Cloning, overexpression and characterization of two peroxiredoxin genes (*alr3183* and *alr4642*) from *Anabaena* PCC 7120

By

Vijay Tailor

Enrollment No. - LIFE01200904008

Bhabha Atomic Research Centre, Mumbai

A thesis submitted to the

Board of Studies in Life Sciences

In partial fulfillment of requirements

for the Degree of

DOCTOR OF PHILOSOPHY

of

HOMI BHABHA NATIONAL INSTITUTE

July, 2016

Homi Bhabha National Institute[1]

Recommendations of the Viva Voce Committee

As members of the Viva Voce Committee, we certify that we have read the dissertation prepared by Vijay Tailor entitled "Cloning, overexpression and characterization of two peroxiredoxin genes (*alr3183* and *alr4642*) from *Anabaena* PCC 7120" and recommend that it may be accepted as fulfilling the thesis requirement for the award of Degree of Doctor of Philosophy.

Chairman – Dr. S. K. Apte	**Date:**
Guide / Convener – Dr. Anand Ballal	**Date:**
Examiner - <Name>	**Date:**
Member 1- Dr. Vinay Kumar	**Date:**
Member 2- Dr. Suprasanna	**Date:**

Final approval and acceptance of this thesis is contingent upon the candidate's submission of the final copies of the thesis to HBNI.

I/We hereby certify that I/we have read this thesis prepared under my/our direction and recommend that it may be accepted as fulfilling the thesis requirement.

Date:

Place: **<Signature>** **<Signature>**

Co-guide (if applicable) **Guide**

[1] This page is to be included only for final submission after successful completion of viva voce.

STATEMENT BY AUTHOR

This dissertation has been submitted in partial fulfillment of requirements for an advanced degree at Homi Bhabha National Institute (HBNI) and is deposited in the Library to be made available to borrowers under rules of the HBNI.

Brief quotations from this dissertation are allowable without special permission, provided that accurate acknowledgement of source is made. Requests for permission for extended quotation from or reproduction of this manuscript in whole or in part may be granted by the Competent Authority of HBNI when in his or her judgment the proposed use of the material is in the interests of scholarship. In all other instances, however, permission must be obtained from the author.

Vijay Tailor

DECLARATION

I, hereby declare that the investigation presented in the thesis has been carried out by me. The work is original and has not been submitted earlier as a whole or in part for a degree / diploma at this or any other Institution / University.

Vijay Tailor

List of Publications arising from the thesis

Journal

1. "Over-expression of Alr4642, a novel Prx-like peroxiredoxin, defends the cyanobacterium *Anabaena* PCC7120 from oxidative stress" (2015) Tailor V., Ballal A., Journal of Applied Phycology, 27(6): 2261-2270.
2. "Novel molecular insights into the function and the antioxidative stress response of a Peroxiredoxin Q protein from Cyanobacteria" (2017) Tailor V., Ballal A. Free Radical Biology and Medicine DOI: 10.1016/j.freeradbiomed.2017.01.031.

Conferences

1. Vijay Tailor and Anand Ballal (2014) "An Atypical Peroxiredoxin 'Alr3183' Protects *Anabaena* PCC7120 from Oxidative Stress". In abstracts of the Society for Research in Free Radicals (SFRR), India-2014 (Jan. 24-30, 2014) conference, held at Lonavala, Maharashtra, India. Pp. 196.

2. Vijay Tailor and Anand Ballal (2015) "A novel Prx-like peroxiredoxin (Alr4642) protects the cyanobacterium *Anabaena* PCC7120 from oxidative stress" In abstract of the DAE-BRNS Life Science Symposium, LSS-2015 (Feb. 3-5, 2015), held at Anushakti Nagar, Mumbai. Pp. 170.

3. Vijay Tailor and Anand Ballal (2017) "Novel molecular insights into the function and the antioxidative stress response of a Peroxiredoxin Q protein from Cyanobacteria" Society for Research in Free Radicals (SFRR), India-2017 (Jan.9-12, 2017) conference, held at Anushakti Nagar, Mumbai, Maharashtra, India. Pp. 149 (Received the best poster award).

Vijay Tailor

Dedicated

to

My Parents

Acknowledgements

Pursuing PhD is a challenge in every aspect; it demanded passion, optimism, commitment and determination. Now as I stand on the edge of its completion, I look back in retrospection and indispensable assistance and guidance of those who were indispensible in letting me achieve my goals. The going has been rough at times and fortunately I have been blessed to have the helpful people around me during those tough times. They have made this journey possible with words of encouragement and support all the time. I would like to thank all people without whom this project would have been a distant reality.

I would like to express my sincere gratitude first to my guide, Dr. Anand Ballal for guiding my work. His encouragement, valuable suggestions and critical inputs were very useful throughout the study, and for improving my scientific writing skills. There is a lot I have learnt from him that will help me throughout my life. This thesis would not have come up to into good shape without his critical evaluation and useful suggestions.

I thank my doctoral committee chairperson Dr. S. K. Apte and Dr. Vinay Kumar, Dr. P. Suprasanna, for their encouragement, valuable suggestions and critical inputs that helped in elevating the standard of this work. I also gratefully thank previous committee members, Dr. TPA Devsagayam, Dr. M. V. Hosur, Dr. A. K. Sharma and Dr. Santosh Kumar, for their suggestions.

I am very thankful to Dr. Hema Rajaram, Dean, Life Sciences, for facilitating all the Ph. D-related paperwork as well as for academic advice. Her help and constant support has helped me complete my thesis.

I wish to thank my lab-mates Dr. Manisha Banerjee, Dr. Rachana Agarwal, Dr. Rajani Kant Chittela, Dr. Alka Gupta, Mr. Dhiman Chakravarty, Ms. Namrata Waghmare and Ms. Anuradha Nair for all their help and moral support all the time and for all the fun we had in past few years. Special thanks to Dr. Bhakti Basu and Dr. Subhash Bihani for their valuable research inputs.

I also thank my friends Archana Mishra, Aparajita Banerjee, Chaturbhuj Srivastav, Surya Kumar Singh, Ravi Sanyal, and Amol for enormous support and well wishes during this period.

I also sincerely thank Mr. Narendra Takade, Mr. Wilton Gaurav and Mr. Avindra Kadam for technical support.

This would never have happened without enormous support from my parents, my in-laws, husband and my family for keeping patience and support in completing my Ph.D. I also extend my heartfelt thanks to my family and well wishers. Motivation from my parents has helped me reach this point in my life. I therefore, dedicate this thesis to my parents.

Finally, I am also thankful to Homi Bhabha National Institute for providing funds required to carry out this work.

To all those, I would like to acknowledge people from whom I received help, and moral support to achieve this feat, thank you very much.

ABBREVIATIONS

Ahp C	Alkyl Hydroperoxide reductase C
Ahp D	Alkyl Hydroperoxide reductase D
Ahp F	Alkyl Hydroperoxide reductase F
AIM	Auto-induction medium
AMS	4-acetamido-4′-maleimidylstilbene-2,2′-disulfonate
Ap	Ampicillin
APS	Ammonium per sulphate
ATP	Adenosine triphosphate
AU	Arbitrary unit
BCPs	Bacterioferritin Comigratory Proteins
bp	Base pairs
BGA	Blue Green Algae
Chl *a*	Chlorophyll *a*
CD	Circular Dichroism
Cm	Chloramphenicol
Cb	Carbenicillin
CBB	Coomassie Brilliant Blue
C_p	Peroxidatic cysteine
C_r	Resolving cysteine
C_pS-OH	Cysteine sulfenic acid
C_pSH	Reduced cysteine
CuX	Cumene-hydroperoxide
Cys	Cysteine
DCHFDA	2′,7′-Dichlorofluorescin diacetate
DIG	Digoxygenin
DLS	Dynamic light scattering
D/W	Distilled water
DTT	Dithiothreitol
EDTA	Ethylene diamine tetra acetic acid

EMSA	Electrophoretic mobility shift assays
ETC	Electron transport chain
GFP	Green fluorescent protein
GSH	Glutathione
GPxs	Glutathione peroxidase
Grx	Glutaredoxin
GR	Glutathione reductase
h	hour/s
H_2O_2	Hydrogen peroxide
HMG-CoA reductase	3-hydroxy-3-methyl-glutaryl-coenzyme A reductase
IR	Ionizing radiation
IPTG	Isopropyl-β-D-thiogalactopyranoside
Kan	Kanamycin
Kb	kilo bases
kDa	kilo Dalton
kGy	kilo Grey
LB	Luria-Bertani
MOPS	3-(N-mopholino) propane sulfonic acid
MALDI-MS	Matrix assisted Laser desorption ionization mass spectrometry
M	Molar
mM	Millimolar
mg	Milligrams
ml	Millilitre
min	Minutes
MV	Methyl-viologen
N	Nitrogen
Ni^{+2}-NTA	Ni^{2+} -nitrilotriacetic acid
NBT-BCIP	Nitro Blue Tetrazolium / 5'Bromo 4' Chloro 3-Indolyl Phosphate
NEB	New England biolabs
Neo	Neomycin

NOX	NADPH oxidases
NTRC	NADPH thioredoxin reductase C
NADH	Nicotineamide-adenine-dinucleotide
NADPH	Nicotineamide-adenine-dinucleotide phosphate
ng	Nanogram
nm	Nanometer
nmoles	Nanomoles
$OH^{\cdot}$	Hydroxyl radicals
OD	Optical Density
ORF	Open Reading Frame
PAGE	Polyacrylamide gel electrophoresis
PCC	Pasteur Culture Collection
PCR	Polymerase Chain Reaction
Prxs	Peroxiredoxins
PrxQ	Peroxiredoxins Q
PSI	Photosystem I
PSI	Photosystem II
RT	Room temperature
ROS	Reactive oxygen species
rpm	Rotation per min
SDS	Sodium dodecyl sulphate
SOD	Superoxide dismutase
SPR	Surface plasmon resonance
$\bullet O_2^-$	Superoxide radical
t-Bx	tertiary-Butyl hydroperoxide
TBE	Tris-Borate EDTA buffer
TEMED	N,N,N`,N`-Tetramethylenediamine
T_m	Melting temperature
Trx	Thioredoxin
TR	Thioredoxin reductase

Tris	Tris (hydroxymethyl)-aminomethane
TSA	Thiol-specific antioxidant
UV	Ultra violet
µg	Microgram
µl	Microliter
µM	Micromloar

Contents

Homi Bhabha National Institute

Ph. D. PROGRAMME

1. Name of the Student: Ms. Vijay Tailor
2. **Name of the Constituent Institution:** Bhabha Atomic Research Centre
3. **Enrolment No.:** LIFE01200904008
4. **Title of the Thesis:** "Cloning, overexpression and characterization of two peroxiredoxin genes *alr3183* and *alr4642*) from *Anabaena* PCC7120"
5. **Board of Studies:** Life Sciences

Cyanobacteria, which originated >3 billion years ago, were among the first organisms to produce oxygen (as byproduct of photosynthesis) in an otherwise reducing environment. Hence, very likely, these organisms have developed elaborate mechanisms to protect their cellular machinery from ROS. The heterocystous, filamentous, cyanobacterium *Anabaena* performs two vital functions, namely photosynthesis and nitrogen fixation, which are extremely sensitive to ROS. Nitrogen-fixing strains of cyanobacteria such as *Anabaena* are economically valuable and eco-friendly source of biofertilizers in the paddy fields of South East Asia (Venkatraman, 1979). Various abiotic stresses (heavy metals, drought, salt, extreme temperatures, high light intensity, herbicides etc.), which lead to over-production of ROS (Choudhury et al., 2013); adversely affect the biofertilizer potential of *Anabaena*. Therefore, understanding the molecular machinery involved in overcoming oxidative stress in *Anabaena* is important for development of newer biofertilizers for use under adverse field conditions.

Reactive oxygen species (ROS), include superoxide (O_2^-), hydrogen peroxide (H_2O_2) and the

hydroxyl radical ($^{\cdot}OH$), and are continuously produced as by-products of normal cellular metabolic activities during aerobic growth. Moreover, formation of ROS is further exacerbated when organisms are exposed to stresses such as light, elevated temperature, salinity, desiccation, radiation etc. Unless effectively scavenged, ROS can damage all major classes of cellular components. Organisms have evolved different strategies that include enzymatic (catalases, superoxide dismutases and peroxidases) and non-enzymatic (e.g. glutathione and ascorbate) defense mechanisms to detoxify ROS.

Peroxiredoxins (Prxs), also called thiol peroxidases, are proteins that detoxify ROS, such as hydrogen peroxide, alkyl hydroperoxides and peroxinitrites. Prxs belong to the Trx (Thioredoxin)-fold superfamily and are ubiquitously present in all domains of life. Prxs possess a catalytic cysteine residue, the peroxidatic cysteine (C_p) that is involved in detoxification of peroxides. During reaction cycle, C_p residue reacts with the peroxide substrate and is oxidized. Many Prxs also have another conserved cysteine residue, the resolving cysteine (C_r), which forms an intermolecular or intramolecular disulfide bond with the oxidized C_p during the reaction cycle. Regeneration of the reduced form of the catalytic cysteine residues is ultimately facilitated by reductants such as thioredoxin, glutaredoxin, cyclophillins etc (Dietz, 2011, Lindahl, and Cejudo 2013).

The role played by the various proteins in overcoming oxidative stress in the filamentous, heterocystous, diazotrophic, cyanobacterium *Anabaena* PCC7120 has generated lot of interest in the recent past (Cha et al. 2007; Agrawal et al. 2014; Panda et al. 2014). Investigating the contribution of peroxiredoxins in overcoming oxidative stress in *Anabaena* PCC7120 is a major research activity being pursued in our laboratory (Banerjee et al. 2012a; Banerjee et al. 2012b; Banerjee et al. 2013, Banerjee et al., 2015). The genome of *Anabaena* PCC 7120 shows

the presence of 10 peroxiredoxin genes (*all1541*, *alr2503*, *all2375*, *all2556*, *alr3183*, *alr4404*, *alr4641*, *alr4642, alr1206, all0513*) (Cui et al. 2012). Of these, the role of *alr3183* and *alr4642* in overcoming oxidative stress was addressed in the present study. Although, Alr3183 had been partially characterized earlier (Cha et al. 2007), its role in oxidative stress resistance *per se* in *Anabaena* PCC7120 had not been ascertained. On the other hand, the ORF *alr4642* (encoding a Prx-like peroxiredoxin) or its orthologs had not been characterized from any bacterial species.

Overall objectives of the thesis:

1) Cloning of *alr3183* and *alr4642* into *E. coli* over-expression vector for over-expression of Alr3183/Alr4642 proteins, their purification and biophysical/biochemical characterization.
2) Expression analysis of Alr3183 and Alr4642 in response to different stresses in *Anabaena*.
3) Construction of suitable plasmid vectors to over-express the above- proteins in *Anabaena* and study stress tolerance of the corresponding over-expression strains *vis-a vis* the wild-type.

Thesis is divided into 5 chapters inclusive of a General Introduction containing review of literature (Chapter 1). The material and methods are described in the Chapter II. Chapters III and IV deal with Results obtained while characterizing Alr3183 and Alr4642 respectively and the relevant discussion. A Summary of major findings of this work is presented at the end, which is followed by a list of references that were used in the study.

Chapter 1: General Introduction

This chapter provides a brief introduction on cyanobacteria and explains why they continue to be a good model system to study responses to abiotic stress. A brief introduction on ROS, pathways that generate ROS and the physiological consequence of oxidative stress i.e.

excessive generation of ROS is described here. The machinery that detoxifies ROS, both non-enzymatic and enzymatic, is discussed. The various types of Prxs and their mechanism of catalysis are highlighted. In addition, the physiological role played by Prxs in different organisms is elaborated. In light of the available information, the objectives and scope of the present study in cyanobacteria is stated.

Chapter 2: Materials and Methods

This chapter describes the materials and experimental methods employed in the study. The source of different bacterial strains, plasmids, enzymes, chemicals culture media and the growth conditions utilized in the study are described here. The procedures followed for polymerase chain reaction (PCR), isolation and cloning of DNA fragments in to plasmid vectors, conjugation of plasmids into *Anabaena* PCC7120 and selection of exconjugants are described. Methodology used to evaluate the oxidative stress resistance of *Anabaena* strains is detailed. The different techniques involved in over-producing the Alr3183/Alr4642 proteins and their subsequent purification are described. Protocols to evaluate the peroxidase activity of Prxs employing different reductants are detailed. Electrophoresis techniques followed by Western/Northern analysis are elaborated. Techniques of gel exclusion chromatography, dynamic light scattering, CD-spectropolarimetry, surface plasmon resonance (SPR) etc are elaborated in this chapter. The different analytical procedures and bioinformatic analyses used in the study are also stated.

Chapter 3: Cloning and characterization of *alr3183*/Alr3183 from *Anabaena* PCC7120

This chapter describes and discusses the results obtained on characterization of the Alr3183 protein from *Anabaena*. Introduction to BCP (bacterioferritin comigratory protein)/PrxQ type of peroxiredoxins and brief review of literature is presented in this chapter. Bioinformatic

analysis indicated Alr3183 to belong to the PrxQ family, wherein the C_p was located within the GCT motif. Further, the cysteine residue at 46th amino acid position was suggested to be C_p whereas the cysteine at 51st position was proposed to be C_r. The *alr3183* gene from *Anabaena* PCC7120 was PCR amplified with suitable primers and cloned into the *E. coli* expression vector, pET16b. This vector adds 10 His codons *in frame* upstream of the 5' end of the gene cloned. Therefore, when expressed, the protein of interest carries a His-tag (at N-terminal) and can be purified by affinity chromatography using IMAC/Ni-NTA agarose. To evaluate the role of catalytic cysteines in the Alr3183 protein, codons corresponding to both the Cys residues were separately mutated to serine by employing a PCR-based strategy that involved the use of mutagenic primers. Similarly, a mutant Alr3183 wherein both the Cys residues were changed to Ser was also generated. The DNA fragments thus obtained, *alr3183C46S*, *alr3183C51S* and *alr3183CDM* (cysteine double mutant) were also cloned into pET16b. After confirming the nucleotide integrity by sequencing, all the plasmid constructs were transformed into *E. coli* BL21(pLysS) for overproduction of proteins. All the over-expressed proteins could be detected with the penta-His antiserum. Furthermore, these proteins were present in the soluble fraction of *E. coli* whole cell extracts and could be purified to near homogeneity by affinity chromatography. The purified Alr3183 protein was employed to raise specific antiserum in rabbits at a commercial facility. All the three above-mentioned proteins immune-cross reacted with anti-Alr3183 antiserum on Western blots.

When resolved on reducing SDS-polyacrylamide gels, all the three proteins migrated with an apparent molecular mass of ~19 kDa, which corresponded to their monomeric size. Incidentally, the Alr3183 protein appeared as two closely spaced bands on reducing SDS-polyacrylamide gels. MALDI-TOF MS-based peptide mass fingerprinting analysis confirmed both the bands to be Alr3183. Results with 4-acetamido-4′-maleimidyl-stilbene-2,2′-

disulfonate (AMS) showed Alr3183 to form intra-molecular disulfide bonds. On non-reducing polyacrylamide gels, only Alr3183 appeared at its monomeric position whereas both Alr3183C46S and Alr3183C51S appeared as dimers. Thus, in the absence of one catalytic cysteine, the other catalytic cysteine (of one monomer) can form intermolecular disulfide bond with its counterpart (from another monomer) and dimerize, whereas, when both the cysteines are present, intramolecular disulphide bond is formed. Gel exclusion chromatography and dynamic light scattering studies also showed Alr3183 to exist as a monomer whereas Alr3183C46S and Alr3183C51S were dimeric. CD spectropolarimetry showed the Alr3183 protein to primarily be an α-helical protein. Reducing the protein with DTT did not significantly alter its secondary structure. Interestingly, Alr3183C46S and Alr3183C51S, in spite of being dimeric, showed only minor changes in the secondary structure when compared with Alr3183, indicating that dimer formation does not cause major alterations in the secondary structure of this protein.

Alr3183 protein showed peroxidase activity with TrxA among the three different reductants (GSH, DTT and TrxA) tested for H_2O detoxification. To monitor physical interaction between TrxA and Alr3183 Surface Plasmon Resonance (SPR) analysis was used. The TrxA protein was immobilized on a bare gold sensor chip while the purified Alr3183 protein was present in the mobile phase for interaction. A concentration-dependent increase in the SPR signal confirmed the physical interaction between Alr3183 and TrxA. The Alr3183 protein was reduced with DTT and allowed to interact with TrxA. Interestingly, the DTT-reduced protein showed decreased binding to TrxA as compared to the control Alr3183 protein (i.e. not treated with DTT). Interaction of Alr3183C46S and Alr3183C51S with TrxA was also performed. At comparable protein concentrations, both Alr3183C46S and the wild-type Alr3183 protein showed similar response units at the end of the assay period. However, a distinctly reduced

interaction was observed when Alr3183C51S was present in the mobile phase. The Alr3183CDM protein bound to TrxA in a manner very similar to that shown by Alr3183C51S. In conclusion, the presence of the resolving cysteine residue appears to enhance the binding of the Alr3183 protein to TrxA.

Alr3183 could decompose H_2O_2, t-butyl hydroperoxide and cumene hydroperoxide in TrxA-dependent manner. On exposure to elevated temperatures, Alr3183 remained fully functional till 40°C, but a severe drop in its activity was observed beyond 45°C, and the protein was completely inactive when exposed to 60°C. Interestingly, unlike other Prxs, such as Alr4641 and All1541 from *Anabaena*, Alr3183 protein was active even after treatment with 10 mM H_2O_2, suggesting that $C_p$was not easily over-oxidized by H_2O_2. The Alr3183C46S protein (that lacks C_p) showed complete absence of peroxidase activity whereas Alr3183C51S (wherein C_r was absent) showed partial activity. However, this activity was 10-fold lower than that observed with the Alr3183 protein. Moreover, Alr3183C51S required relatively higher concentration of TrxA (2 μM or more) to show any peroxidase activity. In contrast, the wild-type protein showed peroxidase activity even with 0.5 μM TrxA.

Expression of the Alr3183 protein was monitored in *Anabaena* in response to stresses such as H_2O_2, methyl viologen, salt etc. No induction of the Alr3183 protein was observed when the total proteins from the stress-treated cells were probed with the Alr3183 antiserum, suggesting the inability of these agents to enhance Alr3183 production in *Anabaena*. Interestingly, Alr3183 protein was found to be distinctly induced in response to γ-radiation. Nitrogen status of the medium did not alter the induction of the Alr3183 protein and even in the under nitrogen-fixing conditions (i.e. absence of combined nitrogen.), production of Alr3183 was observed on exposure to γ-radiation.

Antisense approach was employed to reduce expression of the Alr3183 protein on exposure to gamma radiation. The *alr3183* ORF was cloned in the reverse orientation (i.e. antisense) between a strong light inducible P*psbA1* promoter and the *gfpmut2* gene in pAM1956 (construct denoted pAMAS3183), which was subsequently conjugated into *Anabaena* PCC7120 (to give rise to AnAS3183$^+$). As compared to the wild-type *Anabaena*, a distinct decrease in the synthesis of the Alr3183 protein was observed in AnAS3183$^+$ on exposure to γ-radiation. On exposure to 6 kGy dose, AnAS3183$^+$ showed a reduction in growth as compared to the wild-type, suggesting a role for Alr3183 in overcoming radiation stress.

As the inherent levels of the Alr3183 protein were low in *Anabaena*, it was desired to verify if over-expression of Alr3183 could protect *Anabaena* from oxidative stress. The complete *alr3183* ORF was cloned in between a strong light inducible P_{psbA1} promoter and the *gfpmut2* gene in pAM1956 (construct denoted pAM3183), which was subsequently conjugated into *Anabaena* PCC7120 (to give rise to An3183$^+$). In An3183$^+$, both *alr3183* and *gfp* are co-transcribed but independently translated resulting in co-expression of both proteins. The An3183$^+$ cells that appeared on the selection plates were verified by monitoring expression of GFP microscopically. Intense GFP expression in the filaments under fluorescence microscope showed the presence and transcription of constructs inside the cell. When probed with the Alr3183 antiserum on Western blots, the recombinant An3183$^+$ showed considerable production of the Alr3183 protein. The An3183$^+$ strain showed 5-6 times less levels of ROS than the wild-type strain when exposed to 1mM H_2O_2. Under nitrogen-deficient as well as nitrogen-supplemented conditions, H_2O_2 caused destruction of photosynthetic pigments and cell death in the wild-type *Anabaena* cells, but An3183$^+$ was protected from these deleterious effects.

The 3183C46S protein was also over-produced in *Anabaena* employing the same strategy used to over-express Alr3183. This protein was readily produced in *Anabaena* (An3183C46S). However, unlike the An3183^{+} strain, the An3183C46S^{+} was sensitive to the oxidative effects of H_2O_2, indicating that expression of Alr3183C46S was ineffective in offering any protection from oxidative stress. Thus, peroxidase activity of Alr3183 appears to be essential to protect *Anabaena* from the lethal effects of H_2O_2.

In conclusion, Alr3183 was a monomeric, TrxA-dependent peroxidase whose catalytic cysteines, C_p and C_r, form an intramolecular disulfide bond. The presence of both C_p and C_r prohibits intermolecular disulfide bond formation, but if either of the catalytic cysteine is absent, the protein becomes dimeric due to formation intermolecular C_r-C_r or C_P-C_P linkages. C_p is essential for reacting with the peroxidatic substrate whereas the presence of C_r appears to enhance the protein's capability to interact with TrxA. Reduction of the intra-molecular disulfide bonds decrease the ability of Alr3183 to interact with TrxA, which may be important to facilitate dissociation of the two proteins once the disulfide exchange has occurred. *In vivo*, Alr3183 was found to be a stress-inducible protein whose synthesis was upregulated by γ-radiation. Over-expression of Alr3183 protected *Anabaena* from oxidative stress in nitrogen-supplemented as well as nitrogen-deficient conditions, indicating the potential of An3183^{+} to function as stress-resilient biofertilizer.

Chapter 4: Cloning and characterization of *alr4642*/Alr4642 from *Anabaena* PCC7120

This chapter describes characterization of Alr4642 protein from *Anabaena*. In *Anabaena*, *alr4642* was located immediately downstream of ORF encoding 2-Cys-Prx i.e. *alr4641*. BLAST search showed the ORF *alr4642* (642-bp, encoding 213 amino acids) from *Anabaena* PCC7120 to belong to the thioredoxin superfamily and share homology with the Prx-like2

proteins from many other cyanobacteria. Interestingly, similarity of Alr4642 with the other Prx-like2 proteins was observed only from its second methionine, which was 35 amino acids away from the first annotated methionine. The protein initiating from the second methionine was therefore designated as AlrT4642, (T for truncated). The Prx-like2 domain of Alr4642 extended from 75^{th} to 196^{th} amino acid. Alr4642 showed presence of CXXC motif similar to that present in thioredoxin (Trx). Although, this protein showed conserved peroxidatic cysteine (second C of the CXXC motif), the other two conserved residues (i.e. T & R) of the catalytic triad were absent.

The promoter search program, BPROM, identified a promoter that was located right at the beginning of the full-length *alr4642* ORF with the -35 region overlapping with the start codon of *alr4642* (i.e. the 1^{st} ATG) Although, the -10 of the identified promoter showed a good match with the consensus -10 promoter sequences, the -35 region showed poor match with its respective consensus, indicating that the promoter was inherently a weak promoter. A LexA box that overlapped directly with the -10 sequence was identified bioinformatically. Electrophoretic moblity shift assays (EMSAs) showed that LexA protein from *Anabeana* PCC 7120 bound to the *alr4642* promoter DNA. Northern blotting and hybridization techniques were employed to verify *in vivo* transcription of *alr4642*. In control cells or in response to oxidizing agents such as H_2O_2, methyl-viologen and tertiary-butyl hydroperoxide, the *alr4642* transcript could not be detected. Thus, possibly due to the presence of a weak promoter and/or possible repression by the LexA protein, the *alr4642* ORF was not expressed in *Anabaena*.

Prx-like proteins have not been characterized from any bacterium. Hence, it was desired to purify the Alr4642 protein for biochemical analysis. As homology with the other Prx-like proteins was observed from the second methionine (Met^{36}), along with the full-length *alr4642* ORF, a truncated *alr4642* i.e. *alrt4642* (537-bp, encoding a protein extending from 36^{th}residue

to 213th residue i.e. 178 amino acids) was also cloned in *E. coli* expression vector pET16b for overproduction of N-terminally His-tagged, Alr4642 (10HisAlr4642) or AlrT4642 (10HisTAlr4642). On induction with IPTG, production of the full-length Alr4642 protein or the AlrT4642 protein was clearly observed on denatured polyacrylamide gels. However, in spite of abundant production, 10HisAlr4642 or 10HisAlrT4642 were both insoluble in *E. coli* and located exclusively in the inclusion bodies. Attempts to obtain Alr4642/TAlr4642 in soluble form for purification by (a) lowering the temperature during growth (b) by reducing IPTG concentration, and (c) by employing an alternate medium (e.g. auto-induction medium) were not successful. Similarly, purification under denaturing conditions was also unsuccessful. The over-expressed Alr4642 was eluted from the SDS-polyacrylamide gels and employed to generate polyclonal antiserum in mice. The AlrT4642 protein (along with the thrombin cleavage site) was expressed as a fusion protein with the His-tagged trigger factor (TF, a chaperone) to obtain AlrT4642 in soluble form. The TF-AlrT4642 was soluble when expressed in *E. coli* and could be purified to near homogeneity by affinity chromatography. The fusion protein TF-AlrT4642 was treated with thrombin slurry to cleave AlrT4642 from the His-tagged TF. Although, the proteins were successfully cleaved, the TF remained tightly bound to the AlrT4642 and could not be separated by affinity chromatography or gel filtration.

As Alr4642 could not be expressed in soluble form in *E. coli*, attempts were made to purify Alr4642 after expressing it in *Anabaena*. The complete *alr4642* ORF was cloned in between a strong light inducible P_{psbA1} promoter and a *gfpmut2* ORF in pAM1956 (construct denoted pAMAlr4642), which was subsequently conjugated into *Anabaena* PCC 7120. When exconjugants were probed with the Alr4642 antiserum on Western blots, the recombinant An4642^{+} (but not the wild-type *Anabaena*) showed production of a shorter Alr4642 protein, whose size (20.3 kDa) matched with that of AlrT4642, and not the full length Alr4642. This

indicated that the codon corresponding to the second methionine was the actual start codon *in vivo* in *Anabaena*.

As the above-mentioned results suggested that AlrT4642 (but not Alr4642) was expressed in *Anabaena*, the His-tagged AlrT4642 protein was over-expressed in *Anabaena* for purification. To accomplish this, the *alrt4642* ORF with 6 additional His codons at its 3' end [i.e. *alrt4642(6His)*] was cloned downstream of P_{psbA1} promoter in pAM1956 (pAMT4642) and conjugated into *Anabaena*. Expression of AlrT4642(6His) was verified on Western blots with the Alr4642 antiserum wherein production of a 21.2 kDa protein was observed (the addition of the 6-His tag increased the size of the protein by ~0.9 kDa). This protein was observed in the cytosolic fraction of *Anabaena* extracts indicating that AlrT4642 remained soluble when over-expressed in *Anabaena*. The AlrT4642 protein could be purified to near homogeneity by affinity chromatography employing the Ni-NTA matrix. The identity of purified AlrT4642 was confirmed by probing it with anti-Alr4642 and anti-polyhistidine antibodies. The purified AlrT642 was checked for its ability to protect DNA from oxidative damage using the metal catalyzed oxidation (MCO) assay. In the absence of the AlrT4642(6His) protein or in the presence of BSA (control protein), complete degradation of the plasmid DNA was observed in the metal catalyzed oxidation (MCO) assay. However, when the Alr4642(6His) protein was present, distinct protection of DNA was observed. This protein failed to show TrxA-dependent Prx activity when TrxA from *E. coli* was used, however, a DTT-dependent peroxidase activity was observed**.** The recombinant AnT4642(6His)$^{+}$ and the wild-type *Anabaena* PCC7120 were assessed for oxidative stress resistance in response to hydrogen peroxide. After 2 days of treatment, a pronounced bleaching, indicating loss of photosynthetic pigments, was observed in the wild-type cells but not in AnT4642(6His)$^{+}$, indicating that that over-expression of AlrT4642 can protect *Anabaena* from oxidative stress.

In summary, the *alr4642* ORF from *Anabaena* PCC7120 encoded a protein that showed homology to Prx-like family of Prxs. Sequence analysis showed the presence of another methionine residue, 35 amino acids downstream of the first annotated methionine. Both full length Alr4642 and AlrT4642 (truncated Alr4642, initiating from the second methionine) remained insoluble when over-expressed in *E. coli*, and could not be purified. Interestingly, expression of the complete *alr4642* ORF in wild type *Anabaena* resulted in the production of the truncated AlrT4642 protein, suggesting that the second ATG was the actual *in vivo* start codon of *alr4642* in *Anabaena*. When over-expressed in *Anabaena*, AlrT4642 (with a C-terminal His-tag) was soluble and could be purified by affinity chromatography. The purified AlrT4642 protected the plasmid DNA from oxidative damage and *Anabaena* cells over-expressing AlrT4642 showed improved tolerance to H_2O_2 than the wild-type. These data indicate that AlrT4642 is indeed an antioxidant protein that is capable of protecting *Anabaena* from oxidative stress.

Chapter 5: Summary and Conclusions

The major results obtained during the course of this work and their interpretation and significance is reported in this chapter. Future prospects of research that have risen from the work embodied in this thesis are also discussed.

References: This section will follow chapter 5 and all the relevant literature referred to during the course of this study will be cited here.

References:

1) Agrawal C, Sen S, Singh S, Rai S, Singh, PK, Singh VK and Rai LC (2014) J Proteomics 2014, 96:271-90.
2) Banerjee M, Ballal A, Apte SK (2012a) *Biochem J*, 442:671-80.
3) Banerjee M, Ballal A, Apte SK (2012) *Environ Microbiol*, 14:2891-900.
4) Banerjee M, Raghavan PS, Ballal A, Rajaram H, Apte SK (2013) *Photosynth Res*. 118: 59-70.
5) Banerjee M, Chakravarty D., Ballal A *BMC Plant Biol* 15:60
6) Cha M, Hong SK, Kim IH (2007) *Free Radic Biol Med*, 42:1736-48.
7) Choudhury, S, Panda, P, Sahoo, L (2013) Plant Signal Behav 8: pp. e23681.
8) Cui H, Wang Y, Wang Y, Qin S (2012) *BMC Evol Biol*, 12:220.
9) Dietz KJ (2011) Peroxiredoxins in plants and cyanobacteria. Antioxid Redox Signal.15:1128–59.
10) Panda, B. Basu, B. Rajaram, H. Apte S. K. Proteomics (2014), 14:1895-1904.
11) Venkataraman, G. S. (1979) In Nitrogen and Rice, pp. 311–321. Edited by N. C. Brady. La Banos, Phillipines: International Rice Research Institute.
12) Lindahl, M and Cejudo, FJ (2013) *Methods Enzymol* Elsevier. pp 257-273

Publications:

1. Tailor V., Ballal A. (2015) Over-expression of Alr4642, a novel Prx-like peroxiredoxin, defends the cyanobacterium *Anabaena* PCC7120 from oxidative stress. Journal of Applied Phycology, 27(6): 2261-2270.

Manuscript in preparation

1. Tailor V., Ballal A. (2016) Characterization of a γ-radiation induced peroxiredoxin (Alr3183) from the filamentous, heterocystous, nitrogen-fixing cyanobacterium *Anabaena* sp. PCC 7120.

Conferences attended:

1. Vijay Tailor and Anand Ballal (2014) "An Atypical Peroxiredoxin 'Alr3183' Protects *Anabaena* PCC7120 from Oxidative Stress". SFRR-India-2014 (Jan. 24-30, 2014) conference, held at Lonavala, Maharashtra, India.

2. Vijay Tailor and Anand Ballal (2015) “A novel Prx-like peroxiredoxin (Alr4642) protects the cyanobacterium *Anabaena* PCC7120 from oxidative stress” DAE-BRNS life science symposium LSS-2015 (Feb3-5, 2015), held at Anushakti Nagar, Mumbai.

Signature of the student:

Date:

Doctoral Committee:

S. No.	Name	Designation	Signature	Date
1	Dr. S. K. Apte	Chairman		
2	Dr. Vinay Kumar	Member		
3	Dr. Suprasanna	Member		
4	Dr. Anand Ballal	Convener & Guide		

List of Figures

Chapter- 1

Chapter-3

Chapter-4

List of Tables

Chapter 1 - General Introduction

1.1 Oxygen toxicity, oxidative stress and reactive oxygen species

Molecular oxygen (O_2) is indispensable for the existence of aerobic organisms, but it is also potentially dangerous since reactive oxygen species (ROS) resulting from it are source of cell and tissue injury [1]. It is well known that obligate anaerobes and microaerophiles have considerably reduced tolerance to oxygen. Even aerobic organisms tolerate oxygen only up to a limited extent [2]. In the presence of high concentration of oxygen (i.e. hyperoxia) aerobes too show reduced growth, and beyond a threshold concentration, death may occur, this phenomenon, is termed as oxygen toxicity [3, 4]. Oxygen toxicity arises due to the formation of ROS at increased concentration of oxygen [5]. Incomplete reduction of oxygen to water formed ROS [6, 7]. Superoxide anion radical ($\bullet O_2^-$), hydrogen peroxide (H_2O_2), and hydroxyl radical ($OH^\cdot$) are the biologically important ROS [8, 9, 10]. Singlet oxygen, the excited form of O_2 having spin paired pi-antibonding electrons [11], is generated in photosynthetic organisms.

Molecular oxygen is stable molecule with two unpaired electrons in its pi-antibonding orbitals. These two unpaired electrons exist in the same spin state (Fig. 1.1.1). Due to this structure, oxygen can accept only one electron at a time, making it a weak electron accepter. Since most biological molecules are poor univalent electron donors, oxygen cannot efficiently oxidize them. However, the unpaired electron of oxygen can readily react with the unpaired electrons of transition metals and organic radicals. In contrast, $\bullet O_2^-$, H_2O_2, and $OH^\cdot$ are much stronger univalent oxidants [12] than dioxygen, as evidenced from their values of reduction potentials (Fig. 1.1.2) [13]. Various reactive oxygen species important in biological systems are summarized in Table 1.1.

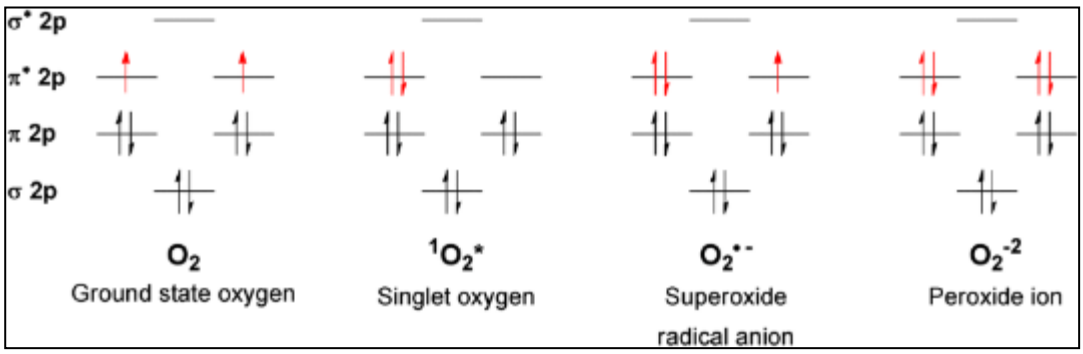

Fig. 1.1.1. Molecular-orbital diagrams of ROS species. Molecular-orbital diagrams of molecular oxygen (O_2), superoxide ($\bullet O_2^-$), peroxide (O_2^{-2}), and singlet oxygen ($^1O_2$) [14].

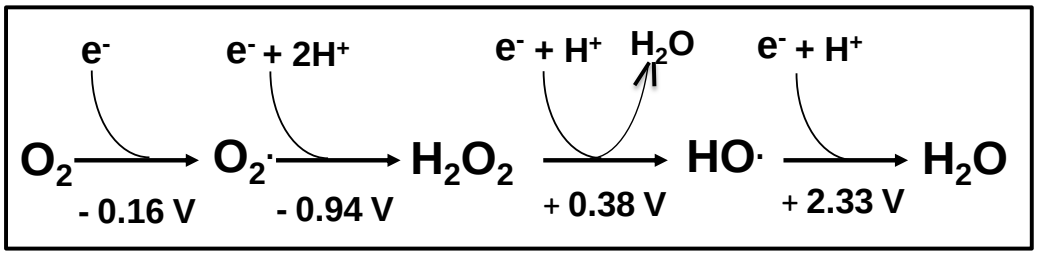

Fig. 1.1.2**. Reduction potentials for oxygen species.** 1 M dioxygen is used as the standard state for the first step [13].

ROS are continuously produced in aerobic cells (13, 12, 15) and their generation is enhanced during stressful conditions. ROS can damage biomolecules [16] which if not repaired effectively, can ultimately lead to cell death. Cumulatively, this is known as oxidative stress. Thus, oxidative stress is an imbalance between ROS generation and its removal or detoxification or repair of damage by a biological system [17, 18].

Table 1.1: Various reactive oxygen species important in biological systems.

Superoxide anion ($\bullet O_2^-$)	Formed in many autoxidation reactions and by the electron transport chain (ETC). Relatively unreactive but can release Fe^{2+} from iron-sulfur proteins and ferritin. Undergoes dismutation spontaneously or by enzymes to form H_2O_2
Hydrogen peroxide (H_2O_2)	Two-electron reduction state, formed as a result of $\bullet O^{2-}$ dismutation or by direct reduction of O_2. Lipid soluble and thus able to diffuse across membranes.
Hydroxyl radical ($\bullet OH$)	Three-electron reduction state, formed mainly by Fenton reaction and peroxynitrite decomposition. Extremely reactive, will attack most cellular components
Organic hydroperoxide (ROOH)	Formed when radicals react with cellular components (such as lipids and DNA)
Alkoxy and RO•, Peroxy radicals ROO•	Organic radicals. Produced in the presence of oxygen by radical addition to double bonds or hydrogen abstraction. Participate in lipid peroxidation reactions
Hypochlorous acid HOCl	Formed from H_2O_2 by myeloperoxidase. Lipid soluble and highly reactive. Will readily oxidize protein constituents, including thiol groups, amino groups and methionine.
Peroxynitrite ONOO-,	Formed in a rapid reaction between $\bullet O_2^-$ and NO•. Lipid soluble and similar in reactivity to hypochlorous acid. Protonation forms peroxynitrous acid, which can undergo homolytic cleavage to form hydroxyl radical and nitrogen dioxide.

Table Source: [19]

1.2 Sources of ROS in living system

Multiple mechanisms lead to ROS generation in a cell and tissue specific manner in organisms [20]. Molecular oxygen is unreactive and hydroxyl radical is short lived (*in vivo* half-life of 10^{-9} sec), thus the rate at which $\bullet O_2^-$ and H_2O_2 are formed inside the cell decides the level of oxidative stress that an organism experiences. In living cells ROS are generated by different sources (Fig. 1.2.), most relevant are those detailed below:

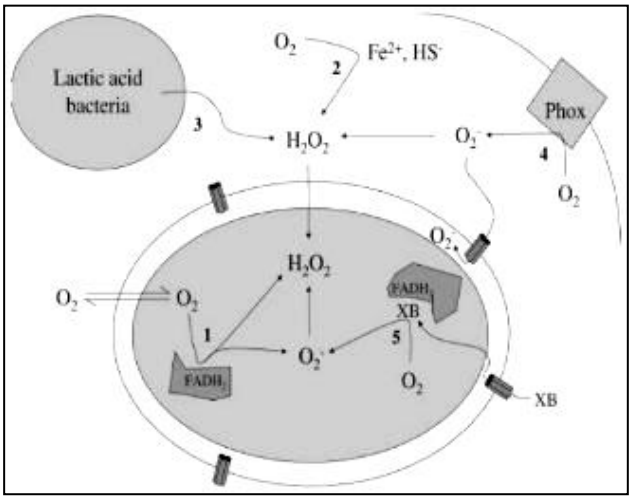

Fig. 1.2. Sources of oxidative stress. Sources for oxidative stress in bacteria include (1) intracellular enzyme autoxidation, (2) environmental redox reactions, (3) H_2O_2 released by competing microbes (e.g. Lactic acid bacteria), (4) phagosomal NADPH oxidase, and (5) redox-cycling antibiotics [20].

1.2.1 Mitochondrial (Respiratory) production of ROS

Oxidative phosphorylation produces usable energy in mitochondria. During this process, proton transport occurs across the inner membrane by the means of electron transport chain (ETC). In ETC, electrons are channeled through a series of proteins via oxidation-reduction reactions, final destination being O_2 and concomitantly generation of water. Under normal conditions approximately, 1–5% of electrons 'flowing' through the ETC are diverted to form

$\bullet O_2^-$ at complex I (NADH/ubiquinone oxidoreductase) and complex III (ubiquinol/cytochrome c oxidoreductase) [12, 21, 22].

ROS Generation in complex I occurs at outer active parts of the enzyme at each end of the cofactor chain. Two distinct but mutually inexclusive sites of O_2 reduction are suggested in complex I as supported by the model for structure of the hydrophillic arm of the respiratory complex I from *Thermus thermophilus* [23]. According to this model, most of the enzyme cofactors are solvent inaccessible, and are not able to react with molecular oxygen. The outer active parts of the enzyme at each end of the cofactor chain: either the reduced flavin moiety or the quinine-binding site seems to be the two sites of ROS generation in complex I [24].

Production of $\bullet O_2^-$ in bc1 complex (complex III): This is the possible site of $\bullet O_2^-$ generation in the periplasm of gram negative bacteria. Auto-oxidation of ubiquinol probably occurs in the momentary presence of semiquinones at Q_n and Q_p, which due to their radical nature react avidly with molecular oxygen. The high auto-oxidation of the bc1 complex in the presence of antimycin, an inhibitor that blocks electron flow to the Q_n site, thereby forcing the accumulation of ubisemiquinone at Q_p supports this hypothesis [25, 26]. The superoxide anions formed are released on the positively charged face of the membrane, i.e. periplasm. The superoxide generated has tendency to get electrostatically attracted to the catalytic iron atom present in the Fe-S clusters. After binding to this cluster, the superoxide radical can univalently oxidize the Fe-S cluster, making it unstable. This ultimately leads to the degradation of clusters and the catalytic iron atom is lost [26, 27].

1.2.2 Production of ROS inside the phagocytic cells (NADPH oxidases or NOX complexes)

The NADPH oxidases are membrane-bound enzymes facing the extracellular space in plasma membranes as well as the phagosome membranes (vesicles used by neutrophils to engulf the microbes). Under normal conditions, the NOX is latent in neutrophils and is activated to assemble in the membranes during respiratory burst [28]. NADPH oxidase can transfer electrons from NADPH inside the cell across the membrane and couple this to molecular oxygen, generating superoxide anion. Myeloperoxidase (MPO) is most abundantly expressed in neutrophils and it produces hypochlorous acid from H_2O_2 and Cl^- ions during the respiratory burst. Using hydrogen peroxide, MPO also produces tyrosyl radical by oxidation of tyrosine. Both the products, H_2O_2 and the tyrosyl radical are cytotoxic.

1.2.3 Ionizing radiation (IR)

Ionizing radiations (X-or-gamma rays) are high energy radiations that have enough energy to free electrons from molecules, thereby creating free radicals. Ionizing radiation can damage molecules directly or indirectly, through radiolysis of water [29]. Radiolysis of water that occurs in the presence of IR is a major source of ROS production. In this process, water loses an electron and becomes highly reactive. Then through a three-step chain reaction, water is sequentially converted to the $^{\cdot}OH$, H_2O_2 and $\bullet O_2^-$ [30]. Since water comprises major portion of all organisms, the probability of radiolysis is quite high under the presence of ionizing radiation.

1.2.4 Photosynthetic production of ROS

The oxygenic photosynthesis is essential for life on earth [31, 32]. Photosynthesis is an important contributor of cellular oxidants [32]. Both the reaction centers of PSI and PSII are the major sources of ROS production in plants. Photoreduction of oxygen to hydrogen peroxide occurs in PSI [33]. Later, Asada [34] showed $\bullet O_2^-$ to be the primary reduction product, and its disproportionation produced H_2O_2 and O_2. In PSII, the ground (triplet) state oxygen is excited to singlet state by the reaction center chlorophyll (Chl) of triplet excited state [35, 36, 37]. Singlet oxygen is unstable and specifically reacts with organic molecules with double bonds. Singlet oxygen is produced in high amount of in plants exposed to high light. These ROS species reduces the photosynthetic efficiency of chloroplasts and excess of singlet oxygen may result in cell death [35].

1.2.5 Futile cycle or redox cycling

Many flavoenzymes and their cofactors are auto-oxidized by aromatic compounds to their anion free radicals [38]. Radicals thus generated can further reduce molecular oxygen to superoxide, and the (unchanged) parent compound is simultaneously regenerated. This behavior of flavoenzymes and their cofactors has been described as futile cycle or redox cycling**.** Examples of redox cycle-inducing molecules includes herbicide paraquat (methyl viologen together with other viologens) and quinones such as menadione [38]. Autoxidation of flavoenzymes yields a mixture of $\bullet O_2^-$ and H_2O_2. More H_2O_2, rather than $\bullet O_2^-$, is produced by NADH dehydrogenase, sulfite reductase, and xanthine oxidase, whereas, succinate dehydrogenase and fumarate dehydrogenase release more $\bullet O_2^-$ than H_2O_2.

Not only the sites of intracellular $\bullet O_2^-$ or H_2O_2 generation, but also the rate at which they are

produced, differ from organism to organism. Hence, even in similar environments, different organisms may experience dissimilar levels of $\bullet O_2^-$ and H_2O_2 stress. This ultimately gives rise to differences in the levels of oxygen tolerated by various species [19].

1.3 Damaging effects of different ROS

Molecular oxygen by itself has a little impact on aerobes. Flint et al. [27], have shown that dioxygen can oxidize the (4Fe-4S) clusters of several dehydratase with a rate constant of about 1 $M^{-1} s^{-1}$.

1.3.1 Effects of superoxide

Superoxide itself is not very reactive, but it can inactivate dehydrogenase enzymes or in its protonated form, hydroperoxyl $HO_2^{\cdot}$, which has a pK_a of 4.8 can also initiate lipid peroxidation [39, 40]. Thus, at physiological pH, the majority of superoxide will exist as $\bullet O_2^-$ (i. e. superoxide anion). Earlier, it was thought that superoxide primarily delivered electrons to adventitious iron on DNA [41]. Later, studies in *E. coli* indicated that superoxide caused damage to DNA by leaching iron from storage proteins (i.e. Fe-S clusters, which are the major source of free iron) or enzymes such as aconitase B and fumarase A/B [42]. This released iron can now deposit on the surface of the DNA and catalyse the Fenton reaction in association with H_2O_2 [42]. This damage to key enzymes causes tricarboxylic acid cycle to lose function during oxidative stress, and hence, non-fermentable substrates can no longer support growth [42].

Recently Baron et al., [43] have suggested acid burst in yeast occurs due to superoxide generation. In mammalian systems, mitochondrial superoxide production causes cellular

oxidative damage and may be the underlying reason for degenerative diseases and aging [42].

1.3.2 Hydrogen peroxide-mediated damage

1.3.3 Hydroxyl radical

The negative charge of $\bullet O_2^-$ reduces its activity with electrons rich molecules, whereas the reactivity of H_2O_2 is reduced by the strength of its oxygen-oxygen bond, but the •OH oxidizes most bio-molecules at diffusion limited rates [45]. Hydroxyl radical formation within a cell occurs mainly by Fenton reaction [46]. Hydroxyl radicals generation by Fenton reaction require iron (or another divalent metal ion, such as copper) and a source of reducing equivalent (possibly NADH) to regenerate the metal [47]. Fenton reaction cause protein carbonylation and membrane peroxidation, its most significant impact is on DNA, because even a single unrepaired DNA lesion can be mutagenic or lethal [47]. A short time exposure to millimolar levels of H_2O_2 creates enough DNA damage to heavily mutagenize or even kill most bacteria [19]. The “free iron,” i.e. the iron that is not incorporated into enzymes or iron-storage proteins, catalyses the Fenton reaction. Nucleic acid are the favored targets of Fenton-mediated damage because nucleic acids have tendency to bind metals, and binding of metals such as iron and copper metals leads to generation of hydroxyl radicals via Fenton reaction when H_2O_2 is present in the vicinity. Hydroxyl radical, due to its non-specific and high reactivity, is unlikely to diffuse far from its origin *in vivo*. Hence, once $HO^{\cdot}$ is generated on DNA, damage to this vital biomolecule is inevitable. $HO^{\cdot}$ can abstract electron from both the sugar and base moieties, and can also react with the unsaturated bases [48, 49]. The resultant radicals finally decompose in multifarious ways and thereby causing different types of lesions. Interestingly, the low reduction potential of guanine facilitates electron movement from G to nearby base radicals, thereby reversing the radical at the original site of oxidation

but leaving guanine with an unpaired electron, which ultimately results in the formation of 8-hydroxyguanine.

Generation of hydroxyl radical occurs by Haber-weiss reaction in the presence of hydrogen peroxide and ferric ion.

In the first step reduction of ferric into ferrous ion with $\bullet O_2^-$:

$$Fe^{3+} + \bullet O_2^- \rightarrow Fe^{2+} + O_2$$

The next step is the Fenton reaction:

$$Fe^{2+} + H_2O_2 \rightarrow Fe^{3+} + {}^-OH + {}^{\cdot}OH$$

Hydroxyl radical is generated inside the body in hypoxic conditions [50]. Moreover, this free radical can be generated *in vitro* under the reducing condition in the presence of ascorbic acid and iron ions. In fact the hydroxyl radical can be made without any additional redox agent. This is considered as special case of a Fenton reaction where one electron from the hydroxyl group of water is transferred to the ferric ion with the formation of a divalent iron and a hydroxyl radical [51]. Thus, the free iron, also called as labile iron, plays an important part in generation of the hydroxyl radical [52].

Membrane damage: Free radicals directly attack polyunsaturated fatty acids in cellular membranes, initiating their (lipid) peroxidation [53]. In mammalian systems, lipid peroxidation is the most prominent result of oxidative stress. During the propagation step, the lipid peroxyl radical extracts an electron from adjacent lipids. Notably, the presence of bis-allylic methylene carbon (present only on polyunsaturated lipids) makes this reaction kinetically efficient. Thus, polyunsaturated lipids that contain such carbon atoms are the main targets of the hydroxyl radical [53]. Contrary to these, studies with model systems indicate that the monounsaturated lipids found in most bacterial membranes are unreactive [54].

Therefore, in the bacterial kingdom, peroxidation occurs only in the polyunsaturated fatty acids present within the thylakoid membranes of photosynthetic bacteria.

The primary effect of membrane damage is the decrease in the membrane fluidity, which alters membrane characteristics and disrupts association of the membrane bound proteins with the membrane. Amplification of lipid peroxidation causes formation of more radicals, and polyunsaturated fatty acids are degraded to a variety of products. Some of these, such as aldehyde, are very reactive and can damage proteins [55]. Aldehydes, unlike the reactive free radicals, are fairly long lived and hence can travel from the site of their production to other targets that are quite away from the initial free-radical event.

1.4 Oxidative stress alleviating machinery

Living organisms have developed a vast array of mechanisms to protect themselves from oxidative stress. These include methods that keep the concentration of ROS at acceptable levels or mechanisms that repair the oxidative damages [19]. These cellular antioxidant defense mechanisms against ROS may be non-enzymatic or enzymatic. Non-enzymatic antioxidants consists of relatively small molecules such as NADPH and NADH pools, carotene, ascorbic acid, tocopherol, and glutathione (GSH) whereas specific enzymes (catalases, peroxiredoxins, superoxide dismutase etc.) form the major component of enzymatic antoxidants [56].

1.4.1 Non-enzymatic antoxidants

These include organic molecules like GSH, Vitamin C, Vitamin E, carotenoids, NADPH and

NADH pools that are constitutively present inside the cell and help to maintain a reducing intracellular environment.

1.4.1.1 Glutathione (GSH)

Glutathione is important antioxidant in all organisms [57, 58, 59, 60, 61, 62]. Glutathione is a tripeptide (L-glutamyl-L-cysteinyl-glycine), having a gamma peptide linkage between the carboxyl group of the glutamate side-chain and the amine group of cysteine. The cysteine residue is attached by normal peptide linkage to the glycine residue [63].

GSH is the major endogenous antioxidant inside the cells and is present at high concentrations (mM**)** in animal and plants [64, 65, 66, 67]. GSH maintained a strong reducing environment inside the. The GSH cysteine thiol can donate a reducing equivalent ($H^+ + e^-$) to ROS other exogeneous antioxidants as vitamin C and E, to keep them in reduced (active) state [68]. GSH also keeps the disulfide bond of proteins in reduced state. Glutathione itself becomes oxidized by donating an electron and readily reacts with another oxidized glutathione to form glutathione disulfide (GSSG). This is possible due to the high glutathione content present within cells. Oxidized glutathione is reduced back to GSH by glutathione reductase (GR), using NADPH as an electron donor. Ratio of reduced glutathione to oxidized glutathione GSSG-to-GSH is the measure of cellular toxicity and an increased value is indicative of oxidative stress. In normal cells/tissues, more than 90% of the total glutathione pool is present as GSH (i.e. in the reduced form) whereas less than 10% exists in the disulfide form (GSSG).

1.4.1.2 Ascorbic acid (Vitamin C)

VitC is naturally occurring organic compound having mild anti-oxidant properties. At

physiological pH, ascorbate ion, the predominant species is stabilized by resonance between the two canonical forms, making ascorbic acid more acidic than otherwise expected if the compound had only isolated hydroxyl group [69]. Due to the resonance-stabilized nature of its own radical ion, semidehydroascorbate, ascorbic acid can transfer a single electron to various acceptors. Ascorbic acid when oxidized forms a radical cation with the loss of one electron and results in the formation of dehydroascorbic acid with the loss of a second electron.

The ascorbate when oxidized is relatively unreactive. However, being a good electron donor, it able initiate free radical reaction in the presence of metal ion. Thus, besides having antioxidant properties, ascorbate is also a potentially toxic pro-oxidative compound. Humans do not have the ability to synthesize ascorbic acid, it is an essential part of nutrition and its deficiency causes scurvy.

1.4.1.3 Vitamin E (VitE)

Vitamin E is a generic term for chain breaking antioxidants and comprises four tocopherol isomers and four tocotrienol isomers. These tocopherols and tocotrienol isomers differ in the number and position of methyl substitutions on the chromanol head [70]. Tocopherols and tocotrienols are closely related chemically, however, they differ in their biological effectiveness [71]. VitE is fat soluble hence, it is incorporated into cell membranes and protect membranes from oxidative damage.

1.4.1.3.1 α-Tocopherol

α-Tocopherol performs its functions as antioxidant in the glutathione peroxidase pathway

[72] and protects the cellular membranes from lipid peroxidation. The α-tocopheroxyl radicals thus generated are recycled back to the active reduced form through reduction by other antioxidants, such as ascorbate, retinol and ubiquinol.

1.4.1.3.2 Tocotrienols

These are the potent antioxidants of the VitE family [73]. Studies have suggested their role in protecting neurons from damage [74]. These are also known to help in reduction of cholesterol [75] by inhibiting the activity of HMG-CoA reductase. Vitamin E is also incorporated into the ultra-high molecular weight polyethylene (UHMWPE) used in hip and knee replacements, to help resist oxidation. VitE is present in a variety of foods including vegetable oils, cereals, meat, poultry, eggs, fruits, vegetables, and wheat germ oil [76].

1.4.1.4 Flavonoids

Flavonoids are phenolic substances occurring ubiquitously in the plant kingdom. Flavonoids have been isolated from wide range of vascular plants known to have strong antioxidant effects [77, 78,]. In humans, flavonoids are degraded into various phenolic compounds, which possess strong anti-oxidative role [79]. Flavonoids naturally occur in fruit, vegetables, and beverages such as tea and wine [79]. The flavonoids have long-term effects on mortality [80] and flavonoid intake inversely correlated with mortality due to coronary heart diseases [81].

In photosynthetic organisms, various substances like carotenoids, tocopherols and plastoquinone quench singlet oxygen.

1.4.1.5 Carotenoids

Carotenoids are class of more than 600 naturally occurring yellow, orange, and red pigments synthesized by plants, algae, and photosynthetic bacteria [82]. Two classes of carotenoids are, carotenes (α-carotene, β-carotene, and lycopene) and xanthophylls (β-cryptoxanthin, lutein, and zeaxanthin). In plants, carotenoids form the major class of compounds that protect against photo-oxidative damage [83] Carotenoids quench the singlet oxygen formed during photosynthesis. α-Carotene, β-carotene, β-cryptoxanthin, lutein, lycopene, and zeaxanthin are the most common dietary carotenoids.

1.4.2 Enzymatic Antioxidants

The main enzymatic machinery that detoxifies the ROS are SOD, catalases and peroxidases [84, 19]. Superoxide dismutases (SOD) catalyzes the dismutation of $\bullet O_2^-$ into O_2 and H_2O_2 [85, 86] while catalases are involved in the decomposition of H_2O_2 to H_2O and O_2. Peroxidases include a large family of enzymes that catalyze reduction of H_2O_2, various organic peroxides or reactive nitrogen species, using different reductants.

1.4.2.1 Superoxide dismutases (SOD)

Superoxide dismutases (EC 1.15.1.1) which catalyzes dismutation of $\bullet O_2^-$, is an important antioxidant that is present in nearly all aerobic organisms [87]. The *Lactobacillus planarum* and related lactobacilli, do not contain SOD, and use a different mechanism to prevent damage from reactive $\bullet O_2^-$ [88, 89]. The dismutation reaction converts the toxic $\bullet O_2^-$ into molecular oxygen and hydrogen peroxide. The general reaction catalyzed by SOD is written as follows.

$$M^{(n+1)+}\text{-SOD} + \bullet O_2^- \rightarrow M^{n+}\text{-SOD} + O_2$$

$$M^{n+}\text{-SOD} + \bullet O_2^- + 2H^+ \rightarrow M^{(n+1)+}\text{-SOD} + H_2O_2.$$

where M = **Cu** (n=1) ; **Mn** (n=2) ; **Fe** (n=2) ; **Ni** (n=2).

The rate constant of spontaneous dismutation of $\bullet O_2^-$ to O_2 and H_2O_2 is quite high (~10^5 $M^{-1}s^{-1}$ at pH 7) and the reaction of $\bullet O_2^-$ with non-radicals is spin forbidden. This implies that, in biological systems the main reaction of $\bullet O_2^-$ is with itself (dismutation) or with another biological radical such as $NO^{\cdot}$ or with a transition-series metal. Superoxide dismutase has the largest K_{cat}/K_M of any known enzyme ~7 * 10^9 $M^{-1}s^{-1}$, with the reaction being diffusion limited.

Three different superoxide dismutases exists and are characterized by the presence of a different metal ion. The Cu-Zn SODs (human and bovine erythrocytes) are blue, The Mn(III)-containing SODs (*E. coli*, rat liver mitochondria) [90, 91], are wine-red whereas the SODs that have Fe(III) [92]. (e.g. *E. coli*) are yellow [92]. Superoxide dismutase is observed in all oxygen-metabolizing cells [93] and have also been found in anaerobic bacteria [94]. SOD enzymes has been isolated from numurous sources such as: *E. coli* [93], *Saccharomyces cerevisiae* [95], *Streptococcus mutans* [96], wheat germ [97], and *Neurospora crassa* [98], signifying that it is a widely characterized enzyme.

1.4.2.2 Catalases

Catalases are ubiquitous enzyme that catalyzes the decomposition of hydrogen peroxide to water and oxygen ($2\ H_2O_2 \rightarrow 2\ H_2O + O_2$). Catalase is a highly reactive enzyme; one catalase can convert approximately 5 million molecules of hydrogen peroxide to water and oxygen each second. The catalases are of two types; one type that contain heme (heme-catalses)

whereas the other type lack heme, but show the presence of Mn in their active site (i.e non-heme or Mn-catalases). The heme-catalases contain four porphyrin heme (iron) groups that allow enzyme to react with hydrogen peroxide. Meanwhile, Mn-catalases are hexameric proteins with four-helix bundle fold, characteristic of the ferritin-like superfamily [99].

Reaction of catalase with peroxide occurs in two stages and is similar to the cytochrome c peroxidase mechanism. The mechanism proposed for heme-catalase is shown below.

$$\text{Fe(III)-E} + H_2O_2 \rightarrow \text{O=Fe(IV)-E(.+)} + H_2O$$

$$\text{O=Fe(IV)-E(.+)} + H_2O_2 \rightarrow \text{Fe(III)-E} + O_2 + H_2O$$

1.4.2.3 Peroxidases

Peroxidases are a large family of enzymes catalysing a reaction of the form: ROOR' + (2e-) + $2H^+ \rightarrow$ ROH + R'OH. The usual substrate for these enzymes can be hydrogen peroxide or in some cases organic hydroperoxides (t-butyl hydroperoxide) or even lipid hydro-peroxide (linoleic acid hydroperoxide). To take part in peroxidase reaction, peroxidases may use a heme cofactor or may use redox active cysteine or selenocysteine in their active site. The nature of the electron donor may vary, for e.g. horshradish peroxidase has an accessible active site and can use variety of organic compounds as electron donors and acceptors. In contrast, the active of cytochrome c peroxidase site is quite closed, thereby only small molecules can donate electrons to it.

Glutathione peroxidase uses glutathione as an electron donor, and are usually selenium-containing enzymes [100]. But, some members of this family are known to contain a catalytically active cysteine. Glutathione peroxidases can detoxify both hydrogen peroxide

and organic hydroperoxide substrates. The glutathione peroxidase catalyzed reaction is:

$$2GSH + H_2O_2 \rightarrow GS–SG + 2H_2O$$

The 2 peroxiredoxins are subject of this thesis, presented below is the detailed information about peroxiredoxins.

1.5 Peroxiredoxins (Prxs)

As this thesis deals with characterization of two peroxiredoxin proteins (Alr3183 and Alr4642); a detailed overview of this important class of proteins is presented below.

Peroxiredoxins (Prx, EC 1.11.1.15) are family of thiol-specific antioxidant proteins (TSA). In literature, these have also been referred to as alkyl hydroperoxide reductase, AhpC (especially in bacteria); thiol peroxidases and thioredoxin peroxidases. These ubiquitous enzymes were first identified in yeast [101, 102] and subsequently in plants [103, 104], animal cells [105], and prokaryotes.

Prxs exert their protective antioxidant role in cells through their peroxidase activity as indicated by the reaction:

$$ROOH + 2H^+ \rightarrow ROH + H_2O$$

In this reaction, hydrogen peroxide, peroxynitrite or a wide range of organic hydroperoxides (ROOH) are reduced and detoxified. A redox-active cysteinyl residue of peroxiredoxins present in the primary catalytic center reacts with the peroxide substrate. The cysteine residue is oxidized to sulfenic acid whereas the peroxide is converted to its corresponding ‘non-toxic’ alcohol or water as in the case of H_2O_2. The sulfenic acid of the peroxidatic cysteine needs to

be regenerated. The electron donors capable of reducing the sulfenic acid back to cysteinyl residue donor includes GSH, thioredoxin, tryparedoxin and the analogous CXXC motif-containing proteins such as glutaredoxins and the bacterial AhpC protein. The specificities for the various e- donor vary considerably between the peroxiredoxin subfamilies.

Prx from yeast in 1988 [101] was found to protect the glutamine synthetase enzyme from oxidative damage caused by Fe(III)/O_2/DTT-mediated oxidase system (i.e. metal catalyzed oxidation). Since the protection was specific for thiol containing mixed-function oxidation systems, the authors proposed that the protector protein [101] functions as a sulfur or an oxygen radical scavenger. Prxs are mainly cytosolic, but few of them may also be found in other cellular compartments (within mitochondria, chloroplasts or peroxisomes). Some of them are also associated with nucleus and membranes. Peroxiredoxins are produced at high levels in cells and they are among the ten most abundant proteins in *E. coli, a*nd compose 0.1-0.8% of the soluble protein in other mammalian cells [106]. Many organisms produce more than one type of Prx. Six Prxs have been identified in mammalian cells, 10 Prx isoforms are observed in Arabidopsis, whereas 3 different Prxs are found in yeast and *E. coli.*

Function of Prx overlaps with catalases and glutathione peroxidases, the two classes of enzymes that have been thoroughly characterized [107]. Abundance of Prx proteins and the presence of a multitude of Prx within cells underscore the importance of Prx in cellular physiology. It is suggested that that AhpC, and not catalase, is responsible for decomposition of endogeneously generated H_2O_2 in *E. coli* [108]. Peroxiredoxins, capable of reducing a broad range of toxic peroxides and peroxinitrites, appear to be fairly indiscriminate with respect to the hydroperoxide substrate.

Initially based on the number of cysteine residues involved directly in catalysis, Prxs proteins

were divided into the 1-Cys and 2-Cys Prxs. Newer structural and mechanistic data, now supports division of 2 -Cys Prxs into the ‘typical’ and ‘atypical’ 2-Cys Prxs.

Detailed sequence analysis indicates that Prxs possess a thioredoxin (Trx)-like fold i.e. belong to the thioredoxin superfamily and are homologues of Trx and glutathione peroxidase (Gpx). Multiple sequence alignment and structural alignment have shown cysteine/selenocysteines of Prx and Gpx to to be structurally similar and both are predicted to work by similar mechanism [109, 110].

The peroxidase reaction mechanism of Prxs is composed of two steps centered around a redox-active cysteine called the peroxidatic cysteine (C_p). In the first step the thiol group of C_p (C_p–SH) attacks the peroxide substrate via nucleophillic attack and gets oxidized to a sulfenic acid intermediate (C_pS-OH). On the basis of available data, all Prx types share the first basic step and hence, the N-terminal cysteine residue (i.e. C_p) is conserved in all Prxs [111]. For the reaction to proceed, a base is required to deprotonate the C_p as well as an acid to protonate the leaving RO^- group. All Prxs have a conserved active site-arginine residue. The guanidine group of the conserved arginine stabilizes thiolate form of the Cp, thereby lowering its pKa [112]. The sequence and structure of the active site is highly conserved among all Prx classes. In the reduced (SH) form, the peroxidatic cysteine is in a narrow, solvent-accessible pocket formed by a loop-helix structural motif. The basic reaction mechanism of Prxs is presented in Fig. 1.5.

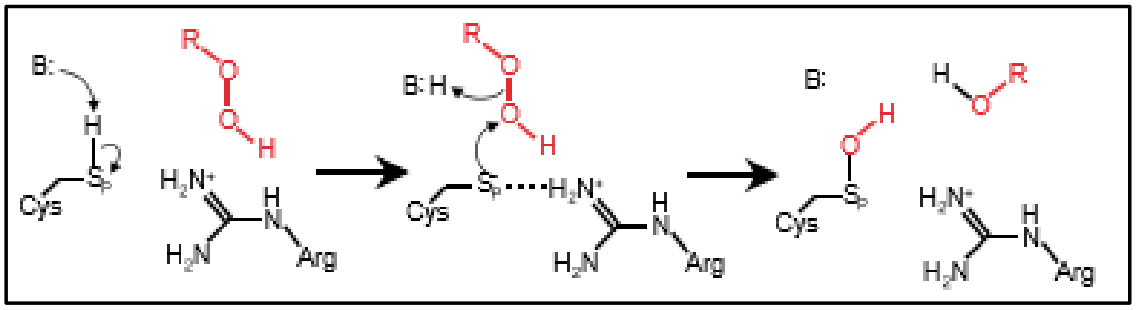

Fig. 1.5. Reaction mechanism of Prxs. The thiolate form of Cp is stabilized by arginine residue and an unknown electron donor, the peroxide reacts with thiolate and converts to corresponding alcohol and Cp is oxidized (112).

The oxidized form of the Prx (cysteine sulfenic acid) is inactive and requires the donation of electron from reduced partner to restore its catalytic activity and to allow its entry into next catalytic cycle. The regeneration of Prx (i.e. conversion of C_pS-OH to C_p-SH) is the second step in the peroxiredoxin mechanism and this step distinguishes the three enzyme classes. In many cases, the presence of another conserved cysteine residue 'the resolving cysteine (C_r)' is required. Depending on the type of Prx, C_r forms an intermolecular or an intramolecular disulfide bond with the C_p. This disulfide bond is ultimately reduced by specific reductants and the active thiol form of the enzyme is regenerated.

The classical 2-Cys Prx are dimeric proteins wherein C_p and C_r are located on different subunits and condense to form an inter-subunit disulfide bond. The atypical 2-Cys Prx are monomers and C_p and C_r are both located on a single polypeptide chain. Reduction of both types of 2-Cys Prxs involves one flavoprotein disulfide reductase and one additional protein (or a domain) containing a CXXC motif (e.g. thioredoxin reductase and thioredoxin, AhpF, tryparedoxin etc. Another category of Prx i.e. 1-Cys Prx also exists. These Prxs have only one catalytic cysteine (Cp) and the mechanism by which the CpS-OH is reduced to Cp-SH after the peroxidatic reaction is quite different from that of 2-Cys Prxs. Reductants of 1-Cys

Prxs include low molecular weight thiols, but physiological partners are unidentified as yet.

Crystal structure studies indicate that all classes of Prxs are similar proteins, having a Trx fold with additional secondary-structure elements present as insertions. The most striking differences is in their oligomeric states. The atypical 2-CysPrxs are monomeric enzymes, whereas both the typical 2-Cys and the 1-Cys Prxs are domain-swapped homodimers in which the C terminus of one subunit reaches across the dimer interface to interact with the other subunit.

1.5.1 Typical 2-Cys Peroxiredoxin

Typical 2-Cys Prx is the largest class of Prxs. This class represents the first Prx to be described and hence termed as the classical Prxs. In this protein, C_p is present generally near residue 50 whereas and C_r is nearer to residue 170 [112]. These are functional homodimers containing two identical active sites. In the second step of the peroxidase reaction, the C_p sulfenic acid (C_pS-OH) from one subunit is attacked by the resolving cysteine (C_r-SH) present at the C terminus of the other subunit and intermolecular disulfide bond (C_pS-SC_r) is formed through condensation reaction. The intersubunit disulfide bond is further reduced by one of the several cell-type specific disulfide reductants (e.g. AhpF, tryparedoxin, thioredoxin or AhpD) regenerating the active enzyme.

The typical 2-Cys Prxs are reported to exist in two different oligomeric forms i.e. dimeric and decameric, with the oligomeric state being linked to its redox state. The dimer is characterized by a compact structure and parallel orientation of the characteristic β-sheet of both subunits [112]. This structural feature allows formation of the intermolecular disulfide bridge during the catalytic cycle. In the typical 2-Cys Prx, the C_r is located in this C-terminal

arm. The amino acid residues Pro-44, Thr-48 and Arg-127 are conserved in all Prxs and are termed as the catalytic triad. The pyrrolidine ring of Pro-44 limits the solvent and peroxide accessibility of the C_p and shields the reactive C_pS-OH intermediate from further oxidation by peroxides. The decameric form of 2-Cys-Prx is doughnut-like in shape while the dimer is characterized by a compact structure.

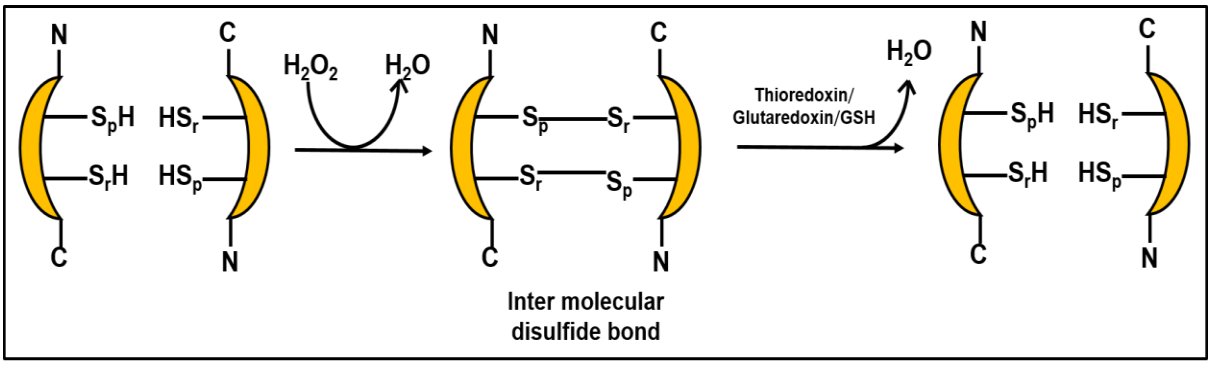

Fig. 1.5.1. Reaction mechanism of typical 2-Cys Prx. H_2O_2 decomposition leads to formation of stable sulfenic acid that subsequently reduced by thiol containing reductants.

In the presence of excess peroxide substrate, the C_pS-OH form gets further oxidized to C_pS-OOH, which is the sulphinic acid form of the catalytic cysteine [113]. Overoxidation, unless reversed, results in inactivation of the enzyme. The over-oxidized form of the active cysteine (i.e. C_pS-OOH) is converted to sulfenic acid sulfiredoxins [114]. Metabolic labelling of mammalian cells with (^{35}S), has shown that the sulfinic form of the PrxI, formed during the exposure of cells to H_2O_2, is rapidly reduced to the catalytically active thiol form [115]**.** In plants, 2-Cys Prx are post-translationally targeted to chloroplasts, and are believed to play important role in protecting the photosynthetic membrane against photo-oxidative damage [116].

1.5.2 Atypical 2-Cys Prx

The second class of Prxs is the atypical 2-Cys Prxs. These proteins essentially follow the same mechanism as that of the typical 2-Cys Prxs, except that these are monomeric [117, 118, 119, 120]. As both C_p and C_r are contained within the same polypeptide, the condensation reaction results in the formation of an intramolecular disulfide bond. Although the C_r of typical and atypical 2-Cys Prxs is not conserved in sequence, they are functionally equivalent. To recycle the disulfide bond, all the known atypical 2-Cys Prxs appear to use thioredoxin as an electron donor [121].

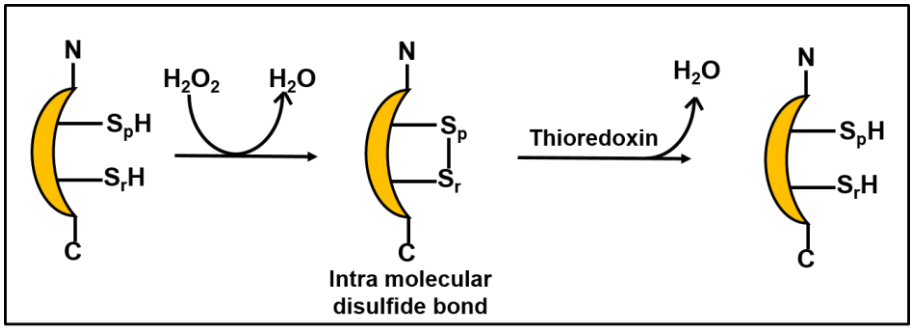

Fig. 1.5.4 Reaction mechanism of atypical 2--Cys Prx. H_2O_2 decomposition leads to formation of stable sulfenic acid that subsequently reduced by thiol containing reductants.

1.5.3 1-Cys Prx

Prxs of this class contain only C_p whereas the C_r is absent [122] (Fig. 1.5.3). Their C_pS-OH formed because of peroxide detoxification is stable in contrast to transient CpS-OH in 2-Cys Prx enzymes. The CpS-OH is presumably reduced by a not yet clear thiol-containing redox partner although proposed electron donors include glutathione, cyclophilin and lipoic acid [123, 124, 125, 126]. It is speculated that one thiol forms a transient mixed disulfide bond with the enzyme, followed by its reduction by a second thiol, thus regenerating the enzyme.

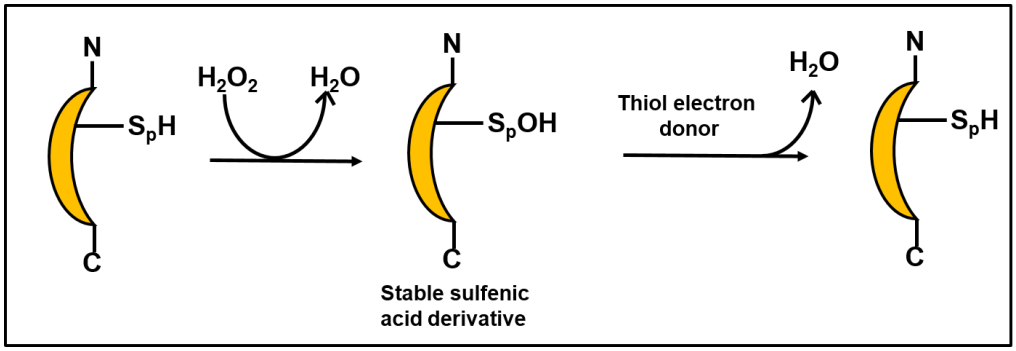

Fig. 1.5.5 Reaction mechanism of 1-Cys Prx. H_2O_2 decomposition leads to formation of stable sulfenic acid that subsequently reduced by thiol containing reductants.

1.5.4 Prx-like Prxs

These types of proteins show sequence similarity to peroxiredoxins. Such proteins have not been characterized from any organism thus far. Generally, the active site region of these Prxs show similarity to active site of other Prxs. These proteins are further divided into Prx-like1 and Prx-like2. In Prx-like1, C_p coincides with the first cysteine in the CXXC motif whereas in the Prx-like2 proteins, the putative C_p is the second cysteine of the CXXC motif.

1.5.5 Function of Prxs

Prxs, a vital part of the antioxidant defense systems in many organisms, are also involved in balancing hydroperoxide production during photosynthesis [124]. Prxs, modulate the level of intracellular level of H_2O_2 and play a key role in cell signaling in eukaryotic cells and are involved in cellular signaling and differentiation, displaying opposite effects [127, 128]**.** Prxs

have been found to be involved in the 24-hour internal circadian clock of organisms [129, 130]. Prxs have been shown to protect proteins and DNA from damage *in vitro* as well as *in vivo* [104]. Peroxiredoxins can be regulated by redox status, oligomerization states, and phosphorylation [112].

1.6 Bacterioferritin co-migratory proteins (BCPs)

BCP/PrxQ proteins are thioredoxin-dependent atypical thiol-peroxidases [117, 131]. The first BCP homolog was identified in *E. coli* as a protein with a molecular mass of 18 kDa, which co-migrated with the bacterioferitin protein on SDS-polyacrylamide gels [132]. Hence, even before its function was known, this protein was named as BCP. As *E. coli* BCP is the prototype and the best studied member of this class of Prx, other atypical 2-Cys Prx are also termed as BCPs.

E. coli BCP is a monomer, which detoxifies both hydrogen peroxide and alkyl hydroperoxides employing TrxA as the electron donor [117]. *E. coli* BCP was found to be monomeric even in the oxidized state, regardless of the presence or the absence of DTT. Non-reducing SDS-PAGE and analytical ultracentrifugation studies of reduced and oxidized BCP showed that the *E. coli* BCP exists as a monomer in solution, eliminating the possibility of intersubunit disulfide bond formation. [120]. *E. coli* BCP contains three cysteine residues (Cys-45, Cys-50, and Cys-99) of which only first cysteine, Cys-45, is absolutely required for activity, and it is thought to be C_p [117]. In contrast, mutation of Cys-99 had no effect on enzymatic activity, whereas mutation of the Cys-50 residue reduced the activity of the enzyme to ~60% of its original activity. Hence, Cys-50 appears to be C_r. As only Cys-45 is essential for activity, BCP also appears to act via 1-Cys pathway, where only the Cys-45 (i.e.

C_p) is utilized during catalytic turnover [117].

Homologoues of BCP are uiquitous in the prokaryotic kigdom, including pathogenic bacteria such as *Mycobacterium Tuberculosis, Hemophilus influenza*e, *Helicobacter pylori*, where these Prxs are described as species-specific marker of pathogenicity. Studies in Helicobacter pylori have linked BCP with bacterial pathogenicity, and BCP was shown to contribute significantly to the ability of the bacteria to colonize the host's stomach [133]. A number of BCP homologs are found in the genomic sequences of lower eukaryotes [134, 135] and plants [102, 118].

Since the name BCP does not provide any insight into its function, homologs of BCP present in plant systems were designated as Peroxiredoxin Q i.e. PrxQ [102]. Poplar, PrxQ is expressed only in leaves and is localized in the chloroplasts and the guard cells of stomata [118]**.** The BCP homolog of Arabidopsis was discovered from the cDNA library as a pre-protein, containing N-terminal signal peptide, which on cleavage formed the mature 17 kDa PrxQ protein. This protein showed a TrxA-dependent activity and could use H_2O_2 as well as organic peroxides as substrates. No GSH-dependent peroxidase activity was observed, and both C_p and C_r were essential for TrxA-dependent peroxidase activity. The PrxQ proteins are known to be monomeric and this status does not change even when the protein in oxidized [118]. MALDI analysis has shown the PrxQ protein from *Sedium lineare* to form an intramolecular disulphide bond [102].

1.7 Cyanobacteria

Cyanobacteria are ancient organisms that originated more than 3 billion years ago [132].

They are also known as Blue Green Algae (BGA) due to the abundance of water soluble blue pigment phycocyanin and green pigment chlorophyll a [133]. Cyanobacteria represent the first simplest oxygenic photosynthetic bacteria [134]. They were the chief primary producers of organic matter and the first organisms to release molecular oxygen by oxygenic photosynthesis into the reductive atmosphere thereby converting the ancient reducing world into an oxidizing one and thus paving the way for evolution of oxygen utilizing organisms [135]. The general features of plasma and thylakoids membranes of cyanobacteria are similar to those of plant chloroplasts in terms of lipid composition and assembly of proteins. [136]. Cyanobacteria possess a higher plant-like photosynthetic apparatus in a prokaryotic cell. Like higher plants, cyanobacteria possesss light harvesting pigments such as chlorophyll a, carotenoids, and phycobillisomes and carryout oxygenic photosynthesis using water as electron donor. Chloroplasts found in plants and eukaryotic algae are believed to have evolved from cyanobacterial ancestors via endosymbiosis [137].

Cyanobacteria are diverse group of microorganisms comprising of 1500 species with various morphologies and species-specific characteristics such as cell movement, cell differentiation, nitrogen-fixation. They exist in increasing order of complexities ranging from unicellular to multicellular cell types. All cyanobacteria have photosynthetic capabilities [138]. Some cyanobacteria have ability to convert the atmospheric nitrogen to ammonia with the help of an oxygen sensitive nitrogenase enzyme complex. These nitrogen-fixing cyanobacteria serve as providers of nitrogen biofertilizer in the cultivation of rice and beans [139] and are economically important as nitrogen biofertilisers in paddy fields [140] of South East Asia. In a related application, the nitrogen-fixing cyanobacteria have been employed to simultaneously reclaim saline/alkaline soils presents in some parts of India and to increase their N status [141, 142].

One major thrust area of today research in biological deals with the stress-tolerance mechanisms of organisms to variety of environmental stresses. Cyanobacteria are found in almost all aquatic and terrestrial habitats: fresh water, oceans, damp soil, bare rock, soil and even antarctic rocks [143]. They also form phototrophic biofilms or occur as planktonic cells**.**

During the course of their evolution, cyanobacteria have been exposed to many unfavourable environmental conditions (extreme heat, cold, pesticides, heavy metals etc). For these reasons cyanobacteria provide a suitable model system, for plants to study the fundamental aspects of adaptive responses to stresses of various kinds. Among the stresses oxidative stress in cyanobacteria, ROS are routinely generated by photosynthetic electron transport, when the intensity of light-driven electron transport exceeds the rate of electron consumption during CO_2 fixation. As cyanobacteria in their natural habitat are often exposed to changing external conditions, their ability to perceive ROS and to rapidly mobilize antioxidant defense systems is important for their survival.

Being photoautotrophs, cyanobacteria have to not only detoxify the reactive oxygen species (ROS) generated by oxygen reduction during respiration chain but also eliminate those ROS generated by the photosynthetic electron transport [144].

1.8 *Anabaena* PCC 7120 and proteins involved in protection from oxidative stress

The filamentous, heterocystous, nitrogen fixing strain of cyanobacteria such as *Anabaena*, serve as naturally abundant source of nitrogen biofertilizers in paddy fields, particularly in India. *Anabaena* PCC 7120 is a filamentous heterocyst-forming, photoautotrophic

cyanobacterium that carries out two physiologically vital processes i.e. photosynthesis and nitrogen fixation [145]. Incidentally, both these processes are sensitive to oxygen.

Anabaenas are known to be resistant to different abiotic stresses like nutrient deficiency, salinity, drought and temperature up shift [146]. A number of abiotic stresses such as heavy metals, drought, salt, extreme temperatures, high light intensity, herbicides and toxins lead to generation of reactive oxygen species (ROS). Recent studies have shown *Anabaena* PCC 7120 to to be highly resistant to gamma radiation (LD_{50}) of 6kGy and desiccation [147] both of which are known to generate high concentrations of ROS.

As techniques for genetic manipulation including an efficient conjugation system is available, *Anabaena* PCC 7120 long been used to study the genetics and physiology of cellular differentiation, pattern formation and nitrogen fixation [148, 149]. The nucleotide sequence of the entire genome of a filamentous cyanobacterium, *Anabaena* sp. strain PCC 7120, has been determined [150], which has further facilitated the study of various genes and proteins.

As *Anabaena* PCC 7120 can tolerate several environmental stresses that are known to generate ROS, it is likely to encode many different proteins to detoxify ROS [151]. In fact, *Anabaena* does encode number of proteins that are known to participate in detoxifying ROS. Among the enzymatic antioxidants, *Anabaena* PCC 7120 possesses 2 SODs and 2 catalases and 10 peroxiredoxins [152, 153, 17, 155, 156, 157].

Superoxide dismutases (SOD) form the first line of defense against ROS. SODs help to remove the superoxide radical by converting it to a more stable hydrogen peroxide via a dismutation reaction. *Anabaena* PCC 7120 has two SODs, namely FeSOD and MnSOD that differ in co-factor requirement. MnSOD is present in the periplasmic lumen as well as cytosol while FeSOD is cytosolic. Both MnSOD and FeSOD activity was reported in the vegetative

cells as well as in the heterocysts [156, 158]. Mn-SOD was found to offer protection against methyl viologen under nitrogen fixing conditions whereas Fe-SOD provided protection under nitrogen-supplemented conditions [157].

The genome of *Anabaena* 7120 shows the presence of two 'Mn-catalases', *alr0998* (KatA) and *alr3090* (KatB). Both the catalases from *Anabaena* have been studied in some detail [152, 159] and over-expression of both the KatA and KatB have been shown to protect the *Anabaena* from oxidative stress [152, 159].

The cell-free extracts of *Anabaena* PCC 7120 show negligible catalase activity under normal conditions [159] indicating that the role of catalases in detoxification of H_2O_2 may be rather limited under normal conditions of growth. The presence of several Prx genes does suggest that these proteins could be the principal players responsible for detoxification of H_2O_2 in *Anabaena* PCC 7120 [160].

Earlier, eight genes/ORFs i.e. *all1541, alr2503, all2375, all2556, alr3183, alr4404 and alr4641, alr4642* had been annotated as *prxs* in *Anabaena* PCC 7120. Recently 2 more *prx-like* ORFs (*all0513* and *alr1206*) were identified by Cui et al, [160]. Based on sequence homology and presence of conserved sequence motifs, Prxs from *Anabaena* PCC 7120 are classified into four groups as described in the introduction section 1.4 [144]. Typical 2-Cys Prx (Alr4641), 1-Cys Prx (Alr4404), BCP/PrxQ proteins (Alr2503, Alr2375, All2556 and Alr3183), and type II Prx (All1541) and Prx-like (Alr4642, All0513 and Alr1206). The Prx proteins that have been characterized from *Anabaena* so far are discussed below.

The typical 2-Cys Prx, Alr4641 is prone to over-oxidation by H_2O_2 and shows the presence of GGVG and YF motifs, which is characteristic of over-oxidation sensitive enzymes. Pascual [161], demostrated that Alr4641 is indeed over oxidized with excess of H_2O_2.

Moreover, the 2-Cys Prx from *Anabaena* is readily and reversibly over-oxidized *in vivo* in response to high light intensity and hydrogen peroxide. The Alr4641 shows both peroxidase (using NTRC as reductant) as well as a chaperone function [162]. Interestingly, unlike 2-Cys Prxs other, the switch from 'peroxidase' to 'chaperone' function is dependents on its redox state and independent of its oligomeric status [162].

The low catalase activity of *Anabaena* PCC 7120 is compensated by the abundant presence of Alr4641 [161]. The Alr4641 protein from *Anabaena* PCC 7120 is induced in response to various abiotic stresses and the *alr4641* promoter is active in vegetative as well as heterocysts [162]. Alr4404, the single 1-Cys-Prx from *Anabaena* PCC 7120, contains VCT (Val-Cys-Thr) motif [17]. Alr4404 is a GSH-dependent peroxidase that is induced under conditions of oxidative stress [163]. This protein is more active against H_2O_2 than other peroxides. Alr4404 is located in heterocyst as well as vegetative cells in *Anabaena*. Over-expression of All4404 has shown to protect *E. coli* as well as *Anabaena* from abiotic stresses [164, 165]. All1541 (encoded by *all1541*) is a glutaredoxin (Grx) domain-containing type II peroxiredoxin (having the conserved TCS motif) from *Anabaena* PCC7120 [162]. Among cyanobacteria, only *Nostoc* and *Anabaena* species contain this type of fused Prx-Grx. All1541 detoxified various peroxides using glutathione (GSH) as reducing agent and the Grx domain was essential for this activity. In *Anabaena* PCC7120, the *all1541* transcript was induced under conditions of oxidative stress, furthermore, recombinant *Anabaena* PCC7120 strains over-expressing All1541 showed superior oxidative stress tolerance to H_2O_2 as compared to the wild-type strain [162].

The 4 BCP/PrxQ homologs (Alr3183, Alr2503, All2375 and All2556) from *Anabaena* contain the GCT motif. These proteins have been shown to be Trx-dependent peroxidases capable of detoxifying hydrogen peroxide and other organic peroxides [166, 144].

1.9 This Study

As described above, the role played by the various proteins in overcoming oxidative stress in the filamentous, heterocystous diazotrophic, cyanobacterium *Anabaena* PCC 7120 has generated lot of interest in the recent past [167, 168, 159]. Our laboratory has been investigating the role played by peroxiredoxins in overcoming oxidative stress in this bacterium [151, 152, 153]. Of the several *prx* genes present in the genome of *Anabaena,* the role of *alr3183* and *alr4642* in overcoming oxidative stress was addressed in this study.

Earlier, gene array studies from our lab had shown *alr3183* to be induced in response to gamma radiation (Dr. Hema Rajaram, unpublished observations), so it was desired to verify its role in radiation/oxidative stress resistance in *Anabaena* PCC 7120. On the other hand, the ORF *alr4642* (encoding a Prx-like peroxiredoxin) or its orthologs had not been characterized from any bacterial species, hence efforts were initiated towards understating the function of this gene in *Anabaena* PCC 7120.

Overall objectives of the thesis:

1) Cloning of *alr3183* and *alr4642* into *E. coli* plasmid vectors for over-expression of Alr3183/Alr4642 proteins, purification of Alr3183/Alr4642 and their biophysical/biochemical characterization.

2) Expression analysis of Alr3183 and Alr4642 in response to different stresses in *Anabaena*.

3) Construction of suitable plasmid vectors to over-express the above-mentioned proteins in *Anabaena* and to study the stress tolerance of the corresponding over-expression strains.

The work carried out is described in the following chapters:

Chapter 2: This chapter describes the materials and experimental methods employed in the study. The different analytical procedures and bioinformatic analyses used in the study are also stated.

Chapter 3: Over-expression, purification and molecular characterization of the Alr3183 protein along with the relevant discussion is described in this chapter.

Chapter 4: Results describing the over-expression, purification and characterization of the Alr4642 protein are detailed and discussed in this chapter.

Chapter 2 - Materials & Methods

2.1 Materials

2.1.1 Chemicals

Luria-Bertani broth components and agar was procured from Becton Dickinson and Company (BD, USA). Chemicals such as CaCl2, protein standard marker (SDS-7), glycine, Tris, IPTG, DTT and antibiotics (kanamycin, ampicillin, chloramphenicol and neomycin), GSH, E. coli ThioredoxinA (TrxA), E. coli Thioredoxin reductase (TR), NADPH, were purchased from Sigma chemicals. Trizol reagent was supplied by Invitrogen and the Peroxoquant kit was purchased from (Thermo Scientific). Nitrocellulose membrane was obtained from GE healthcare limited whereas X-ray film, developers, fixers were supplied by Kodak, India. Other molecular biology grade fine chemicals were purchased locally.

Plasmid isolation kit, gel purification kit, Ni-NTA agarose beads were purchased from Qiagen, Germany. Protein assay kit was obtained from Lowry's (Lowry, USA). Restriction enzymes (BamHI, SalI, SmaI, XhoI, EcoRI), DNA molecular weight markers 100 bp ladder and 1 kb ladder was purchased from New England Biolabs, (NEB, UK). DNTPs, $MgCl_2$, T4-DNA ligase. Q-Sepharose, terminal transferase, digoxigenin (DIG) labeled ddUTP, anti-DIG antibody, nitrocellulose membrane, and NBT-BCIP solutions were obtained from Roche life sciences, UK. Taq DNA polymerase was purchased from BRIT (India).

2.1.2 Bacterial strains, plasmids and primers used in the study

The wild-type *Anabaena* PCC 7120 was used from our lab collection. *Escherichia coli* strain DH5α was used as cloning host and *E. coli* BL21 (plysS) was used for over-production of the

recombinant proteins. All the bacterial strains used in this study are shown in Table 2.1. The pET16b vector (Novagen) was used for over-expression of recombinant proteins in *E. coli*. The pFPN plasmid was used to add a light inducible promoter, P_{psbA1}, upstream of the gene of interest for subsequent cloning into the promoter-less *Anabaena*/*E. coli* shuttle vector, pAM1956 (courtesy Prof. James Golden, A&M University, Texas). The vector pAM1956 was used for over-expression of the proteins in *Anabaena*. All the plasmids used in this study are listed in Table 2.3.

Table 2.1 Bacterial strains used in this study.

Strain	Description	Source
***E. coli* strains**		
DH5α	*F- recA41 endA1 gyrA96 thi-1 hsdR17 (rk- mk-) supE44 relAλ lacU169*	Lab collection
BL21(pLysS)	*Cmr F– ompThSdSB (rB- mB-) gal dcm (DE3) pLysS*	Novagen
HB 101	*F- mcrBmrr hsdS20(rB- mB-) recA13 leuB6 ara-14 proA2 lacY1 galK2 xyl-5 mtl-1 rpsL20(SmR) glnV44 λ-*	Lab collection
HB101R2	Donor strain carrying pRL623 (encoding methylase) and pRL443 (conjugal plasmid)	[169]
***Anabaena* strain**		
Anabaena PCC7120	Wild-type strain	[170]

An3183^{+}	Nm^{r}, *Anabaena* PCC 7120 harbouring pAM3183	This study
An3183C46S^{+}	Nm^{r}, *Anabaena* PCC 7120 harbouring pAM3183C46S	This study
AnAs3183^{+}	Nm^{r}, *Anabaena* PCC 7120 harbouring pAMAs3183	This study
An4642^{+}	Nm^{r}, *Anabaena* PCC 7120 harbouring pAM4642	This study
AnT4642^{+}	Nm^{r}, *Anabaena* PCC 7120 harbouring pAMT4642(6His)	This study
AnT4642(6His)$^{+}$	Nm^{r}, *Anabaena* PCC 7120 harbouring pAMT4642(6His)	This study

Table 2.2 Primers used in this study

Primer	Sequence (5'-3')
Alr3183fwd	CGGGATCCCATATGCCAGTTAAAGTTGGAGACTC
Alr3183rev	CGGGATCCCTATTTACTCGCCAACTGTTGC
3183C46Sfwd	ACACCAGGATCTACAGCAGAATC
3183C46Srev	GATTCTGCTGTAGATCCTGGTGTATC
3183C51Sfwd	AGCAGAATCTTCCGCTTTCCGCG
3183C51Srev	CGCGGAAAGCGGAAGATTCTGCT
3183Promfwd	CGAGCTCGGTCAACAACCACAGCATCGAGAAC
3183Promrev	GGGGTACCCCAACTTTAACTGGCATATAAAATTAATAAAC

Antisense3183fwd	CGCATATGCTATTTACTCGCCAACTGTTGC
Antisense3183rev	CGGGATCCATGCCAGTTAAAGTTGGAGACTC
*alr*3183_mut_fwdup	CCGCTCGAGCTGCTATATACATATCGCCCGC
*alr*3183_mut_rev_up	AACTGCAGCTATACATTTCTTTATATTCTAGGACTATTTG
*alr*3183_mut_fwd_down	AACTGCAGCCCGGGCGGTGATGAAATTTACCACCTGCC
*alr*3183_mut_rev_down	CGGGATCCGAAGCAGGAAGTCAAAACAGCCATTG
*alr4642*fwd	CGGGATCCCATATGAACGCAGATAGACACAG
*alr4642*rev	CGGGATCCTTAATCAAATTTTCCTAACAACTTTTCG
*alrT4642*fwd	GCGCGGCATATGTTAACTTCAACAGATTTCAGTGG
alrT4642rev(6His)	GGATCCTTAATGATGGTGATGGTGATGATCAAATTTT CCTAACAACTTTTCG
4642LexA212site_fwd	CTTTATTTAGAAACCTTCCAAC
4642LexA212site_rev	ACTTCAACAGATTTCAGTGGC
4642LexA3site_rev	GAATTTTCACAGAAAAGCAATATTGC

Table 2.3 Plasmids used in the study

Plasmid	Description	Source/Reference
pET16b	*E. coli* over-expression vector	Novagen
pFPN	*Anabaena* integrative expression vector	[171]
pAM1956	*E. coli* /*Anabaena* shuttle vector	[172]
pET3183	pET16b carrying *alr3183*	This study
pET3183C46S	pET16b carrying *alr3183C46S*	This study
pET3183C51S	pET16b carrying *alr3183C51S*	This study

pET3183CDM	pET16b carrying *alr3183*CDM	This study
pET4642	pET16b carrying *alr4642*	This study
pETT4642	pET16b carrying *alrt4642*	This study
pETTF-T4642	pET16b carrying *alrTF-t4642*	This study
pFPN3183	pFPN carrying *alr3183*	This study
pFPN3183C46S	pFPN carrying *alr3183*C46S	This study
pFPN4642	pFPN carrying *alr*4642	This study
pFPNT4642(6His)	pFPN carrying *alrt4642(6His)*	This study
pFPNT4642	pFPN carrying *alrt4642*	This study
pAM3183	pAM1956 carrying *alr3183*	This study
pAM3183C46S	pAM1956 carrying *alr3183*C46S	This study
pAM3183C51S	pAM1956 carrying *alr3183*C51S	This study
pAM3183CDM	pAM1956 carrying *alr3183*CDM	This study
pAM4642	pAM1956 carrying *alr4642*	This study
pAMT4642	pAM1956 carrying *alr*T4642	This study
pAMT4642(6His)	pAM1956 carrying *alr*T4642(6His)	This study

2.2 Methods

2.2.1 Bioinformatic approaches

2.2.1.1 Primer designing

The primers required for the amplification of different genes were designed based on the nucleotide sequence of the concerned genes available at www.kazusa.or.jp/cyanobase. The GC percentage, T_m values, secondary structure and the possibilities of dimer formation (among primers) were analyzed using DNAMAN software (Lynnon Biosoft, Germany). Two different restriction enzyme site (NdeI and BamHI) that were not present within the gene of interest (verified using NEB cutter v 2.0. URL: http://www.tools.neb.com/NEB cutter2/index.php) were incorporated at the 5' end of the forward (NdeI) or the reverse primer (BamHI). Additional bases were added to the primer sequence to facilitate digestion with the appropriate restriction endonuclease. The list of primers used this study are presented in table 2.2.

2.2.1.2 Amino-acid sequence analysis, multiple sequence alignment and phylogeny analysis

Amino acid sequence was analyzed using BLAST (http://blast.ncbi.nlm.nih.gov/blast) or SMART (http://smart.embl-heidelberg.de/) algorithms [173, 174]. Multiple sequence alignment was performed with the ClustalW software available at www.ch.embnet.org/software/ClustalW.html.

2.2.1.3 Promoter analysis

The *alr4642* promoter was identified by a promoter search program available at www.softberry.com. *Anabaena* LexA-binding sequence (TAGTACTAATGTTCTA) [175] was used to identify similar sites in the *alr4642* promoter region using the lalign software (www.ebi.ac.uk/Tools/psa/lalign)

2.2.2 Medium and growth conditions

Anabaena sp. strain PCC7120 was grown in BG-11 medium [176], pH 7.2 with combined nitrogen (17 mM $NaNO_3$) i.e. BG-11N$^+$ or in the absence of combined nitrogen (BG-11N$^-$). For growth on solid medium, 1.5% agar (Difco) was added to the BG-11N$^+$/BG-11N$^-$ medium. Cultures were grown at 27°C ± 2ºC under continuous illumination (30 μE m^{-2} s^{-1}). Depending upon the requirement, cultures were grown under static conditions or aerated (2 L min^{-1}) or kept shaking (150 rpm). *E. coli* strains DH5α or BL21 (plysS) were grown in Luria Bertani (LB) medium at 37°C at 100-120 rpm with appropriate antibiotics (if required).

Antibiotics were used at 100 μg mL-1 carbenicillin (Cb), 33 μg mL-1 chloramphenicol (Cm) or 50 μg mL-1 kanamycin (Km) for *E. coli* and 25 μg mL^{-1} neomycin (Nm) in agar media or 12.5 μg mL^{-1} in liquid BG-11$^+$ media for selection of *Anabaena* ex-conjugants. All glassware and solutions were sterilized by autoclaving at 120ºC for 20 minutes.

2.2.3 Recombinant DNA techniques - Cloning of gene into *E. coli*

Standard molecular biology techniques were used for cloning of genes into *E. coli* [177]. Briefly the ORFs were amplified using gene specific primers by PCR (see 2.2.1.1 for primer designing). For directional cloning into the desired vector appropriate restriction

endonuclease sites were incorporated in the specific primer used. The amplified gene product was eluted from the gel and digested with appropriate restriction enzymes, ligated to the similarly digested vector, and transformed into chemically competent *E. coli* cells. The transformants were analyzed by colony PCR using gene specific primers. The plasmid was isolated from the PCR-positive colonies and analyzed by restriction-digestion. Finally, the cloned inserts were sequenced to confirm the nucleotide integrity of the gene. Individual steps are detailed below.

2.2.3.1 Isolation of chromosomal DNA

Total DNA was isolated from *Anabaena* PCC 7120 cells using method described by Apte and Haselkorn [178]. All the reagents used are detailed in Table 2.4. Briefly ten ml of *Anabaena* PCC 7120 culture (10 µg/ml chlorophyll equivalent) was centrifuged for 10 min at 5000 rpm. The pellet was dissolved in 10 ml of NaCl (1M) and centrifuged immediately at 5000 rpm for 10 min. The pellet was washed twice with TES (20 ml) and resuspended in 10 ml of $T_{10}E_{25}$. Subsequently, 1ml of freshly prepared lysozyme (2 mg/ml in $T_{10}E_1$) was added to above, and the cell-suspension was incubated with gentle shaking at 37°C for 1h. Freshly prepared, 1.2 ml of sarcosyl/proteinase K mix (130 mg lauryl sarcosine in 0.5 ml of 20 mg/ml proteinase K solution) was added to the cell-suspension and incubation continued for another hour. Equal amount of phenol (equilibrated with 100 mM Tris-HCl, pH 8.0) was added to suspension, gently mixed and centrifuged (5000 X g 5 min) to separate aqueous (DNA) phase from organic (phenol) phase. Aqueous layer was extracted with phenol once more and subsequently with chloroform: isoamyl alcohol (24:1). Chromosomal DNA was spooled after gently mixing the aqueous layer with $1/10^{th}$ volume of sodium acetate (3M), pH 5.2 and 2.5 volumes of chilled absolute ethanol. The spooled DNA was washed with 70% ethanol, air

dried and dissolved in $T_{10}E_1$.

2.2.3.2 Agarose gel electrophoresis

Agarose gels were prepared in TBE 1X (Tris Borate EDTA) buffer. DNA samples were mixed with appropriate volume of bromophenol blue dye containing 10X DNA loading buffer. Electrophoresis was carried out using at 80 V for 30 minutes to 2 h at room temperature. To visualize the DNA gels were stained with ethidium bromide (0.5 µg/ml in 1X TBE) and visualized under ultraviolet transilluminator and photographed on a Gel Doc (Fusion SL, Vilber Lourmat). In order to quantify the DNA and estimate its size, DNA molecular weight markers 100 bp ladder, and 1 kb ladder (NEB) were used.

Table 2.4: List of reagents used for nucleic acid purification and electrophoresis

Reagent	Composition
TES	10 mM Tris, 25 mM EDTA, pH 8.0, 150 mM NaCl
$T_{10}E_{25}$	10 mM Tris-HCl, 25 mM EDTA, pH 8.0
$T_{10}E_1$	10 mM Tris-HCl, 1mM EDTA
TE_{100}	100 mM Tris-HCl, 100 mM EDTA, pH 8.0
10X loading dye	0.4% bromophenol blue, 0.4% Xylene cyanol, 50% Glycerol
1X Tris borate EDTA buffer (TBE)	8.9 mM Trizma base, 8.9 mM Boric acid, 0.2 mM EDTA

2.2.3.4 PCR amplification, gel extraction of DNA and plasmid isolation

PCR amplification was performed using 200 ng of *Anabaena* PCC 7120 genomic DNA.

Primers at 0.1 μM concentrations and dNTPs at 200 μM concentration were used. Primer sequences used are summarized in Table 2.2. The amplification was carried out for 30 cycles and involved repeating steps of denaturation at 95°C, annealing in the range of 52-64°C (depending on individual primer set) and extension at 72°C. The PCR products thus obtained were resolved on 0.8%-1.0% agarose gel and visualized under UV illumination after EtBr staining. The DNA amplicon was excised from the gel using sterile scalpel. The amplified PCR product was eluted from the gel piece with the DNA gel extraction kit (Qiagen) by following the protocol as described by the manufacturer. Plasmid DNA was isolated by the alkaline lysis method with the help of a plasmid DNA isolation kit (Qiagen).

2.2.3.5 Restriction enzyme digestion

Restriction digestion was carried out using kit from New England Biolabs Ltd following manufacturer's protocol. The digested DNA was mixed with with the appropriate amount of loading dye and resolved on 0.8% agarose gel. DNA fragments were visualized under UV trans-illuminator. The DNA marker (100 bp and/or 1kb, NEB) were used to estimate sizes of the products.

2.2.3.6 Ligation of restriction digested DNA fragments to respective vectors

The ligation reaction was carried out using quick DNA ligase (T4 DNA ligase, Roche Biochemicals) as per the manufacturer's protocol. The insert to vector ratio was maintained in molar ratio 3:1- 5:1 for sticky end ligation. Total DNA concentration was kept at 200 ng/20 μl. After incubation period, the ligation mix was directly used for transformation.

2.2.3.7 Transformation of *E. coli* cells and screening of positive transformants

The ligated DNA (100-200 ng) or plasmid (50 ng) was used to transform the competent *E. coli* cells. Competent cells of *E. coli* were prepared using calcium chloride/Rubidium chloride [179]. Transformation of *E. coli* cells was performed using standard protocol [180]. Colony PCR was performed to assess the putative transformants. Using *E. coli* cells as template, PCR reaction was performed with the gene specific primer set for the corresponding ORFs as described earlier. The amplification products obtained were analyzed by agarose gel electrophoresis. Colony PCR that yielded a product of appropriate size indicated successful cloning of the respective gene. Plasmid was isolated from positive clones, and the release of the appropriately-sized DNA insert was verified by restriction digestion and sequencing.

2.2.3.8 DNA sequencing

Clones were sequenced on both strands using the automated DNA sequencer by Sanger's dideoxy method at commercial facility (Bangalore Genei, Bangalore). The sequence identity of cloned fragments with *Anabaena* sp. strain PCC 7120 genome sequence was evaluated using the BlastN program at cyanobase.

2.2.4 Site-directed mutagenesis

Site-directed mutagenesis using overlapping PCR with mutagenic primers was performed to replace the cysteine codon (AGA) of *alr3183* with serine (GGA). The recombinant pET*alr3183* was subjected to two step PCR-directed mutagenesis using mutagenic oligonucleotide primers (listed in Table 2.2) containing mismatch base (i.e. GGA instead of AGA) at the desired location. The mutagenic PCR involved the generation of two PCR products that overlapped in sequence containing the same mutation introduced by the mutagenic PCR primers. A subsequent re-amplification of these fragments with *alr3183*

cloning primers (see Table 2.2) resulted in the enrichment of the full-length *alr3183* having desired mutations. The mutation thus introduced was confirmed by sequencing.

2.2.5 RNA isolation and Northern blotting

2.2.5.1 Isolation of RNA from *Anabaena* PCC 7120

Fifty ml *Anabaena* PCC 7120 (4-6 μg chlorophyll *a*/ml) were harvested by centrifugation (5000 x g) and immediately shock frozen in liquid nitrogen. One ml of RNA isolation reagent Trizol (Invitrogen) was added to the cells along with 0.5 ml of autoclaved glass beads (~ 500 μm, Sigma). The cell suspension was vortexed (hard, 3 min x 3), and RNA isolated as per the recommended protocol. The RNA pellet was resuspended in DNAseI reaction buffer (0.1M sodium acetate pH 5.0, 5 mM $MgSO_4$) and subjected to DNAseI treatment (RNAse free, 5U, Roche) treatment. At the end of 45 min, LiCl (2M final concentration) was added to the tubes and the tubes kept at -20˚C for at least 1 hour. The RNA was collected by centrifugation (15000 x g, 20) min) at 4˚C. The RNA pellet was washed with 75% ethanol, air dried and dissolved in RNAase free water.

Following relationship was used to determine the concentration of RNA

$$A_{260} = \quad 1 \quad = 40 \text{ μg/ml RNA.}$$

2.2.5.2 Electrophoretic separation of RNA

RNA samples were electrophoretically resolved in formaldehyde MOPS buffer on a 1.2% agarose gel. The gel was pre-run for 15 min at 100 V before loading RNA samples. RNA samples were prepared in RNA loading dye (1X) and incubated at 65˚C for 10 min before loading. Electrophoresis was carried out in MOPS buffer (1X) for 4h at 5 V/cm. After

electrophoresis, gel was stained with ethidium bromide for 30 min and then destained with water. RNA ladder (NEB) was used to calculate the size of RNA fragments.

Table 2.5: Reagents used in RNA electrophoresis.

MOPS (10X)	200 mM MOPS, 50 mM sodium acetate, 10 mM EDTA, pH 7.0
RNA loading dye (2X, 10 ml)	2X MOPS (2ml of 10X MOPS), 64% Formamide, (6.4 ml), 8% sucrose (0.4 ml of 50% sucrose solution), 4.4% formaldehyde (1.2 ml of 37% formaldehyde), 0.2% xylene cyanol 0.2% bromophenol blue,
RNAse free water	1 ml of DEPC (Diethylpyrocarbonate, Sigma) was added to 1 litre of double distilled water, mixed thoroughly, allowed to stand for 18h at 37˚C and autoclaved

2.2.5.3 DIG labeling of probes

The DNA fragment to be used as a probe for hybridization was denatured by boiling for 10 min and followed by immediate chilling on ice. To this, hexanucleotide random primer and digoxigenin (DIG) labeling mix were added, as per the recommended by manufacturer protocol (Roche biochemicals), and this mix was incubated at 37˚C for 20 hrs. The labeled DNA was purified using Sephadex G-50 columns to remove the unincorporated nucleotides.

2.2.5.4 Northern blotting and hybridization

The electrophoretically separated RNA molecules containg agarose gel, was blotted by capillary blotting in SSC (10X) overnight onto positively charged nylon membrane. The transferred RNA was UV–cross linked to the nylon membrane. Pre-hybridization was performed at 50˚C for 1 h in DIG Easy Hyb buffer (Roche). The DIG labeled DNA probe was hybridized to the RNA on membrane overnight in DIG Easy Hyb buffer at 50 ˚C. After

hybridization, the membranes were washed twice with solution A (2X SSC, 0.1% SDS) for 15 min at room temperature and twice with solution B (0.1X SSC, 0.1% SDS at 66˚C) for 15 min at 66˚C. The chemiluminescent detection was carried out using DIG systems user's guide for filter hybridizations (Roche) as per the instructions provided.

2.2.6 Protein extraction, resolution and detection of cellular proteins

2.2.6.1 Extraction of total or soluble proteins from *Anabaena* PCC 7120

For the preparation of the whole cell extracts, cells were harvested by centrifugation at 5000 rpm for 5 mintues, washed twice with Tris (20 mM pH 8.0) and re-suspended in appropriate volume of 20 mM Tris. Glass beads (100 mm) were added equivalent to the volume of initial pellet, mixed by vigorous vortexing (5 times) with intermittent incubation on ice. This cell suspension was mixed with equal volume of the SDS sample buffer and boiled for 5 minutes at 95°C for 5 minutes. The supernatant obtained after 5 min of centrifugation (12000 x g) was used as total cell-extract. Total soluble proteins were isolated from *Anabaena* using following protocol (at 4°C). Briefly, the cells were harvested by centrifugation at 6000 rpm for 5 minutes and the cell pellet was re-suspended in buffer (Tris 20 mM, pH 8.0). Subsequently, cell suspension was frozen in liquid nitrogen and thawed on ice. This process was repeated 3 times. For more effective lysis, glass beads (equal in volume to the initial cell pellet) were added and cells were subjected to vigorous vortexing (3 cycles of 3 m. each) with incubation on ice (5 minutes each) after each vortex step. Finally, the cell suspension was centrifuged at 10000 rpm for 20 min and supernatant thus obtained was used as soluble protein.

2.2.6.2 Estimation of protein content

The protein estimation was carried out as described earlier [181] with slight modifications. Briefly the purified protein sample or cellular extract was added to 500 µl of deionized water. The protein was subsequently precipitated by adding 50 µl of 1.5 mg/ml of Deoxycholate (DOC, SIGMA, India) and 50µl of 92% Trichloroacetic acid solution (TCA, SRL, India), followed by centrifugation at 12000 x g for 15 minutes. The precipitated protein was subsequently resuspended in 500 µl of Lowry's reagent (SIGMA Aldrich, India) and another 500 µl of deionized water was added to the tube. After incubation for 30 min, 250 µl of Folin C solution (18 ml 2N Folin C and 90 ml of water) was added and the reaction mix was incubated for 30 minutes. The samples were analyzed spectrophotometrically at 750 nm. The linear standard graph of protein concentration was made by using defined concentrations of BSA.

2.2.6.3 Electrophoretic separation and visualization of protein (SDS-PAGE)

SDS-PAGE analysis is an important technique for resolving proteins under denaturing conditions 30% acrylamide solution (containing 0.8% bis-acrylamide), 1.5 M Tris-HCl pH 8.8, and 10% SDS were used to prepare (12-14%) resolving gels. APS (0.1% final concentration) and TEMED (10 µl per 20 ml of gel mix) were used as free radical generator and catalyst respectively. The gel solution was poured between two glass plates (10 x 8cm) having 1 mm thickness and allowed to polymerize for at least 1h. The top portion of the gel was buffered with water saturated butanol or isopropanol to avoid contact with air. After polymerization, the top layer of water saturated butanol/isopropanol was drained off. The stacking gel solution (4% acrylamide/bisacrylamide, 125 mM Tris-HCl, pH 6.5, and 0.1% SDS) was poured on top of the resolving gel by appropriately diluting stock solutions of 30% acrylamide, 0.5 M Tris-HCl pH 6.8, 10% SDS and was allowed to polymerize for at least 0.5

h. Appropriate wells were generated while pouring the stacking gel solution by using standard sized combs. After removing the comb, the space between the gel plates and combs was flushed with distilled water and then comb was removed slowly to avoid any damage to wells. The wells thus formed were rinsed twice with distilled water to any loose gel pieces. The gel with properly formed wells were subsequently used for resolving proteins under denaturing conditions. After estimation of protein using Lowry's (SIGMA, USA), equal amount of protein (20 µg to 60 µg) was mixed with 5X loading dye (0.06 M Tris-Cl pH 6.8, 2% SDS, 40% glycerol, 0.025% bromophenol blue) and denatured by heating at 100°C for 5 m. The sample proteins were then loaded into SDS-polyacrylamide gels desired percentage of acrylamide gel and resolved in 1X Tris glycine buffer (25 mM Tris, 250 mM glycine, 0.1% SDS) at 30 mA current with voltage 150 V till the dye front reached gel. After completion of electrophoresis, the protein bands were visualized by staining with Coomassie blue staining solution (0.5% Coomassie blue, 50% methanol, 10% acetic acid) followed by de-staining (10% methanol, 10% acetic acid) or processed for immunoblotting as described below.

1.2.6.4 Western blotting and immunodetection

The polyacrylamide gel after electrophoresis was equilibrated in transfer buffer for 1h (See table 2.5). The proteins were tranferrred to nitrocellulose membeane using electroblotting at 300-350 mA for 1 h. After transfer blot was stained with nonspecific protein staning reagent Poncaeu-S to verify the transfer of protein. Subsequently, blot was immersed in Tris-saline buffer (TSB) containg 1% blocking reagent for 1h. Desired primary antibody, at appropriate dilution (1:5000) in 1X blocking buffer was added and the blot was incubated overnight at 4°C. The blot was washed twice with TBS buffer for 20 min each, followed by incubation with secondary antibody in TBS buffer for 1h. The blot was washed again (twice) with TBS

buffer for 15 min each. The blot was briefly rinsed with reaction buffer and color reaction carried out using NBT/BCIP (Nitro blue tetrazolium chloride/5-bromo-4-chloro-3-indolyl phosphate, toluidine salt) stock solution in dark. The reaction was stopped by rinsing the blot in water.

Table 2.6: Reagent for protein electrophoresis and western blotting

Reagent	Composition
2X Cracking Buffer	0.5 M Tris-HCl,, pH 6.8, 5% (w/v) 2-mercaptoethanol, 2% (w/v) SDS, 20% Glycerol, 0.1% BPB,, 0.076 EGTA, 0.2% Sodium azide, 0.02% PMSF
Running Buffer	0.3% Trizma base, 1.44% Glycine, 0.1% SDS
Destaining Solution	I: 10% Glacial acetic acid, 50% Methanol II: 10% Glacial acetic acid, 10% Methanol, 2% Glycerol
Coomassie Brilliant Blue G250	0.2% Coomassie Brilliant Blue G250, 20% Glacial acetic acid, 40% Methanol
Transfer Buffer	0.125 M Trizma Base, 0.192 M Glycine, 20 % methanol
Tris Saline Buffer	0.05 M Trizma Base, 0.9% NaCl
Maleic Acid Buffer	0.1 M Maleic acid, 0.15 M NaCl
Reaction Buffer	0.1 M Trizma Base, 0.1 M NaCl

2.2.6.5 Extraction of spot, trypsin digestion and peptide mass fingerprinting and peptide mass-finger printing, MASCOT identification

For MALDI identification of two bands that appeared on SDS-PAGE, the purified Alr3183

was resolved on SDS-PAGE (12% gel), stained with Coomassie R-250. After destaining, the two bands corresponding to the Alr3183 protein were excised out of the gel using a sterile scalpel. The gel pieces were digested *in gel* with trypsin overnight. The trypsin-digested protein used for generation of peptide mass finger print in a MALDI- mass spectrometer (Bruker-Daltonics). The peptide peaks obtained were searched for masses of peptides using MASCOT server.

2.2.7 Protein over-expression and purification

2.2.7.1 Over-expression, solubility and purification of the Alr3183 protein from *E. coli*

Single colony of *E. coli* BL21(pLys) carrying the appropriate plasmid was picked from a petri plate, transferred into 5 ml Luria Broth (LB) and grown for 16-18 h at 37°C. Two ml of this culture was seeded into main culture of 200 ml of fresh LB broth (i.e. 2% inoculum) and incubated at 37°C for another 4h, or till the absorbance of the culture at 600 nm (A_{600}) reached ~ 0.6. At this stage, a aliquot of cells was kept as un-induced control. The inducer, isopropyl β-D-1-thiogalactopyranoside (IPTG, 1 mM) was added to the culture and incubation continued for another 4h. Cells were harvested by centrifugation at 5000 rpm for 10 minutes and the cell pellet was stored at -80°C. A small aliquot of these cells was kept for SDS-PAGE analysis to determine the extent of protein induction.

To verify if the protein was present in the soluble or the insoluble fraction, the cell pellet (stored at -80^{o}C) was suspended in 25 ml ice-cold lysis buffer (50 mM Tris-Cl pH 8, 200 mM NaCl, 1 mM PMSF, 2 mM β-mercaptoethanol) and lysed by sonication on ice (10 sec bursts

at 200-300 W with a 10 sec cooling pulse between each period). The cell lysate was centrifuged at 5000 x g for 5 minutes to remove the unlysed cells and the supernatant thus obtained was further centrifuged at 12,000 x g for 20 minutes. The supernatant contained the soluble proteins whereas the pellet contained the insoluble or the inclusion body fraction. Both the soluble and the insoluble fractions were resolved on SDS-PAGE to determine the solubility of the recombinant protein.

The soluble recombinant protein was purified from supernatant fraction by affinity chromatography. The supernatant was allowed to interact with the Ni-NTA matrix (300 µl slurry, Qiagen, Germany) for 18 h at 4°C. To remove the non-specifically bound proteins, the matrix was washed with ~20 ml of the native lysis buffer solution followed by washing with wash buffers containing increasing concentration of imidazole (Sigma Chemicals, St, Louis, MO). The slurry was washed five times with 5 mL buffer B (50 mM Tris, 200 mM NaCl, 5 mM imidazole; pH 8.0) and three times with 5 mL buffer C (50 mM Tris, 200 mM NaCl, 20 mM imidazole; pH 8.0). Final elution was performed in buffer D (50 mM Tris, 200 mM NaCl, pH 8.0 containing 250 or 500 mM imidazole). The eluted protein was dialyzed against 20 mM Tris–HCl (pH 8.0) with 4 buffer changes (150 ml each) for a total time of 18 h. For gel-exclusion analysis, the purified protein was dialyzed against buffer containing 20 mM Tris–HCl 150 mM NaCl, pH 8.0 The affinity purified proteins were separated on a 12% or 15% SDS-PAGE to verify their purity.

2.2.7.2 Over-expression, solubility and purification of the Alr4642 protein

2.2.7.2.1 Purification trials of Alr4642 protein from *E. coli* in denaturing conditions

To purify Alr4642 in denaturing conditions, 50 ml of overnight IPTG-induced *E. coli* BL21/pET4642 culture was harvested, the cell pellet was dissolved in 6M Guanidium hydrochloride (Gn.HCl) and allowed to bind to the Ni-NTA resin. After appropriate washing, flow through, wash and elution fractions were analyzed on SDS-polyacrylamide gels.

2.2.7.2.2 Over-expression, solubility and purification of Alr4642 protein from *Anabaena* PCC7120

For purification of AlrT4642(6His), AnT4642 $(6His)^{+}$ cells were grown with aeration (2 L min^{-1}) in the presence of light for 8–10 days until chlorophyll *a* density of 8–10 μg mL^{-1} was reached. Cells were harvested by centrifugation, washed thoroughly with lysis buffer and stored at -80˚C. Solubility of over-expressed Alr4642 was verified as described (2.2.7.1). Purification of AlrT4642 using Ni-NTA affinity chromatography was performed as described for Alr3183 with little modifications. The frozen *Anabaena* cell pellet was thawed on ice and resuspended in 25 ml ice-cold lysis buffer (50 mM Tris-Cl pH 8, 200 mM NaCl, 1 mM PMSF, 2 mM β-mercaptoethanol) and lysed by sonication on ice. The cell lysate was centrifuged at 12,000 × g for 30 min to remove the debris, and the supernatant was allowed to interact with the Ni-NTA matrix (300 μl slurry, Qiagen, Germany) for 18 h at 4 °C. To remove the non-specifically bound proteins the matrix was washed with almost 50 ml of native lysis buffer solution. Subsequently, the matrix was washed five times with 5 mL buffer B (50 mM Tris, 200 mM NaCl, 5 mM imidazole; pH 8.0) and three times with 5 mL buffer C (50 mM Tris, 200 mM NaCl, 20 mM imidazole; pH 8.0). Final elution was performed in buffer D (50 mM Tris, 200 mM NaCl, 250 mM imidazole; pH 8.0). The eluted protein was dialyzed against 20 mM Tris–HCl (pH 8.0) with 4 buffer changes (150 ml each) for a total time of 18 h.

2.2.8 Antibody generation against Alr3183 and Alr4642

Purified Alr3183 or Alr4642 proteins were individually loaded in all the wells of a 14% or a 12% denaturing polyacrylamide gel. After electrophoresis, single lane was cut out of the rest of the gel and stained briefly with Coomassie brilliant blue (CBB-R 250) to locate the position of the protein. Once the protein band was visualized, this lane was kept next to the rest of the unstained gel. The stained protein band served as a marker that located the position of the protein on the unstained gel. The desired portion of the gel (expected to contain the purified protein) was excised with a sterile scalpel. The excised gel was sliced into small pieces and incubated in a buffer (Tris-NaCl, 20 mM; NaCl, 50 mM; pH 8.0,) over-night at 25^{o}C with mild agitation. The elution of protein was confirmed by resolving a small aliquot on SDS-polyacrylamide gels. The quantity of protein was estimated by the modified Lowry's method. The proteins were lyophilized and 1-2 mg of each protein (Alr3183 and Alr4642) was given to a commercial facility (Banglore Genei, India) for production of specific antiserum. The anti-Alr3183 was raised in rabbit whereas the anti-Alr4642 was raised in mouse. The polyclonal antiserum thus obtained was tested for its ability to cross-react with the purified protein (i.e. the protein used for generation of antiserum) on Western blots.

2.2.9 Biophysical methods

2.2.9.1 Determination of oligomeric status of purified proteins by gel-exclusion chromatography

Oligomeric status of Alr3183 and its cysteine mutants was determined by gel permeation chromatography employing the Superdex-200 gel-exclusion column with a bed volume of 24 ml (GE Healthcare, UK). Bovine serum albumin (66 kD), carbonic anhydrase (29 kD), and

cytochrome C (12.4 kD) were used as protein standards. Approximately 250 µl (1 µg/µl) of each protein was individually passed through the column at a flow rate of 0.6 ml per min. All the fractions were collected and resolved on 14% SDS-PAGE.

2.2.9.2 Hydrodynamic size of Alr3183, Alr3183C46S and Alr3183C51S using dynamic light scattering

Hydrodynamic size of Alr3183/Alr3183C46S/Alr3183C51S was determined using dynamic light scattering (Malvern zetasizer, nanoseries) at 0.4 µg/µl concentration of protein in buffer (20 mM Tris, pH 8). 1 ml cuvette was used for this purpose.

2.2.9.3 Circular Dichroism (CD) spectral analysis

For CD-spectral analysis, the purified proteins were dialyzed against a buffer containing 20 mM Tris-Cl (pH 8), and CD spectra in the far-UV (190-250 nm) and near-UV (230-350 nm) region were recorded on a Jasco J-720 spectropolarimeter using cylindrical quartz cuvettes of path length 1 and 10 mm respectively. Each spectrum is the average of five successive scans performed at a scan speed of 20 nm/minute. Appropriate baseline subtraction and noise reduction analysis were performed.

2.2.9.4 Surface plasmon resonance (SPR) analysis to verify interaction between Alr3183 and *E. coli* TrxA

SPR analysis with a bare gold sensor chip was performed using the Autolab Esprit SPR system. At 20°C, about 200 response units of TrxA was loaded onto the bare gold chip employing the EDC-NHS chemistry (Autolab ESPIRIT User manual SPR) followed by

extensive washing with buffer H (20 mM Tris, 100 mM NaCl, pH 7.5). The Alr3183/Alr3183C46S/Alr3183C51S/Alr3183CDM proteins were injected separately onto the TrxA-bound sensor chip at 33.3 μL min^{-1} flow rate in independent experiments. The Alr3183 proteins were allowed to interact with the immobilized TrxA for 300 s before washing off with buffer H containing 0.1% SDS. The Alr3183 protein was reduced with DTT (20 mM) in the above-mentioned buffer for 1 h and the excess DTT was subsequently removed by dialysis. The DTT-reduced protein was also allowed to interact with the immobilized TrxA. The data were processed using Autolab kinetic evaluation software (V5.4) provided with the instrument.

2.2.9.5 Electrophoretic mobility shift assays (EMSAs)

To confirm the ability of the purified LexA to bind to the putative LexA-binding sequence electrophoretic mobility shift assays (EMSAs) were performed. Two complementary oligonucleotides (39 nt each) that encompassed the putative LexA-binding site were annealed to form the double stranded i.e. dsLexA-binding DNA. The purified *Anabaena* LexA protein (kindly provided by Mr. Arvind Kumar and Dr. Hema Rajaram) in increasing amounts was allowed to bind to the above-mentioned 38 bp dsDNA in DNA binding buffer (Roche). After the assay, the contents of each reaction were resolved on agarose gel and visualized by staining with ethidium bromide.

2.2.10 Biochemical Assays

2.2.10.1 Modification of the proteins with AMS (4-acetamido-4′-maleimidylstilbene-2,2′-disulfonate).

The alkylating agent AMS, which covalently binds to the reduced form of the protein (containing a free thiol group), was used to verify whether Alr3183 formed an intramolecular disulfide bond or not. Purified proteins were incubated in a reaction mixture containing 100 mM DTT or 2 mM H_2O_2 at 20°C for 20 min. After the incubation period, proteins were precipitated with 10% TCA and dissolved in 20 µl of a freshly prepared solution containing 1% SDS, 50 mM Tris/HCl (pH 7.5) and 15 mM AMS. Proteins were initially incubated with agitation at 20°C for 30 min after which they were transferred to 37°C for 10 min. Finally, proteins were resolved by SDS/PAGE (14% gel) under non-reducing conditions and visualized by staining with CBB.

2.2.10.2 MCO (metal-catalysed oxidation) assay for antioxidant activity

The pBSK (plasmid pBluescript) was subjected to MCO in the presence of Fe^{3+} and DTT wherein the highly reactive hydroxyl radicals ($^{\cdot}OH$, formed by the Fenton reaction) degrade the DNA. Purified proteins (0.2–2 µg) were incubated with 5 mM DTT and 3 µM $FeCl_3$ for 30 min at room temperature (25°C). pBSK DNA (1 µg) was added to each of the reaction mixtures and the samples were further incubated for 4 h. Subsequently, the DNA integrity was assessed by electrophoresis of reaction samples on agarose gels.

2.2.10.3 Peroxidase activity

For the DTT-dependent peroxidase assay, a reaction mixture (1 ml) containing 50 mM HEPES/NaOH buffer (pH 7.0) and the desired concentrations of Prx proteins were pre-incubated with DTT (3 mM) for 10 min at 37°C, followed by the addition of H_2O_2 (200-250 μM). The residual H_2O_2 remaining in tubes was measured with the peroxoquant kit (Thermo Scientific). The amount of residual H_2O_2 remaining in the reaction was estimated from a

standard calibration curve prepared using known concentrations of H_2O_2. For GSH-dependent peroxidase activity, the typical reaction mixture contained 50 mM HEPES/NaOH (pH 7.0), NADPH (0.25 mM), glutathione reductase (GR, 0.2 μM), 1 μg of purified Alr3183 protein and GSH (5 mM). The reaction was started by the addition of 200 μM H_2O_2 and the decrease in the absorbance of NADPH (at 340 nm) was monitored. The TrxA-dependent peroxidase activity of various Alr3183 constructs was measured by monitoring the decrease in absorbance of NADPH at 340 nm using TrxA (1-5 μM) and H_2O_2 (200 μM) as the substrate. For calculation of kinetic parameters, the reaction was started by the direct addition of H_2O_2 (ranging from 5 to 250 μM) and the activity was monitored for 5 min. A molar absorption coefficient of 6220 $cm^{-1}M^{-1}$ for NADPH was used to calculate the enzyme activity [166]. For verifying its resistance to H_2O_2, the purified Alr3183 protein was incubated with 5 mM H_2O_2 for 4 h, dialyzed to remove H_2O_2 and analyzed for the TrxA-dependent peroxidase activity. Purified Alr3183 was incubated at different temperatures (30, 40, 45, 50, 60, 70˚C) for 10 minutes and the TrxA-dependent activity was measured as described above.

2.2.11 *In vivo* role of Prxs in *Anabaena* PCC 7120

2.2.11.1 Treatment with various stresses

Three-day-old cultures of the wild-type *Anabaena* PCC 7120 (WT) as well as various recombinant strains were inoculated in a fresh growth medium at a chlorophyll *a* density of 3 μg mL^{-1} and subjected to stresses such as hydrogen peroxide (H_2O_2), tertiary-butyl hydroperoxide (tBx), Cumene-hydroperoxide (CuX) in tubes (without shaking) under illumination for 2 days. For radiation and desiccation stresses, cells were centrifuged and re-suspended at a chlorophyll *a* density of 10 μg mL^{-1}.

2.2.11.2 Overexpression of proteins in *Anabaena* PCC7120

In order to evaluate the *in vivo* role of Alr3183/Alr4642, it was desired to over-express these proteins in *Anabaena*. Briefly, appropriate plasmid constructs were made to over-express specific proteins in the wild-type *Anabaena*. These were subsequently transferred to *Anabaena* by tri-parental conjugation. The *alr3183* knock down construct was made by overexpressing antisense *alr3183* RNA in *Anabaena* PCC7120.

2.2.11.2.1 Construction of pAM1956 vectors for transfer to *Anabaena*

The DNA fragment corresponding to the ORF were excised out of the appropriate pET16b construct by employing the restriction enzymes and the fragment was inserted downstream of the strong light inducible *psbA1* promoter (P_{psbA1}) in the pFPN vector [171], employing the above-mentioned restriction enzymes (NdeI and BamHI). Subsequently, the desired ORF along with the P_{psbA1} promoter was transferred as a XmaI-SalI fragment from pFPN plasmid to similarly digested *E. coli*/*Anabaena* shuttle vector pAM1956 [172] to obtain the plasmid to be conjugated into *Anabaena* PCC 7120. The presence of the appropriate gene in this construct was verified using restriction digestion and nucleotide sequencing. The pAM1956 vector also contains a gene encoding green fluorescent protein (GFP) which can be monitored by fluorescence microscopy and thus GFP expression can be used as a marker to identify cells that contain the plasmid of interest. The GFP fluorescence can be visualized under fluorescence microscope (λ_{Ex} = 488 nm; λ_{Em} = 507 nm).

Using a conjugal *E. coli* donor strain [HB101(pRL623+pRL443)], the pAM1956 constructs having protein of interest were conjugated into *Anabaena* PCC7120 individually as described earlier [148]. Ex-conjugants were selected on BG-11/N^+ agar plates supplemented with

neomycin (25 µg/ml) on HATF membranes. Individual isolated colonies that appearing on the HATF membrane were inoculated in $BG11N^+$ liquid with the antibiotic neomycin (12.5 µg/ml) and repeatedly sub-cultured in the same medium. The transformed *Anabaena* strain thus obtained was maintained on $BG\text{-}11/N^+$ plates containing neomycin. For detection of desired protein, total protein extracts or cytosolic extract of or the wild-type or recombinant *Anabaena* PCC 7120 was made and probed with the specific antiserum on Western blots.

2.2.11.3 Measurement of growth

The photoautotrophic growth of wild type *Anabaena* PCC7120 and its various recombinant strains were monitored by determining the content of chlorophyll *a* per ml of culture as described by Mackinney [182]. Growth of *E. coli* strains was measured by estimating absorbance at 600 nm of appropriate dilutions.

2.2.11.4 Fluorescence microscopy

The fluorescence microscopy of the wild-type *Anabaena* 7120 was performed under green light excitation (excitation 511 ±8 nm). This wavelength is specifically absorbed by the blue pigment phycocyanin which transfers the energy to chlorophyll *a*. The chlorophyll *a* shows a typical red autofluorescence (emission ~710). The red auto fluorescing image of filament was recorded by a Carl Zeiss Axioscop 40 microscope with 40X and 100X objectives. The green fluorescent protein (GFP) expressing images of *Anabaena* 7120 were obtained under blue light excitation (excitation 480 ± 8 nm) and the fluorescence (emission 511 ±8 nm) was captured with a charge-coupled device (CCD) Axiocam MRc (Zeiss) camera attached to the microscope.

2.2.11.5 Estimation of total ROS content using DCHFDA method

Total ROS content of the whole cells were estimated using 2′,7′-Dichlorofluorescin diacetate (DCHFDA, SIGMA Aldrich, USA), a cell-permeable, non-fluorescent probe. DCHFDA is de-esterified intracellularly and turns to highly fluorescent 2′,7′-dichlorofluorescein upon oxidation. This allows sensitive and rapid quantitation of oxygen-reactive species in response to any conditions that perturbs the ROS status of the cell. Briefly, 1 ml of cells were taken in 1.5 ml eppendorf tubes, DCHFDA (10 µM final concentration) was added to cells and the suspension was incubated at 37^{o}C in dark with shaking (150rpm). After 1 h of incubation, florescence was estimated in triplicates (λex = 490 nm, λem = 520 nm).

Chapter 3 - Characterization of Alr3183

3.1 Introduction

The Alr3183 protein belongs to the PrxQ subfamily of Prxs i.e. it is an atypical 2-Cys Prx. The first atypical 2-Cys Prx was identified in *E. coli* as a protein with a molecular mass of 18 kDa, which comigrated with the bacterioferritin protein [129, 102]. Hence, even before its function was known, this protein was named as bacterioferitin comigratory protein (BCP). As *E. coli* BCP is the prototype and the best studied member, this family of proteins is termed as the BCP family. Subsequently, the *E. coli* BCP protein was found to be a member of AhpC/TSA family with a general alkyl hydroperoxidase activity that required thioredoxin A (TrxA) as an electron donor [116, 183, 184, 185, 119]. The plant homologs of BCP are named as PrxQ proteins. BCP/PrxQ proteins in general are 149 to 154 amino-acid long polypeptides that contain two catalytic cysteines, the peroxidatic cysteine (C_p) and the resolving cysteine (C_r), which form an intramolecular disulphide bond. The peroxidatic cysteine of these proteins is located in the conserved GCT motif. However, the position of the resolving cysteine is not conserved and, interestingly, in some members, the resolving cysteine may not be not present at all [186, 166, 187]. Unlike other Prxs, BCP/PrxQ members exists as a monomer and the regeneration of the sulfenic acid form of the C_p takes place by intra-molecular disulphide bond formation. BCP/PrxQ proteins generally use thioredoxin as reducing agent and are therefore considered to be thioredoxin-dependent thiol peroxidases [116, 183, 84, 185, 119].

Although not found in mammals, the PrxQ homologs have been observed in plants [102, 103, ,188, 189] and other non-pathogenic bacteria [116, 166, 187], including cyanobacteria [166, 190]. The poplar PrxQ protein is targeted to chloroplasts, suggesting its possible role in maintaining the redox status of that organelle [103, 191, 192]. Over-expression of *Gentiana*

triflora (Gt) PrxQ resulted in resistance to fungal infection and methyl viologen in *Nicotiana tabacum* [193], whereas over production of *Suaeda salsa* PrxQ led to tolerance to cold stress in Arabidopsis [194].

Although *Anabaena* possesses two genes encoding catalases, the inherent catalase activity in *Anabaena* appears to be low under normal conditions of growth [153, 161]. In view of this, it is proposed that Prxs could be the principal proteins that detoxify H_2O_2 in *Anabaena* [195]. This reasoning is supported by the occurrence of many genes encoding Prxs in *Anabaena* [166]. All the major categories of Prxs are found in *Anabaena*, including four that belong to the BCP/PrxQ subtype (i.e. Alr2503, All2375, All2556 and Alr3183) [150, 166, 17]. Chloroplasts are the organelle with highest content of Prxs in plant cells and the antioxidant system in chloroplasts, is supposed to have evolved from cyanobacteria. Similar to *Anabaena*, chloroplasts also show the presence of the multiple PrxQ proteins and low catalase activity [195, 153]. The Alr3183 protein (Q8YSA6) from *Anabaena* PCC 7120 was named as GCT1 [166], due to the presence of C_p in the conserved GCT motif. In phylogenetic analysis, Alr3183 clustered with plant PrxQs, suggesting that plants PrxQs probably originated from their cyanobacterial counterparts [196]. The characterization of the Alr3183 protein from *Anabaena* PCC 7120 is described in this chapter.

3.2 Bioinformatic analysis of the *alr3183*/Alr3183

3.2.1 Genomic context

The *alr3183* ORF (gi Q8YSA6) that encodes the Alr3183 protein is located on *Anabaena* main chromosome at the chromosomal location 3852775…3853236, on the direct strand. The schematic representation of the location of the *alr3183* ORF is shown in the Fig. 3.2.1.1 The

alr3183 ORF is located downstream of the ORF encoding glucose inhibited division protein B (*alr3182*), whereas *all3184*, ORF that encodes light-repressed protein (LrtA) is located downstream of the *alr3183*, but is present in the reverse orientation.

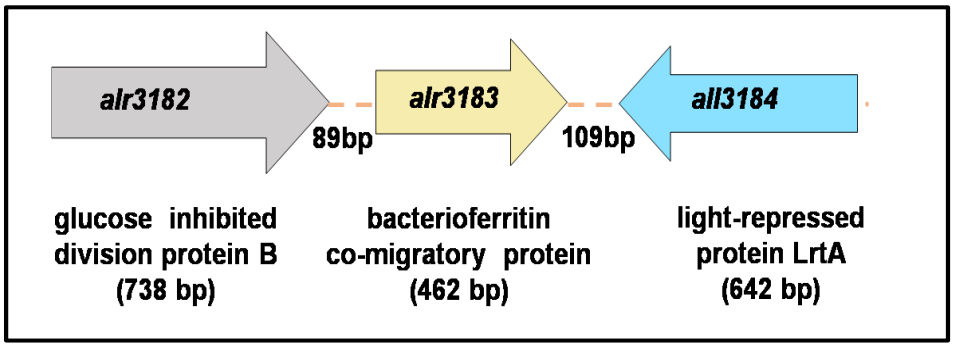

Fig. 3.2.1. Schematic representation of the *alr3183* gene on the genome of *Anabaena* PCC 7120. The *alr3183* (yellow) and its neighboring ORFs are shown with their sizes (in bp). The intergenic regions are depicted by dashed lines and the direction of arrowheads depicts the direction of transcription.

3.2.2 Homology search and multiple sequence alignment of Alr3183

Analysis with the BLASTp algorithm (http://blast.ncbi.nlm.nih.gov/Blast.cgi) using the Alr3183 amino acid sequence from the cyanobase database (http://genome.microbedb.jp/cyanobase/Anabaena/genes/alr3183.faa) as subject sequence and all non-redundant GenBank protein sequences as target database revealed that the Alr3183 protein belonged to the bacterioferritin comigratory protein (BCP) subfamily of peroxiredoxin family, indicating that it was an atypical 2-Cys Prx.

Multiple sequence alignment of Alr3183 homologs from different organisms is shown in the Fig. 3.2.2. The Alr3183 homologs appear to be present in bacteria, archaea, plants and lower

eukaryotes, but surprisingly not found in animals. More significant matches (> 60% identity, > 80% positives) were seen with the BCP/PrxQ type of proteins from cyanobacteria but lower homology was observed with the non-cyanobacterial homologs (http://blast.ncbi.nlm.nih.gov/Blast.cgi).

```
                        10        20        30        40        50        60
                ....|....|....|....|....|....|....|....|....|....|....|....|
Anabaena        ------------------------------------------------------------
Nostoc          ------------------------------------------------------------
Ava_3881        ------------------------------------------------------------
Synpcc7942      ------------------------------------------------------------
Streptomyces    ------------------------------------------------------------
Myxococcales    ------------------------------------------------------------
Escherichia     ------------------------------------------------------------
Haemophilus     ------------------------------------------------------------
Klebsiella      ------------------------------------------------------------
Mycobacterium   ------------------------------------------------------------
Salmonella      ------------------------------------------------------------
Saccharomyces   ----------MGEALRRSTRIAISKRMLEEEESKLAPISTPEVPKKKIKTGPKHNANQA
Poplar          ---MASISLPKHSLPSLLPTLKPITSSSQNLPILSKSSQSQFYGLKFSHSTSLSIPSSSS
Oryza           MAFAVSTACRPSLLLPPRQRS----SPPRPRPLLCTPSTAAFRRGALSATTTPTPARAAL
Zea             MAFTPATACCKASLALAPRASPRGPAACAQAALLCTPSTSVFRGLRAPASAAPAPRRRRS
Arabidopsis     MAASSSSFTLCNHTTLRTLPLRKTLVTKTQFSVPTKSSESNFFGSTLTHSSYISPVSSSS
Sedum           ------------------------------QTLQTSSQSQFHGLKFSHASSFKSPSAPL
Clustal Consensus
```

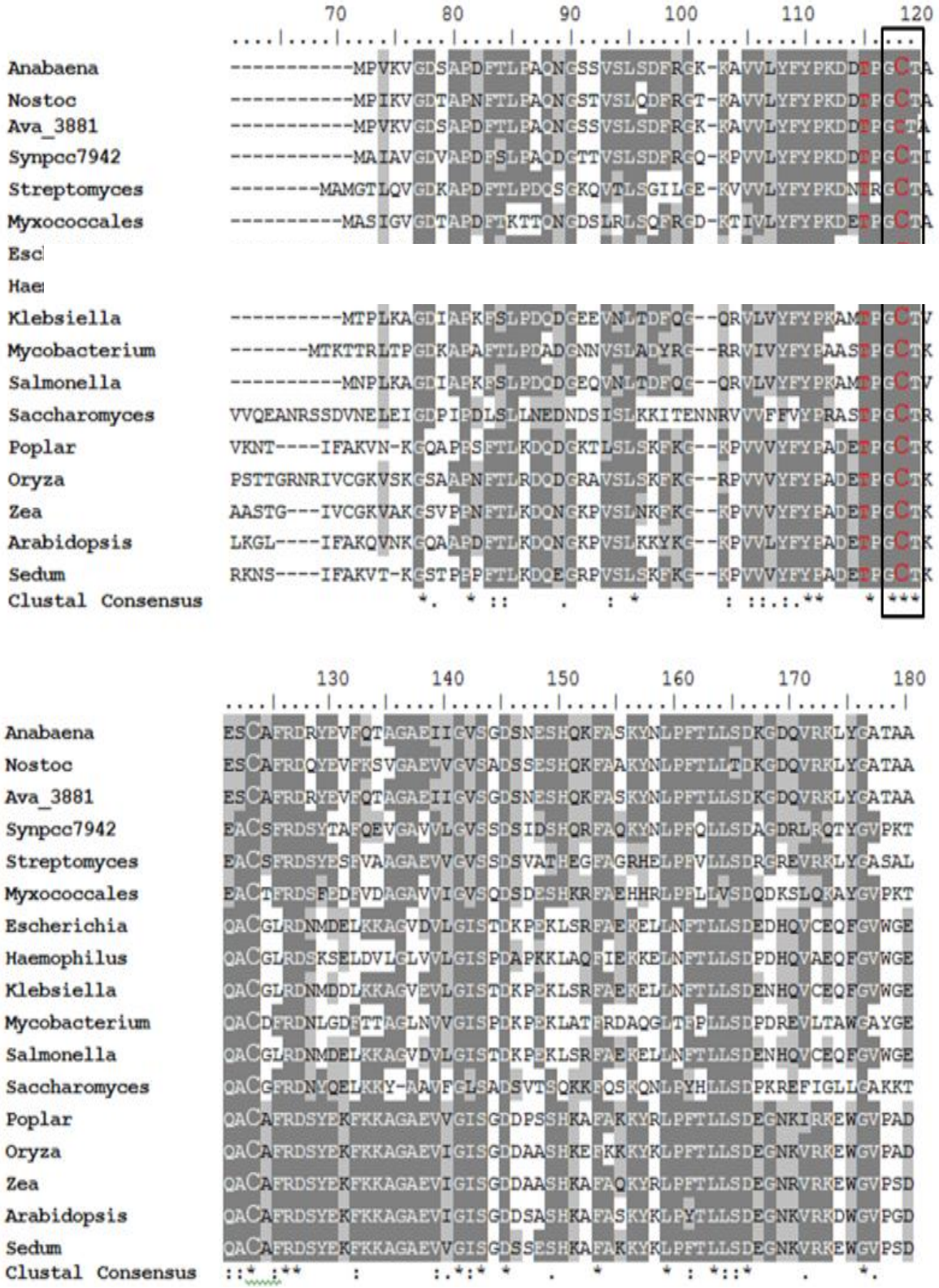
70
80
90
100
110
120
Anabaena
Nostoc
Ava_3881
Synpcc7942
Streptomyces
Myxococcales
Esc
Hae
Klebsiella
Mycobacterium
Salmonella
Saccharomyces
Poplar
Oryza
Zea
Arabidopsis
Sedum
Clustal Consensus
130
140
150
160
170
180
Anabaena
Nostoc
Ava_3881
Synpcc7942
Streptomyces
Myxococcales
Escherichia
Haemophilus
Klebsiella
Mycobacterium
Salmonella
Saccharomyces
Poplar
Oryza
Zea
Arabidopsis
Sedum
Clustal Consensus

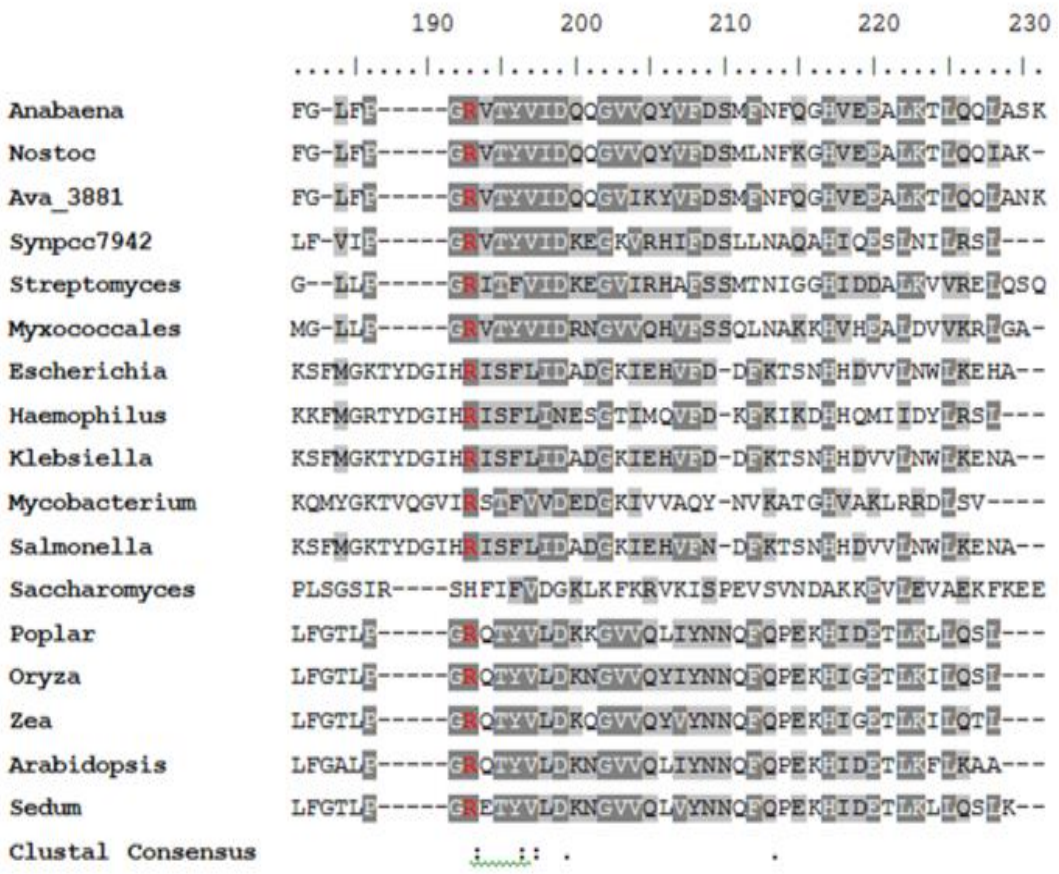

Fig. 3.2.2. Multiple sequence alignment of the Alr3183 protein with BCP/PrxQ proteins from various organisms. Alignment was performed using ClustalW using standard parameters *Anabaena* PCC7120 (Alr3183, Q8YSA6), Ava_3881 (aba23486.1), *Synpcc7942* (WP_006516077), *Streptomyces* sp. NRRL F-5123 (WP_031519847.1), *Myxococcales* (gb|KPK14909.1), *Escherichia coli* (AAC75533), *Haemophilus influenza* (AAC21920), *K. pneumonia* (GI: 152971345), *Mycobacterium tuberculosis* H37Rv (CAA16017), *Salmonella enterica Typhimurium* str. LT2 (Q8XF67), *S. cerevisiae* (CAA86239), *Poplar* (AY530803), *Oryza sativa* (NP_001057052.1), *Zea mays* (NP_001150063.1), Arabidopsis thaliana (NP_189235.1), *Sedium lineare* (BAA90524) were employed for comparison. The residues of catalytic triad (T, C, and R) are shown in red, the two catalytic cysteines are depicted in an enlarged font, and the catalytic GCT motif is boxed.

On the basis of homology with homologous BCP/PrxQ proteins, cysteine residues at positions 46 (Cys-46) and 51 (Cys-51) of Alr3183 appeared to be the putative C_p and C_r residues, respectively. The C_p (Cys-46) was present in the GCT motif, which is characteristic of the BCP proteins. The 4 amino acids spacing between the two putative catalytic cysteines placed Alr3183 into the α-subgroup of the BCP/PrxQ proteins [183, 186].

3.2.3. Primary sequence analysis of the Alr3183 protein

The 462-bp long *alr3183* ORF along with its amino acid sequence (153 amino acids, mol. wt. 16.7 kDa) is shown in Fig. 3.2.3 The residues of the catalytic triad (T, C, and R) are located at amino acid residue no. 43, 46 and 115, respectively. The C_p is the 46th amino acid residue from the N-terminal and the C_r is situated 4 amino-acids away from it (The 51th amino acid residue).

Fig. 3.2.3. Sequence analysis of *alr3183*/Alr3183. The 462 bp long *alr3183* ORF that encodes 153 amino-acid long polypeptide. Peroxidatic and resolving cysteine's are depicted in larger font size; the catalytic GCT motif having the peroxidatic cysteine is shown in box. Residues of the catalytic triad (T, C, and R) of Prxs are depicted in red color.

3.2.4 Domain analysis using SMART program

Analysis with the SMART program (http://smart.embl-heidelberg.de/) showed the Alr3183 protein to have the AhpC/TSA domain (extending from the 6th amino acid to the 129th amino acid). This AhpC/TSA family contains proteins related to bacterial alkyl hydroperoxide reductase (AhpC) and yeast thiol-specific antioxidant (TSA). AhpC/TSA domain is characteristic of the thioredoxin-like super-family.

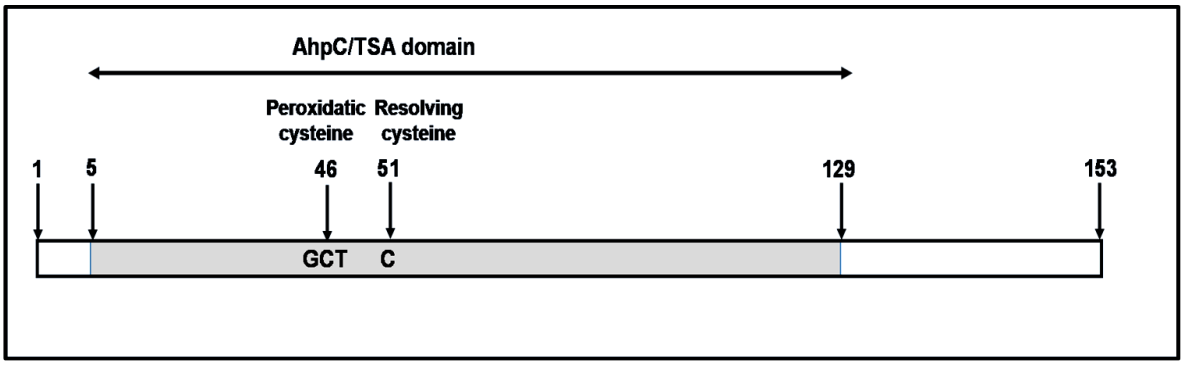

Fig. 3.2.4. Schematic representation of the Alr3183 protein. The predicted 153 amino-acid long Alr3183 protein consists of an AhpC/TSA domain. The position and the amino acid residue number of the conserved 'GCT' motif (typical of the BCP/PrxQ type of Prx), and the putative peroxidatic and resolving cysteine residues are indicated.

3.2.5. Protparam parameters

The biophysical parameters for Alr3183 protein were calculated using protparam tool at Expasy server (http://web.expasy.org/cgi-bin/protparam/protparam) using amino acid sequence of Alr3183 protein obtained from Cyanobase database as the query sequence. The Alr3183 protein was a polypeptide of molecular weight 16768.8 Da. The theoretical pI was 5.63. Total negatively charged residues (Asp + Glu) wwere 17 and positively charged residues (Arg + Lys) were 15 and the protein did not contain any Trp residues. As predicted

by SOSUI **(http://harrier.nagahama-i-bio.ac.jp/sosui/cgi-bin/adv_sosui.cgi)**, the protein did not have any transmembrane regions and appeared to be cytosolic.

3.3 Cloning of *alr3183* in expression vector pET16b and over-expression in *E. coli*

3.3.1. Cloning of *alr3183* in *E. coli* expression vector pET16b.

For biochemical and biophysical characterization of proteins, it is essential to obtain the protein of interest in pure form and in large amounts. For this purpose, it was desired to over-produce the Alr3183 protein with an *in frame* His-tag in *E. coli*. The His-tag would not only enable purification of the Alr3183 protein by affinity chromatography using the Ni-NTA matrix but also facilitate easy detection with the monoclonal anti-polyhistidine antiserum on Western blots.

The *alr3183* ORF was PCR amplified using gene specific primers *alr3183*fwd and *alr3183*rev. (Table 2.2 in material and methods and Fig. 3.3.1A). Amplification of ~ 0.5 kb DNA was observed only when both the reverse and the forward primers were used in the PCR reaction, whereas no amplification was observed when only the single (forward or reverse) primer was present in the reaction mix (Fig. 3.3.1A). The PCR product was eluted from the gel, digested with the restriction enzymes NdeI & BamHI, ligated into similarly digested pET16b vector and transformed into *E. coli* DH5α cells. Next morning the colonies that appeared on the (carbenecillin) plate were verified for the presence of the *alr3183* ORF using colony PCR. Colonies (Fig. 3.3.1B) that showed the presence of the *alr3183* amplicon in the PCR were subsequently employed for plasmid isolation. The purified plasmid (pET3183) was assessed for the presence of the *alr3183* insert by restriction digestion (Fig.

3.3.1C) and the nucleotide integrity of the cloned fragment was confirmed by sequencing.

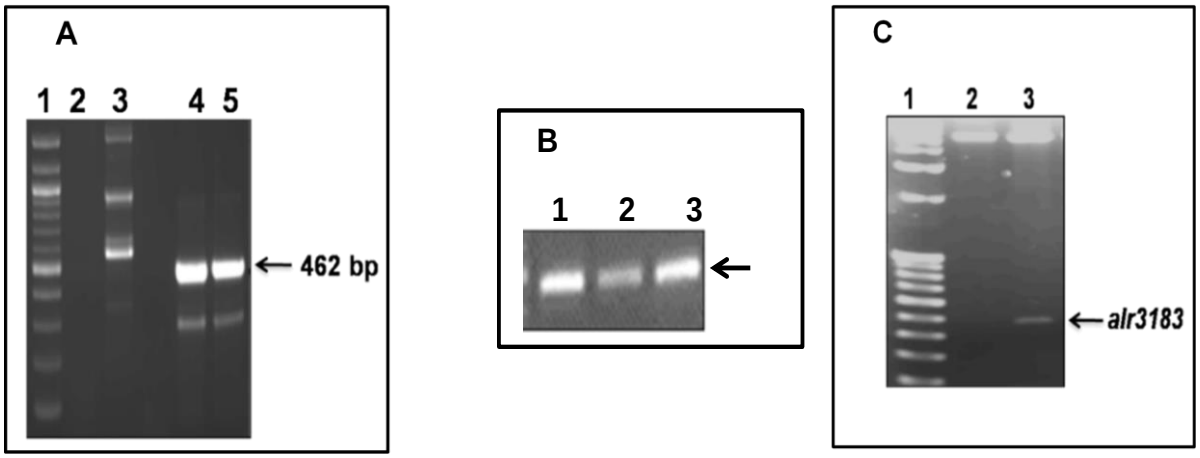

Fig. 3.3.1. Cloning of *alr3183* in pET16b. (A) PCR amplification of *alr3183* from genomic DNA of *Anabaena* PCC 7120. Lane 1, DNA marker (100 bp ladder, NEB); lane 2, PCR with only *alr3183fwd*; lane 3, PCR with only *alr3183rev*; lanes 4 & 5, PCR with both *alr3183fwd* and *alr3183rev.* (B) Colony PCR. *E. coli* colonies that arose after transformation were analyzed for the presence of the *alr3183* gene. The primers *alr3183fwd* and *alr3183rev* were used for amplification. The colony no is depicted on top of the lanes and the specific PCR product obtained is shown by an arrow. (C) Restriction digestion of pET3183. Lane1, Mol. wt. marker (100 bp ladder & 1 kb ladder, NEB); lane 2, undigested pET3183; lane 3, pET3183 digested with NdeI and BamHI. The 462 bp *alr3183* insert released after digestion is indicated.

3.3.2 Over-expression of Alr3183 in *E. coli* and immuno-detection with the monoclonal anti-polyhistidine antiserum

When any gene is inserted between the NdeI-BamHI restriction sites of pET16b, 10 His codons are added in frame to the 5' end of the gene and hence, the over-expressed protein carries an N-terminal 10-His tag. This addition increases the size of the protein by ~2.5 kDa. For overproduction of Alr3183, pET3183 was transformed into the appropriate expression host, *E. coli* BL21pLysS. *E. coli* BL21 pLysS/pET3183 cells were grown in LB medium at

37°C till the culture OD_{600} reached 0.6. Subsequently, temperature was reduced to 20ºC and 30 minutes later, the culture was induced with IPTG. Aliquots were removed after 4h or 24 h and the total cellular proteins were analyzed on SDS-polyacrylamide gels under reducing conditions. As seen in the Fig. 3.3.2A, two very closely spaced protein bands of ~19 kDa were found to be induced in the presence of IPTG. To confirm the presence of the histidine tag, the total cellular proteins were electro-blotted onto nitrocellulose membrane and probed with the monoclonal anti-polyhistidine antiserum. On developing the blot, two bands of ~19 kDa, identical to those observed in Fig. 3.3.2A, were visualized (Fig. 3.3.2B), thus confirming the presence of the His-tagged Alr3183 protein. It should be noted that no signal was seen in the lane where the empty vector (i.e. –ve control) was used for expression.

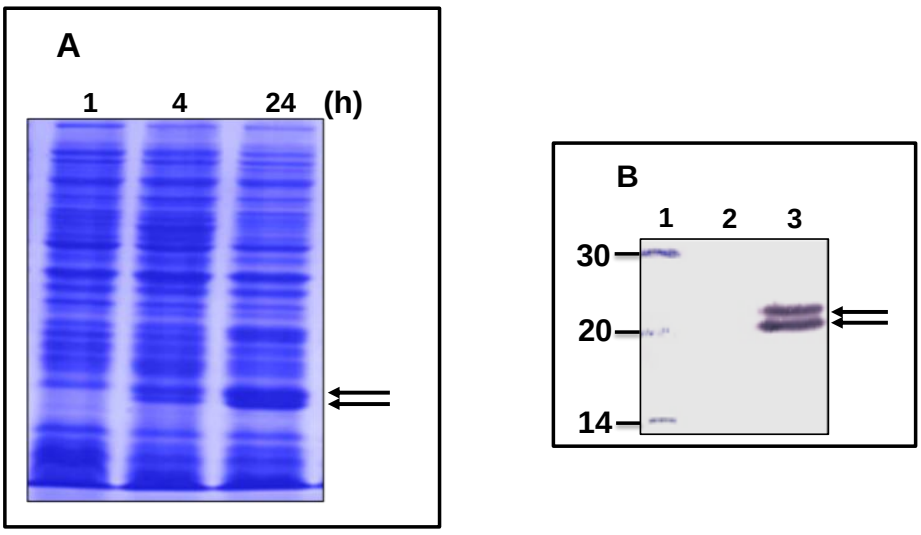

Fig. 3.3.2. Over-expression of Alr3183 in *E. coli.* (A) The E. coli strain BL21pLysS/pET3183 was induced with IPTG (1 mM) and aliquots were removed at the time points indicated. The total cellular proteins were solubilized in Lamelli's buffer, resolved on SDS-PAGE and visualized after staining with CBB. The two Alr3183 bands (~19 kDa) are shown by arrows. (B) Western blot. Total protein extracts from cells induced with IPTG or the uninduced (control) cells were resolved on SDS-PAGE, transferred onto nitrocellulose membrane and probed with the monoclonal anti-His antibody. Lane1, Molecular weight standard; lane2, *E. coli* BL21/pET16b; lane3, *E. coli* BL21pET3183. The Alr3183 bands observed on developing the blot are shown by arrows.

3.4 Purification of the His-tagged Alr3183 using affinity chromatography

3.4.1 Solubility of the over-expressed recombinant Alr3183 protein in *E. coli*

After over-expression in *E. coli*, a protein may exist either in soluble form (i.e. remain cytosolic) or may form inclusion bodies. Unlike the proteins present in the inclusion bodies, proteins that remain soluble are expected to be properly folded and can be purified under native conditions. To verify if the over-expressed Alr3183 was present in the soluble fraction (or formed inclusion bodies), *E. coli* cells overproducing Alr3183 were lysed by sonication and the cytosolic fraction was separated from the inclusion bodies. When resolved on denaturing polyacrylamide gels, the over-expressed Alr3183 was observed to be predominantly present in the soluble fraction (Fig. 3.4.1), thus allowing purification trials under native conditions.

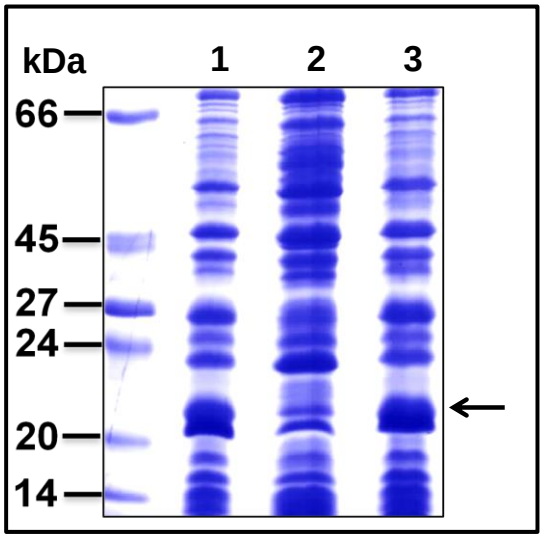

Fig. 3.4.1. Localization of the Alr3183 protein in *E. coli*. The E. coli BL21pLysS/pET3183 cells were induced with 1mM IPTG at 20^{o}C for 18 h. Total cell lysate was separated into soluble or insoluble fraction. These fractions were solubilized in Lamelli's buffer containing DTT, resolved on SDS-PAGE and stained with CBB. Lane 1, induced cells; lane 2, Inclusion-body (insoluble fraction); lane 3, soluble fraction.

3.4.2 Purification of Alr3183

Purification of Alr3183 was performed by affinity chromatography using the Ni-NTA matrix under native conditions. *E. coli* cells overproducing the Alr3183 protein were lysed by sonication and the soluble fraction obtained was loaded onto Ni-NTA slurry. After thorough washing with imidazole containing buffers, the protein was eluted by the elution buffer containing imidazole 250 mM. Different fractions were analyzed on SDS-PAGE and as seen in Fig. 3.4.2, the Alr3183 protein could be obtained in relatively pure form in the elution fractions.

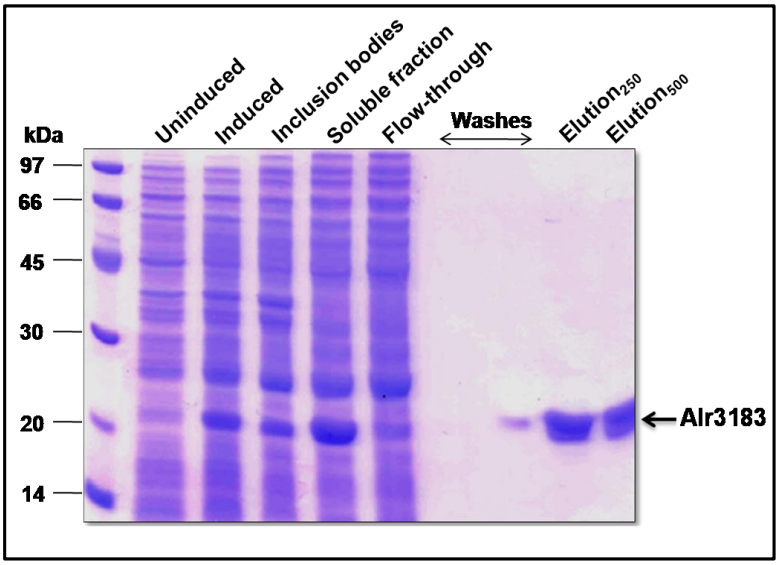

Fig. 3.4.2. Purification of Alr3183. Alr3183 was purified using affinity chromatography. Aliquots from different fractions (as indicated) were solubilized in Lamelli's buffer containing DTT, resolved on 12% SDS-PAGE and visualized by staining with CBB. The molecular mass of standard is indicated on the left side of the gel.

3.5 Generation of anti-Alr3183 anti-serum in rabbit

To detect expression of the Alr3183 protein *in vivo* in *Anabaena*, it was desired to raise

polyclonal antiserum against the purified Alr3183 protein. To obtain the highly pure Alr3183 protein for this purpose, the affinity-purified Alr3183 protein was resolved on SDS-polyacrylamide gels and eluted there from. A small aliquot of from this this elution was resolved by SDS-PAGE to verify the presence of the Alr3183 protein (Fig. 3.5A). This protein was subsequently employed to raise specific anti-serum in rabbit at a commercial facility (Merck, Bangalore).

For antiserum generation in rabbit, 1 mg of Alr3183 was used for primary immunization whereas 500 μg protein was employed for each of the 3 subsequent booster doses. The antiserum supplied by the company was tested by cross-reacting it with the purified Alr3183 protein on Western blots. At 1:5000 dilution, the antiserum could easily detect 50 ng of the purified protein (3.5B). The pre-immune serum, employed as a control (1:5000 dilution), did not cross-react with the Alr3183 protein.

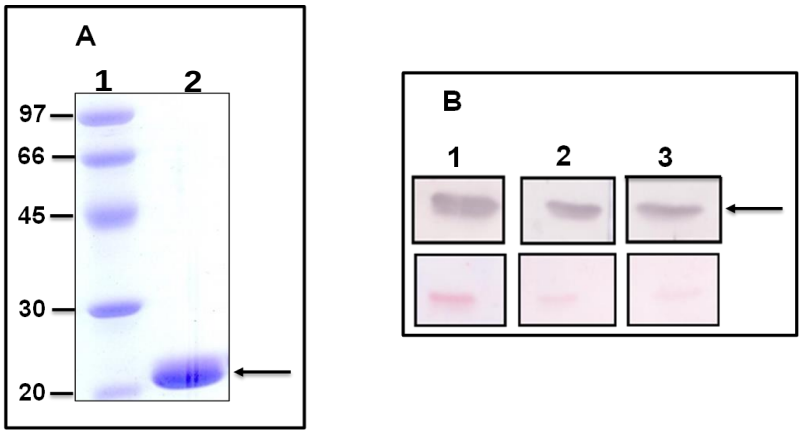

Fig. 3.5. Alr3183 used for antiserum generation and titre of antiserum obtained from rabbit. (A) Protein sample used for antiserum generation lanes1 molecular wt. standard lane2 purified Alr3183. (B) Immunodetection of the purified Alr3183 protein with the specific antiserum. Different concentrations of the purified Alr3183 protein (1, 250 ng; 2, 100 ng; 3, 50 ng) were resolved on SDS-PAGE, electro-blotted onto nitrocellulose membrane, probed with Alr3183 antiserum (1:5000 dilution) and developed with NBT-BCIP. The Ponceau S-stained gel is shown as loading control in lower panel.

3.6 The Alr3183 protein forms intra-molecular disulphide bond

In general, Prxs are characterized by the presence of two catalytic cysteine residues, which may form inter-molecular or intra-molecular disulphide bonds. To investigate if this protein formed intermolecular dimers, Alr3183 was resolved on SDS-PAGE in the presence or the absence of DTT (reducing agent) (Fig. 3.6A). Under reducing (+DTT) conditions, the Alr3183 protein appeared as two closely spaced bands (monomeric forms) while no dimeric forms were observed. However, under non-reducing conditions (-DTT), the Alr3183 protein was visualized mainly as a single band (monomeric form) that co-migrated with the lower band of the two bands observed in presence of DTT.

The alkylating agent AMS (4- acetamido-4'-maleimidyl-stilbene-2, 2'-disulfonate) was used to verify the possibility of Alr3183 to form an intra-molecular disulphide bond (Fig. 3.6B). AMS specifically and covalently binds to the reduced form of a protein (i.e. a protein containing a free thiol group). On being alkylated with a molecule of AMS, the molecular weight of the protein increases by approximately 0.5 kDa. Hence, the AMS-bound and the AMS-free form of the protein can be identified on SDS-PAGE on the basis of their different mobility. The oxidized form (treated with H_2O_2) or the reduced form (treated with DTT) of the Alr3183 protein was reacted with excess of AMS and resolved on SDS-PAGE. The DTT-treated form of the protein displayed retarded mobility as compared to the H_2O_2-treated form of Alr3183. This showed that AMS bound to reduced, but not oxidized, form of the Alr3183 protein. The unavailability of the free thiol group to bind to AMS in the oxidized state indicated the presence of an intra-molecular disulfide bond in the Alr3183 protein.

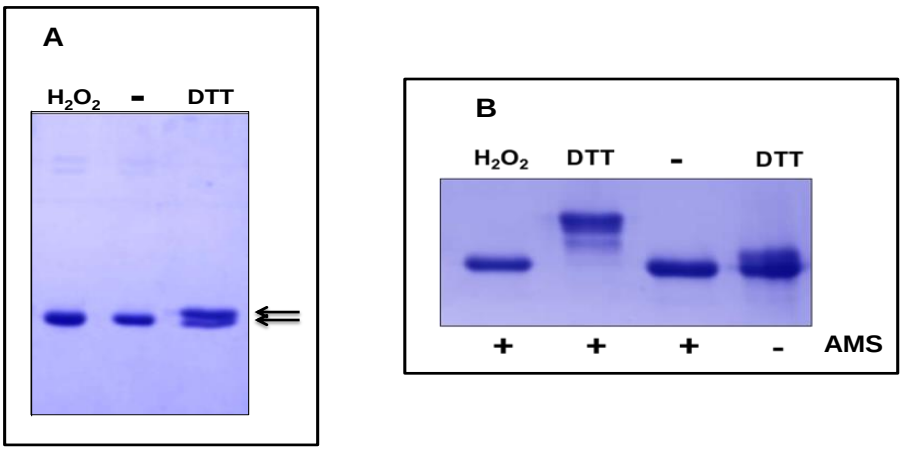

Fig. 3.6. Formation of inter or intra molecular disulphide bond in Alr3183. (A) SDS-PAGE analysis of purified Alr3183 under reducing, non-reducing and oxidizing conditions. Alr3183 (2 μg) treated with DTT (10 mM), H_2O_2 (2 mM) or left untreated (as indicated on top of the gel) was solubilized in Laemmli's sample buffer without DTT, electrophoretically separated by SDS-PAGE (12% gel) and visualized by staining with CBB. Reduced (red) and oxidized (ox.) protein is indicated by an arrow. Molecular weight standards are shown at left of the gel. (B) AMS modification of Alr3183. Purified Alr3183 protein was incubated with H_2O_2 (2 mM) or DTT (100 mM), reacted with AMS (AMS- 4-acetamido-4′-aleimidylstilbene-2, 2′-disulfonic acid) and precipitated with TCA. The precipitated proteins were solubilized in Laemmli's sample buffer and resolved by SDS-PAGE (14% gel) and visualized by staining with CBB.

3.7 Mass-spectrometric analysis of the two Alr3183 bands observed on SDS-PAGE

Matrix-assisted laser desorption/ionization -time of flight-mass spectrometry (MALDI-TOF-MS) technique was employed to determine the identity of the two protein bands (~19 kDa) observed on SDS-PAGE under reducing conditions. The Purified Alr3183 protein was solubilized in sample buffer containing DTT and resolved on SDS-polyacrylamide gels and stained with CBB-250. Both the bands were excised with a scalpel, digested with trypsin and subjected to MS-analysis. The mass spectrum obtained was searched against nrNCBI database using MASCOT server (http://www.matrixscience.com/server.html). Mass-

spectrometric analysis revealed both the bands to be the Alr3183 protein from *Anabaena* PCC7120.

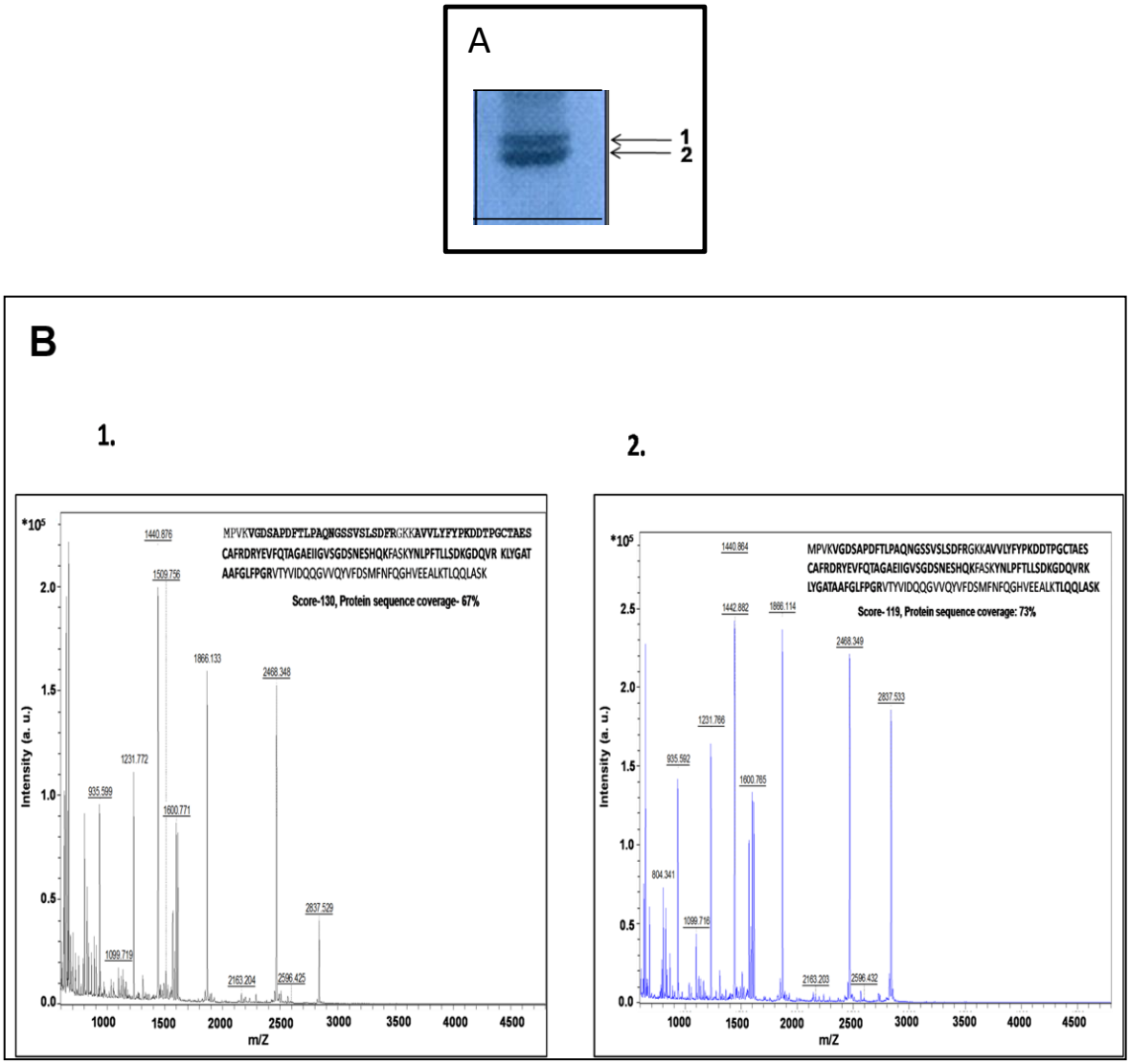

Fig. 3.7. Identification of the 2 bands in Alr3183 preparations. (A) The purified Alr3183 was resolved on denaturing PAGE and visualized after staining with CBB. Lane1, molecular weight marker; lane 2, Alr3183 protein (1 µg). The 2 bands are depicted by arrows. (B) Mass-spectra obtained after the tryptic digestion of the individual Alr3183 bands.

Table 3.1: Positions and masses (expected and calculated) of peptides in upper band.

Start	End	Observed	Mr(expt)	Mr(calc)	ppm	M	Peptide
5	28	2467.3825	2466.3753	2466.1663	84.7	0	K.VGDSAPDFTLPAQNGSSVSLSDFR.G
32	40	1099.7163	1098.7090	1098.6114	88.9	0	K.AVVLYFYPK.D
41	54	1586.7464	1585.7391	1585.6137	79.1	0	K.DDTPGCTAESCAFR.D
55	80	2837.5325	2836.5253	2836.3264	70.1	1	R.DRYEVFQTAGAEIIGVSGDSNESHQK.F
57	80	2566.3847	2565.3774	2565.1983	69.8	0	R.YEVFQTAGAEIIGVSGDSNESHQK.F
85	95	1310.8043	1309.7970	1309.6918	80.3	0	K.YNLPFTLLSDK.G
85	100	1866.1136	1865.1063	1864.9683	74.0	1	K.YNLPFTLLSDKGDQVR.K
101	115	1568.9735	1567.9662	1567.8511	73.4	1	R.KLYGATAAFGLFPGR.V
102	115	1440.8640	1439.8567	1439.7561	69.8	0	K.LYGATAAFGLFPGR.V
146	153	888.5987	887.5915	887.5076	94.5	0	K.TLQQLASK.-

Table 3.2: Positions and masses (expected and calculated) of peptides in lower band.

Start	End	Observed	Mr(Expt)	Mr(calc)	ppm	M	Peptide
5	28	2467.3668	2466.3595	2466.1663	78.3	0	K.VGDSAPDFTLPAQNGSSVSLSDFR.G
32	40	1099.7188	1098.7115	1098.6114	91.2	0	K.AVVLYFYPK.D
41	54	1586.7507	1585.7434	1585.6137	81.8	0	K.DDTPGCTAESCAFR.D
55	80	2837.5291	2836.5219	2836.3264	68.9	1	R.DRYEVFQTAGAEIIGVSGDNESHQK.F
57	80	2566.3829	2565.3756	2565.1983	69.1	0	R.YEVFQTAGAEIIGVSGDSNESHQK.F
85	95	1310.8079	1309.8007	1309.6918	83.1	0	K.YNLPFTLLSDK.G
85	100	1866.1328	1865.1255	1864.9683	84.3	1	K.YNLPFTLLSDKGDQVR.K
101	115	1568.9922	1567.9849	1567.8611	85.4	1	R.KLYGATAAFGLFPGR.V
102	115	1440.8764	1439.8691	1439.7561	78.5	0	K.LYGATAAFGLFPGR.V

3.8 Secondary structural analysis of the Alr3183 protein using CD-spectropolarimetry

Circular dichroism is shown by molecules containing chiral chromophores (light absorbing groups) and is the difference in the absorption of right-handed circularly polarised light (R-CPL) and left-handed circularly polarised light (L-CPL) [197]. Different structural elements in proteins show different CD spectra. Thus, each molecular structure has a circular dichroism signature, and this signature can be used to identify various structural elements present and to follow changes in the structure of macromolecules in different conditions [198, 199, 200]. The most widely studied circular dichroism signatures are the proteins secondary structural elements (α-helix and the β sheet). The CD spectra below 260 nm (far-UV) can be used to predict the percentages of each secondary structural element in the structure of a protein.

Purified Alr3183 protein in native (untreated) or reduced (treated with DTT) form was subjected to CD analysis, and on the basis of CD spectrum obtained (Fig. 3.8), the relative content of the different types of secondary structures (α-helix, β-strand, turns and unordered residues) were calculated using the program CDNN. Results showed the native Alr3183 to exist primarily as alpha helical structure (α- helix, 42.40%; β-turn, 15.40% and random-coil, 27.60%, (Table 3.3). The CD spectra of the DTT-reduced protein (Table 3.3) was also very similar to that of the native (i.e. non-reduced) Alr3183, indicating that reduction/oxidation did not appreciably change the secondary structure of Alr3183 (Fig. 3.8).

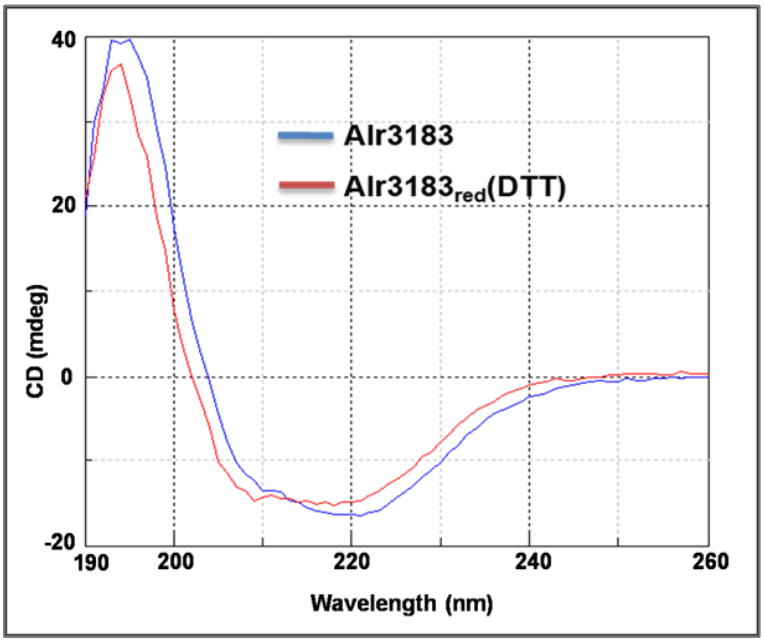

Fig. 3.8. CD spectropolarimetric analysis of Alr3183. Native (untreated) or reduced (treated with DTT) form of the purified Alr3183 protein (0.4 µg/µl) was subjected to CD analysis. The relative content of different types of secondary structures (α-helix, β- strand, turns and unordered residues) were calculated using a program CDNN.

Table 3.3: Secondary structural elements in native (untreated) and reduced (DTT treated) Alr3183.

Native							
	180-260 nm	185-260 nm	190-260 nm	195-260 nm	200-260 nm	205-260 nm	210-260 nm
Helix	n.d.	n.d.	42.40%	42.20%	39.20%	39.70%	39.20%
Antiparallel	n.d.	n.d.	3.70%	5.50%	7.00%	6.60%	6.80%
Parallel	n.d.	n.d.	7.00%	6.80%	7.40%	7.40%	7.50%
Beta-Turn	n.d.	n.d.	15.30%	15.30%	15.80%	15.70%	15.80%
Rndm. Coil	n.d.	n.d.	27.60%	27.30%	28.80%	29.00%	29.40%
Total Sum	-	-	96.00%	97.30%	98.30%	98.50%	98.70%
DTT							
	180-260 nm	185-260 nm	190-260 nm	195-260 nm	200-260 nm	205-260 nm	210-260 nm
Helix	n.d.	n.d.	45.40%	46.60%	43.10%	41.90%	40.20%
Antiparallel	n.d.	n.d.	4.80%	4.90%	5.00%	5.40%	5.90%
Parallel	n.d.	n.d.	7.10%	6.70%	6.20%	5.90%	5.70%
Beta-Turn	n.d.	n.d.	14.70%	14.00%	13.70%	13.90%	14.60%
Rndm. Coil	n.d.	n.d.	24.40%	25.40%	30.20%	31.50%	29.90%
Total Sum	-	-	96.30%	97.70%	98.30%	98.70%	96.20%

3.9 Biochemical analysis of Alr3183

3.9.1 ThioredoxinA (TrxA) dependent peroxidase activity

Among the three reducing agents tested (DTT, GSH and TrxA), the purified Alr3183 protein could detoxify H_2O_2 only with TrxA (Fig. 3.9.1A). As shown in Fig. 3.9.1B, the TrxA-dependent peroxidase activity showed an obvious protein concentration-dependence. Ability of Alr3183 to detoxify different peroxide substrates was also ascertained. Along with H_2O_2, Alr3183 could also decompose organic peroxides such as t-butyl hydroperoxide (t-Bx) and cumene hydroperoxide (CHP) using TrxA as the reducing agent Fig. 3.9.1C.

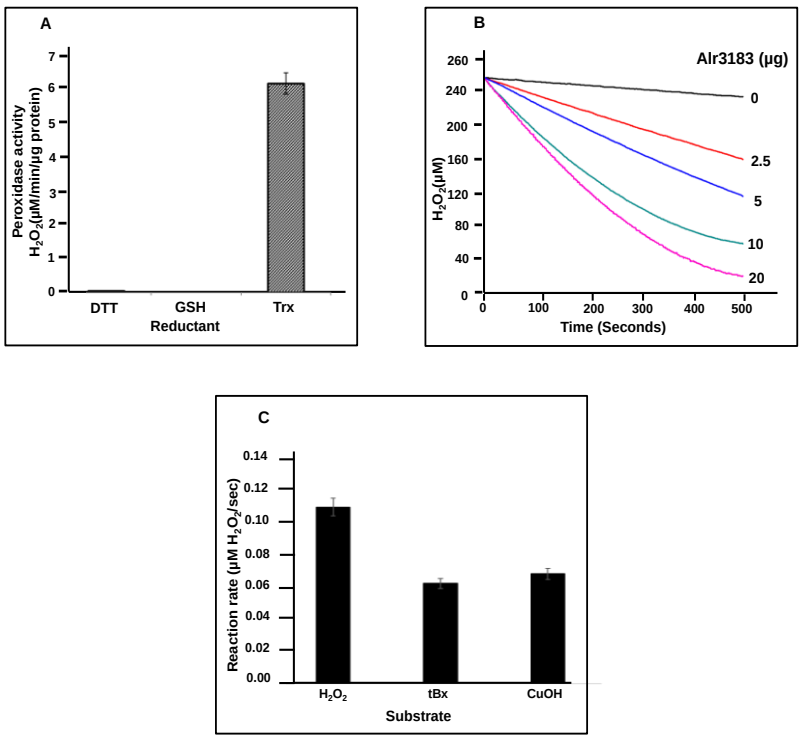

Fig. 3.9.1. Peroxidase activity of the Alr3183 protein. (A) Peroxidase activity of the purified Alr3183 protein with different reductant systems using H_2O_2 as substrate. (B) Protein concentration dependent peroxidase activity of Alr3183. Decomposition of H_2O_2 (200 μM) in the presence of increasing concentrations of Alr3183 was monitored. Reaction was measured by monitoring the decrease in absorbance of NADPH at 340 nm. The amount of protein used in a reaction is indicated in the figure. (C) Decomposition of different substrates: Hydrogen peroxide (H_2O_2), tertiary butyl hydroperoxide (Tbx) and cumene hydroperoxide (CHP) by Alr3183 was monitored by measuring the decrease in NADPH.

3.9.2 Activity of Alr3183 after exposure to elevated temperatures

It was desired to verify if the Alr3183 protein remained functional after exposure to elevated temperatures. Different aliquots of the purified protein were incubated at predetermined temperatures (30, 40, 45, 50, 60, 70º C) for 10 minutes (Fig. 3.9.2) and subsequently assayed at the room temperature. The activity decreased slightly on exposure to 40ºC, but a sharp decrease in the activity was observed at 45 ºC. The Alr3183 protein was completely inactivated at 70 ºC. These results show that Alr3183 is not a thermostable protein

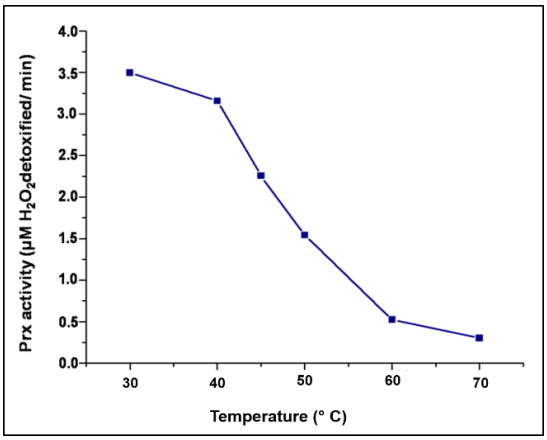

Fig. 3.9.2. Alr3183 is not a thermostable protein. Purified Alr3183 was incubated at different temperatures (30, 40, 45, 50, 60, 70° C) for 10 minutes, after which peroxidase activity was monitored.

3.9.3 Kinetic parameter for H_2O_2 decomposition

Different kinetic parameters of the peroxidase activity of Alr3183 with respect to decomposition of H_2O_2 were determined (Fig. 3.9.3 and Table 3.4). The reaction was started by the direct addition of H_2O_2 (ranging from 5 to 250 µM) and the activity was monitored for 5 min. A molar absorption coefficient of 6220 $cm^{-1} \cdot M^{-1}$ for NADPH at this wavelength was used to calculate the enzyme activity.

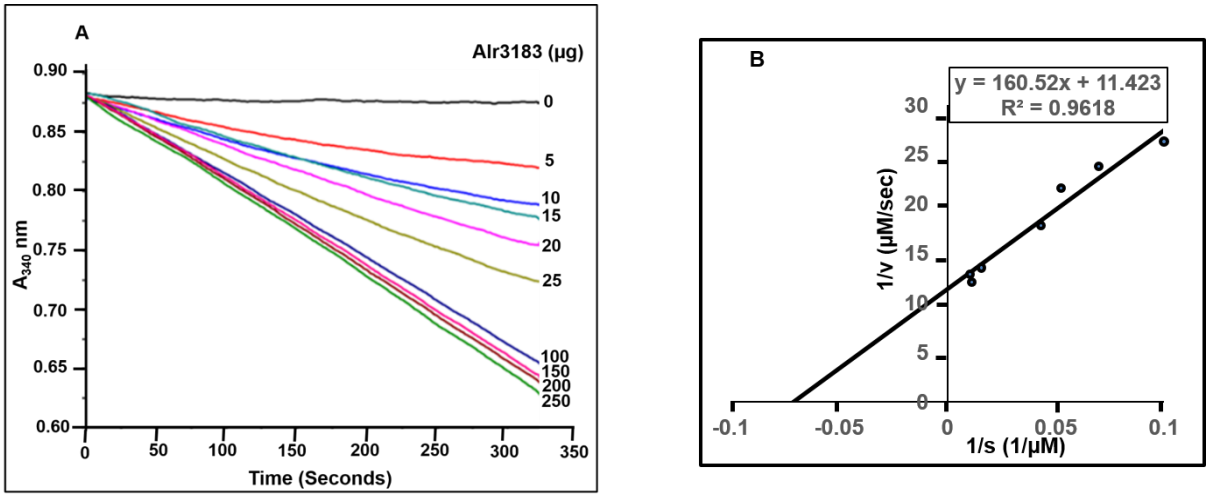

Fig. 3.9.3. Kinetic parameters for H_2O_2 decomposition were estimated at varying concentration of H_2O_2 using NADPH decomposition assay. (A) Change in the absorbance NADPH at 340 nm with time. (B) The corresponding Lineweaver Burk plot.

Table. 3.4. Kinetic parameter for H_2O_2 decomposition

Kinetic Parameters	V_{max} (µM/min)	K_M (µM)	Kcat $Vmax/E_T$ (Sec^{-1})	Catalytic efficiency $(Kcat/K_M) *10^3$
	5.25	**14**	**0.42**	**30**

3.9.4 Kinetic parameter with respect to utilization of TrxA

To calculate the various kinetic parameters for the TrxA-dependent peroxidase activity of Alr3183 with respect to utilization of TrxA, the concentration of the substrate, H_2O_2, was kept constant while the concentration of TrxA was varied in the reaction mix. The reaction was started by the direct addition of H_2O_2 (250 µM) and the activity was monitored for 5 min (Fig. 3.9.4). The kinetic parameters obtained are are shown in (Table 2.5)

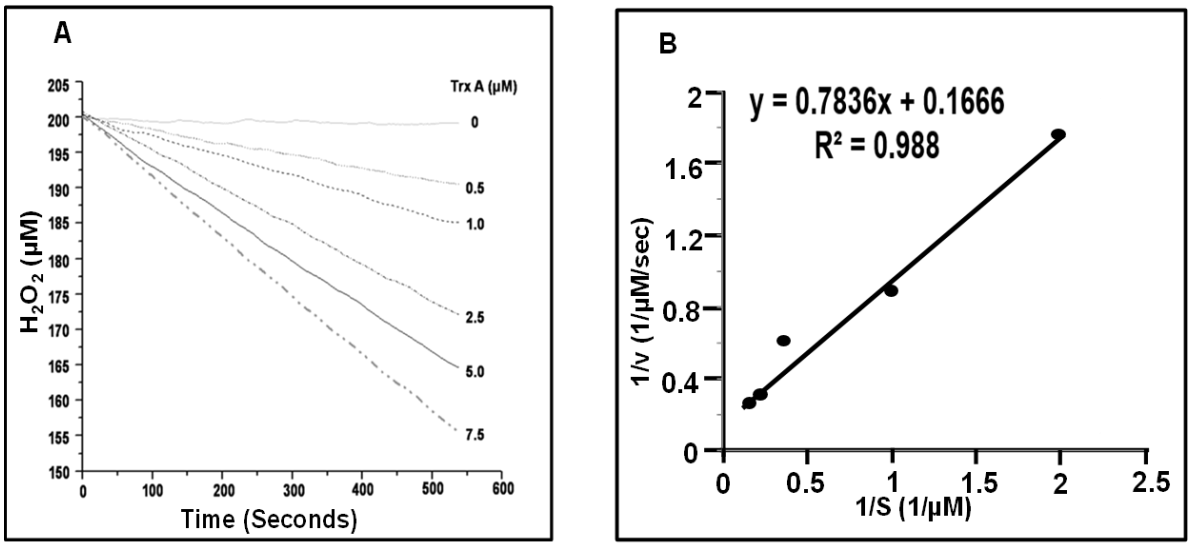

Fig. 3.9.4. Kinetic parameters for TrxA utilization. Kinetic parameters for TrxA utilization were estimated by monitoring decomposition of H_2O_2 (250 µM) at varying concentration of TrxA using NADPH decomposition assay. (A) Decrease in the absorbance of NADPH (340 nm) with time. (B) Plot of initial rate versus substrate concentration. (C) The corresponding Lineweaver Burk plot of B.

Table 3.5 Kinetic parameter for TrxA utilization

Kinetic Parameters	**V_{max} (µM/min)**	**K_M (µM)**	**Kcat Vmax/E_T (Sec^{-1})**	**Catalytic efficiency ($Kcat/K_M$) *10^3**
	15	**4.7**	**$9.6 * 10^{-3}$**	**2.04**

3.9.5 Alr3183 is not inactivated by high concentrations of hydrogen peroxide.

Prxs are known to be inactivated by an excess of peroxide substrate. The –SH group of C_p gets over-oxidized (i.e. converted to its sulfinic acid form), which renders C_p incapable of attacking another molecule of peroxide. The purified Alr3183 protein was treated with 5 mM

H_2O_2 for 4 h and subsequently monitored for TrxA-dependent peroxidase activity (Fig. 3.9.5). Interestingly, The H_2O_2-treated Alr3183 protein showed TrxA dependent activity that was very similar to that observed with the control Alr3183 protein, suggesting that the catalytic cysteine was not prone to over-oxidation.

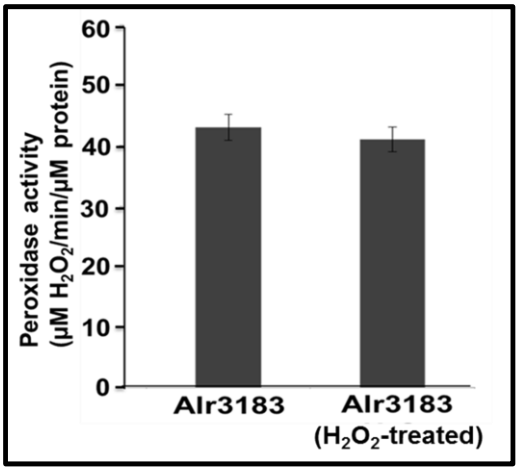

Fig. 3.9.5. Effect of H_2O_2 treatment on peroxidase activity of Alr3183. Peroxidase activity of the untreated Alr3183 protein or the protein exposed to H_2O_2 (5 mM) for 4h was monitored.

3.10 Analysis of the physical interaction of Alr3183 and TrxA using surface plasmon resonance

Surface Plasmon Resonance (SPR), a powerful technique for measuring biomolecular interactions, enables monitoring of label-free interactions in real time between two biomolecules [201]. Technically, the term Surface Plasmon Resonance (SPR), refers to an optical phenomenon that permits monitoring of changes in refractive index, which occurs only when two molecules interact. The technique has found widespread use in protein-protein interaction studies [202].

The physical interaction of Alr3183 with TrxA was studied by Surface Plasmon Resonance (SPR) technique. The TrxA protein was immobilized on a bare gold sensor chip while the

purified Alr3183 proteins were present in the mobile phase for interaction. A concentration-dependent increase in the SPR signal confirmed the physical interaction between Alr3183 and TrxA (Fig. 3.10.1).

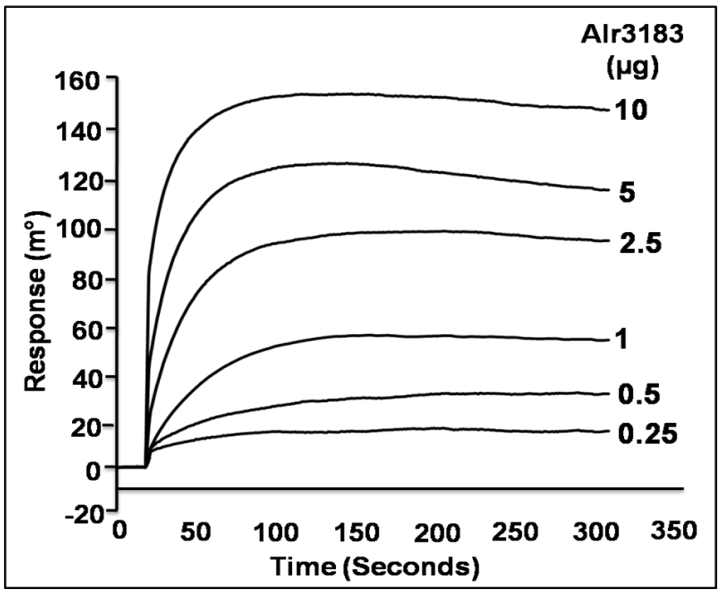

Fig. 3.10.1 Interaction of Alr3183 with immobilized TrxA. Different concentrations of the Alr3183 protein (as indicated in the figure) were injected onto the Alr3183-immobilized sensor chip at 33.3 µl/min flow rate in independent experiments.

Ability of the reduced Alr3183 protein to interact with TrxA was also verified. The Alr3183 protein was reduced with DTT and allowed to interact with TrxA. Interestingly, the DTT-reduced protein showed decreased binding to TrxA as compared to the control Alr3183 protein (i.e. not treated with DTT) (Fig.3.10.2).

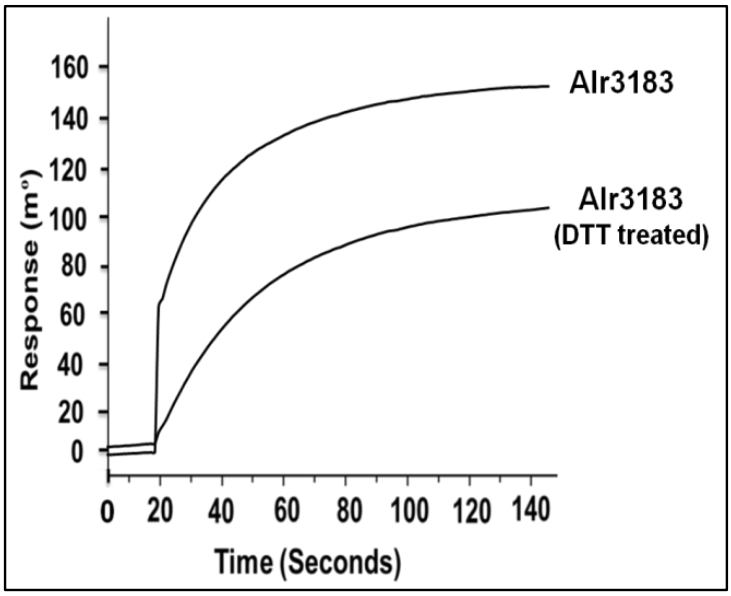

Fig. 3.10.2 Comparison of TrxA binding of untreated and reduced Alr3183 using SPR. The Alr3183 protein was reduced with DTT and subsequently the DTT was removed by dialysis. The reduced protein was allowed to interact with TrxA immobilized on to the gold sensor chip.

3.11 Role of cysteine residues in the catalysis

The atypical 2-Cys proteins have 2 cysteines that take part in catalysis. The Alr3183 has C_p at 46^{th} position whereas C_r is located 4 amino acids away from it (i.e. it is the 51^{st} amino acid). To verify the role of the Cys residues in Alr3183, the C_p or C_r was replaced with serine (S) to give rise to Alr3183C46S (C_p replaced by Ser) or Alr3183C51S (C_r replaced by Ser) employing a PCR-based site-directed mutagenesis strategy (described in section 3.11.1). Another mutant form of Alr3183 wherein both the cysteines were converted to serine (i.e. cysteine double mutant, Alr3183CDM) was also constructed. The peroxidatic TrxA-dependent peroxidatic activity of these mutant proteins and their ability to interact with TrxA was analysed.

3.11.1 Generation of alr3183C46S, alr3183C51S and alr3183CDM

Replacement of the Cys residue (s) of Alr3183 with Ser by PCR-mediated site-directed mutagenesis was performed using the strategy described in Fig. 3.11.1. The mutation at the desired location was obtained by using mutagenic primers that contained the Ser codon in place of the Cys codon. The *alr3183* ORF was subjected to two-step PCR using the above-mentioned oligonucleotide primers (mentioned in Table 2.2). The first mutagenic PCR reaction involved generation of two PCR products that overlapped in sequence containing the desired mutation. A subsequent re-amplification of these fragments with *alr3183*fwd/rev primers resulted in the enrichment of the full-length *alr3183*C46S or *alr3183*C51S.

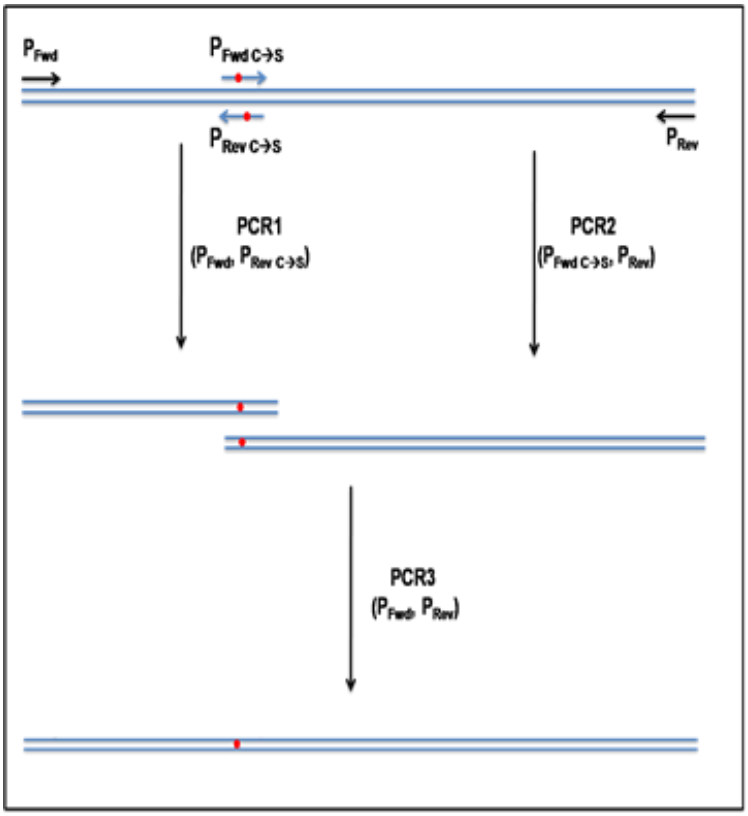

Fig. 3.11.1.1. Strategy in PCR mediated site specific mutagenesis. The template DNA was subjected to 2 PCR reactions separately with mutagenic primers that overlapped in sequence at the desired location. The amplified products were mixed in 1:1 ratio and subjected to the PCR3 reaction with native primers.

Briefly, for generation of *alr3183C46S*, 2 PCR reaction were performed one with *3183C46Sfwd* & *alr3183rev* (PCR1), and second with *alr3183fwd* & *3183C46Srev* (PCR2), finally. The amplicon from PCR1 and PCR2 were mixed in equal proportion and subjected to third PCR reaction with *alr3183fwd* and *alr3183rev* (PCR3). Similarly, for generation of *alr3183C51S* PCR1 was done with *3183C51Sfwd* and *alr3183rev* whereas PCR2 performed with *alr3183fwd* and *3183C51Srev*. PCR1 and PCR2 products were pooled and subjected to PCR 3 for amplification of *alr3183C51S* with native primers (*alr3183fwd* and *alr3183rev*). For constructing *alr3183CDM*, the *alr3183C46S* DNA was employed as a template for the initial PCRs (PCR1 and PCR2) with the primers used to generate *alr3183C51S*. Subsequently, the two products obtained were pooled and subjected to PCR with *alr3183fwd* and *alr3183rev*.

All these PCR products were individually cloned into the pET16b vector at the NdeI and BamHI sites. Transformants were verified by colony PCR for the presence of the *alr3183* gene (Fig. 3.11.1.2). The purified plasmid from a PCR-positive colony was verified by restriction digestion with appropriate enzymes for the presence of the gene. All the respective inserts were sequenced to confirm the presence of the desired mutation.

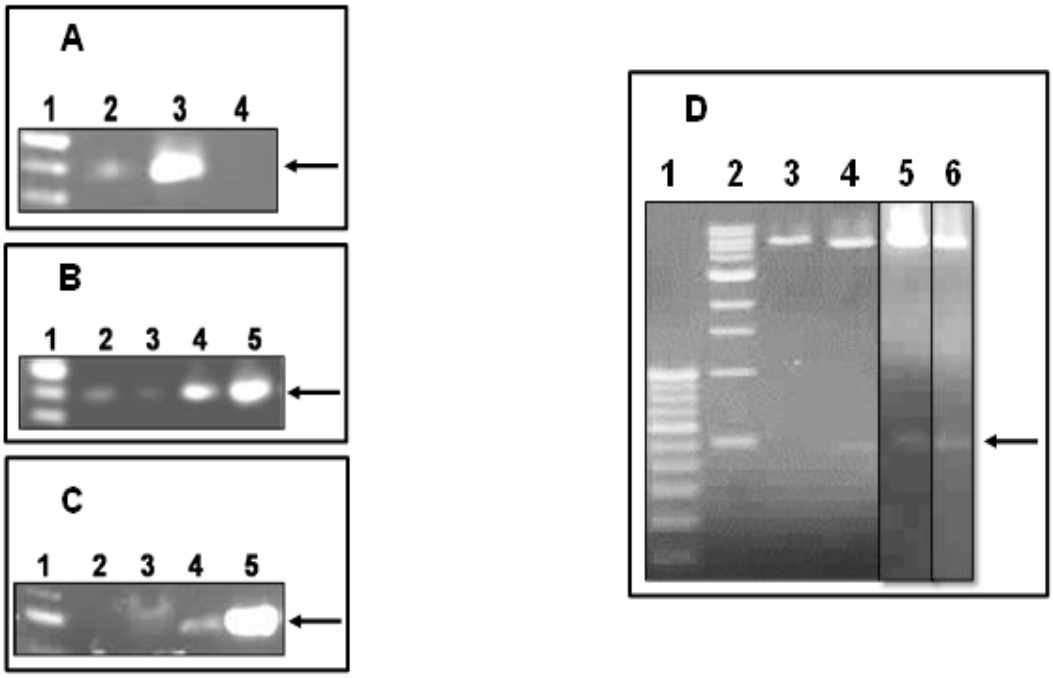

Fig. 3.11.1.2. Generation of *alr3183C46S*, *alr3183C51S* and *alr3183CDM*. PCR of (A) DH5α/pETalr3183C46S (B) DH5α/pETalr3183C51S (C) DH5α/pETalr3183CDM, colonies using *alr3183fwd* and *alr3183rev* primers. Lane 1, marker 100 bp (NEB); lane 2, PCR of colony no #1; lane 3, PCR of colony no #2; lane 4, PCR of colony no #3; lane5, PCR of colony no#4. The PCR product is shown by arrow. (D) Restriction digestion of isolated plasmids. Lane1, 100 bp ladder NEB; lane 2, 1kb ladder; lane 3, pET3183CDM undigested control; lane 4, pET3183CDM digested with NdeI and BamHI; lane 5, pET3183C46S digested with NdeI and BamHI; lane 6, pET3183C51S digested with NdeI and BamHI. The ~460 bp insert released after digestion is shown by an arrow.

3.11.2 Purification of Alr3183C46S, Alr3183C51S and Alr3183CDM from *E. coli*

The Alr3183 cysteine variants were over-expressed in *E. coli* and purified by affinity chromatography as described for Alr3183 (Fig. 3.11.2 A-C). These proteins were probed with the Alr3183 antiserum or the Anti-His antibody on Western blots. As is seen in Fig. 3.11.2D, all the proteins cross-reacted with Alr3183 antiserum as well as with the Anti-His antibody, thus confirming the presence of the recombinant proteins.

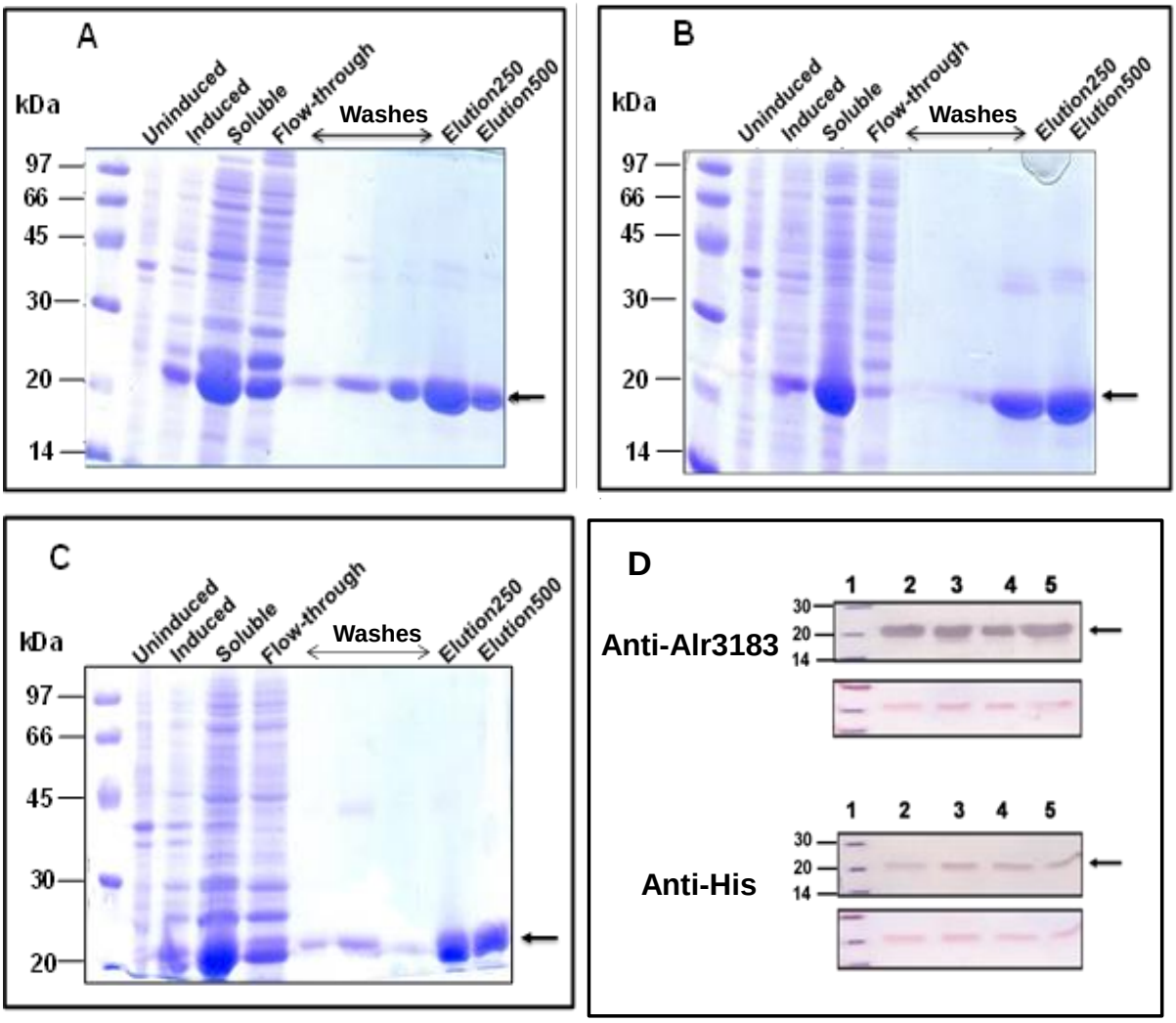

Fig. 3.11.2. Purification of various cysteine mutants of Alr3183 protein from *E. coli*. Purification of (A) Alr3183C46S (B) Alr3183C51S and (C) Alr3183CDM. The BL21pET*alr3183C46S*, BL21pET*alr3183C51S* and BL21pET*alr3183CDM* cells were induced with IPTG (1 mM final concentration) and the respective proteins purified by affinity chromatography employing the Ni-NTA matrix. 20 µl of the different fractions (as indicated in the figures) were resolved by electrophoresis and the proteins were visualized by staining with CBB. Molecular weight markers are shown at the left side of the gels. (D) Western blot analysis of the various Alr3183 proteins. The soluble fraction of the IPTG-induced cells was mixed with Laemmli's buffer (without DTT), resolved on 12% SDS-PAGE, transferred to nitrocellulose membrane and probed with the Alr3183 antiserum (upper panel) or the Anti-His antibody (lower panel). Lane molecular weight standard; lane2, Alr3183; lane 3, Alr3183C46S; lane4, Alr3183C51S; lane5, Alr3183CDM.

3.11.3 Biophysical analysis of the wild-type Alr3183 and its cysteine mutants

3.11.3.1 The Alr3183 and Alr3183CDM are monomeric whereas Alr3183C46S and Alr3183C51S are dimeric.

The purified proteins were incubated with DTT (to reduce the protein) or left untreated and visualized on non-reducing SDS-PAGE. Both the cysteine mutants (Alr3183C46S and Alr3183C51S) were mostly present as dimers when left untreated whereas Alr3183 and Alr3183CDM were monomeric. In reduced conditions (i.e. in the presence of DTT) all the proteins were present in their monomeric forms (Fig. 3.11.3.1A and B).

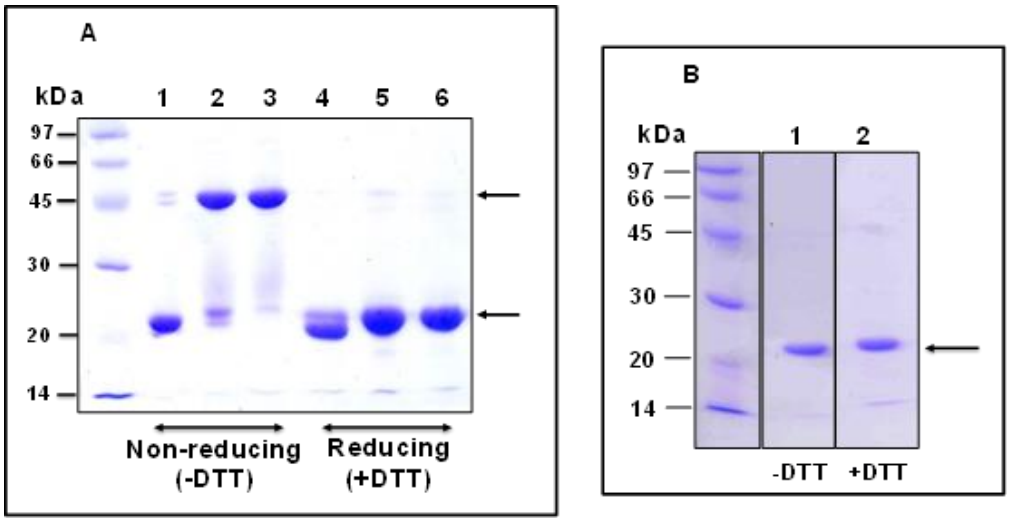

Fig. 3.11.3.1. SDS-PAGE analysis of purified Alr3183 and its cysteine variants under reducing or non-reducing conditions. (A) Alr3183, Alr3183C46S and Alr3183C51S (5 μg each), untreated or reduced with DTT (100 mM) as indicated on the bottom of the gel, were solubilized in Laemmli's sample buffer without DTT, electrophoretically separated by SDS/PAGE (12% gel) and visualized by staining with CBB. Molecular weight standards are shown at left of the gel. (B) Alr3183CDM (2 µg), untreated or reduced (100 mM DTT) as indicated on the bottom of the gel, and resolved on SDS-PAGE as mentioned in (A).

3.11.3.2 Analysis of the various Alr3183 proteins by size-exclusion chromatography

Prxs are known to form different oligomeric forms and the presence of these can be detected by size exclusion chromatography [120, 203, 204, 205]. To verify if Alr3183 or its cysteine mutants could form oligomers, the purified Alr3183, Alr3183C46S, Alr3183C51S and Alr3183CDM were subjected to size-exclusion chromatography on Superdex 200 column. Elution profile of Alr3183 and mutant proteins was compared with the elution profile obtained from standard proteins of known size (Fig.3.13.1). Largely, the Alr3183 and Alr3183CDM appeared at monomeric position while Alr3183C46S and Alr3183C51S were dimeric. These results were in good agreement with data obtained from SDS-PAGE analysis, which also indicated these proteins to exist mostly as monomers (Alr3183 & Alr3183CDM) or dimers (Alr3183C46S and Alr3183C51S).

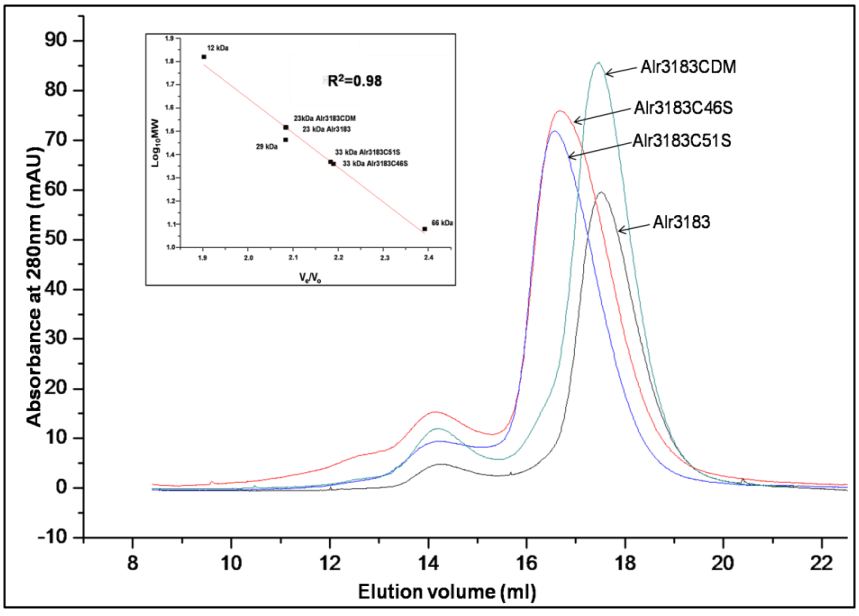

Fig. 3.11.3.2. Gel-exclusion chromatography. Elution profile of the various Alr3183 proteins on a Superdex 200 10/300 GL column. The column was pre-equilibrated with buffer (20 mM Tris, 50 mM NaCl, pH 7.2) and a 100 µl aliquot of protein (200 µg) was injected. The retention volumes obtained with standard proteins were employed to draw a standard curve (depicted in the insert) that was used to determine the masses of the proteins.

3.11.3.3 Determination of volumetric distribution of sizes of Alr3183, Alr3183C46S, and Alr3183C51S

Hydrodynamic sizes of Alr3183, Alr3183C46S, and Alr3183C51S were determined using dynamic light scattering. The size of native Alr3183 was found to be 3.7 nm, whereas the size of Alr3183C46S and Alr3183C51S was 7.4 and 7.6 nm respectively. This result supports the earlier polyacrylamide gel electrophoresis and size-exclusion data wherein too Alr3183 was present as monomer while both Alr3183C46S and Alr3183C51S were observed to be dimeric.

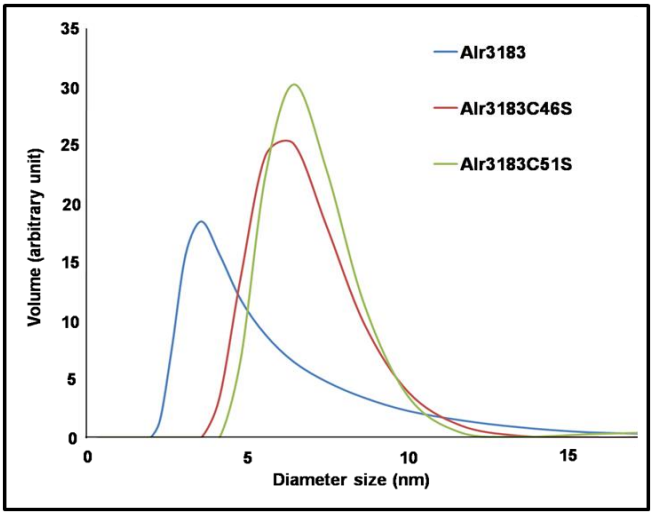

Fig. 3.11.3.3. DLS analysis of the Alr3183, Alr3183C46S and Alr3183C51S. The dynamic light scattering (DLS) profile of the purified Alr3183, Alr3183C46S and Alr3183C51S (in 20 mM Tris, pH 7.2).

3.11.3.4 CD spectropolarimetry of Alr3183, Alr3183C46S and Alr3183C51S

To see whether the absence of either of the two catalytic cysteines caused any change in the secondary structure of Alr3183, CD-spectropolarimetry technique was employed. As evidenced from the Fig. 3.11.3.4, change of the any of the catalytic cysteines to serine did not cause any major change in the secondary structure of the protein. It appears that formation of disulfide linkages do not have any bearing on the overall secondary structure of the Alr3183

protein.

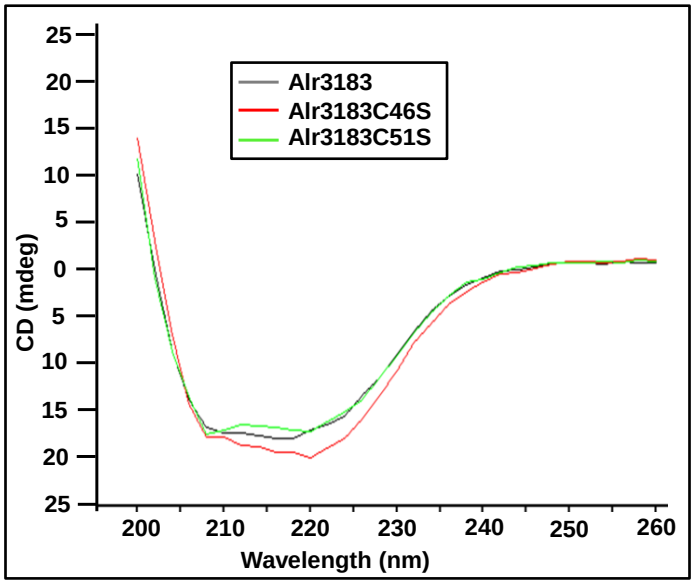

Fig. 3.11.3.4. CD-spectropolarimetry of the Alr3183, Alr3183C46S and Alr3183C51S. Purified proteins (100 µl) were taken at equivalent concentration (0.4 µg/µl), were analyzed using CD-spectropolarimeter in far-uv light region**.**

3.11.4 Biochemical analysis of the Alr3183 cysteine mutants.

3.11.4.1 Alr3183C46S and Alr3183CDM are inactive whereas Alr3183C51S shows reduced activity

As Alr3183 showed TrxA-dependent peroxidase activity, ability of the Alr3183C46S, Alr3183C51S and Alr3183CDM to detoxify H_2O_2 using TrxA as reductant was monitored. The Alr3183C46S or the Alr3183CDM protein was completely inactive whereas, when compared with Alr3183, Alr3183C51S showed more than 5-fold reduced activity than that observed with the wild-type Alr3183.

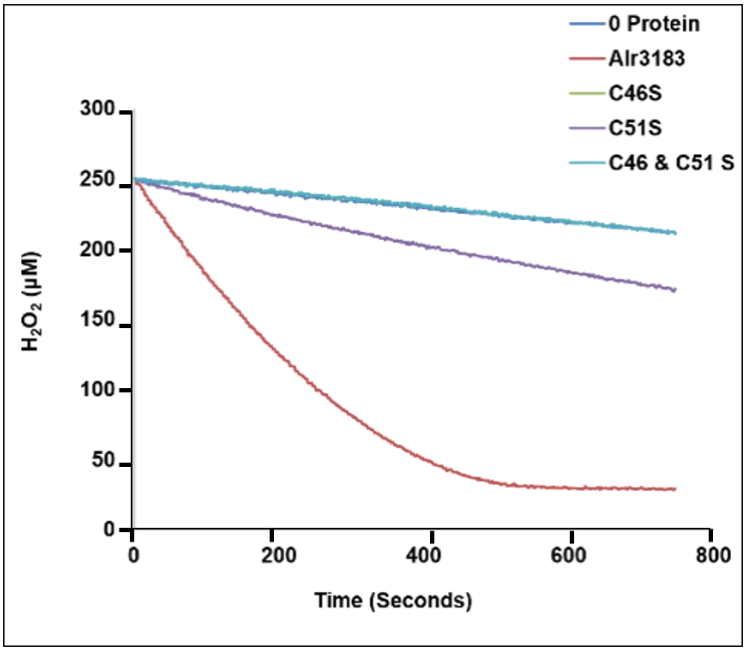

Fig. 3.11.4.1. TrxA dependent peroxidase activity of Alr3183 and mutants. TrxA dependent peroxidase activity of Alr3183, Alr3183C46S, Alr3183C51S and Alr3183CDM were measured by monitoring the decomposition of NADPH. The reaction was started by addition of 250 µM H_2O_2. Please note that the no protein control, Alr3183C46S and Alr3183CDM showed an identical response.

In this assay, the wild-type Alr3183 protein could completely decompose most of the H_2O_2 in 10 minutes whereas AlrC46S3183 protein was completely inactive. The Alr3183C51S showed substantially reduced activity and could detoxify ~20% of the initial H_2O_2. Activity of wild-type protein was 35 µM H_2O_2 decomposed/min/µg protein while that of Alr3183C51S was 7 µM H_2O_2 decomposed/min/µg protein (Fig. 3.11.4.1). These results indicate that Cys-46 is indeed the C_p as its mutation causes protein to lose its activity completely. On the other hand, considerable (but not complete) loss of activity on mutating Cys-51 shows that it is the C_r. These observations, supported by bioinformatic predictions, indicate Cys-46 and Cys-51 are indeed the C_p the C_r residues, respectively.

3.11.4.2 Alr3183C51S requires higher concentration of TrxA for peroxidase activity

Increasing concentrations of TrxA were used in H_2O_2 decomposition reaction with the wild-type Alr3183 or the Alr3183C51S. In the absence of TrxA, no activity was observed with both the proteins, whereas, on increasing the concentration of TrxA, a concomitant increase in the peroxidase activity of Alr3183 was observed. Unlike the Alr3183 protein, Alr3183C51S required relatively higher concentration of TrxA to show any peroxidase activity i.e. peroxidase activity was observed only when TrxA concentration was 2.5 µM or more (Fig. 3.11.4.2).

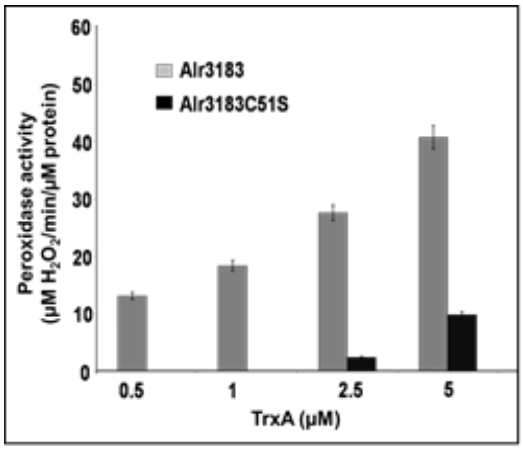

Fig. 3.11.4.2. Comparison of Peroxidase activity of Alr3183 and Alr3183C51S at different concentration of TrxA.

3.12. Surface Plasmon Resonance analysis to monitor the physical interaction of the various Alr3183 proteins with TrxA

SPR experiments were performed to assess if the absence of cysteine residues affected ability of the Alr3183 protein to interact with TrxA. Interaction of Alr3183C46S, Alr3183C51S and Alr3183CDM with TrxA is shown in the Fig. 3.14A. At a comparable concentration, both

Alr3183C46S and the wild-type Alr3183 protein showed similar response units at the end of the assay period (Fig. 3.14). However, a distinctly reduced interaction was observed when Alr3183C51S or Alr3183CDM was present in the mobile phase Fig. 3.12A. The Alr3183CDM protein bound to TrxA in a manner similar to that shown by Alr3183C51S Fig. 3.12A. To confirm that equal amount of each purified protein was used in the SPR assays, equal volumes of the respective protein preparations were resolved on SDS-PAGE. On staining with CBB, the content of all the proteins appeared to be similar; indicating that comparable amount of each protein was used in the assays (Fig. 3.12B).

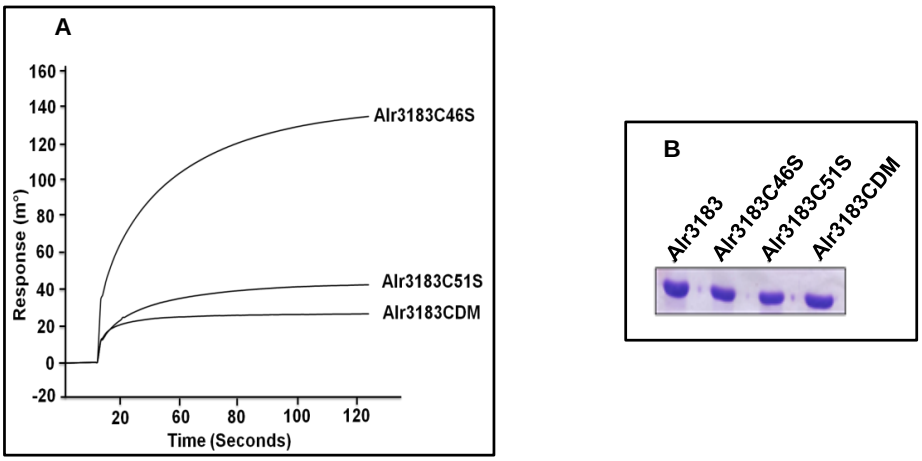

Fig. 3.12. **Interaction of Alr3183** cysteine mutant with TrxA. TrxA (250 µM) was immobilized onto the bare gold chip employing the EDC-NHS chemistry. 10 µg of each protein were injected onto the TrxA-bound sensor chip at 33.3 µL/min flow rate in independent experiments. (B) 2.5 µl of each of the protein preparation (1mg/ml) used for SPR analysis was resolved on SDS-PAGE and visualized by staining with CBB.

3.13 Deciphering the *In-vivo* role of Alr3183 in *Anabaena* PCC 7120

3.13.1 Expression of Alr3183 in response to different stresses.

Prxs are known to be induced in response to different stresses in several organisms, including

cyanobacteria [206, 144, 185]. In *Anabaena* PCC 7120, Prxs such as All1541 and Alr4641 are induced by oxidative stresses mediated by H_2O_2 or methyl viologen (MV) [152, 162]. To verify if the same held true for Alr3183, expression of the Alr3183 protein, on exposure to different oxidative stresses was monitored in the wild-type *Anabaena* PCC 7120. Three day old cultures of *Anabaena* PCC 7120 were subjected to various agents that cause oxidative stresses i.e. methyl viologen (MV), t-butyl-hydroperoxide (tBx), cumene hydroperoxide (CuX) and hydrogen peroxide. After 6 h, cells were harvested; total protein was isolated, resolved on SDS-polyacrylamide gels, transferred to a nitrocellulose membrane and probed with the Alr3183 anti-serum. No induction, but in fact a decrease in the amount of the Alr3183 protein was observed on exposure to these agents. Thus, Alr3183 is apparently not induced in response to oxidizing agents in *Anabaena*.

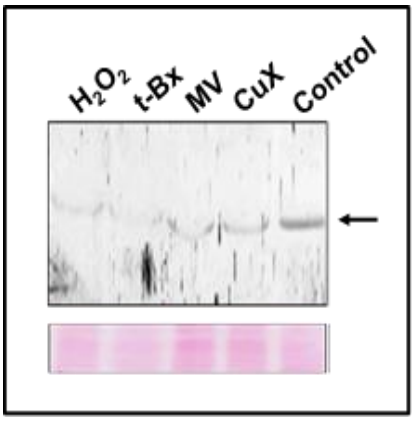

Fig. 3.13.1. Induction of Alr3183 protein in *Anabaena*. Total proteins (50 µg per lane) were resolved by SDS/PAGE (12% gel), electro-blotted on to nitrocellulose membrane, and probed with anti-Alr3183 antiserum (1:2000 dilution). The 17 kDa Alr3183 band is shown by an arrow. PonceauS-stained part of the nitrocellulose membrane is shown as a loading control in the bottom.

3.13.2 Over-expression of Alr3183 in the wild-type *Anabaena* PCC7120

Although the purified Alr3183 protein showed good peroxidase activity in vitro, this protein was poorly expressed in *Anabaena*. Moreover, as described earlier, there was a further reduction in the in vivo content of Alr3183 on exposure to the oxidizing agents. Apparently, Alr3183 was not synthesized in adequate amounts so as to offer protection from oxidative stresses. Hence, to gain insights into the ability of Alr3183 to protect *Anabaena* from oxidative stress, it was desired to over-express Alr3183 in *Anabaena* PCC 7120. For this purpose, a plasmid vector to over-express the Alr3183 protein was constructed. Subsequently, this vector was transferred to *Anabaena* by tri-parental conjugation and the over-expression of the Alr3183 protein in the recombinant *Anabaena* strain ($An3183^{+}$) was confirmed using the Alr3183 antiserum. The oxidative stress tolerance of the $An3183^{+}$ was assessed and compared with that of the wild-type *Anabaena.* All these aspects are presented in the ensuing sections.

3.13.2.1 Cloning of *alr3183* into pAM1956

The methodology employed to obtain a suitable plasmid construct to over-express Alr3183 in *Anabaena* is shown in Fig. 3.15.1. The plasmid, pAM1956, an *Anabaena*/*E. coli* shuttle vector, which carries the promoter-less *gfpmut2* was used for this purpose. As this plasmid does not have a promoter, a strong promoter was required to be inserted upstream of the *alr3183* ORF prior to transfer to pAM1956. The strong *Anabaena* promoter, P_{psbA1}, was used to drive the expression of the *alr3183* gene *in vivo*. Earlier, the P_{psbA1} promoter was cloned in the *Anabaena* PCC 7120 integrative vector pFPN [171]. Using NdeI and BamHI restriction sites, the *alr3183* ORF was released from the pET3183 and cloned downstream of the P_{psbA1} in pFPN (to give rise to pFPN3183). Subsequently, the *alr3183* ORF along with the P_{psbA1}

promoter was excised out of pFPN3183 (with XmaI and SalI restriction enzymes) and cloned upstream of *gfpmut2* in the similarly digested pAM1956 (to obtain pAM3183). In pAM3183, the *alr3183* and *gfp* are co-transcribed, but independently translated, resulting in production of both the proteins. Hence, the presence of pAM3183 can be verified by monitoring GFP expression by fluorescence microscopy.

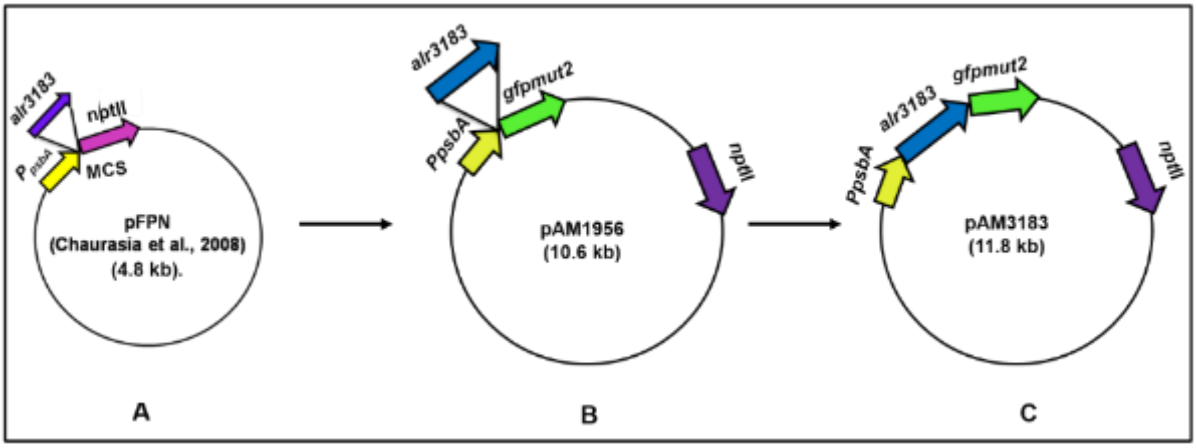

Fig. 3.13.2.1.1. Schematic representation of steps involved in preparation of construct for over-expression of Alr3183 in wild-type *Anabaena*. (A) Cloning of alr3183 into pFPN. The *alr3183* orf was excised out of pET*alr3183*, and ligated into similarly digested pFPN, to obtain pFPN3183. (B) PpsbA1-*alr3183* was excised from pFPN3183 using XmaI/SalI digestion and sub-cloned into pAM1956 vector, (C) In the resulting vector, pAM3183, PpsbA1 promoter drives expression of *alr3183* as well as gfpmut2.

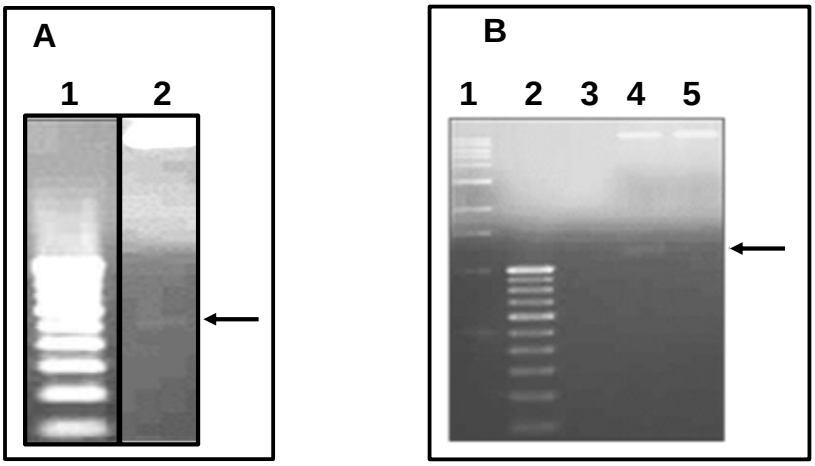

Fig. 3.13.2.1.1. Cloning of *alr3183* into pFPN and pAM. (A) Restriction digestion of pFPN3183. Lane1, 100 bp ladder (NEB); pFPN3183 digested with NdeI and BamHI. 450 bp long ORF is shown by arrow. (B) Restriction digestion of pAM3183. Lane1, 1kb DNA ladder (NEB); lane 2, 100bp DNA ladder (NEB); lane3, empty; lane 4, pAM3183 digested with XmaI and SalI; lane 5, undigested pAM3183. The 1.1 kb insert released is indicated by an arrow.

3.13.2.2 Over-expression of the Alr3183 protein in *Anabaena* PCC 7120.

For over-expression of Alr3183 in *Anabaena*, the pAM3183 construct was conjugated into *Anabaena* using a conjugal *E. coli* donor by tri-parental mating. The ex-conjugants ($An3183^+$) were selected on $BG11N^+$ agar medium supplemented with neomycin. Individual isolated colonies that appeared on the plate were inoculated in $BG11N^+$ medium with neomycin. The presence of pAM3183 was verified by monitoring expression of green fluorescence protein (GFP) under fluorescence microscope (Fig. 3.13.2.2A). On visual inspection, $An3183^+$ (*Anabaena* PCC7120 carrying pAM3183) cells showed green GFP florescence, indicating presence of pAM3183. In contrast, the untransformed wild-type *Anabaena* PCC 7120 strain appeared red due to the auto fluorescence of chlorophyll *a* (Fig. 3.13.2.2A).

For detection of Alr3183 protein in $An3183^+$, the cytosolic extract of $An3183^+$ was probed

with anti-Alr3183 antiserum. On developing the Western blot, an intense ~17 kDa band corresponding to Alr3183 was clearly observed in An3183^{+} cells whereas no such signal was observed in the wild-type cells. The ~17 kDa signal was not observed when the blot was probed with the control pre-immune serum suggesting that the ~17 kDa band was indeed Alr3183 and not some non-specific cross-reaction (Fig. 3.13.2.2B).

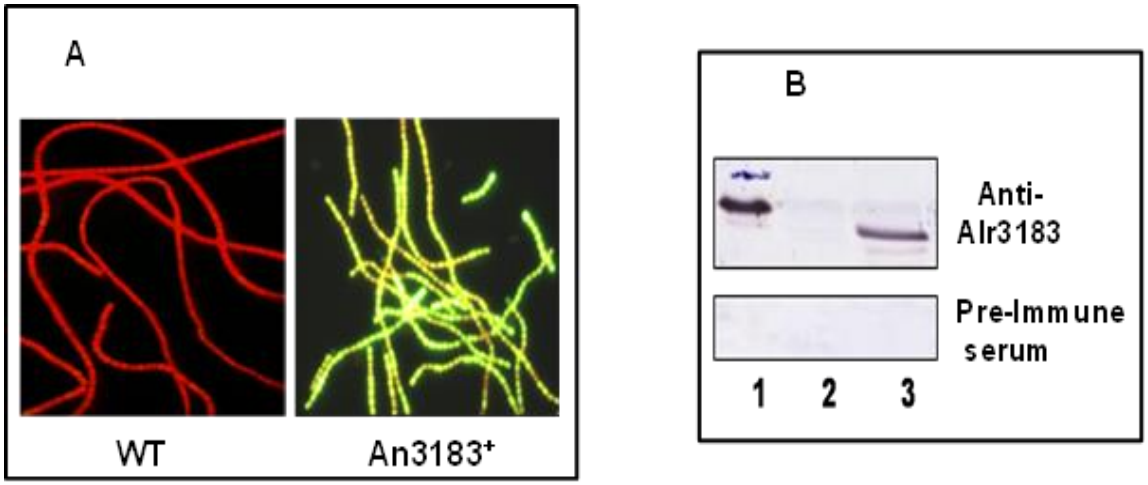

Fig. 3.13.2.2. Over-expression of Alr3183 in wild-type *Anabaena*. (A) Fluorescence micrographs. The recombinant An3183^{+} or wild-type *Anabaena* (WT) cells were grown in BG-11 medium for 3 days and fluorescence microphotographs (500X magnification) using Hg-Arc lamp (excitation BP, 450-490 nm and emission LP, 515 nm) were captured. (B) Over-expression of the Alr3183 protein in An3183^{+} strain. The WT *Anabaena* PCC 7120 or *Anabaena* PCC 7120 cells over-expressing Alr3183 (An3183^{+}) cells were harvested, cell-free extracts were prepared, proteins (20 μg per lane) were resolved by SDS/PAGE (12% gel), and immuno-detected with the anti-Alr3183 antiserum (1:10000 dilution) or pre-immune serum (as indicated). Lane 1, His-tagged Alr318 purified from *E. coli*; lane 2, wild-type *Anabaena* PCC 7120; lane 3, An3183^{+}.

3.13.3 Oxidative stress tolerance of the An3183^{+} and its comparison with the wild-type *Anabaena* PCC7120

3.13.3.1 Total ROS levels in response to H_2O_2

The intracellular levels of ROS in the wild-type *Anabaena* PCC7120 or *An*3183^{+} cells exposed to H_2O_2 (1 mM) were assessed with the fluorogenic probe DCHFDA. Under control conditions, ROS levels were very low in both types of cells. However, on exposure to 1 mM of H_2O_2, about 5-6 fold higher levels of ROS were observed in the wild-type *Anabaena* PCC7120 cells as compared to An3183^{+} cells (3.13.3.1). These results suggest that overproduction of Alr3183 reduces H_2O_2-mediated ROS generation in *Anabaena*.

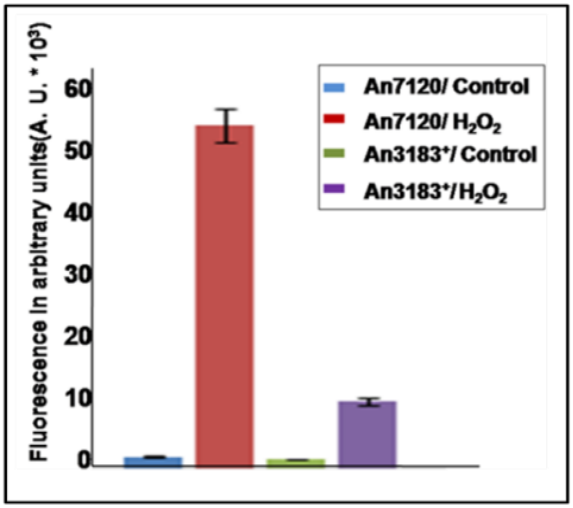

Fig. 3.13.3.1. Intracellular ROS formation in response to H_2O_2. The wild- type *Anabaena* PCC 7120 (An7120) or An3183+ cells were cells were grown for 3 days in BG11 medium and treated with H_2O_2 (1 mM) for 1h. Subsequently, cells were incubated with DCHFDA (10 µM final concentration) for 20 min and fluorescence emission (λ_{ex} = 490 nm, λ_{em} = 520 nm) was measured on a spectrofluorimeter. The relative fluorescence of control (untreated cells) nd H_2O_2-treated cultures is shown in the figure.

3.13.3.2 Oxidative stress tolerance of the An3183^{+}

Exponentially growing cultures of the wild-type *Anabaena* or An3183^{+} grown in BG-ll/N^{+} were subjected to H_2O_2 at 1 mM final concentration stress under stationary conditions. Two days treatment with H_2O_2 showed pronounced bleaching (Fig. 3.13.3.2.1A) caused by a sharp

reduction in the chlorophyll *a* content in the wild-type *Anabaena* PCC7120 stressed with H_2O_2, but the An3183$^+$ cells were fairly protected (Fig. 3.13.3.2.1B). After treatment with H_2O_2, filaments of the wild-type *Anabaena* PCC 7120 were completely fragmented and wide-spread lysis was observed. In contrast, filaments An3183$^+$ culture remained intact and cell lysis was not observed. (Fig. 3.13.3.2.2A). At the same point of time, the Alr3183 protein was clearly present in An3183$^+$ cells while none was observed in the corresponding wild-type cells (Fig. 3.13.3.2.2B). The An3183$^+$ cells successfully survived treatment with 1 mM H_2O_2 and could grow on agar plates whereas the wild-type cells showed complete loss of survival upon such treatment and did not form any colonies on plate (Fig. 3.13.3.2.3.).

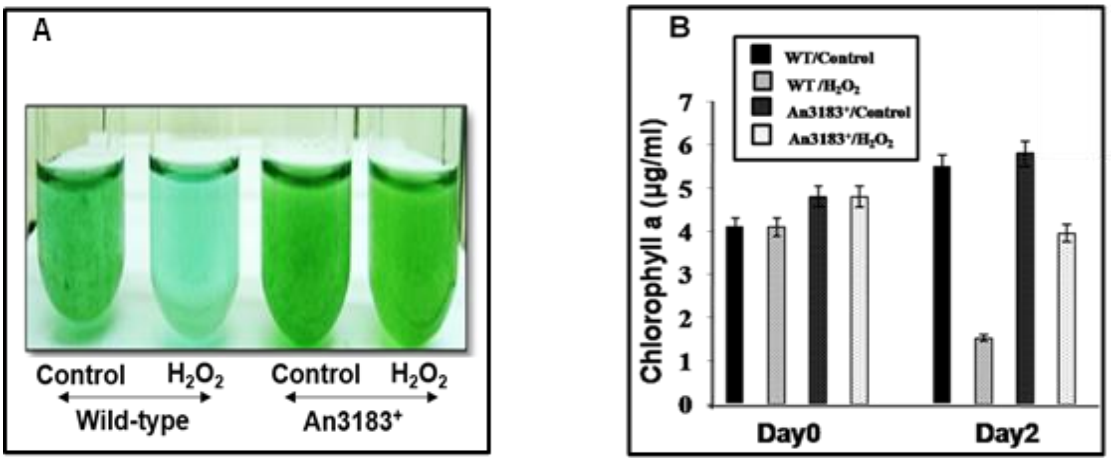

Fig. 3.13.3.2.1 Treatment of An3183$^+$ with 1 mM H_2O_2. (A) Three-day old wild-type *Anabaena* PCC7120 (WT) or An3183$^+$ were inoculated in fresh growth medium, subjected to H_2O_2 stress for 2 days and subsequently photographed. C, control; H_2O_2, 1 mM H_2O_2 (B) The chlorophyll *a* content of the wild-type *Anabaena* PCC7120 (WT) and An3183$^+$ shown in (A) was determined immediately (Day 0) or after 2 days of exposure to H_2O_2 (Day 2).

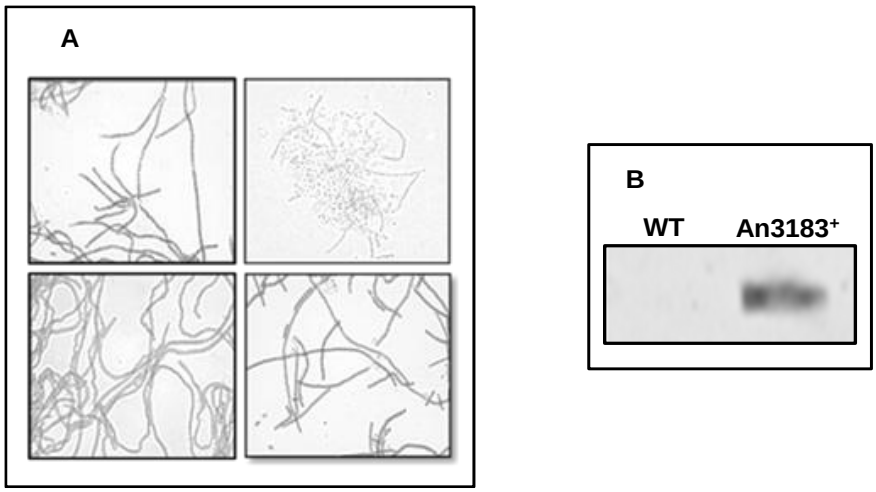

Fig. 3.13.3.2.2. Cell-lysis and Western blot. (A) WT or An3183$^+$ or cells were grown for 3 days in BG11 medium and subsequently treated with H_2O_2 (1 mM). After 2 days, these cultures were viewed under light microscope (500X magnification). (B) The cell-free extracts were prepared from the wild-type *Anabaena* (WT) or An3183$^+$ treated with 1 mM H_2O_2 were resolved (20 μg per lane) by SDS/PAGE and immuno-detected with the anti-Alr3183 antiserum (1:10 000 dilution). The **~17** kD Alr3183 is shown by an arrow.

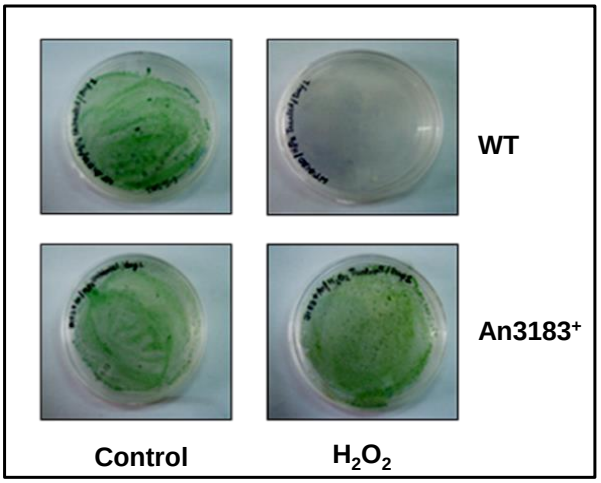

Fig. 3.13.3.2.3. Survival of *Anabaena* cultures in response to H_2O_2 (1mM). 100 µl culture of control or H_2O_2-treated *Anabaena* cells (after 2 days of treatment with H_2O_2) were plated on BG11N$^+$ agar plates. The plates were incubated under continuous illumination for 14 days and photographed.

Not only under nitrogen supplemented conditions, under nitrogen-deficient conditions too, An3183$^+$ was protected from the toxic effects of H_2O_2, whereas the wild-type remained susceptible.

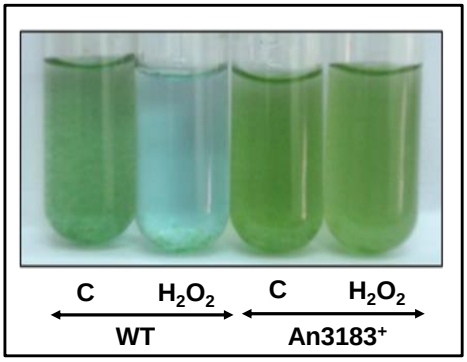

Fig. 3.13.3.2.4. WT or An3183^{+} or cells were grown for 3 days in BG11/N^{-} medium and subsequently treated with H_2O_2 (1 mM). The cultures were photographed after 2 days.

3.13.4 Over-expression of Alr3183C46S does not protect *Anabaena* from oxidative stress.

To confirm that the peroxidase activity of Alr3183 was indeed essential for protection from oxidative stress, the Alr3183C46S protein (that lacks the peroxide activity) was over-expressed in *Anabaena*. The strategy employed to over-express Alr3183 was also followed to over-produce Alr3183C46S in *Anabaena*. The *alr3183C46S* gene was cloned downstream of the strong light inducible P*psbA1* promoter in the pFPN vector (Fig.3.13.4.1). This ORF along with the P_{psbA1} promoter was subsequently sub-cloned into *E. coli-Anabaena* shuttle vector, pAM1956 (construct denoted as pAM3183C46S) Fig.3.13.4.2. This plasmid was conjugated into *Anabaena* PCC 7120 to obtain the An3183C46S^{+} strain.

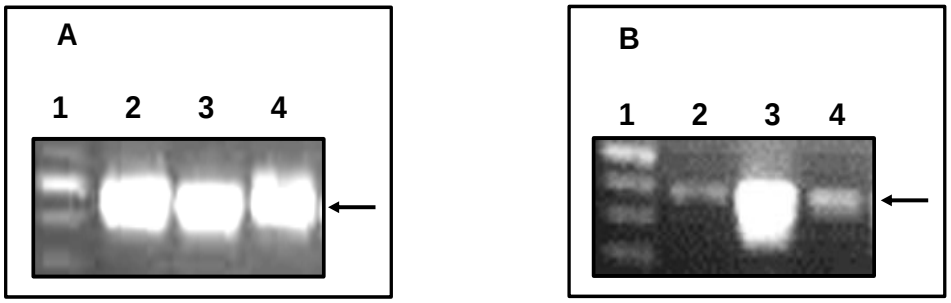

Fig. 3.13.4.1. Cloning of *alr3183C46S* into pFPN and pAM. (A) Cloning of *alr3183C46S* into pFPN. PCR of *E. coli* pFPN3183C46S colonies with *alr3183* cloning primers i. e. *alr3183fwd* and *alr3183rev*. Lane 1, 100 bp ladder (NEB); lane2, PCR of colony # 1; lane3, PCR of colony # 2; lane 4, PCR of colony #4. The PCR product is shown with arrow. (B) Cloning of *alr3183C46S* into pAM1956 (1) PCR of *E. coli* pAM*3183C46S* colonies using Alr3183fwd and $P_{alr3183rev}$. Lane 1, 100 bp ladder (NEB), lane2, PCR of colony # 1; lane3, PCR of colony # 2; lane 4, PCR of colony #4. The PCR product is shown by arrow.

The recombinant strain, An3183C46S$^+$, showed expression of the GFP, and the Alr3183C46S protein too was readily produced in An3183C46S$^+$ (Fig. 3.13.4.2A and B). The ability of An3183C46S$^+$ to withstand oxidative stress was verified. Logarithmic phase cultures of the wild-type *Anabaena* or An3183C46S$^+$ were subjected to H_2O_2 (1 mM) stress under stationary conditions in BG11/N$^+$ medium. Treatment with H_2O_2 for 2 days resulted in pronounced bleaching of filaments and a sharp reduction in the chlorophyll *a* content in the wild-type *Anabaena* as well as the recombinant An3183C46S$^+$ (Fig. 3.13.4.3A and B). These results indicated that An3183C46S$^+$ was not able to protect the *Anabaena* from H_2O_2-mediated damage and was as sensitive as the WT *Anabaena.*

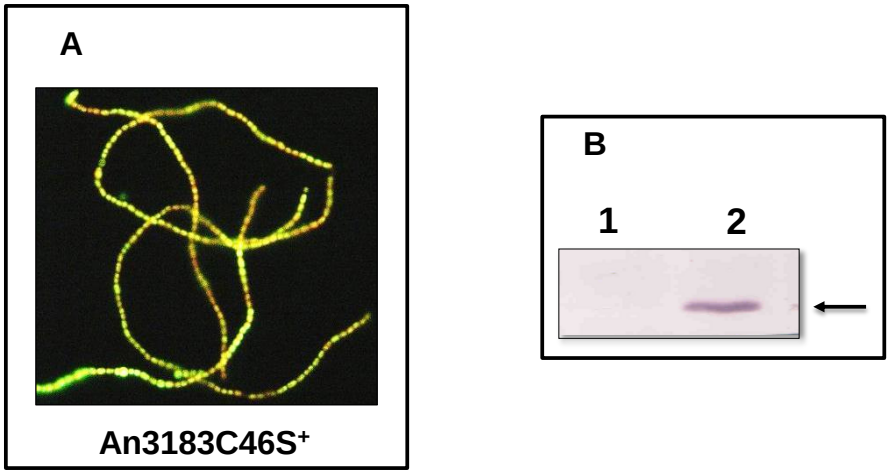

Fig. 3.13.4.2. Over-expression of Alr3183C46S in *Anabaena.* (A) The An3183C46S^{+} culture was visualized under fluorescence microscope microscope using Hg-Arc lamp (excitation BP, 450–490 nm and emission LP, 515 nm). (B) Cell-free extracts from wild- type *Anabaena* (WT) or An3183C46S^{+} were resolved by SDS-PAGE (30 µg per lane), electro blotted on to nitrocellulose membrane, and probed with the Alr3183 antiserum (1:10000 dilution). The ~17 kDa Alr3183C46S band is shown by an arrow.

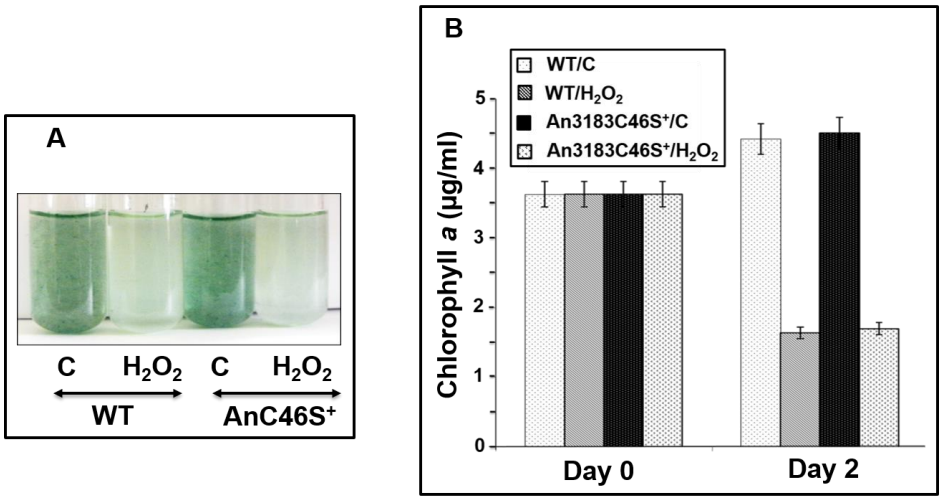

Fig. 3.13.4.3. Over-expression of Alr3183C46S in *Anabaena.* (A) Three-day old wild-type *Anabaena* PCC 7120 (WT) or An3183C46S^{+} were subjected to 1mM H_2O_2 stress in tubes and photographed after 2 days. (B) The chlorophyll *a* content of the wild-type *Anabaena* (WT) or An3183C46S^{+} shown in (A) was determined immediately (Day 0) or after 2 days of exposure to H_2O_2 (Day 2).

3.14 Alr3183 is induced in response to ionizing radiation and mitomycin C

Earlier micro-array experiments from our laboratory had shown *alr3183* to be induced in response to ionizing-irradiation. To verify if Alr3183 was indeed induced *in vivo*, the wild-type *Anabaena* PCC 7120 was irradiated with different doses of gamma radiation and inoculated in fresh medium. Subsequently, production of the Alr3183 protein during recovery was verified on Western blots with the Alr3183 antiserum. Interestingly, Alr3183 protein was found to be distinctly induced in response to γ-radiation (Fig. 3.14.1A). At lower doses (0.5 and 1 kGy), the Alr3183 protein was observed 3 h post irradiation and could be clearly observed till day 3, after which it subsequently disappeared by day 5. With increasing dose of γ-radiation (3 and 6 kGy), the levels of Alr3183 protein remained high for a longer duration and gradually decreased with time. For example, noteworthy amount of the Alr3183 protein was observed even after 8 days of exposure to 6 kGy dose of γ-radiation (Fig. 3.14.1A). Nitrogen status of the BG11 medium did not affect the induction of the Alr3183 protein and even in the absence of combined nitrogen (i.e. under nitrogen-fixing conditions); production of Alr3183 was observed on exposure to γ-radiation (Fig. 3.14.1B).

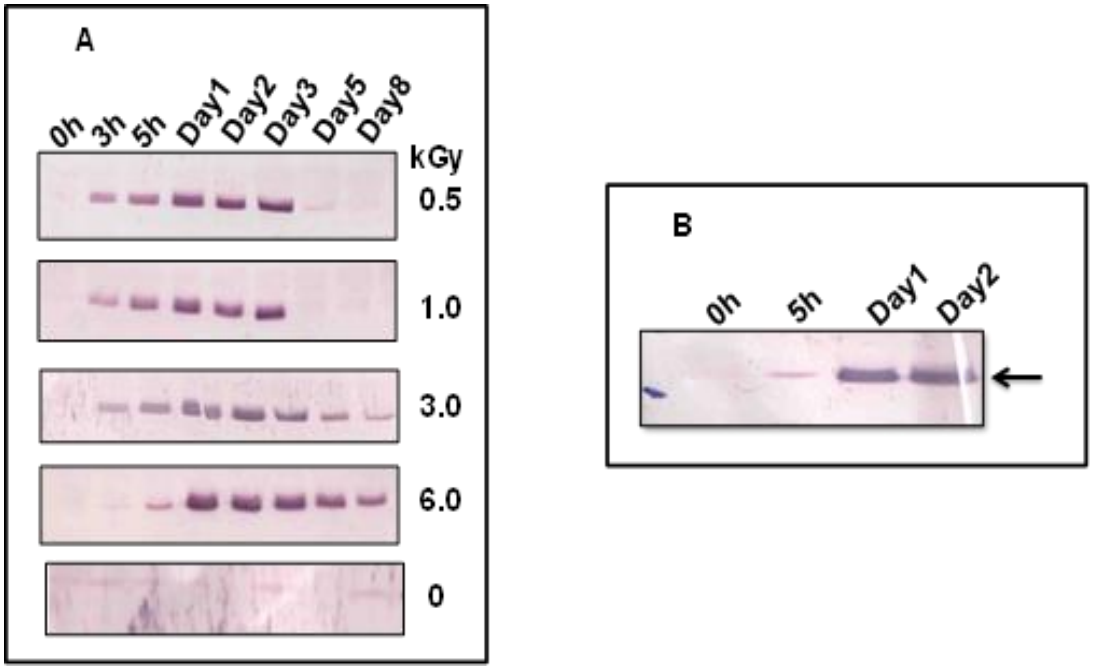

Fig. 3.14.1. Induction of Alr3183 in *Anabaena* PCC7120 in response to gamma radiation. (A) Four-day old *Anabaena* PCC7120 cells grown in $BG11N^{+}$ medium were subjected to different doses of gamma radiation, total proteins were extracted at the time points indicated in the figure and probed with the Anti-Alr3183 antiserum. (B) *Anabaena* PCC7120 culture was grown in $BG11N^{-}$ medium (lacking combined nitrogen) for 4 days, exposed to 6 kGy of gamma radiation and processed as mentioned in (B).

Ability of mitomycin C, another agent that causes DNA double stranded breaks, to induce expression of Alr3183 was monitored in *Anabaena*. As shown the Fig. 3.14.1, addition of mitomycin clearly induced expression of the Alr3183 protein in *Anabaena*.

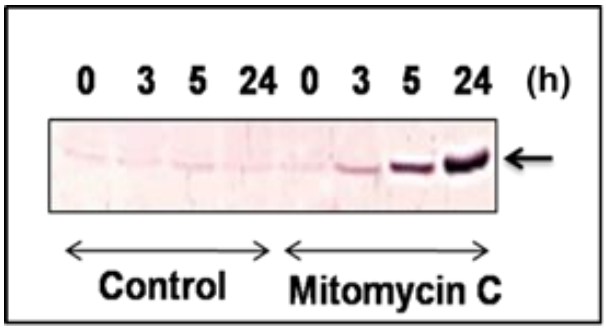

Fig. 3.14.2. Induction of Alr3183 in *Anabaena* PCC7120 in response to mitomycin C. Four-day old *Anabaena* PCC7120 cells grown in $BG11N^+$ medium was treated with mitomycin C (2.5 µg/ml), total proteins were extracted at the time points indicated in the figure probed with the Anti-Alr3183 antibody.

3.16 Knock-down of *alr3183* in *Anabaena* PCC7120 and the response of the knock-down strain to gamma radiation

Antisense RNA–mediated approach was employed to reduce expression of the Alr3183 protein on exposure to gamma radiation. The complete *alr3183* ORF was cloned in the reverse orientation (i.e. antisense) downstream of the light inducible P_{psbA1} promoter in the pFPN vector (pFPNAS3183) (Fig.3.15.1A). The DNA fragment containing the P_{psbA1} promoter and antisense *alr3183* was afterwards transferred to pAM1956 (construct denoted pAMAS3183), upstream of the *gfp*. The pAMAS3183 was sequenced to confirm the appropriate orientation of the *alr3183* ORF in this construct. The pAM3183 is schematically depicted in Fig.3.15.1A. The pAMAS3183 construct was subsequently conjugated into *Anabaena* PCC7120, to give rise to $AnAS3183^+$. The efficiency of the antisense-mediated decrease in the production Alr3183 was monitored on Western blots after exposure to radiation. As compared to the wild-type *Anabaena*, a distinct decrease in the synthesis of the Alr3183 protein was observed in $AnAS3183^+$ on exposure to γ-radiation (Fig.3.15.1B). The wild-type *Anabaena* PCC7120 and $AnAS3183^+$ were both exposed to 3 kGy dose and their

growth was monitored over a two-week period post irradiation. The AnAS3183^{+} showed a decreased growth as compared to the wild-type (Fig. 3.15.2), suggesting a role of Alr3183 in overcoming radiation stress.

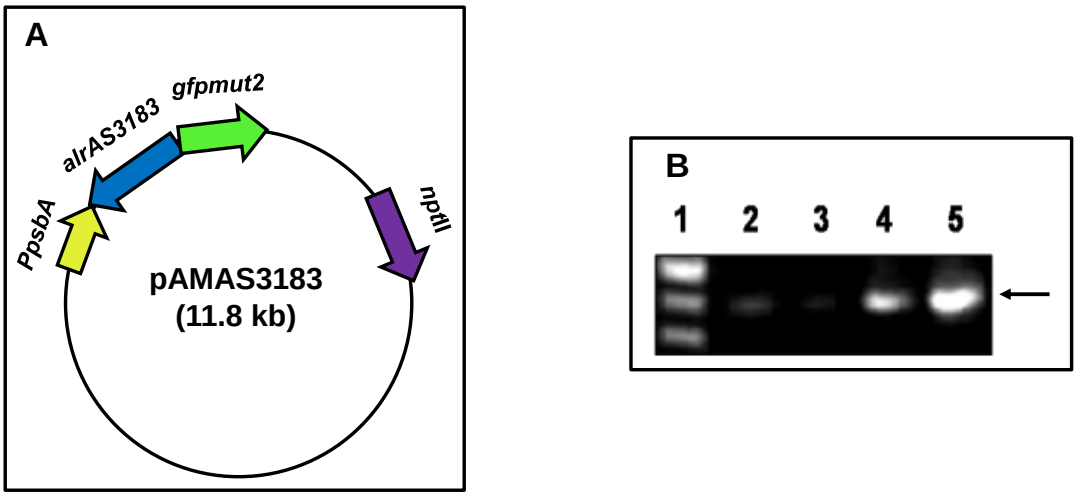

Fig. 3.15.1. Cloning of AS3183 **in *Anabaena*.** (A) Schematic representation of the AnAS3183^{+} construct. Various elements and size of the plasmid are shown. (B) PCR of DH5α pAM*alrAS3183* colonies using *alr3183* cloning primers. Lane 1, 100 bp ladder (NEB), lane 2, PCR of colony #1; lane 3, PCR of colony #2, lane 4, PCR of colony #3; lane 5, PCR of colony # 4. PCR product is shown by arrow.

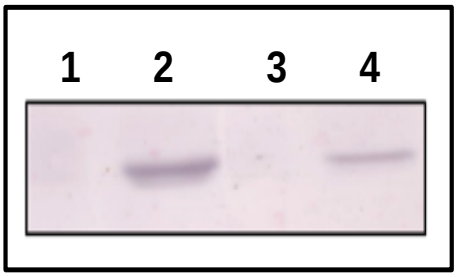

Fig. 3.15.2. Reduction of Alr3183 in AnAS3183^{+} strain in response to gamma radiation. Four-day old *Anabaena* PCC7120 and AnAS3183^{+} cells, grown in BG11N^{+} medium were left untreated or exposed to gamma radiation (3.0 kGy), total proteins were extracted at day 1 of post-irradiation recovery probed with the Anti-Alr3183 antibody.

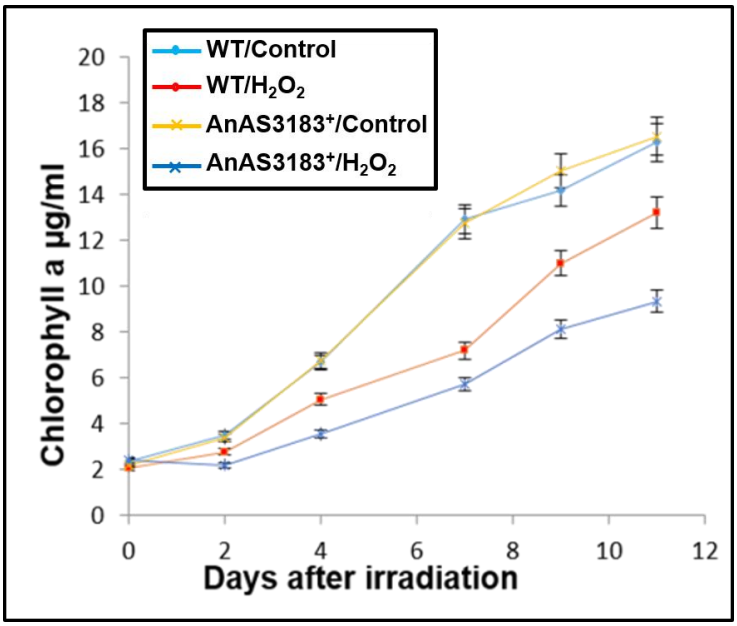

Fig. 3.15.3. Growth of *Anabaena* on exposure to radiation. The wild-type (WT) or the AnAS3183$^+$ strain was exposed to 3 kGy dose of gamma radiation and allowed to recover in fresh BG-11/N$^+$ medium under usual growth conditions. Growth was measured as increase in the content of chlorophyll *a* for 12 days.

3.14 Discussion

The PrxQ/BCP proteins are widely distributed in bacteria, archaea, plants and lower eukaryotes. Initially, BCP/PrxQ proteins were observed to be present in few pathogenic bacteria such as *Mycobacterium tuberculosis* and were hypothesized to play a role in pathohenesis [116, 102]. Presently, analysis of sequenced genomes shows them to be present in many different genera of bacteria, including several non-pathogenic ones [116]. Interestingly, such proteins appear to be absent in higher animals [116]. PrxQ proteins have been found in all the sequenced cyanobacterial genomes [160], suggesting that these may play an important role in cyanobacterial physiology. Among cyanobacteria, Alr3183 like proteins are observed both in filamentous cyanobacteria (e. g. *Anabaena*), as well as in

unicellular cyanobacteria (e.g. *Synechococcus*). In this study role of Alr3183, a PrxQ-like protein from a filamentous cyanobacterium *Anabaena* was evaluated.

The *alr3183* ORF from *Anabaena* PCC 7120 was cloned and over-expressed in *E. coli*. The overexpressed Alr3183 protein was located in the soluble fraction and could be purified using affinity chromatography (Fig. 3.4.2.1) However, the purified protein was observed as two bands at its monomeric position when resolved on reducing PAGE (Fig. 3.16.1A). Mass-Spectrometric analysis identified both the bands as Alr3183. Electrophoretic mobility of a reduced protein (i.e. free –SH group present) is known to be differ from that of its oxidized form (i.e. when disulfide linkages are present) [207, 208]. The oxidized form, because of its more compact structure moves slightly faster than the reduced form. As the two bands at the monomeric position were conclusively identified to be Alr3183, the lower band likely to correspond to the oxidized Alr3183 protein (i.e. C_p-C_r form disulphide bond) whereas the upper bond is possibly the reduced form of Alr3183 (i.e. C_p-SH and C_r-SH are free and not disulfide bonded). It should be noted that at the concentration used, DTT could not completely reduce Alr3183, and some oxidized Alr3183 (i.e. lower band) was always observed on gels along with the reduced form. However, in the absence of DTT, only a single band that matched the position of the lower band of the DTT-treated sample was observed. These results indicate that the Alr3183 protein isolated from *E. coli* exists in oxidized form.

The nature of the disulfide bond formed (i.e. intermolecular/intramolecular) by a Prx not only depends on the Prx subfamily that particular Prx belongs to, but also depends on the availability of the catalytic cysteines. For example, the wild-type All1541 (Type II Prx from

Anabaena) is distributed among its monomeric and dimeric forms. However, a mutant version of this protein that lacks the C_p is monomeric, whereas All1541 without the C_r isdimeric [152]. In Alr4641, the 2-Cys-Prx from *Anabaena* PCC 7120, dimerization occurs due to disulphide bond formation between the C_p of one subunit and the C_r of another subunit [162]. But, if any of the two-cysteine residue is lost, the 2-Cys-Prx protein is unable to dimerize [162]. The wild-type Alr3183 exists as a monomer, and interestingly, in contrast to All1541 or Alr4641, when either of the cysteine residue is lost (Alr3183C46S or Alr3183C51S) the protein forms intermolecular disulfide bond and becomes dimeric (Fig.3.12.1A and 3.12.1). So, the presence of both the cysteines appears to preclude the formation of intermolecular disulfide bond and intermolecular disulfide bond formation predominates in Alr3183.

The Alr3183 protein showed a high TrxA-dependent peroxidase activity, whereas the DTT-dependent or the GSH-dependent peroxidase activity was very low (Fig.3.9.1A). These results are in agreement with the study of Cha et al. [166] who also showed PrxQ proteins from *Anabaena* to show a TrxA-dependent activity. The wild-type Alr3183 showed the best peroxidase activity, Alr3183C51S showed considerably reduced activity whereas Alr3183C46S was completely inactive (Fig.3.13.1). Thus, the formation of disulfide bonds alone is not adequate for peroxidase activity; these bonds have to form in the right context, with the right partner. The presence of both C_p and C_r prohibits intermolecular disulfide bond formation, but, if either of the catalytic cysteine is absent, the protein becomes dimeric due to formation intermolecular C_p-C_p or C_r-C_r linkages.

The SPR technique can be gainfully utilized to explore the influence of the cysteine residues/disulfide bonds on the ability of Prxs to interact with Trxs. Recently, Hara and Hisabori [209] used this technique to observe the interaction of chloroplast peroxiredoxin Q

(PrxQ) from *Arabidopsis thaliana* with its cognate Trx, Trxh1. However, in their study, the PrxQ protein failed to interact with the wild-type Trxh1 protein, but interaction could be observed only with a mutant $Trxh1_{CS}$ that lacked the second cysteine in its catalytic domain. In contrast, in the present study, the wild-type Alr3183 protein readily interacted with the immobilized TrxA. During the reaction cycle, for regenerating the free thiol form of C_p, the oxidized Prx has to interact with TrxA (for reduction), and once reduced, Prx has to dissociate from TrxA, so that Prx can undergo the next round of reaction [210]. The purified Alr3183 protein (which exists in oxidized state), showed enhanced association with TrxA as compared to the Alr3183 protein that was reduced with DTT (Fig. 3.10.2). Thus, reduction of Alr3183 appears to decrease its ability to interact with TrxA, which in turn may facilitate the dissociation between the two once the disulfide bond exchange has occurred.

The Alr3183 lacking the C_r (Alr3183C51S) also functions as a peroxidase, albeit poorly. Similar to Alr3183C51S, the C_r mutants of PrxQ from Poplar or *Rhodobacter sphaeroides* also dimerize and show peroxidase activity. All the PrxQ homodimers that lack the resolving cysteine are suggested to form an atypical active site that contains the two peroxidatic cysteine residues [183]. It should be noted that Alr3183C51S requires higher concentration of TrxA to show detectable peroxidase activity *in vitro* (Fig. 3.9.4.1). Interestingly, the Alr3183C51S (or Alr3183CDM) that lack C_r show decreased ability to interact with TrxA than the wild-type Alr3183 protein or the Alr3183C46S, which have C_r (Fig.3.10.1). Taken together, these two aspects underscore the importance of C_r for promoting interaction between Alr3183 and TrxA for efficient peroxidase function. The presence of C_r appears to facilitate the recruitment of TrxA, which would rapidly reduce the oxidized cysteines, consequently speeding up the reaction.

On exposure to excess of H_2O_2, the thiol group of the peroxidatic cysteine undergoes

overoxidation to form sulphinic acid (SO_3H) [161, 152]. This modification renders the Prx inactive, i.e. it can no longer function as a peroxidase [161]. In fact, both Alr4641 and All1541 from *Anabaena* PCC 7120 have been shown to be easily inactivated by high concentrations of H_2O_2, [152, 162]. In comparison, the Alr3183 protein remained active even after exposure to 5 mM H_2O_2, indicating that it was more recalcitrant to over-oxidation than the two above-mentioned Prxs, and can work in more oxidizing conditions than other 2-Cys Prx.

Why does *Anabaena* encode so many PrxQ proteins? The presence of multiple PrxQs in *Anabaena*, apparently catalyzing similar reactions, may not be a case of redundancy. A particular PrxQ may be induced in response to a specific stress in *Anabaena*. For example, All2375 alone is induced by NaCl and diamide whereas Alr2503, All2375 and All2556 are all induced by t-butyl hydroperoxide, but Alr3183 is not [166]. Among the various stresses/oxidizing agents tested, the Alr3183 protein was induced only in response to gamma radiation. Ionizing radiation such as gamma radiation not only causes double stranded breaks (dsbs) in DNA, but also causes severe oxidative stress [17]. Along with other ROS, exposure to gamma radiation also leads to the formation of H_2O_2 and lipid peroxides [211], both of which are substrates of Alr3183 [166]. Moreover, reduced growth of the AnAS3183 strain in response to 3 kGy gamma radiation does argue for a role of Alr3183 in overcoming oxidative stress. The induction of Alr3183 by gamma radiation, but not by peroxides is perplexing. Interestingly, Alr3183 expression was also observed when *Anabaena* PCC 7120 was exposed to mitomycin C, an agent that causes DNA double strand breaks (Fig. 3.13.5.2). Thus, there appears to be a link between expression of Alr3183 and the formation of DNA dsbs in *Anabaena*.

In particular, the filamentous strains of cyanobacteria, including *Anabaena*, are very sensitive to the oxidative effects of H_2O_2 [212, 153]. Under normal (i.e. unstressed) conditions,

Anabaena shows very poor catalase expression and no catalase activity can be detected on zymograms [153]. In fact, H_2O_2 and methyl viologen also fail to induce catalase expression in *Anabaena*. As *Anabaena* shows a preponderance of genes that encode Peroxiredoxins, it is believed that these may be the proteins that defend *Anabaena* from peroxides such as H_2O_2. H_2O_2 and methyl-viologen both induce Alr4641 & All1541, but do not elicit production of Alr3183 in *Anabaena* PCC 7120. Likely, Alr4641 and All1541 (but not Alr3183) could be the principal players that protect cell from H_2O_2 under normal physiological conditions. However, it should be noted that induction of Alr4641 or All541 that normally occurs in response to externally added H_2O_2 is not adequate to protect *Anabaena* from its toxicity. Addition of as little as 1 mM of H_2O_2 causes rapid degradation of chlorophyll *a*, resulting in complete collapse of *Anabaena* cultures and cell death (Fig. 3.13.1) However, if Alr3183 is over-expressed in *Anabaena,* cells are protected from the damaging consequences of H_2O_2, both under nitrogen-supplemented as well as nitrogen-deficient conditions. Unlike the wild-type, on exposure to H_2O_2, the An3183$^+$ strain showed substantially reduced ROS formation, lower damage to pigments and consequently, the cells remained viable d (Fig.3.13.2).

Although known to function primarily as peroxidases, Prxs are now also known to be involved in redox signalling [213] or function as chaperones [214, 162] or phospholipases [215]. In fact, other activity as the phospholipase or the chaperone activity of Prxs has been shown to be independent of the catalytic cysteine residues. To exclude the possibility that Alr3183 would mediate its protective role (against H_2O_2) independent of the peroxidase activity, the mutant Alr3183C46S protein (that lacks the peroxidase activity) was over-expressed in *Anabaena*. Like the wild-type strain, the Alr3183C46S$^+$ strain was also very susceptible to H_2O_2. This demonstrates that the protective role of Alr3183 protein in *Anabaena* against H_2O_2 mediated oxidative stress is due to the peroxidase activity mediated

by peroxidatic cysteine. This highlights the importance of peroxidatic cysteine of Alr3183 protein for *in vivo* detoxification of H_2O_2 in *Anabaena*. In response to different abiotic stresses, the *alr3183* gene transcript was not enhanced in *Anabaena.* Gamma radiation (a physical agent that causes oxidative stress) can increase production of the *alr3183* transcript/ Alr3183 protein (Fig. 3.12.3).

Treatment of the *Anabaena* PCC 7120 with H_2O_2 (a) increased production of ROS (b) decrease in photosynthetic activities and (c) loss in viability. In the cyanobacterium *Microcystis aeruginosa*, H_2O_2 treatment caused enhanced ROS accumulation, which results in destruction of pigment synthesis and led to cell death [216]. However, all the above mentioned deleterious effects were alleviated in An3183$^+$ strain, indicating that Alr3183 can protect *Anabaena* from oxidative stress.

In conclusion, Alr3183 was found to be a monomeric, TrxA-dependent peroxidase whose C_p and C_r, formed an intramolecular disulfide bond. The presence of both C_p and C_r prohibited intermolecular disulfide bond formation, but, if either of the catalytic cysteine was absent, the protein became dimeric due to the formation of intermolecular C_p-C_p or C_r-C_r linkages. C_p was essential for reacting with the peroxidatic substrate whereas the presence of C_r appeared to improve the protein's capability to interact with TrxA. *In vivo*, Alr3183 was found to be a stress-inducible protein whose synthesis was upregulated by γ-radiation. Over-expression of Alr3183 protected *Anabaena* from oxidative stress in nitrogen-supplemented as well as nitrogen-deficient conditions, indicating the potential of An3183$^+$ to function as stress-resilient biofertilizer.

Chapter 4 - Characterization of Alr4642

4.1 Introduction

The Alr4642 protein from the heterocystous filamentous cyanobacterium *Anabaena* PCC7120 is a member of the Prx-like family of peroxiredoxins. Prx-like family of peroxiredoxins represent the recently identified sub-family of peroxiredoxins [160]. Initially, members of this family were annotated as hypothetical proteins. The Prx-like proteins contain the CXXC motif, which is characteristic of thioredoxins (Trx) and glutaredoxins (Grx) proteins [160]. The Prx-like proteins belong to the thioredoxin (TRX)-like superfamily, which is a large and diverse group of proteins that show the presence of a TRX fold. Members of this family also show the characteristic AhpC/TSA domain (https://www.ncbi.nlm.nih.gov/ Structure/cdd/wrpsb.cgi).

The Prx-like proteins are further subdivided into Prx-like1 and Prx-like2. In Prx-like1, the conserved peroxidatic cysteine aligns with the first cysteine of the CXXC motif, whereas, in the Prx-like2 proteins, the peroxidatic cysteine corresponds to the second cysteine of the above-mentioned motif. Although these proteins (Prx-like1 and Prx-like2 proteins) have the conserved peroxidatic cysteine, the other two conserved residues of the catalytic triad (Tyr & Arg) of peroxiredoxins are absent. The Alr4642 protein is a Prx-like2 subfamily of Peroxiredoxins.

In Prx-like2 proteins, the CXXC motif is present close to the N-terminal end of the protein, usually between amino residues 44-67. 17 Prx-like2 proteins have been annotated (i.e. 6.96% of the total peroxiredoxins found) among the 37 cyanobacterial genomes sequenced so far, Interestingly, all the five filamentous cyanobacteria whose genome has been sequenced (*Anabaena* sp. PCC 7120, *Anabaena variabilis* ATCC 29413, *Arthrospira platensis* NIES-39, *Nostoc punctiforme* ATCC 29133, and *Trichodesmium erythraeum* IMS101), show the presence of the Prx-like2 proteins.

As mentioned in the introduction, the role played by various peroxiredoxins in overcoming oxidative stress in the filamentous, heterocystous diazotrophic, cyanobacterium *Anabaena* PCC7120 has generated lot of interest in the recent past [166, 152, 167, 162]. However, in spite of garnering all this attention, some Prxs from *Anabaena*, especially those belonging to the Prx-like family, have not been studied at all. In fact, not only from *Anabaena*, Prx-like proteins have not been characterized from any bacterium so far. Hence, it was desired to elucidate the role of Alr4642, a Prx-like2 protein from *Anabaena* PCC 7120.

4.2 Bioinformatic analysis of Alr4642

4.2.1 Chromosomal location, nucleotide and amino acid sequence

In *Anabaena* PCC7120, *alr4642* (642 bp) is located between nucleotide position 5545507 to 5546148 on the main chromosome (Fig. 4.2.1.1) and is annotated as putative thiol-specific antioxidant protein. Just upstream of *alr4642* lies the gene *alr4641* that encodes 2-Cys-Prx protein (i.e. Alr4641), whereas *alr4643*, ORF that encodes the chaperone, DnaJ, is present downstream of the *alr4642* ORF, but in the reverse orientation, (http://genome.microbedb.jp/cyanobase/*Anabaena*/genes/alr4642).

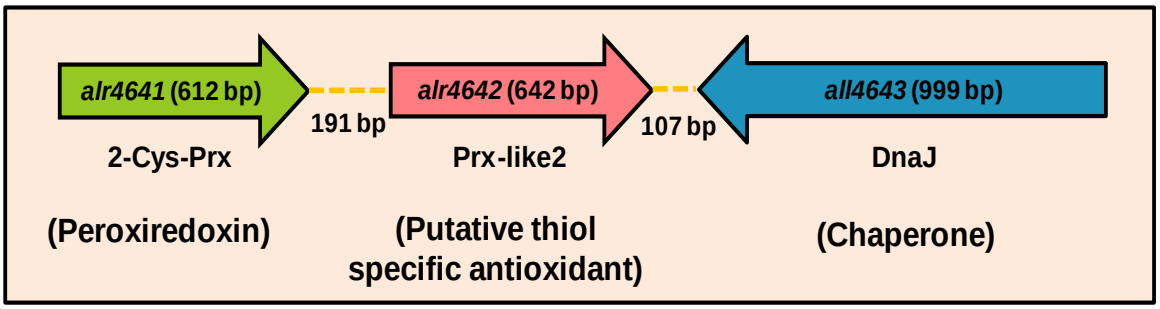

Fig. 4.2.1.1. Schematic depiction of *alr4642* on *Anabaena* PCC7120 chromosome. Along with the *alr4642* ORF, ORFs present in the vicinity of *alr4642* are also shown. The respective nucleotide sizes are indicated in the figure. The protein encoded by the respective ORF is depicted below the ORF. Arrowheads indicate direction of the transcription. The length (in bp) of the intergenic region (dashed line) is also represented.

The 642 bp long nucleotide sequence of the complete *alr4642* ORF along with its translated 213 amino acid sequence (obtained from http://genome.microbedb.jp/cyanobase /Anabaena/genes/*alr4642*) is shown in the Fig. 4.2.1.2. The Alr4642 protein has methionine residues located at the 1st and the 36th amino acid position, respectively. The putative catalytic cysteine (second cysteine in the CXXC motif) is the 111th residue of the polypeptide chain. Hereafter, the full-length protein (initiating from first methionine codon) is designated as Alr4642, whereas the protein initiating from the second methionine is designated as AlrT4642, (T for truncated). The AlrT4642 is 178 amino acids long.

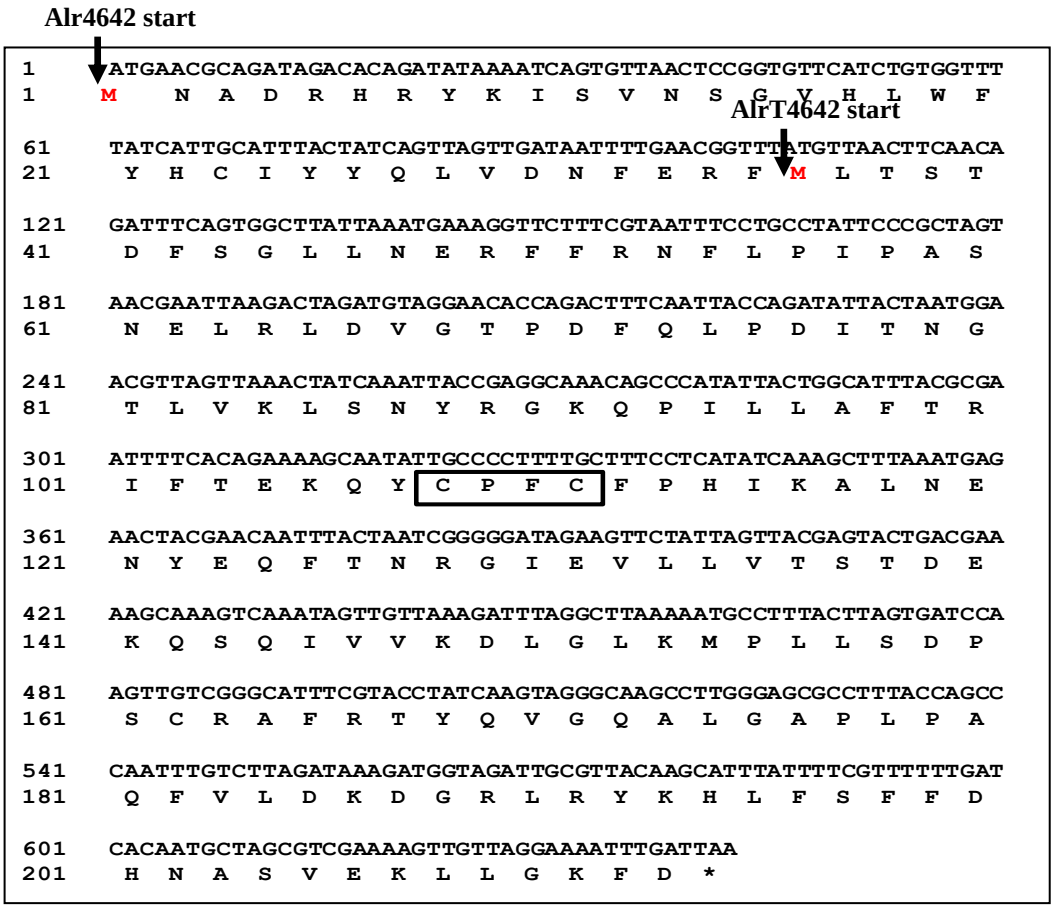

Fig. 4.2.1.2 Primary sequence analysis of *alr4642*/Alr4642. The 213 amino-acid long Alr4642 polypeptide is shown as one letter symbol along with its coding nucleotide sequence. The First and the second methionine are shown in red colour. The CXXC motif (CPFC in Alr4642), which is a characteristic of Prx-like2 proteins is boxed. The full-length protein (i.e. initiating from first methionine codon) is designated as Alr4642 whereas the protein initiating from the second methionine is designated as AlrT4642, (T for truncated). The AlrT4642 is 178 amino acids long.

4.2.2 Alr4642 protein shows similarity to other Prx-like2 proteins from its second methionine residue

BLASTp search for proteins homologous to Alr4642 using its amino acid sequence as query and the cyanobacterial genome sequences as the target sequence (http://blast.ncbi.nlm.nih.gov/Blast.cgi) revealed the Alr4642 protein to be a putative thiol-specific antioxidant (TSA) protein having similarity to Prxs (Fig 4.2.2). Among Prxs, the

Alr4642 protein showed extensive homology to Prx-like2 family of peroxiredoxins, which are hypothetical proteins with sequence similarity to Prxs. Interestingly, the BLASTp analysis showed the Alr4642 protein to display similarity with other Peroxiredoxins from its second methionine residue that was 35 amino acids away from the first (Fig. 4.2.2). Also, most of the homologous cyanobacterial proteins showed similarity to Alr4642 only from the 36th amino acid. The ORF initiating from the second ATG codon was therefore designated as *alrt4642* (wherein t stands for truncated). Not surprisingly, in this analysis, the highest similarity (identity, 70-80%, positives, 80-90%) was observed with related proteins from filamentous cyanobacteria e.g. *Nostoc*, *Anabaena*, *Fischerella* etc. Relatively lower homology was observed with similar proteins from unicellular cyanobacteria such as *Thermosynechococcus elongates* (identity, 58%, positives, 74%).

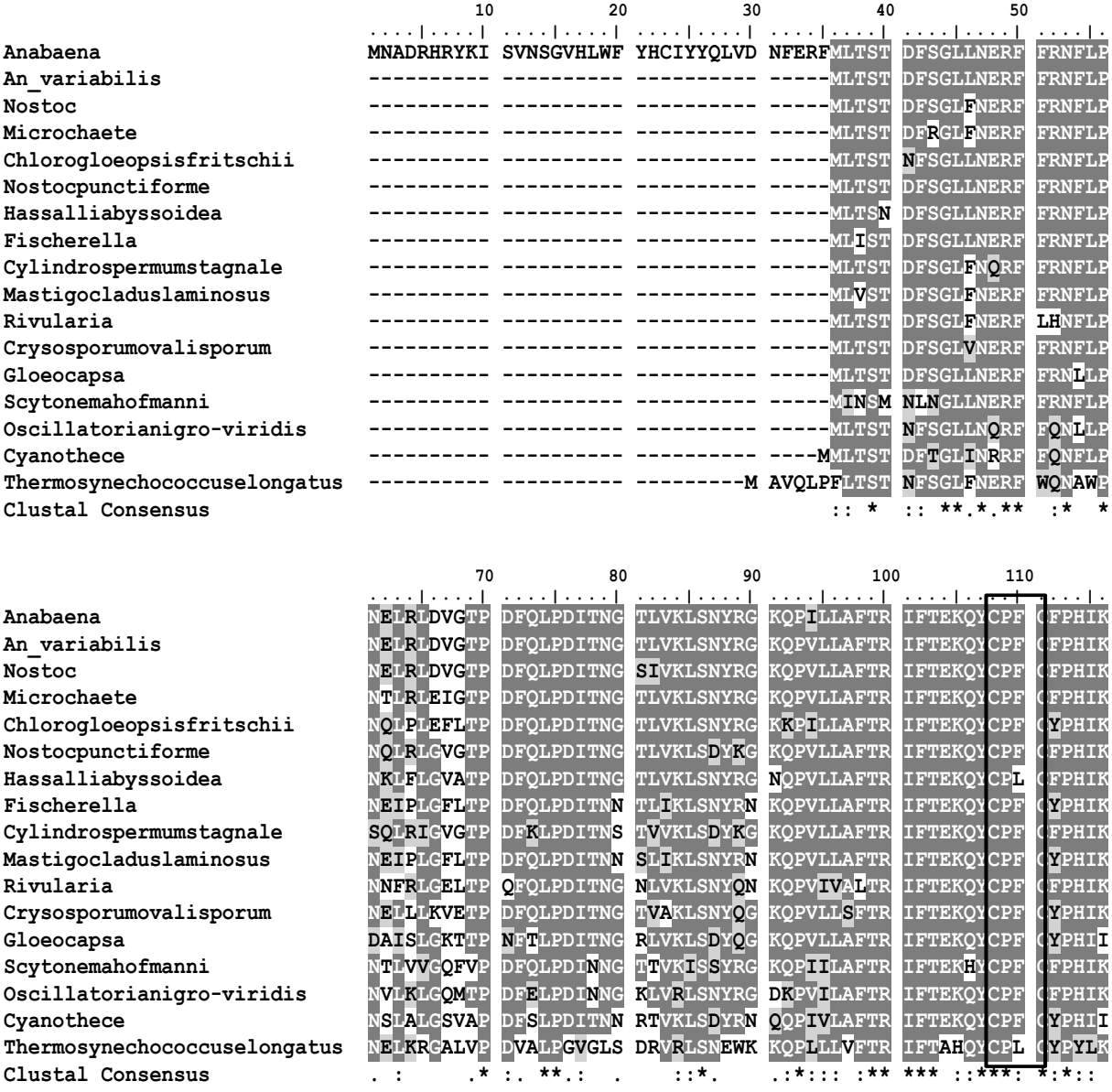

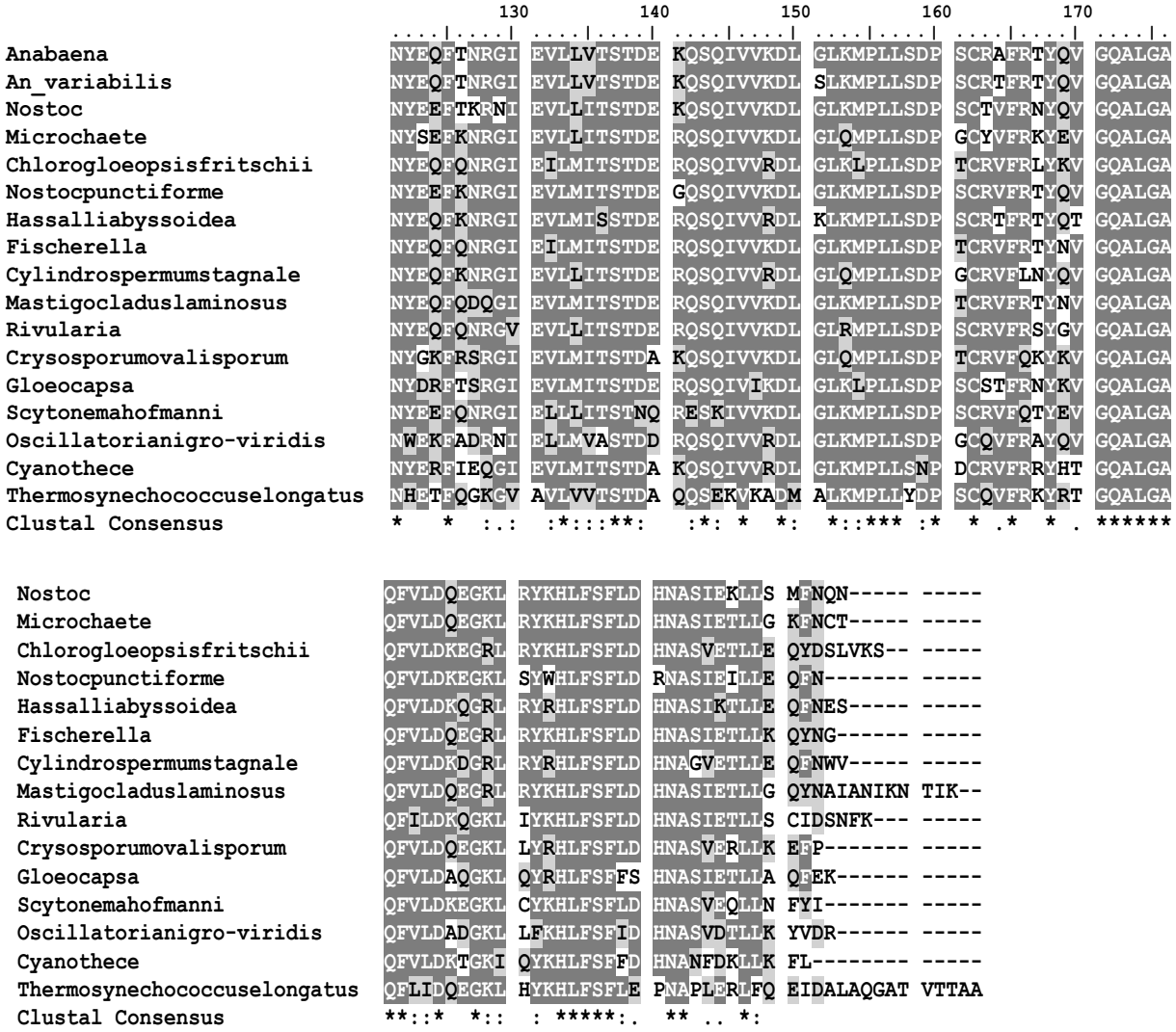

Fig. 4.2.2. Multiple sequence alignment. ClustalW software was employed to obtain alignment of Alr4642-like proteins from different bacteria. Identical amino acids are depicted by (*), conservered amino acids are depicted by (:), whereas semi-conserved amino acids are depicted by (.). The CXXC motif is boxed. The proteins compared include, *Anabaena* [*Anabaena* sp. PCC 7120_BAB76341.1]; An_variabilis (*Anabaena variabilis* ATCC 29413_CP000117.1); Nostoc [*Nostoc punctiforme*_WP_012412313.1]; Microchaete [*Microchaete sp.* PCC 7126_ WP_026100224.1]; Chlorogloeopsisfritschii [*Chlorogloeopsis fritschii;* WP_016874252.1]; Hassallia byssoidea [*Hassallia byssoidea;* WP_039741944.1]; *Fischerella* [*Fischerella* sp. PCC 9431_ WP_026720910.1]; Cylindrospermumstagnale [*Cylindrospermum stagnale*; WP_015208910.1]; Mastigocladuslaminosus [*Mastigocladus laminosus*_ WP_044447082.1]; Rivularia [*Rivularia* sp. PCC; WP_015118879.17116]; Chrysosporumovalisporum [*Chrysosporum ovalisporum* ILC-164; AJW31582.1], Gloeocapsa [*Gloeocapsa* sp. PCC 7428; WP_015189048.1]; Scytonemahofmanni [*Scytonema hofmanni*; WP_017744500.1]; Oscillatorianigro-viridis [*Oscillatoria nigro-viridis;* WP_015178161.1]; Cyanothece [*Cyanothece* sp. PCC 8802; ACV01365.1]; Thermosynechococcuselongatus [*Thermosynechococcus elongatus*_ P_011057129.1]. The name of the bacterium and accession no. of the protein as mentioned in the UniprotKB/Swissprot databases is shown in parenthesis.

4.2.3 Domain analysis on the Alr4642

Domain analysis using blastp and SMART revealed the Alr4642 protein to possess the Cd02970: Prx-like2 domain, which extended from amino acid position no. 68 to 196 (e value of 1.30 e-27; Fig. 4.2.3). The putative proteins that show sequence similarity to Prxs show the presence of this domain. These proteins contain CXXC motif similar to Trx (for e.g. CPFC in Alr4642) and second cysteine of this motif corresponds to the catalytic cysteine of Prxs.

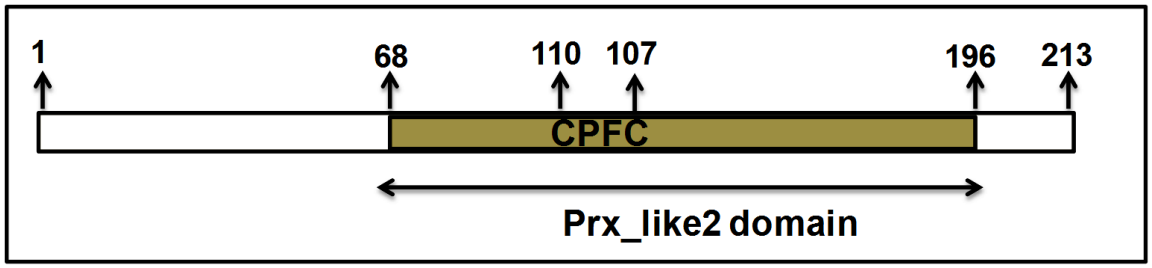

Fig. 4.2.3. Domain analysis of Alr4642. Position of the Prx-like2 domain on the primary sequence of the Alr4642 is shown. The position and the amino acid residue number of the CXXC motif (CPFC) in the primary sequence of the Alr4642 protein are depicted**.**

4.2.4 The *alr4642-like* homologs appear to be absent in non-cyanobacterial genomes

To identify Alr4642 homologs in non-cyanobacterial organisms, a BLASTp search was performed using Alr4642 protein as the subject and NCBI non-redundant protein database as target. The cyanobacterial genomes were excluded in this search. Alr4642 showed some similarity to different types of proteins such as AhpC, 2-Cys Prxs, BCP proteins, redoxin, thiol-disulfide oxidoreductase resA, etc. However, in all these cases, the overall homology was quite poor and was limited to short stretches of amino acids. The pair-wise sequence

alignment of the top four non-cyanobacterial Alr4642 homologs with Alr4642 is shown in Fig. 4.2.4. In fact, best homology was observed with the annotated AhpC gene from *Chloroflexus*. It was observed that not only the homology between the respective protein pairs was poor but the overall coverage was also very less. These observations do suggest that genes encoding the Prx-like2 homologs are likely to be present only in cyanobacterial genomes.

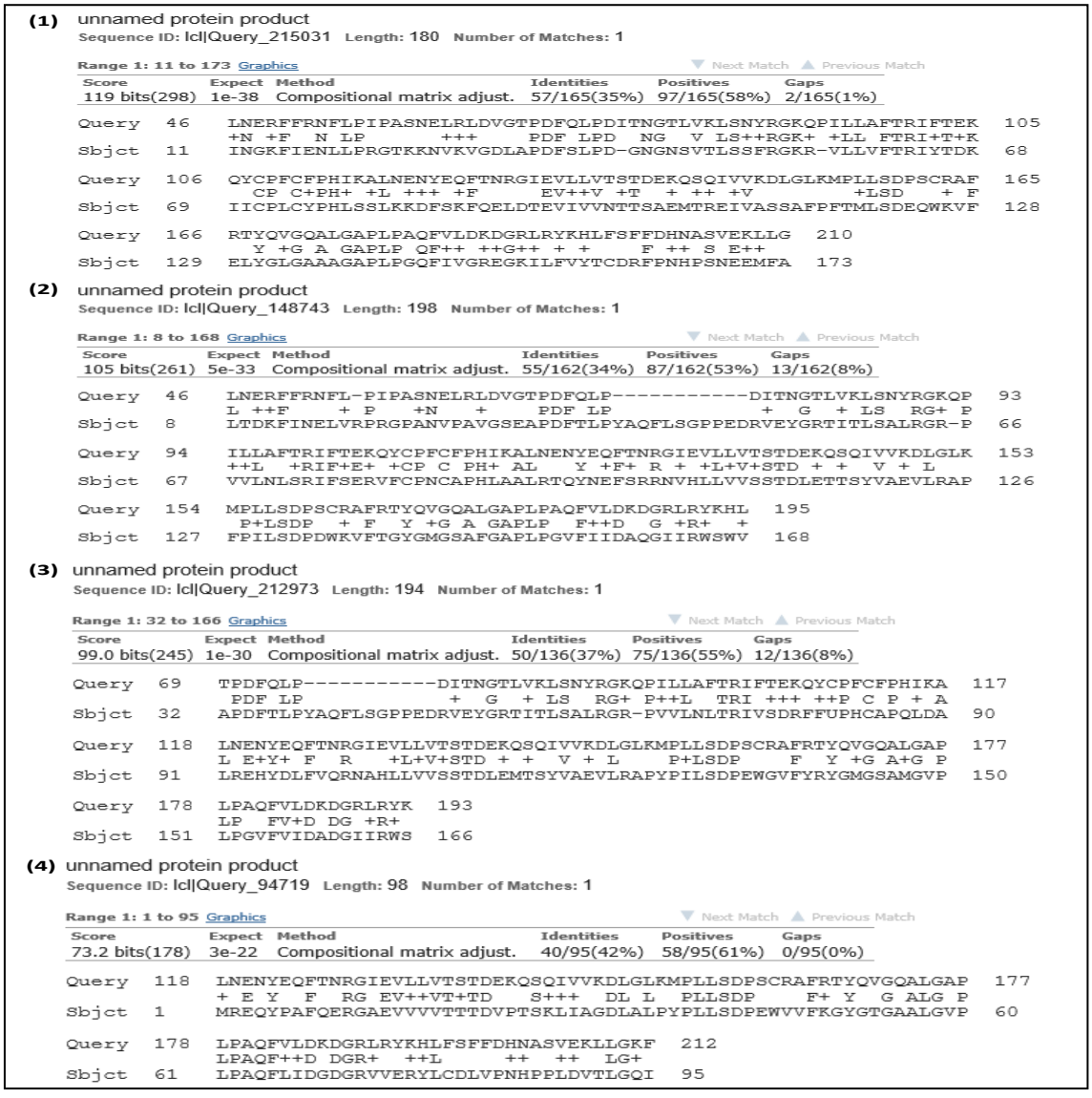

(1) unnamed protein product
Sequence ID: lcl|Query_215031 Length: 180 Number of Matches: 1

Range 1: 11 to 173 Graphics — Next Match — Previous Match

Score	Expect	Method	Identities	Positives	Gaps
119 bits(298)	1e-38	Compositional matrix adjust.	57/165(35%)	97/165(58%)	2/165(1%)

```
Query   46   LNERFFRNFLPIPASNELRLDVGTPDFQLPDITNGTLVKLSNYRGKQPILLAFTRIFTEK   105
             +N +F   N LP       +++     PDF LPD   NG   V LS++RGK+ +LL FTRI+T+K
Sbjct   11   INGKFIENLLPRGTKKNVKVGDLAPDFSLPD-GNGNSVTLSSFRGKR-VLLVFTRIYTDK   68

Query   106  QYCPFCFPHIKALNENYEQFTNRGIEVLLVTSTDEKQSQIVVKDLGLKMPLLSDPSCRAF   165
               CP C+PH+ +L +++ +F      EV++V +T   + ++ +V          +LSD    + F
Sbjct   69   IICPLCYPHLSSLKKDFSKFQELDTEVIVVNTTSAEMTREIVASSAFPFTMLSDEQWKVF   128

Query   166  RTYQVGQALGAPLPAQFVLDKDGRLRYKHLFSFFDHNASVEKLLG   210
               Y +G A GAPLP QF++ ++G++ + +     F ++ S E++
Sbjct   129  ELYGLGAAAGAPLPGQFIVGREGKILFVYTCDRFPNHPSNEEMFA   173
```

(2) unnamed protein product
Sequence ID: lcl|Query_148743 Length: 198 Number of Matches: 1

Range 1: 8 to 168 Graphics — Next Match — Previous Match

Score	Expect	Method	Identities	Positives	Gaps
105 bits(261)	5e-33	Compositional matrix adjust.	55/162(34%)	87/162(53%)	13/162(8%)

```
Query   46   LNERFFRNFL-PIPASNELRLDVGTPDFQLP-----------DITNGTLVKLSNYRGKQP   93
             L ++F     + P    +N    +     PDF LP              +  G   + LS   RG+ P
Sbjct   8    LTDKFINELVRPRGPANVPAVGSEAPDFTLPYAQFLSGPPEDRVEYGRTITLSALRGR-P   66

Query   94   ILLAFTRIFTEKQYCPFCFPHIKALNENYEQFTNRGIEVLLVTSTDEKQSQIVVKDLGLK   153
             ++L   +RIF+E+ +CP C PH+ AL    Y +F+ R + +L+V+STD + +  V + L
Sbjct   67   VVLNLSRIFSERVFCPNCAPHLAALRTQYNEFSRRNVHLLVVSSTDLETTSYVAEVLRAP   126

Query   154  MPLLSDPSCRAFRTYQVGQALGAPLPAQFVLDKDGRLRYKHL   195
              P+LSDP   + F   Y +G A GAPLP   F++D   G +R+   +
Sbjct   127  FPILSDPDWKVFTGYGMGSAFGAPLPGVFIIDAQGIIRWSWV   168
```

(3) unnamed protein product
Sequence ID: lcl|Query_212973 Length: 194 Number of Matches: 1

Range 1: 32 to 166 Graphics — Next Match — Previous Match

Score	Expect	Method	Identities	Positives	Gaps
99.0 bits(245)	1e-30	Compositional matrix adjust.	50/136(37%)	75/136(55%)	12/136(8%)

```
Query   69   TPDFQLP-----------DITNGTLVKLSNYRGKQPILLAFTRIFTEKQYCPFCFPHIKA   117
              PDF LP           +  G   + LS   RG+ P++L   TRI +++ ++P C P + A
Sbjct   32   APDFTLPYAQFLSGPPEDRVEYGRTITLSALRGR-PVVLNLTRIVSDRFFUPHCAPQLDA   90

Query   118  LNENYEQFTNRGIEVLLVTSTDEKQSQIVVKDLGLKMPLLSDPSCRAFRTYQVGQALGAP   177
             L E+Y+ F   R    +L+V+STD + +   V + L     P+LSDP     F   Y +G A+G P
Sbjct   91   LREHYDLFVQRNAHLLVVSSTDLEMTSYVAEVLRAPYPILSDPEWGVFYRYGMGSAMGVP   150

Query   178  LPAQFVLDKDGRLRYK   193
             LP   FV+D DG +R+
Sbjct   151  LPGVFVIDADGIIRWS   166
```

(4) unnamed protein product
Sequence ID: lcl|Query_94719 Length: 98 Number of Matches: 1

Range 1: 1 to 95 Graphics — Next Match — Previous Match

Score	Expect	Method	Identities	Positives	Gaps
73.2 bits(178)	3e-22	Compositional matrix adjust.	40/95(42%)	58/95(61%)	0/95(0%)

```
Query   118  LNENYEQFTNRGIEVLLVTSTDEKQSQIVVKDLGLKMPLLSDPSCRAFRTYQVGQALGAP   177
             + E Y   F   RG EV++VT+TD    S+++   DL L   PLLSDP     F+ Y   G ALG P
Sbjct   1    MREQYPAFQERGAEVVVVTTTDVPTSKLIAGDLALPYPLLSDPEWVVFKGYGTGAALGVP   60

Query   178  LPAQFVLDKDGRLRYKHLFSFFDHNASVEKLLGKF   212
             LPAQF++D DGR+   ++L      ++   ++   LG+
Sbjct   61   LPAQFLIDGDGRVVERYLCDLVPNHPPLDVTLGQI   95
```

Fig. 4.2.4. Pair-wise protein sequence alignment of Alr4642 with from non-cyanobacterial homologs. The Alr4642 sequence was chosen as the query and used for BLASTp excluding cyanobacteria. Of the different sequences that came up in the search, the top four homologs were used for pair-wise sequence alignment. The organisms used for alignment and accession no of respective proteins are (1) *Chloriherpetons thalasum*

(WP_012501141.1); (2) *Chloroflexus aggregans* (WP_012616427.1); (3) *Chloroflexus auranticus* (WP_012255975.1); (4) *Thermonema rassanum* (WP_051633048.1).

4.2.5 Protparam parameters

The 642 bp long *alr4642* ORF encodes protein Alr4642 with a calculated molecular weight of 24731.4 Da (213 amino acid) and an expected pI of 8.62 (http://web.expasy.org/cgi-bin/protparam/protparam). Number of negatively charged residues (Asp + Glu) was 22 whereas 25 positively charged residues (Arg + Lys) were present. The theoretical extinction coefficient (at 280 nm) measured in water, was estimated to be (1) 19160 L mol^{-1} cm^{-1}; Abs 0.1% (i.e. 1 g/l) = 0.775, assuming all pairs of Cys residues form cystines and (2) 18910 L mol^{-1} cm^{-1} Abs 0.1% (i.e. 1 g/l) = 0.765, assuming all Cys residues are reduced. The Alr4642 was not found to have any transmembrane regions as predicted by SOSUI (http://harrier.nagahama-i-bio.ac.jp/sosui/cgi-bin/adv_sosui.cgi). The AlrT4642 protein was also searched for the same parameters. The calculated molecular of this protein weight was 20326.4 Da; with number of amino acids, 178 and a theoretical pI of 8.43. The number of negatively charged residues (Asp + Glu) was 19, whereas 21 residues were positively charged. The theoretical extinction coefficient (at 280 nm) measured in water, was estimated to be (1) 7575 L mol^{-1} cm^{-1}; Abs 0.1% (i.e. 1 g/l) = 0.373 0.367, assuming all pairs of Cys residues form cystines and (2) 7450L mol^{-1} cm^{-1} Abs 0.1% (i.e. 1 g/l) = 0.367, assuming all Cys residues were reduced.

4.3 *alr4642*/Alr4642 is not expressed in *Anabaena*

Several peroxiredoxins in *Anabaena* are not only constitutively expressed, but also induced in response to oxidative and other stresses. Expression of Alr4642 was monitored under control

conditions (i.e. in the absence of any stress) on in response to abiotic stresses on Western blots with the Alr4642 antiserum[1] whereas synthesis of the *alr4642* transcript was monitored on Northern blots with the DIG labeled *alr4642* DNA probe.

The 4 day old wild-type *Anabaena* was exposed to different oxidative stress-inducing agents. At various time points after stress treatment, total proteins were isolated, resolved on SDS-PAGE and probed with the Alr4642 antiserum (generation of Alr4642-specific antisrum is described in section 4.7). Alr4642 protein expression in the cell free protein extracts of unstressed *Anabaena* PCC 7120 could not be detected on Western blots (Fig. 4.3A). Even after exposure to oxidizing agents like methyl-viologen or H_2O_2, expression of the Alr4642 protein could not be observed in *Anabaena* PCC 7120 (Fig. 4.3B). Other stresses like salinity, desiccation or sucrose also gave similar results (Fig. 4.3C).

Similarly, the *alr4642* transcript could not be detected in total RNA isolated from control or H_2O_2/MV-treated cells on Northern blots with the *alr4642* probe (4.3C). These results clearly showed that the *alr4642* gene was not expressed in *Anabaena*. It should be noted that the gene present immediately present upstream of *alr4642*, *alr4641*, is not only constitutively expressed but is also highly induced in response to several stresses (Banerjee et al., 2015). In this context, non-expression of *alr4642* is indeed surprising.

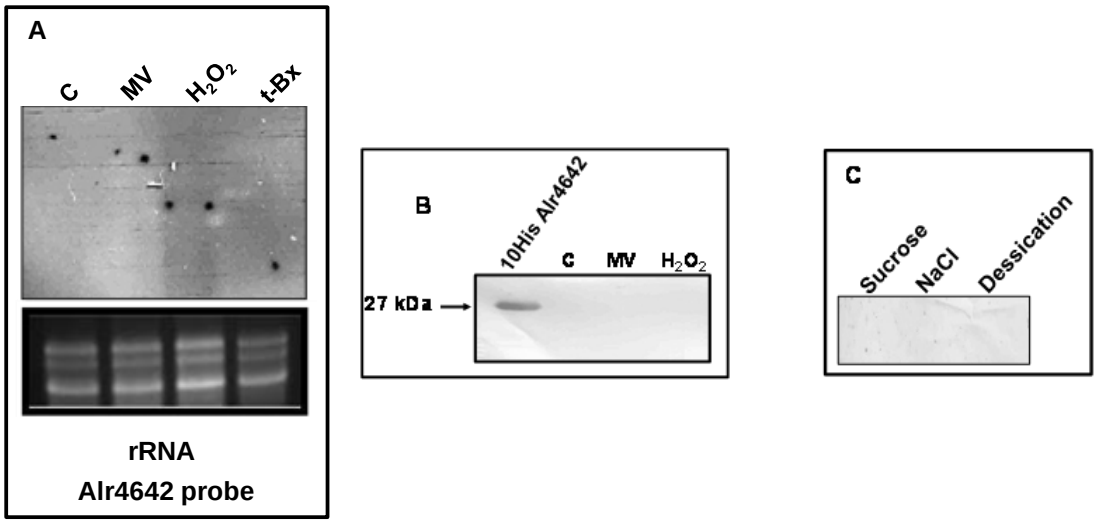

Fig. 4.3. ***In vivo*** **expression analysis of** ***alr4642*****/Alr4642.** (A) Northern blot. Exponentially- grown wild-type *Anabaena* PCC 7120 cells were exposed to various stresses (methyl-viologen, MV; hydrogen peroxide, H_2O_2 and t-butyl hydroperoxide, t-Bx), after 1 h, total RNA was isolated, resolved on agarose gel, blotted onto nylon membrane and hybridized with the DIG-labelled *alr4642* probe. The rRNA bands are given as control on lower panel. (B) Western blotting-immunodetection analysis with the Alr4642 antiserum. Total protein was isolated from *Anabaena* PCC 7120 cells grown in BG11 medium without or with (B) 2 µM MV (MV) or 1 mM H_2O_2 (H_2O_2) These proteins (50 µg per lane) were resolved on denaturing polyacrylamide gels and electro-blotted onto the nitrocellulose membrane. Subsequently, the blot was allowed to cross-react with the Alr4642 antiserum (1:2000), followed by secondary anti-mouse IgG (1:5000) coupled to alkaline phosphatase. The 27 kDa band shown by the purified (i.e. eluted from polyacrylamide gels) His-tagged Alr4642 is depicted by an arrow. (C) Exponentially growing wild type *Anabaena* cells were exposed to 50 mM Sucrose (Sucrose), 200 mM NaCl (NaCl), 6 days of dessication (Dessication). The samples were processed and developed as described in (B).

4.4 The *alr4642* gene shows the presence of a weak promoter and the repressor LexA binds to the *alr4642* promoter

4.4.1 Analysis of the *alr4642* promoter

To determine the probable reason for the lack of *alr4642* expression, DNA upstream of the *alr4642* ORF was analyzed for the presence of promoter elements. The promoter identified by a promoter search program (BPROM) is shown in (Fig. 4.4.1). Interestingly, this promoter

sequence was located right at the beginning of the *alr4642* ORF, and in fact the −35 region of the identified promoter overlapped with the start codon of the full length *alr4642*. Although the −10 region of the identified promoter showed a good match with the consensus −10 promoter sequences, the −35 region showed poor match with its respective consensus, indicating that the promoter was inherently a weak promoter. Homology search with *Anabaena* PCC 7120 LexA protein-binding sequence (Mazón et al., 2004) showed the presence of a LexA-binding site that overlapped directly with the −10 sequence (Fig. 4.4.1).

Fig. 4.4.1. Promoter analysis. The nucleotide sequence corresponding to the -10 and -35 region of the promoter are underlined. The ATG codons for Alr4642 and AlrT4642 are indicated while the LexA-binding sequence that overlaps with the −10 region is depicted by a thick line

4.4.2 The repressor LexA binds to the *alr4642* promoter

To confirm the ability of the purified LexA to bind to the putative LexA-binding sequence (shown in Fig. 4.4.1), electrophoretic mobility shift assays (EMSAs) were performed. Two complementary oligonucleotides (39 nt each) that encompassed the putative LexA-binding site were annealed to form the double stranded i.e. dsLexA-binding DNA. The purified LexA protein of *Anabaena* PCC 7120 (kindly provided by Mr. Arvind Kumar and Dr. Hema Rajaram, Molecular Biology Division, BARC) was allowed to bind to the above-mentioned

38 bp dsDNA in a suitable binding buffer. The LexA protein bound to this DNA and as seen in the Fig. 4.4.2, a slight shift, corresponding to the protein-DNA complexes, was observed. This result indicated the ability of the LexA protein to bind to the LexA-site present around the -10 region of the promoter.

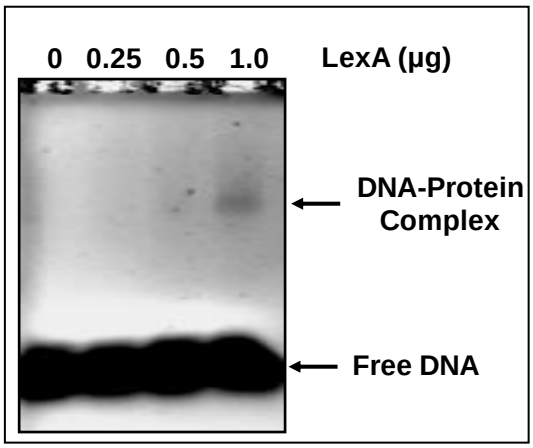

Fig. 4.4.2. EMSA. Increasing amount (as indicated) of *Anabaena* LexA protein was allowed to bind to 39 bp *alr4642* promoter DNA that contained the LexA-binding site. After the assay, the contents of each reaction were resolved on agarose gel and visualized by staining with ethidium bromide. The free DNA and the DNA-protein complex are depicted in the figure**.**

4.5 Cloning of *alr4642* in pET16b and over-expression in *E. coli*

Although large scale genome sequencing projects have unearthed the presence of several Prx-like proteins, they have not been experimentally characterized from any organism so far. Hence, to gain insights into its biochemical function, it was desired to over-express the Alr4642 protein in *E. coli* and purify it there from. As similarity of Alr4642 with other Prx-like2 peroxiredoxins (from several cyanobacteria) was observed from its second annotated methionine residue (Section 4.2.2 and Fig. 4.2.3), attempts were also made to express and purify a slightly truncated Alr4642, i.e. initiating from the second methionine, designated as AlrT4642 (where 'T' denotes truncated).

4.5.1 Cloning of *alr4642* and *alrT4642* into pET16b

The *alr4642* or *alrT4642* ORF was PCR amplified using gene-specific primers, *alr4642fwd* and *alr4642rev* or *alrT4642fwd* and *alr4642rev* respectively (Table 2), employing *Anabaena* PCC 7120 chromosomal DNA as template (Fig 4.5.1.1A, B and C). The PCR products were digested with the restriction enzymes NdeI and BamHI and cloned separately into similarly digested pET16b to obtain pET4642 and pETT4642 respectively. The plasmids pET4642 and pETT4642 were sequenced to confirm the nucleotide sequence integrity of the cloned gene.

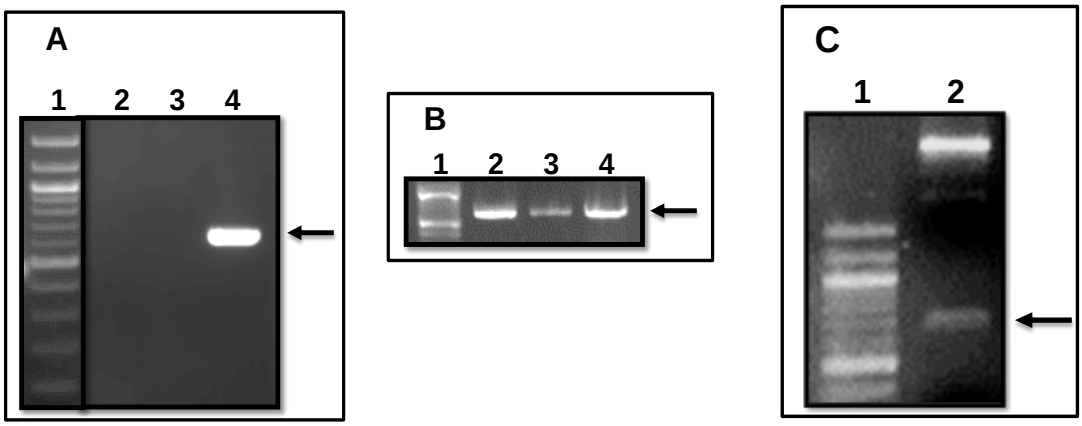

Fig. 4.5.1.1. Cloning of *alr4642* into pET16b. (A) PCR amplification of *alr4642* from genomic DNA of *Anabaena* PCC 7120. Lane1, molecular weight standard (100 bp ladder, NEB); lane 2, PCR with *alr4642fwd* primer alone (single primer control); lane 3, PCR with *alr4642*rev primer alone (single primer control); lane 4, PCR with *alr4642fwd* and *alr4642*rev primer in the reaction mixture. (B) Colony PCR of *E. coli* DH5α transformants to identify pET4642 containing colonies. Lane 1, 100 bp ladder, NEB; lane 2, PCR of colony # 1; lane 3, PCR of colony # 2; lane 4, PCR of colony # 3. The ~650 bp PCR product is indicated by an arrow in A and B. (C) Restriction digestion of pET4642. Lane 1, 100 bp ladder (NEB); lane 2 pET4642 digested with NdeI and BamHI. The insert released (~650 bp) is indicated by an arrow.

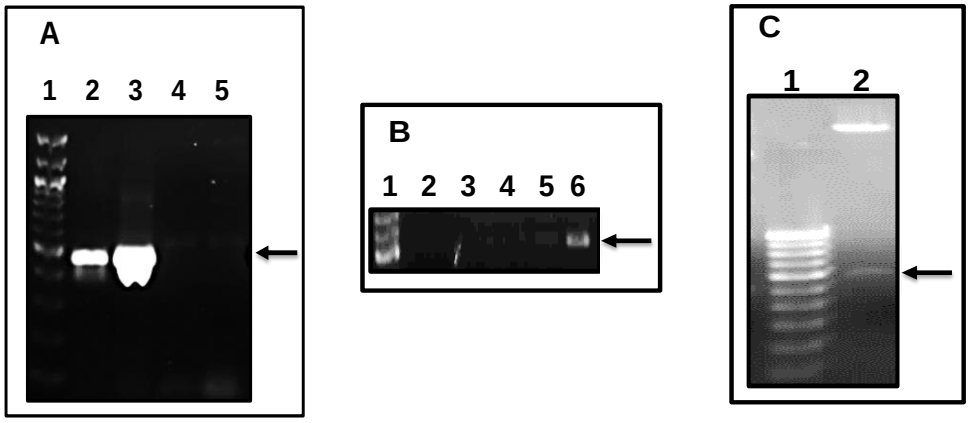

Fig. 4.5.1.2. Cloning of *alrT4642* into pET16b. (A) PCR amplification of *alrt4642* from genomic DNA of *Anabaena* PCC 7120. Lane1, molecular weight standard (100 bp ladder, NEB); lane 2 and 3, PCR with *alrt4642fwd* and *alr4642*rev; lane 4, PCR with *alrt4642fwd* primer alone (single primer control); lane 4, PCR with *alr4642*rev primer alone (single primer control). (B) Colony PCR of *E. coli* JM109 transformants to identify pETT4642 containing colonies. Lane 1, 100 bp ladder, NEB; lane 2, PCR of colony # 1; lane 3, PCR of colony # 2; lane 4, PCR of colony # 3; lane 5, PCR of colony # 4; lane 6, PCR of colony # 5; lane 7, PCR of colony # 6. The ~540 bp *alrt4642* PCR product is indicated by an arrow in A and B. (C) Restriction digestion of pETT4642. Lane 1, 100 bp ladder (NEB); lane 2, pETT4642 digested with NdeI and BamHI. The insert released (~540 bp) is indicated by an arrow.

4.5.2 Over-expression of Alr4642 using IPTG

As mentioned in the previous chapter, cloning of any ORF at NdeI and BamHI sites of pET16b plasmid results in the addition of 10 *in frame* His codons to the 5' end of the ORF. Therefore, the over-expressed proteins contain an N-terminal 10 histidine (10-His) tag. The plasmid pET4642 or pETT4642 was separately transformed into *E. coli* BL21 pLysS/codon plus cells. The recombinant *E. coli* cells were grown in Luria-Bertani (LB) medium with appropriate antibiotics to an optical density at 600 nm (OD_{600}) of ~1.0 and induced with 1 mM isopropyl-thiogalactopyranoside (IPTG) for over-production of proteins. Four hours after induction, cells were harvested by centrifugation, lysed and the total cellular proteins were analyzed on denaturing polyacrylamide gels. Production of the full-length 10HisAlr4642

protein or the truncated 10HisAlrT4642 protein was clearly observed on denatured polyacrylamide gels (Fig. 4.5.2A). The identity of the proteins was further confirmed by immunodetection with the penta-His antiserum (Fig. 4.5.2B).

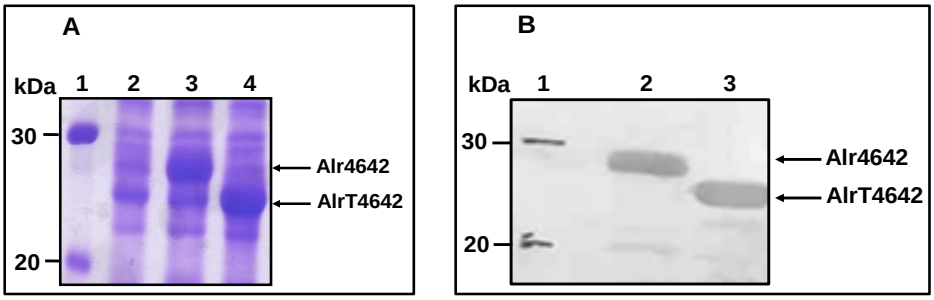

Fig. 4.5.2. Over-expression of Alr4642/AlrT4642. (A) Production of Alr4642 in *E. coli* BL21 pLysSAlr4642 or 10HisAlrT4642 were over-produced in *E. coli* employing the pET16b expression vector. 4 h after induction with IPTG, proteins (20 µg) were resolved by SDS-PAGE and visualized by staining with Coomassie brilliant blue (CBB). Lane 1, mol. wt. marker; lane 2; BL21pLys/pET16b; lane 3, BL21pLysS/pET4642; lane 4, BL21pLysS/pETT4642. (B) Western blot analysis. Total protein fractions from *E. coli* cells over-producing 10HisAlr4642 (lane 2) or 10HisAlrT4642 (lane 3) were probed with the polyhistidine antiserum. The His-tagged Alr4642/ AlrT4642 proteins are depicted by arrows. Molecular weight standards were loaded in lane 1.

4.6 Attempts to purify Alr4642 from *E. coli*

4.6.1 Solubility of Alr4642/AlrT4642 in *E. coli*

Solubility of the heterologously expressed recombinant protein in *E. coli* plays an important role in choosing the subsequent method of purification. The soluble proteins are easier to purify whereas the insoluble proteins require more tedious ways of purification i.e. purification under denaturing conditions followed by refolding of the protein. To see whether the Alr4642/ AlrT4642 were present in the soluble or insoluble fraction, the total cell lysate was centrifuged to separate the soluble fraction and the inclusion bodies. Both these fractions were resolved electrophoretically on SDS-PAGE. However, in spite of production in

abundant amount, both the over-expressed proteins were located exclusively in the inclusion bodies fraction and not in soluble fraction (Fig.4.6.1 A & B).

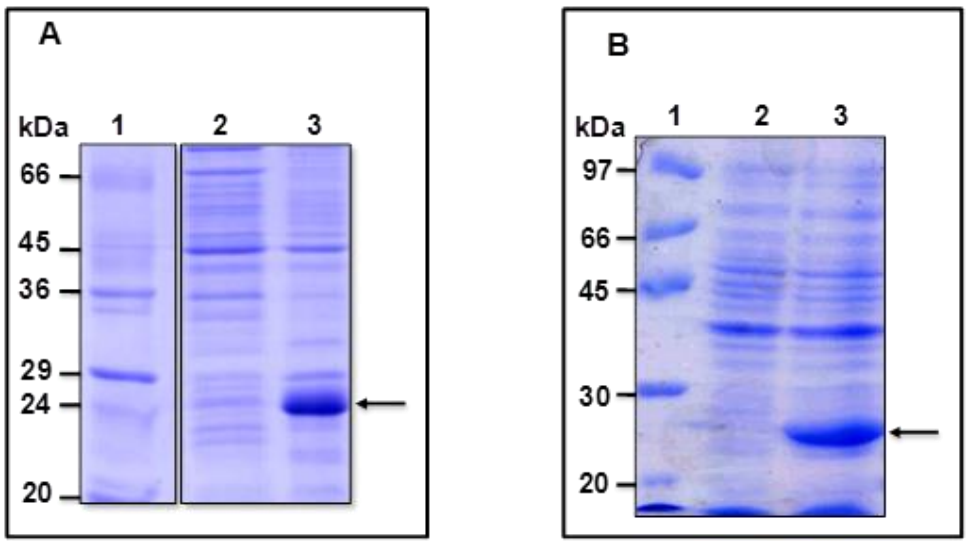

Fig. 4.6.1. Solubility of over-expressed Alr4642 and AlrT4642 in *E. coli.* Soluble and inclusion body fractions were prepared from *E. coli* cells over-producing (A) Alr4642 or (B) AlrT4642, proteins (20 µg) were resolved by SDS-PAGE and visualized by staining with Coomassie brilliant blue (CBB). Lane 1, Molecular weight standard; lane 2, soluble fraction; lane 3, inclusion body fraction. The 27 kDa His tagged Alr4642 (A) and the 22 kDa His tagged AlrT4642 (B) are indicated by arrow.

4.6.2 Expression at lowered temperature to obtain soluble protein

Protein expression at lower temperature, between 15–20°C allows cells time to properly fold the protein, thereby improving the solubility of the protein. To see the effect of lowering of temperature on solubility of 10HisAlr4642, *E. coli* cells were induced with IPTG at 16°C. Subsequently, soluble and inclusion body fractions obtained from these cells were analyzed on the SDS-PAGE. As seen in the Figure 4.6.2, even after inducing cells at low temperature, the over-expressed protein was located exclusively in the inclusion body fraction.

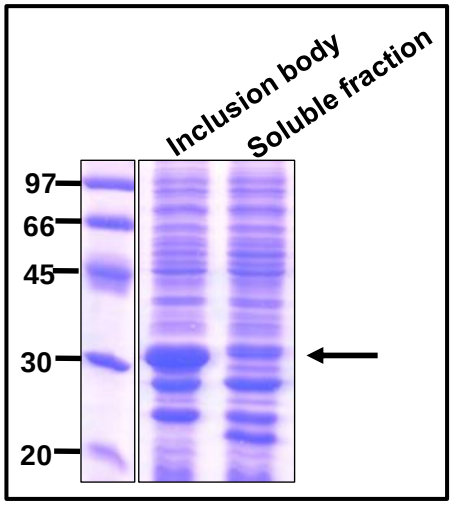

Fig. 4.6.2. Solubility of Alr4642 at low temperature. The soluble fraction or the inclusion body fraction from *E. coli*/pET4642 induced with IPTG at 16ºC. These were resolved on SDS-PAGE and visualized after staining with CBB-250. The 27 kDa 10HisAlr4642 is indicated by arrow.

4.6.3 Over-expression under micromolar concentration of IPTG

Decreasing the concentration of the inducer IPTG is known to increase the solubility of the over-expressed protein. *E. coli* BL21/pET4642 cultures were allowed to grow with appropriate antibiotics to OD_{600}~0.8 and induced with different concentrations of IPTG (25µm, 50µm, 100µm) for 4 h. After induction, cells were disrupted by sonication and the inclusion body fraction was separated from the cytosolic fraction for each sample. On analysis, production of Alr4642 was observed at all concentrations of IPTG, but in all the cases the Alr4642 protein remained insoluble i.e. present in inclusion bodies. (Fig. 4.6.3)

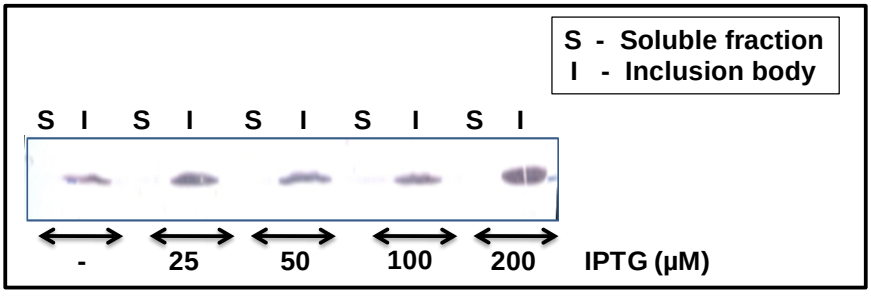

Fig. 4.6.3. Induction of 10HisAlr4642 with different concentrations of IPTG. *E. coli* BL21 carrying pETAlr4642 was induced with various concentration (as indicated) of IPTG for 4 h, soluble and inclusion body fraction were prepared, resolved on SDS-PAGE, transferred to nitrocellulose membrane and probed with the Alr4642 antiserum.

4.6.4 Use of auto-induction medium (AIM) for protein over-production

The principle of AIM media is based on carbon sources in the medium that are metabolized differentially to promote high density cell growth and automatically induce protein expression from *lac* promoters. With AIM media (which contain both glucose and lactose) a high-density cell growth is followed by a spontaneous induction of protein expression. Thus, there is no need to monitor the cell density and no induction with IPTG is necessary. Initially, glucose is metabolized preferentially during growth, which prevents uptake of lactose until the glucose is depleted. As the glucose is depleted, lactose is taken up and converted by β-galactosidase to the inducer allolactose, which ultimately leads to expression of the desired protein [217, 218].

E. coli BL21/pET4642 was inoculated in AIM and grown at 37ºC over-night. From this pre-culture, the main culture was inoculated at 1:100 ratio and further allowed to grow for 24 h. After induction, cells were disrupted by sonication and the inclusion body fraction was separated from the cytosolic fraction. On analysis, high quantity of Alr4642 was observed to be produced, but, despite this, the entire Alr4642 protein remained insoluble i.e. present in inclusion bodies.

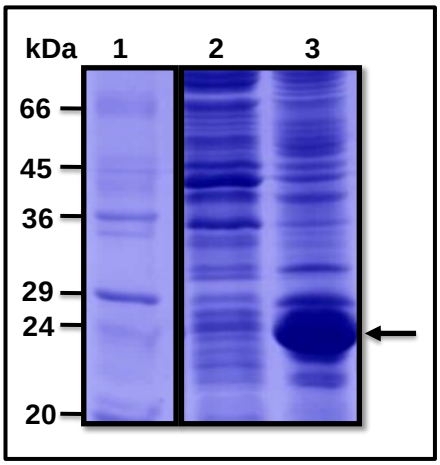

Fig. 4.6.4. Over-production of Alr4642 using AIM medium. *E. coli* cells were grown in auto-induction for 24 h. Subsequently, cells were lysed and the soluble fraction separated from the inclusion body fraction by centrifugation. These fractions were resolved on SDS-PAGE and visualized after staining with CBB. Lane 1, protein marker; lane 2, soluble fraction; lane 3, inclusion body fraction. The 27 kDa His tagged Alr4642 is indicated by an arrow. Sizes of the standards are depicted at the left side of the gel.

4.6.5 Over-expression of Alr4642 or AlrT4642 with a C-terminal Histidine tag

Another strategy attempted to obtain the AlrT4642 protein in soluble was to move the histidine tag from the N-terminal to the C-terminal of the protein. For this purpose, the corresponding ORF was sub-cloned in pET29b, a vector that introduces a C-terminal 6-histidine tag when an ORF is cloned between the NdeI and XhoI restriction sites. The pET4642 was digested with restriction enzymes NdeI & XhoI and the released insert was sub-cloned into similarly digested pET29b vector to yield pET29bT4642. This plasmid was transformed to *E. coli* BL21 cells and expression of AlrT4642(6His) protein was analyzed after induction with IPTG. Although, the protein was produced in substantial quantity, it continued to be present in the inclusion body fraction (Fig. 4.6.5).

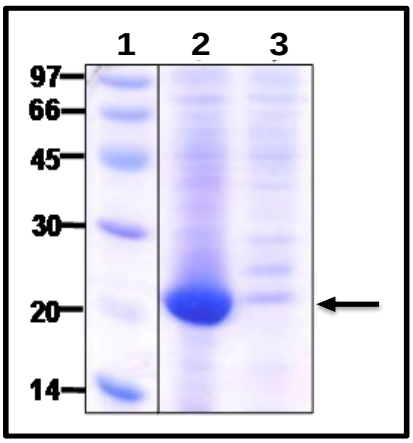

Fig. 4.6.5. Solubility of the over-expressed AlrT4642(6His) protein. Soluble and inclusion body fractions were separated from *E. coli* cells over-producing AlrT4642(6His). Proteins (20 µg) were resolved by SDS-PAGE and visualized by staining with Coomassie brilliant blue (CBB). Lane 1, molecular weight standard; lane 2, inclusion body fraction; lane 3, soluble fraction. The 21.2 kDa AlrT4642(6His) protein is indicated by arrow.

4.6.6 Purification under denaturing conditions guanidinium-hydrochloride.

As attempts to purify Alr4642 under native conditions were not successful, it was desired to purify Alr4642 under denaturing conditions using chaotropic agents such as guanidine. To achieve this, overnight IPTG-induced *E. coli* BL21/pET4642 culture was harvested, the cell pellet was dissolved in 6M guanidium hydrochloride (Gn.HCl) and allowed to bind to the Ni-NTA resin. After appropriate washing, flow through, wash and elution fractions were analyzed on SDS-polyacrylamide gels. A relatively pure 10HisAlr4642 protein fraction could be obtained from Gn.HCl-treated cells (Fig.4.6.6). However, on dialyzing out the Gn.HCl, the entire protein precipitated, rendering it unsuitable for biochemical analysis.

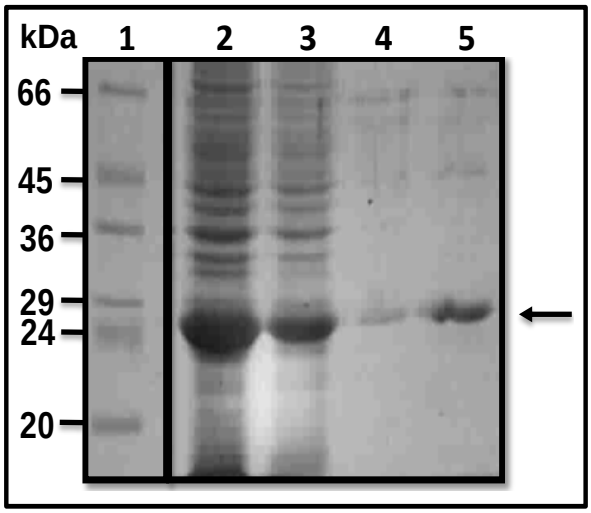

Fig. 4.6.6. Alr4642 purification under denaturing conditions. Purification of Alr4642 with Gn-HCl. The inclusion body pellet was dissolved in Gn.HCl (6M) and used for purification of 10HisAlr4642 using affinity chromatography. Lane1. Molecular weight standards; lane 2, Inclusion bodies solublized in Gn.HCl; , lane 3, unbound proteins; lane 4, wash; lane 5, purified 10HisAlr4642.

4.7 Generation of the Anti-Alr4642 antiserum

The Gn-HCl purified 10HisAlr4642 protein was used for generation of anti-Alr4642 antiserum. The purified protein was further resolved on SDS-PAGE and the 10HisAlr4642 protein was eluted from the gel and subsequently used to immunize mouse. To raise specific antiserum, the primary immunization (with 100 μg of the 10HisAlr4642 protein) and three booster immunizations (50 μg purified protein per booster) in mouse and collection of antiserum were performed at a commercial facility (Merck, India). The anti-serum obtained was verified for its ability to cross-react with the 10HisAlr4642 protein. The antiserum could easily detect 50 ng of the purified protein on Western blots.

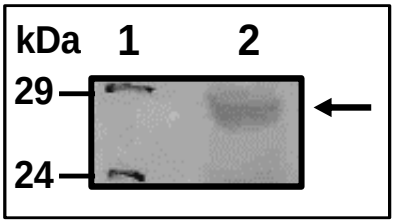

Fig. 4.7. Immunodetection of the 10HisAlr4642 with specific antiserum. 50 ng of Alr4642 protein was resolved on SDS-PAGE, electro-blotted onto nitrocellulose membrane, probed with Anti-Alr4642 anti-serum (1:5000 dilution) and developed with NBT-BCIP.

4.8 Expression of Trigger factor-Alr4642 fusion protein employing the pCold TF vector

Co-expression of one or more chaperone proteins during expression of a heterologous target protein has been proven to be effective for obtaining increased amounts of soluble recombinant protein in *E. coli*. The plasmid pColdTF (Takara Bio, vector map is shown in appendix C) is a fusion expression vector that expresses the target protein as a fusion with (His-tagged) trigger factor (TF), an *E. coli* chaperone (that helps in proper folding of proteins) (Fig. 4.8.1). The schematic diagram of the pCold vector, relevant to this section, is shown in the Fig.4.8.1. Expression is under the control of the cold shock protein A (*cspA*) gene promoter. The TEE (translational enhancer element), enhances the level of translation for the protein. The insertion of a gene of interest at appropriate sites (in MCS) in this vector results in expression of a fusion protein i.e. TF and the protein of interest. The fusion protein can be purified by affinity chromatography with the Ni-NTA matrix and the protein of interest can be separated from TF by cleavage with thrombin.

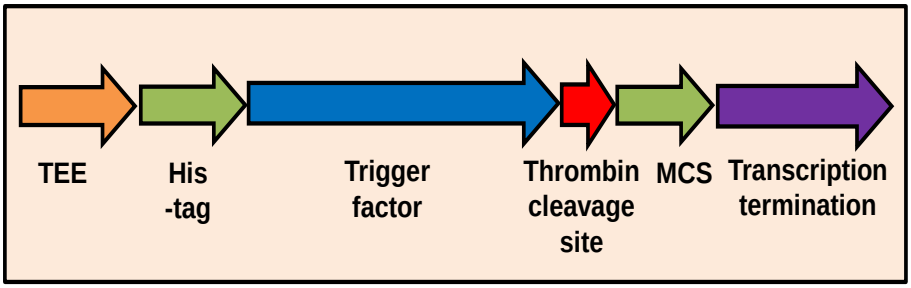

Fig. 4.8. Schematic representation of pColdTF vector. The various elements of the pCold TF vector are shown. TEE (translational enhancer element), TF (Trigger factor), Thrombin cleavage site, MCS (multiple cloning site). For the sake of clarity, these elements are not drawn to scale**.**

4.8.1 Cloning of *alr4642* in pColdTF expression vector

The *alrt4642* DNA fragment was PCR amplified and ligated to the pColdTF vector (resultant construct was named as pColdTFT4642). The pColdTFT4642 was verified for the presence of the appropriate insert by restriction digestion as well as sequencing (Fig. 4.8.1). Subsequently, this plasmid was transformed to *E. coli* BL21plysS for over-production of the fusion protein.

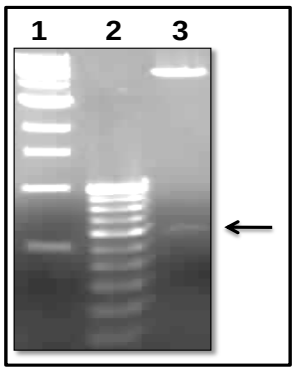

Fig. 4.8.1. Restriction analysis of pColdTFT4642. Lane 1, 1 kb ladder (NEB); lane 2, 100 bp ladder (NEB); lane3, pColdTFT4642 digested with NdeI and BamHI.

4.8.2 Production of fusion protein AlrT4642-TF in *E. coli*

On induction with IPTG, production of a ~73 kDa protein (Trigger factor-Alr4642 fusion protein) was observed on SDS-polyacrylamide gels (Fig.4.8.2A). Unlike the previously over-expressed His-tagged Alr4642/AlrT4642, this fusion protein remained soluble (Fig.4.8.2B) and could be purified to near homogeneity by affinity chromatography employing the Ni-NTA matrix (Fig.4.8.2.C).

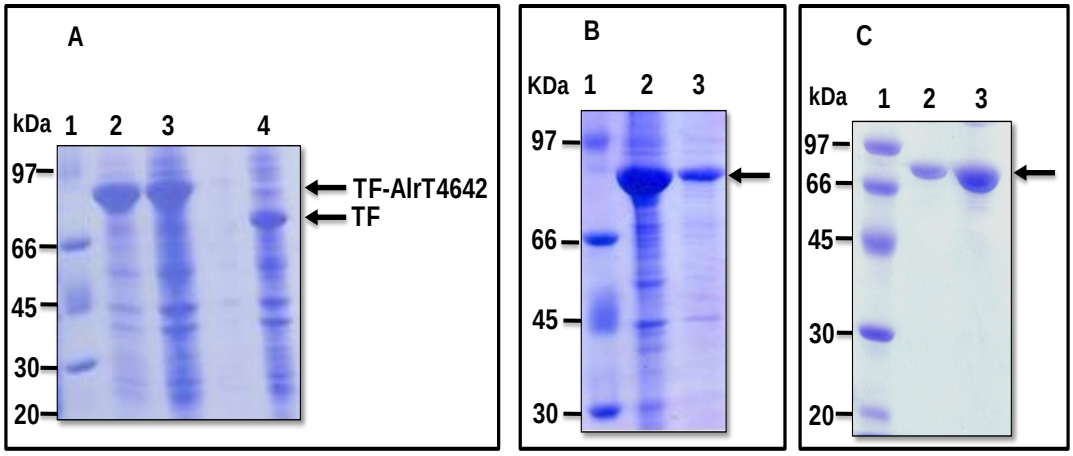

Fig. 4.8.2. Over-expression of AlrTF-T4642 in *E. coli.* (A) Cells were induced with 1 mM IPTG, total proteins extracted in Laemmli's sample buffer and resolved on SDS-PAGE. Lane 1, molecular weight marker; lanes 2 & 3, *E. coli* Bl-21/pColdTFT4642 induced with 1 mM IPTG; lane 4, *E. coli* Bl-21/pColdTF induced with IPTG. (B) Solubility of TF-T4642. Cell lysate of the IPTG-induced *E. coli* Bl-21/pColdTFT4642 was separated into soluble and inclusion body fraction and aliquots were resolved on SDS-PAGE. Lane 1, molecular weight marker; lane 2 soluble fraction; lane 3, inclusion body fraction. A total of 30 µg protein was loaded in lanes 2-4. (C) Purified AlrTF-T4642 fusion protein. The AlrTF-T4642 was purified by affinity chromatography employing the Ni-NTA matrix as described in the methods section. Lane 1; mol wt. marker; lane 2, purified protein (2 µg); lane 3; purified protein (6 µg).

4.8.3 Cleavage of AlrTF-T4642 with thrombin

The purified AlrT4642-TF fusion protein was dialyzed against the thrombin cleavage buffer and incubated with the thrombin slurry (Sigma Aldrich) for cleaving the Alr4642 protein

from the His-tagged TF. To monitor the progress of cleavage, aliquots obtained after 1 h, 6 h and 24 h were resolved on SDS-polyacrylamide gels and visualized. As seen in the Figure 4.8.3, almost complete cleavage was observed at the end of 24 hrs.

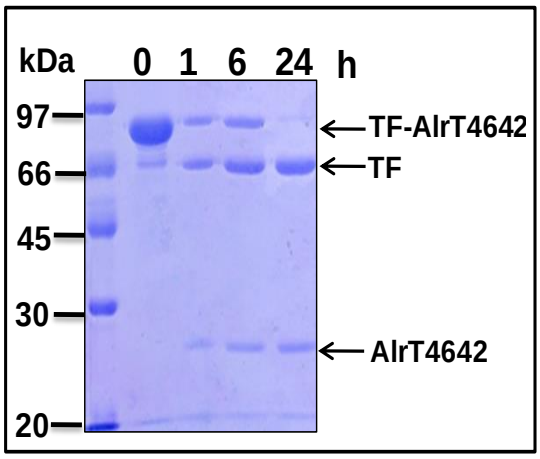

Fig. 4.8.3. Cleavage of TF-T4642 with thrombin slurry. 15 µg of purified AlrTF-T4642 was incubated with thrombin slurry in equilibration buffer and aliquots were taken at various time points (as indicated on top of the gel), mixed with Laemmli's sample buffer resolved on SDS-PAGE and visualized after staining with CBB.

4.8.4 Separation of AlrT4642 and trigger factor

Attempts were made to separate AlrT4642 from the trigger factor by using (1) Ni-NTA affinity chromatography to remove the His-tagged TF protein and (2) size exclusion chromatography.

When incubated with the Ni-NTA resin, a decrease in the concentration of TF was observed in the first few hours. However, the entire TF could not be removed on longer incubation (24 h) with the resin or on adding aliquots of fresh Ni-NTA resin. These results suggested that even after cleavage by thrombin, a portion of the TF protein remained tightly bound to the AlrT4642 protein. Size exclusion chromatography was attempted to separate TF from AlrT4642. In this case, minor amounts of the AlrT4642 and TF proteins were both observed

in the fraction that eluted first (peak 1, that eluted first) whereas in the second peak (peak 2), only the TF protein was observed (Fig.4.9.3B). Thus, it appears that TF binds very tightly to Alr4642 and hence detergents like SDS are required to separate them.

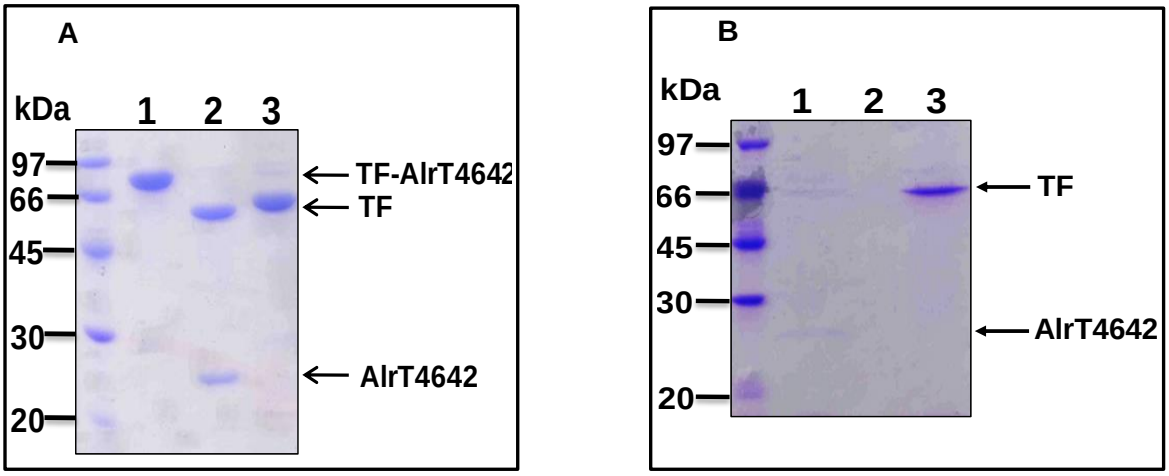

Fig. 4.8.4. Separation of TF and AlrT4642 TF-AlrT4642. (A) Thrombin cleavage of TF-T4642, lines lane 1, TF-T4642 lane 2. 2, thrombin-cleaved TF-T4642; lane 3, TF control. Molecular weight Standard is shown at the left corner of the gel. The sample shown in lane 2 was used for size exclusion chromatography. (B) Size-exclusion chromatographic separation of thrombin cleaved TF-T4642 Lane1, peak1; lane 2, empty lane; lane 3, peak 2. The molecular weight Standard is shown at the left corner of the gel.

4.9 Over-expression of *alr4642* in *Anabaena* PCC7120

4.9.1 Construction of pAM4642 for over-expression of *alr4642* in *Anabaena*

As Alr4642 could not be expressed in soluble form in *E. coli*, attempts were made to verify if Alr4642 remained soluble after over-expressing it in *Anabaena*. For this purpose, the *alr4642* DNA fragment (642-bp) from pET4642 was sub-cloned, downstream of the strong P_{psbA1} promoter, into the pFPN vector [171] employing the restriction enzymes NdeI and BamHI (plasmid called pFPN4642) (Fig. 4.9.1). Subsequently, the *alr4642* gene along with the P_{psbA1}

promoter was transferred as a SalI–XmaI fragment from pFPN4642 to appropriately digested *E. coli/Anabaena* shuttle vector pAM1956 [172] to obtain pAM4642. The presence of the *alr4642* insert in pAM4642 was verified by PCR with appropriate primers and sequencing. Using a conjugal *E. coli* donor [HB101 (pRL623 + pRL443)], pAM4642 was conjugated into *Anabaena* PCC7120 as described earlier [148]. Ex-conjugants were selected on BG-11/N^+ agar plates containing neomycin (25 µg mL^{-1}), transferred to BG-11/N^+ liquid medium containing neomycin (10 µg mL^{-1}) and repeatedly sub-cultured. The transformed *Anabaena* strain thus obtained (designated An4642$^+$) was maintained on BG-11/N^+ plates containing neomycin.

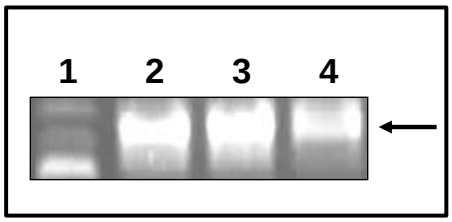

Fig. 4.9.1. Identification of pAM4642-containing colonies PCR. Colony PCR of *E. coli* DH5α transformants to identify colonies with pAMT4642. Lane 1, 100 bp ladder, NEB; lane 2, PCR of colony # 1; lane 3, PCR of colony # 2; lane 4, PCR of colony # 3. The ~650 bp PCR product is indicated by an arrow.

4.9.2 Expression of *alr4642* in *Anabaena* PCC 7120 leads to production of AlrT4642

For comparison, the different Alr4642/AlrT4642 proteins (relevant to this section) along with their respective mol. wt. are schematically depicted in Fig. 4.9.2.1. The An4642$^+$ cells that appeared on the selection medium were verified by monitoring expression of GFP (Fig. 4.9.2.2). Soluble extracts of An4642$^+$ were prepared to monitor production of Alr4642 on Western blots. Along with the An4642 extract, the thrombin-digested TF-AlrT4642 was also

subjected to electrophoretic separation on the same gel. When probed with the Alr4642 antiserum on Western blots, the recombinant An4642^{+} showed production of a shorter Alr4642 protein, whose size (20.3 kDa) matched exactly with that of AlrT4642 obtained after digesting TF-AlrT4642 with thrombin (Fig. 4.9.2.3). This implied that the full length Alr4642 protein was not synthesized from the *alr4642* ORF and further indicated that the codon corresponding to the second methionine was the actual *in vivo* start codon in *Anabaena*.

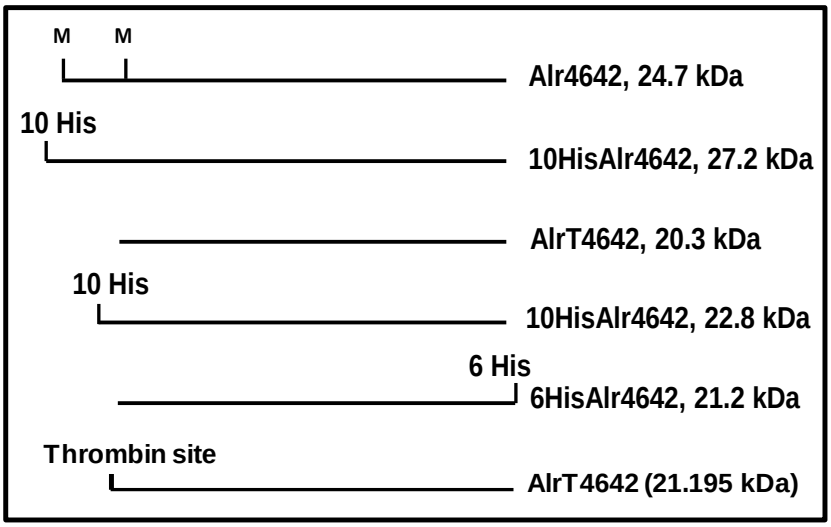

Fig. 4.9.2.1. Schematic representation of the various Alr4642 proteins employed in the study along with their expected molecular weights.

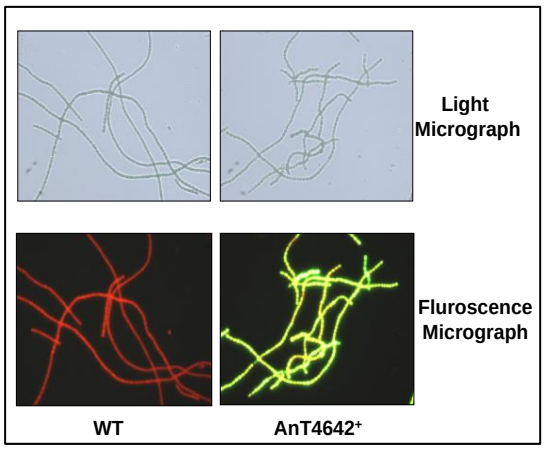

Fig. 4.9.2.2. Over-expression of Alr4642 in *Anabaena* PCC7120. (A) Wild type *Anabaena* and An4642$^+$. Cultures were grown in BG-11 medium for 3 days and visualized microscopically. Light micrographs and fluorescence micrographs (excitation BP, 450-490 nm and emission LP, 515 nm) are depicted. WT, wild-type *Anabaena* PCC 7120; An4642$^+$, recombinant *Anabaena* PCC 7120 transformed with pAM4642.

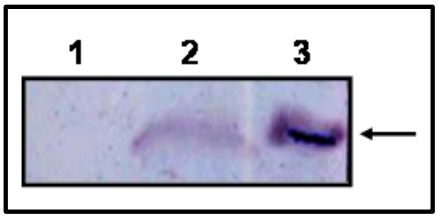

Fig. 4.9.2.3. Western blot analysis. Total proteins were isolated from the wild-type *Anabaena* PCC 7120 or the An4642$^+$ strain (20 µg per lane) and the TF-Alr4642 protein digested with thrombin (200 ng), were resolved on SDS-PAGE, electro-blotted onto a nitrocellulose membrane and probed with the Alr4642-specific antiserum. Lane 1, wild-type *Anabaena* PCC 7120; lane 2, An4642$^+$ and lane 3, thrombin-digested TF- T4642. The position of the AlrT4642 protein band is indicated by an arrow.

4.10 Purification of Alr4642(6His) from *Anabaena*

Homology of Alr4642 with the other Prx-like2 proteins commenced from its second methionine that was 36 amino acids away from the first methionine annotated in the database (Fig. 4.2.3). Moreover, in *Anabaena*, expression of the complete *alr4642* ORF (An4642$^+$) resulted in production of a smaller protein whose size corresponded to that of AlrT4642 (Fig. 4.9.2.3). Both these results indicated that the second methionine was the *in vivo* start codon of *alr4642*. As AlrT4642 was present in the soluble fraction of *Anabaena* extracts, it was desired to purify this protein from *Anabaena*. Hence, to enable rapid purification by affinity chromatography, attempts were made to over-express a His-tagged AlrT4642 protein in *Anabaena*.

4.10.1 Strategy for construction of *alrt4642(6His)*

For purification by Ni-NTA affinity chromatography, the presence of a histidine tag is essential. For this reason, 6 *in frame* histidine codons were added to the reverse primer employed to amplify the *alrt4642* ORF. Thus, the expressed protein would have a C-terminal hexa-histidine tag. The strategy for over-expression of *alrt4642*(6His) in *Anabaena* and the subsequent purification of AlrT4642 from the resulting strain AnT4642(6His)$^{+}$ is described below.

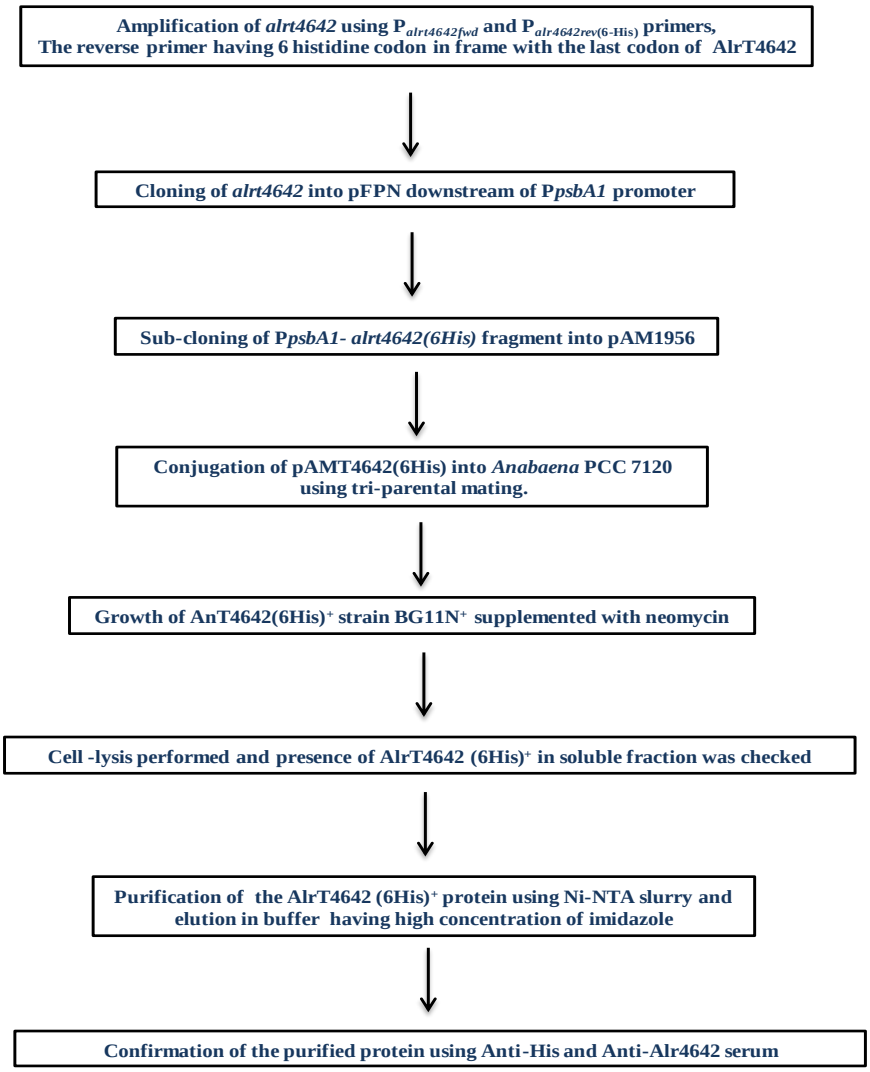

Fig. 4.10.1. Schematic representation of AnT4642^{+} construction and its purification.

4.10.2 Cloning of *alrt4642(6His)* in pAM1956

Anabaena PCC 7120 chromosomal DNA was subjected to PCR with *alrt4642fwd* and *alrt4642rev(6His*) so as to obtain the *alrt4642(6His)* PCR product (Fig. 4.10.2.1). This PCR product was ligated to appropriately digested pFPN plasmid to yield, pFPNT4642(6His) (Fig. 4.10.2.1). Subsequently, Alr*T4642(6His)* insert along with the P_{psbA1} promoter was transferred as a SalI–XmaI fragment to pAM1956 to form pAMT4642(6His), wherein the *alrt4642(6His)* gene is present upstream of the *gfp* (green fluorescent protein) gene (Fig. 4.10.2.2 A & B). In this construct, both *alrt4642* as well as *gfp* are co-transcribed but independently translated.

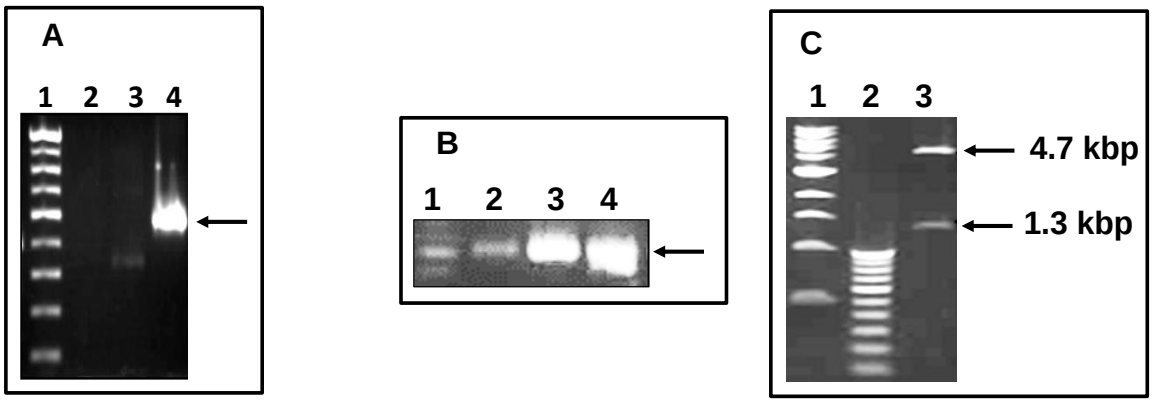

Fig. 4.10.2.1. Cloning of *alrt4642(6His)* in pFPN. (A) PCR amplification of *alrt4642(6His)* from genomic DNA of *Anabaena* PCC 7120. Lane1, molecular weight standard (100 bp ladder, NEB); lane 2, PCR with *alrt4642fwd* primer alone (single primer control); lane 3, PCR with alrt4642rev(6His) primer alone (single primer control); lane 4, PCR with *alrt4642fwd* and *alrt4642rev(6His*) in the reaction mixture. (B) Colony PCR of *E. coli* DH5α primer in the reaction mixture. (B) Colony PCR of *E. coli* 19ransformants to identify pFPNT4642(6His)-containing colonies. Lane 1, 100 bp ladder, NEB; lane 2, PCR of colony # 1; lane 3, PCR of colony # 2; lane 4, PCR of colony # 3 The ~540 bp PCR product is indicated by an arrow in A and B. (C) Restriction digestion of pFPNT4642(6His) lane 1. Plasmid digested with XmaI and SalI; Lane M1, 100 bp ladder (NEB); Lane M2, 1 kb ladder (NEB). The size of the plasmid and that of the released insert is indicated in the figure.

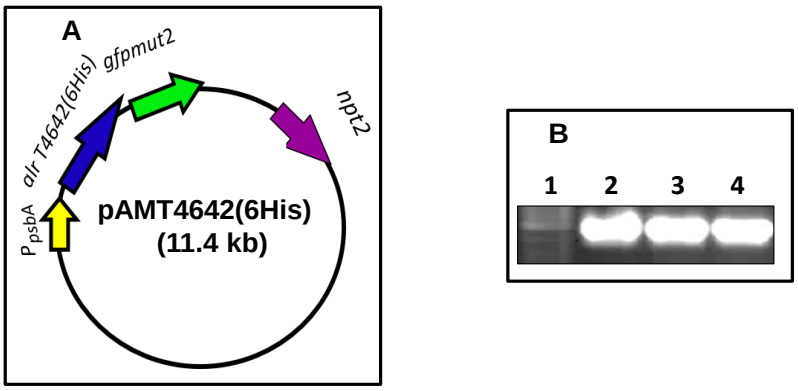

Fig. 4.10.2. Cloning of *alrt4642(6His)* in pAM1956. (A) Schematic representation of pAMT4642(6His). The arrows indicate the direction of transcription. (B) Colony PCR. To identify transformants containing pAMT4642(6His), *E. coli* DH5α colonies were subjected to PCR with primers. Lane 1, 100 bp ladder, NEB; lane 2, PCR of colony # 1; lane 3, PCR of colony # 2; lane 4, PCR of colony # 3.

4.10.3 Over-expression of AlrT4642 (6His)

The pAMT4642 (6His) was conjugated into *Anabaena* PCC 7120 and the corresponding ex-conjugants [AnT4642 (6His) $^{+}$] were identified by visualizing expression of GFP (4.10.3A). Production of the AlrT4642 (6His) protein in the above-mentioned exconjugants was verified on Western blots. For appropriate comparison, the total soluble proteins obtained from AnT4642(6His)$^{+}$ or An4642^{+} or the wild-type *Anabaena* PCC 7120 (along with the thrombin-digested TF-AlrT4642) were resolved on denaturing gels and probed with the Alr4641 antiserum. Production of the 21.2 kDa protein, whose size matched with that of AlrT4642 (arising from the thrombin-cleaved TF-AlrT642), was observed in AnT4642 (6His) $^{+}$ extract. (Fig. 4.10.3B). Due to the presence of the hexa-histidine tag, AlrT4642 (6His) showed slightly decreased mobility than AlrT4642 that was present in the An4642^{+} extracts (Fig 4.10.3). The presence of the AlrT4642 (6His) protein in the cytosolic fraction of *Anabaena*

extracts indicated that like AlrT4642, AlrT4642 (6His) too remained soluble when over-expressed in *Anabaena*. (Fig. 4.10.3).

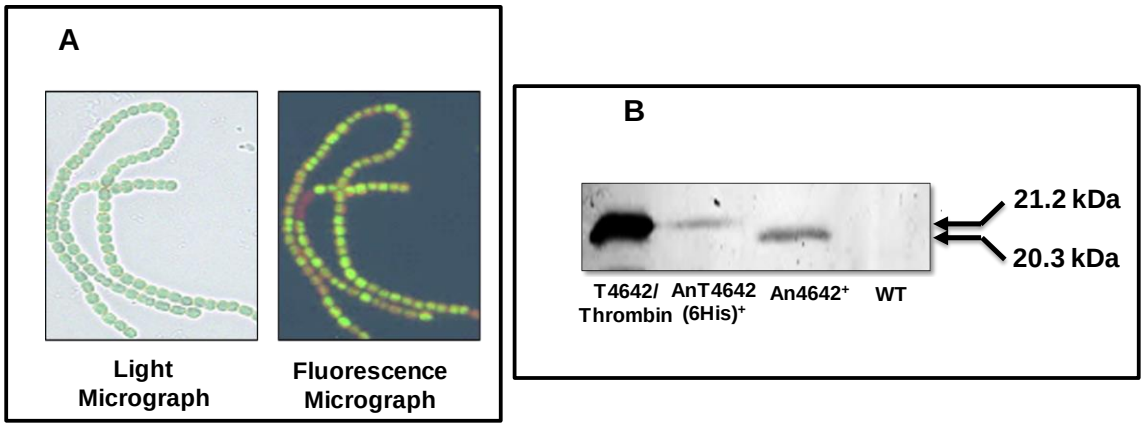

Fig. 4.10.3. Over-expression of AlrT4642 (6His) in *Anabaena* PCC 7120. (A) Light and fluorescence micrographs of AnT4642^{+}, recombinant *Anabaena* PCC7120 transformed with pAMT4642. *Anabaena* cells grown in BG-11 medium for 3 days were viewed under a fluorescent microscope (excitation BP, 450-490 nm and emission LP, 515 nm). (B) Total proteins from wild-type *Anabaena* PCC7120, An4642^{+} or AnT4642^{+}(6His) (20 µg per lane) along with TF-AlrT4642 (500 ng) digested with thrombin, were separated on SDS-PAGE and probed with the Alr4642-specific antiserum. Size (kDa) of the two proteins is depicted.

4.10.4 Purification of AlrT4642 (6His) by Ni-NTA affinity chromatography

For purification of the AlrT4642 (6His) protein, the AnT4642(6His)$^{+}$ cells were inoculated in BG11-N^{+} medium at chlorophyll *a* density of 1.0 – 1.2 µg per ml and allowed to grow for 7 days. After 7 days of growth, cells were harvested by centrifugation, washed once with lysis buffer containg 5 mM imidazole and stored at -80ºC till further processing. Subsequently, cells were allowed to thaw on ice, disrupted by sonication and the cytosolic fraction obtained was allowed to bind to the Ni-NTA slurry. After incubation for 3 h, the slurry was washed thoroughly with lysis buffer (containing 20 mM imidazole) and finally the bound proteins were eluted in a buffer containing 250 mM imidazole. Aliquots of each of the fractions were

kept aside to ascertain the progress of purification on denaturing PAGE. As shown in the Fig. 4.10.1A, the AlrT4642(6His) protein could be purified fromAnT4642(6His)$^{+}$ using Ni-NTA affinity chromatography. The identity of purified AlrT4642(6His) was confirmed by probing it with anti-Alr4642 or the anti-polyhistidine antiserum (Fig. 4.10.4.B 1 & 2).

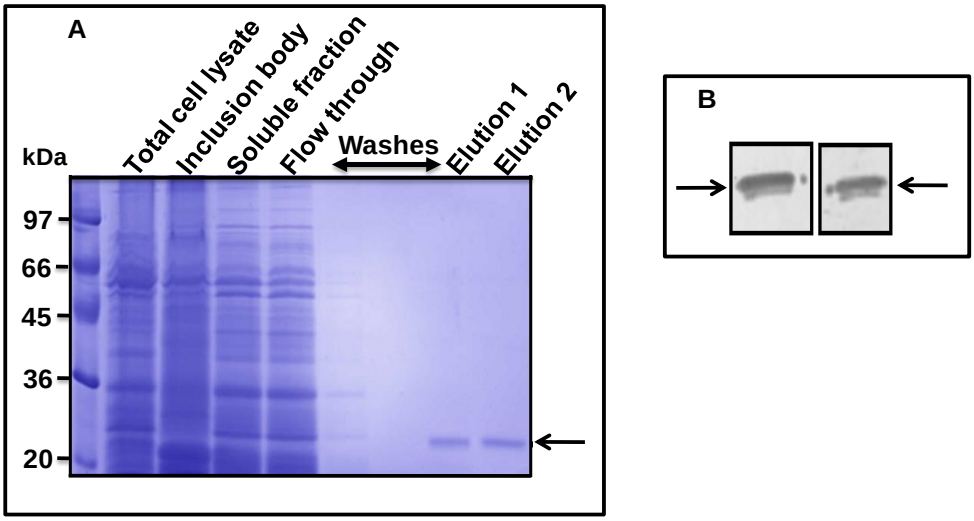

Fig. 4.10.4. Purification of AlrT4642(6His) from AnT4642^{+}(6His). (A) AnT4642^{+}(6His) culture was grown (with aeration) for 7 days and purification of the AlrT4642(6His) protein was performed as described in the methods section. Equal volume of different fractions (20 µl each) as indicated in the figure were resolved on SDS-PAGE and visualized by staining with CBB. 21.2 kDa AlrT4642 is shown by an arrow. Molecular weight standard is shown at left of the gel. (B) The purified AlrT4642(6His) was probed with the polyhistidine antiserum (left panel) or with the Alr4642-specific antiserum (right panel). The 21 kDa AlrT4642 protein band that appeared after developing the blot is shown by an arrow.

4.11 AlrT4642 protects the supercoiled plasmid from ROS mediated damage and shows DTT-dependent peroxidase activity.

In the metal-catalyzed oxidation (MCO) assay, hydroxyl radicals are generated by incubating $FeCl_3$ with DTT at room temperature. If production of these radicals in not inhibited, these

can degrade any DNA molecule that is present in the vicinity. The DNA integrity can be easily visualized by electrophoresis of samples on agarose gels. The ability of Alr4642(6His) to protect pBluescript from oxidative was verified by the MCO assay. In the absence of the AlrT4642(6His) protein or in the presence of BSA (control protein), complete degradation of the plasmid DNA was observed. However, when the Alr4642(6His) protein was present (Fig.4.11.1A), a major amount of plasmid DNA was converted only to the linear (L) form and not degraded completely. Also, the proportion of the covalently closed circular (CCC) form of plasmid DNA increased with increasing concentration of the Alr4642(6His) protein. Thus, the addition of purified AlrT4642(6His) conferred considerable protection to DNA from oxidative damage.

The DTT-dependent peroxidase activity assay was performed to verify if the purified Alr4642 protein showed peroxidase activity. In this assay, H_2O_2 was used as the substrate whereas DTT was employed as the reducing agent. A distinct reduction in concentration of H_2O_2 was observed in the presence of the Alr4642(6His) protein. However, no peroxidase activity was observed when TrxA was used as the substrate.

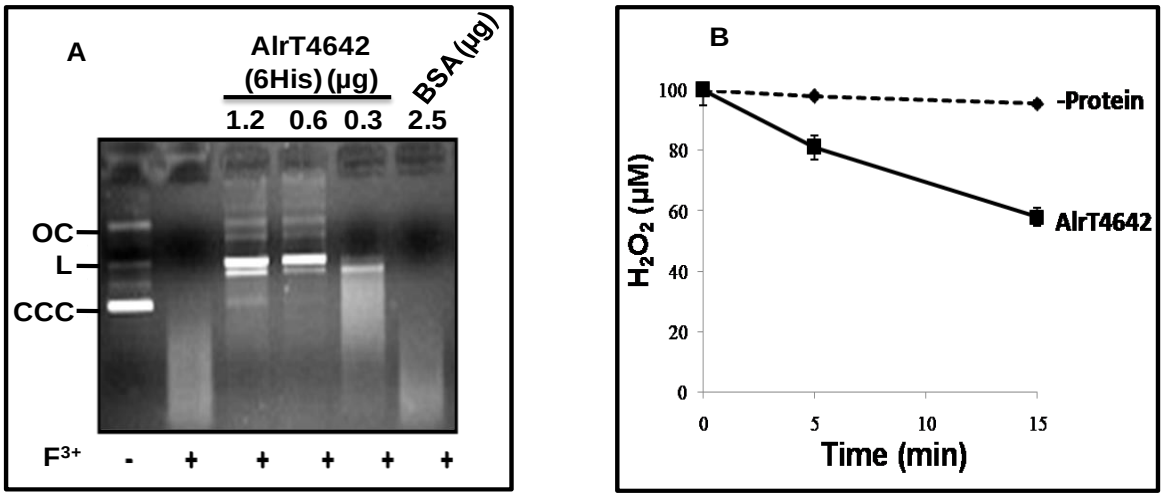

Fig. 4.11. Anti-oxidant activity of AlrT4642(6His)$^+$. (A) Metal catalyzed oxidation (MCO) assay. One microgram of pBluescript DNA (lane 1) was subjected to oxidative damage using the MCO reaction (5 mM DTT +3 µM Fe^{3+}, depicted by Fe^{3+}) to generate ROS in the absence (lane 2) or in the presence of purified AlrT4642(6His) (lanes 3–5) or BSA (lane 6) as indicated. The integrity of DNA was assessed by electrophoresis on a 1%agarose gel followed by staining with ethidium bromide. The covalently closed circular (CCC), linear (L) and open circle (OC) forms of the plasmid DNA are indicated. (B) DTT-dependent peroxidase activity. Decomposition of H_2O_2 by the purified Alr4642(6His) protein (5 µg) using DTT as reductant. Dashed line, no protein; solid line, Alr4642(6His).

4.12 Over-expression of Alr4642 protects *Anabaena* from H_2O_2 mediated oxidative stress

As the purified AlrT4642(6His) protein showed antioxidant activity *in vitro*, it was desired to verify if over-expression of AlrT4642 would protect *Anabaena* from oxidative stress. To accomplish this, AnT4642(6His)$^+$ and the wild-type *Anabaena* PCC 7120 were assessed for oxidative stress resistance in response to hydrogen peroxide. As seen in Fig.4.12.A, after 2 days of treatment, a pronounced bleaching, indicating loss of photosynthetic pigments, was observed in the wild-type cells but not in AnT4642 (6His)$^+$. AnT4642(6His)$^+$showed

chlorophyll *a* content comparable to the unstressed AnT4642(6His)$^{+}$ cells, whereas a clear reduction in chlorophyll *a* was observed in the wild-type cells after 2 days of H_2O_2 stress (Fig.4.12 B).

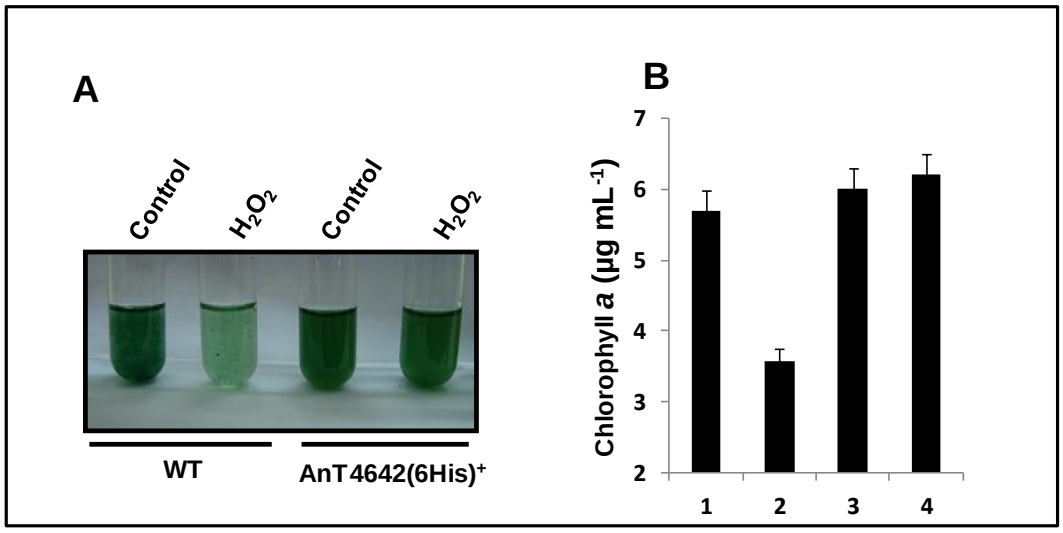

Fig. 4.12. AlrT4642 protects *Anabaena* from oxidative stress. (A) Three-day old cultures were inoculated in fresh BG11N^{+} and subjected to 1 mM H_2O_2 stress for 2 days. Subsequently, the cultures were photographed. WT, wild-type *Anabaena* PCC7120 and AnT4642+, recombinant *Anabaena* PCC7120 over-expressing AlrT4642(6His). (B) The chlorophyll *a* content of the cultures shown in (A) was determined after 2 days of exposure to H_2O_2. 1, WT/contol; 2, WT/H_2O_2; 3, AnT4642^{+}/control and 4, AnT4642^{+}/H_2O_2.

4.13 Discussion

Reactive oxygen species (ROS) such as superoxide anion ($\cdot O_2$), hydroxyl radical ($\cdot OH$), and hydrogen peroxide (H_2O_2), constantly formed in all aerobic organisms, can cause damage to a wide range of biomolecules, including DNA molecules and proteins [19]. ROS are formed by

partial reduction of oxygen during cellular metabolism. Environmental stresses, e.g. salinity, sudden osmotic alterations, desiccation, non-ionizing radiations, metal toxicity, high light intensity etc., result in enhanced generation of ROS, indicating an obvious cross-talk between these stresses and oxidative stress [219].

Hydrogen peroxide (H_2O_2) is a very common ROS in biological systems and cyanobacteria, in particular, have been shown to be generally more susceptible to H_2O_2 than other phototrophs [220]. Being photoautotrophs, cyanobacteria have to not only detoxify (ROS) generated by the photosynthetic electron transport chain, but also scavenge those generated during respiration i.e. reduction of oxygen [144]. H_2O_2, though relatively stable, can undergo Fenton reaction to generate the most damaging ROS, i.e. ·OH [221]; hence, it is particularly important to remove intracellular H_2O_2. Detoxification of H_2O_2 is largely mediated by peroxidases and catalases that convert H_2O_2 into harmless water [206]. As *Anabaena* shows extremely low levels of catalase activity, it is proposed that thiol peroxidases such as Prxs may be the principal components that eliminate H_2O_2 [153, 161]. This view is supported by the relatively large number of *prx* genes present in the genome of *Anabaena* PCC7120 [150].

The role of hitherto uncharacterized *alr4642* ORF, encoding the Alr4642 protein, was explored in this study. The Alr4642 protein, which showed similarity to Prx-like2 group of Prxs, was found to be highly conserved in cyanobacteria and was present in diverse species ranging from the filamentous forms such as *Fischerella muscicola* to unicellular forms such as *Synechococcus* PCC7335 and *Gloeobacter violaceus*. All the nitrogen-fixing cyanobacteria, e.g. *Nostoc* sp., *Anabaena* sp. and Cyanotheceae, also showed the presence of Alr4642-like ORFs. Typically, homolologs of Alr4642 were found mostly in cyanobacteria and not in other heterotrophic bacteria, indicating that these may play a unique role in

cyanobacteria.

The LexA protein, a transcriptional repressor, is believed to regulate genes involved in DNA repair (SOS response) in *E. coli* and in other bacteria. LexA protein from *E. coli* specifically binds to the *E. coli* SOS box, an imperfect 20-bp palindrome that contains the sequence CTG$(TA)_5$ CAG [175, 222]. In *E. coli*, function of the LexA protein is regulated by RecA. The RecA protein gets activated in response to DNA damage, and this activation in turn induces the autocatalytic cleavage of LexA. On cleavage, the LexA protein loses its ability to bind DNA and thus, no longer function as repressor. More recently, the hypothesis that LexA regulates only the genes involved in SOS repair has been contested in many prokaryotes, including cyanobacteria. In *Synechocystis* sp. strain PCC 6803, LexA was shown to control expression of few genes involved in carbon metabolism. Subsequently, LexA was postulated to be involved in redox-responsive gene expression in *Synechocystis* PCC 6803 [223], indicating that LexA does also regulate genes that are not directly involved in SOS response. The LexA protein has been shown to be expressed in *Anabaena* PCC 7120 and interestingly, stresses that induce SOS-response did not influence the cellular content of the LexA protein nor did bring about cleavage of LexA in *Anabaena* [224]. Bioinformatic analysis of the *alr4642* promoter showed the presence of the sequence that resembled the *E. coli* LexA box. Moreover, the purified LexA protein also bound to this DNA sequence in vitro, suggesting that expression of *alr4642* may be repressed by the LexA protein in *Anabaena*.

In spite of being located downstream of a gene that is highly expressed (*alr4641* that encodes 2-Cys-Prx) [162], expression of the *alr4642* mRNA or the Alr4642protein could not be detected under any of the conditions tested. Clearly, there is no read through from the *alr4641* promoter into the *alr4642* promoter. Not only in the present study, but other large scale

proteomic studies in response to various stress (including oxidative) have also failed to detect expression of the Alr4642 protein in *Anabaena*. Bioinformatic analysis showed the presence of a weak promoter upstream of the *alr4642* ORF. Thus, probably due the absence of a strong promoter and the presence of LexA binding site within this promoter, the *alr4642* is not transcribed efficiently, consequently, this leads to the absence of the Alr4642 protein in *Anabaena*.

Interestingly, homology of Alr4642 with the other Prx-like2 proteins commenced from its second methionine that was 36 amino acids away from the first methionine annotated in the database (Fig. 4.2.3). Moreover, in *Anabaena*, expression of the complete *alr4642* ORF (from pAM4642) resulted in production of a smaller protein whose size corresponded to that of AlrT4642 (Fig. 4.9.2.3) suggesting that the second ATG codon may be the actual *in vivo* start codon of *alr4642* in *Anabaena*.

Solubility of proteins that are over-expressed employing the pET system in *E. coli* is a major problem, and in many cases, the over-produced protein is exclusively present (presumably in inactive form) in the inclusion bodies. Similarly, both Alr4642 and AlrT4642 could not be produced in *E. coli* in soluble form. In frame fusion of a protein of interest which is insoluble in *E. coli* with a chaperone protein is known to increase solubility of the protein. Fusion of AlrT4642 with trigger factor (TF) resulted in the production of AlrT4642-TF which remained soluble in *E. coli*. However, it was not possible to separate the AlrT4642 from TF even after cleaving the two polypeptides, indicating tight binding of TF with the AlrT4642 (4.8.4). These results suggest AlrT4642 remains soluble only when associated with chaperone proteins like TF.

However, over-expression of *alr4642* or *alrT4642(6His)* in *Anabaena* PCC 7120 led to production of soluble AlrT4642 and AlrT4642(6His), respectively (Fig. 4.10.3). In fact, AlrT4642(6His) expressed in *Anabaena* could be purified to near homogeneity by affinity chromatography with the Ni- NTA matrix (Fig. 4.10.4). To our knowledge, this is the first instance wherein a *Anabeana* protein after over-expression in *Anabaena*. In an earlier study, Mn-catalase from *Anabaena* PCC 7120 (Alr0998) was over-expressed in *E. coli* and resulted in production of insoluble protein that could not be purified [152]. When over-expressed in *Anabaena*, the Alr4642 protein not only remained soluble, but was also active. These data show the potential use of *Anabaena* PCC 7120 strain for generation of soluble proteins in cases where it is not possible to do so in *E. coli*.

Prxs from *Anabaena* PCC7120 are known to show TrxA-dependent (e.g. Alr3183) or GSH-dependent (e.g. All1541 & Alr4404) or NTRC-dependent (e.g. Alr4641) peroxidase activity. However, the purified Alr4642 protein could not utilize any of the above-mentioned electron donors for peroxide activity. The exact reason for this is not clear, but Prxs are known to use their cognate TrxA partners more efficiently (as reducing agents) to decompose peroxides. *Synechocystis* PCC6803 shows the presence of 5 Prxs (2-Cys-Prx, PrxQ, 1-Cys-Prx, PrxQ1 and PrxQ2) and the three TrxA homologs (TrxA, TrxB and TrxQ). Each Prx utilized the TrxA/TrxB/TrxQ with different efficiencies. PrxII used TrxQ more efficiently than TrxB whereas PrxQ1 could utilize *Synechocystis* TrxA and TrxB as electron donors but failed to utilize PrxQ. For Alr4642, *E. coli* TrxA was employed in the assays. It is likely that due to the absence of the appropriate TrxA equivalent from *Anabaena*, Alr4642 did not show any peroxidase activity. *Anabaena* PCC 7120 also shows the presence of 3 TrxA homologs (TrxA, TrxA2 and TrxA3). Possibly, if TrxA equivalents from *Anabaena* are employed in the reaction, Alr4642 may indeed show TrxA-dependent activity with at least one of them.

A metal-catalyzed oxidation (MCO) assay was performed to verify if Alr4642 could protect a vital molecule such as DNA *in vitro*. In MCO, in the presence of electron donor such as DTT, Fe^{3+} catalyzes reduction of atmospheric O_2 to H_2O_2 and is itself converted to Fe^{2+}. H_2O_2 formed is rapidly converted to hydroxyl radicals ($^{\cdot}OH$) via the Fenton reaction. These radicals damage and degrade the DNA, which can be visualized by electrophoresis. However, in the presence of active peroxidases (e.g. Prxs), the H_2O_2 generated is rapidly decomposed, resulting in reduced production of $^{\cdot}OH$ and consequently, DNA is protected. The purified Alr4642 protein could confer considerable protection to the plasmid in the MCO assay. This clearly suggests that Alr4642 can detoxify H_2O_2, i.e. function as a peroxidase and eventually prevent formation of $OH^{\cdot}$. Many studies have employed DTT as reducing equivalent to study the peroxide activity of Prxs as DTT can act as a non-specific electron donor. The purified Alr2503 protein (from *Anabaena* PCC 7120) showed a poor TrxA-dependent activity whereas a distinct DTT-dependent capacity to detoxify hydrogen peroxide was observed [144]. Akin to Alr2503, the Alr4642 protein from *Anabaena* PCC 7120 showed DTT-dependent capability to detoxify H_2O_2, indicating that it could indeed function as a peroxidase. Hence, when over-expressed in *Anabaena*, the AlrT4642(6His) protein was not only soluble but was also biologically active.

The presence of H_2O_2 in the medium is known to cause severe toxicity to filamentous cyanobacteria. On its own, H_2O_2 is a weak oxidant, but in the presence of Fe^{2+}, it forms $^{\cdot}OH$, the most deleterious radical, which can directly or indirectly (via generation of protein radicals and lipid peroxides) damage all the cellular macromolecules. The BG-II culture medium has traces of transition metals, including iron. So, in the presence of H_2O_2, the hydroxyl radical can be readily formed within cells. Protein synthesis *per se* is also known to be a specific target of H_2O_2 in cyanobacteria. Inhibition of protein synthesis prevents the

repair of photosystems from photodamage and eventually leads to disruption of photosynthesis and pigment loss. However, if proteins that decompose H_2O_2 (Prxs/catalases) are adequately present, they can effectively detoxify H_2O_2 and protect the cellular components from H_2O_2-mediated oxidative damage.

In cyanobacteria, chlorophyll *a* content is a reliable indicator of growth and is routinely used to assess resistance to various stresses. Other studies have shown *Anabaena* PCC7120 to be very sensitive to H_2O_2 [153, 162] or methyl viologen [157] and addition of these agents to the culture medium results in the considerable reduction of chlorophyll *a*, indicating cessation in growth. In *Chrysosporum ovalisporum* ILC, an akinite forming cyanobacterium, growth inhibition was observed with as little as 0.1 mM H_2O_2 and addition of just 0.5 mM H_2O_2 resulted in complete collapse of this culture [212]. In the present study, treatment of H_2O_2 led to distinct reduction in the chlorophyll *a* content, in the wild-type *Anabaena* PCC7120 whereas in contrast, under similar conditions, AnT4642(6His)$^+$ did not bleach and the chlorophyll *a* content remained similar to that of the non-stressed cells. These results clearly demonstrate that AlrT4642, a Prx-like2 protein, can protect *Anabaena* PCC7120 from oxidative stress mediated by H_2O_2.

In conclusion, *alrT4642* is not expressed in *Anabaena*, possibly due to the presence of a weak promoter and probable repression by the LexA protein. In spite of being insoluble in *E. coli*, the AlrT4642 protein remained soluble when over-expressed (from a strong promoter) in *Anabaena*. The second methionine was identified as the actual start codon of Alr4642in *Anabaena*. The AlrT4642(6His) protein, purified from *Anabaena*, protected DNA from oxidative damage suggesting that it is indeed an antioxidant protein. Over-expression of AlrT4642 protected *Anabaena* from oxidative stress mediated by H_2O_2. These results

demonstrate the possible use of prx-like genes for construction of stress-tolerant *Anabaena* strains for use as biofertilizers.

Chapter 5 – Summary and Conclusions

Reactive oxygen species, which include superoxide (O_2^-), the hydroxyl radical ($^{\cdot}OH$), and hydrogen peroxide (H_2O_2) are constantly made as by-products of normal cellular metabolic activities in the course of aerobic growth. Cyanobacteria, due to their close association with molecular oxygen, have developed elaborate mechanisms to protect their cellular machinery from ROS. The heterocystous, filamentous, cyanobacterium *Anabaena* performs two vital functions, namely photosynthesis and nitrogen fixation, which are very sensitive to ROS. Nitrogen-fixing strains of cyanobacteria such as *Anabaena* are economically valuable and eco-friendly source of biofertilizers in the paddy fields of South East Asia [225]. The various abiotic stresses (drought, salt, extreme temperatures, high light intensity, herbicides etc.) lead to over-production of ROS [226], which adversely affects the biofertilizer potential of *Anabaena*. Hence, a deeper understanding of the molecular machinery that alleviates oxidative stress in *Anabaena* is important for development of biofertilizers for use under unfavorable field conditions.

Organisms have evolved different strategies that include enzymatic (catalases, superoxide dismutases and peroxidases) and non-enzymatic (e.g. glutathione and ascorbate) defense mechanisms to detoxify ROS. Peroxiredoxins (Prxs), also called thiol peroxidases, are proteins that detoxify ROS, such as hydrogen peroxide, alkyl hydroperoxides and peroxinitrites. Prxs possess a catalytic cysteine residue, the peroxidatic cysteine (C_p) that is involved in detoxification of peroxides. During reaction cycle, C_p residue reacts with the peroxide substrate and is oxidized. Many Prxs also have another conserved cysteine residue, the resolving cysteine (C_r), which forms an intermolecular or intramolecular disulfide bond with the oxidized C_p during the reaction cycle. Regeneration of the reduced form of the catalytic cysteine residues is ultimately facilitated by reductants such as thioredoxin,

glutaredoxin, cyclophillins etc [119, 227].

The role played by the various proteins in overcoming oxidative stress in the filamentous, heterocystous, diazotrophic, cyanobacterium *Anabaena* PCC7120 has generated lot of interest in the recent past [166, 167, 168, 151, 162, 228]. The genome of *Anabaena* PCC 7120 shows the presence of 10 peroxiredoxin genes [160]. Of these, the role of *alr3183* and *alr4642* in overcoming oxidative stress was addressed in the present study.

Bioinformatic analysis indicated Alr3183 to belong to the PrxQ family of Prxs, wherein the C_p was located within the GCT motif. Further, the cysteine residue at 46^{th} amino acid position was suggested to be C_p whereas the cysteine at 51^{st} position was proposed to be C_r. The *alr3183* gene from *Anabaena* PCC7120 was cloned into the expression vector, pET16b, and the His-tagged Alr3183 protein over-expressed in *E. coli* was subsequently purified by affinity chromatography. To evaluate the role of catalytic cysteines in the Alr3183 protein, codons corresponding to both the Cys residues were separately mutated to serine by site directed mutagenesis. Similarly, a mutant Alr3183 wherein both the Cys residues were changed to Ser was also generated. The DNA fragments thus obtained, *alr3183C46S*, *alr3183C51S* or *alr3183CDM* (cysteine double mutant) were also cloned into pET16b and the corresponding proteins were purified after over-expression.

When resolved on reducing SDS-polyacrylamide gels, all the four proteins migrated with an apparent molecular mass of ~20 kDa, which matched their monomeric size. Incidentally, the Alr3183 protein appeared as two closely spaced bands on reducing SDS-polyacrylamide gels. MALDI-TOF MS-based peptide mass finger printing analysis confirmed both the bands to be Alr3183. Results with 4-acetamido-4′-maleimidyl-stilbene-2,2′-disulfonate (AMS) showed Alr3183 to form intra-molecular disulfide bonds. On non-reducing polyacrylamide gels,

Alr3183 and Alr3183CDM appeared at monomeric position whereas both Alr3183C46S and Alr3183C51S appeared as dimers. Thus, in the absence of one catalytic cysteine, the other catalytic cysteine (of one monomer) can form intermolecular disulfide bond with its counterpart (from another monomer) and dimerize, whereas, when both the cysteines are present, intramolecular disulphide bond is formed. Gel exclusion chromatography and dynamic light scattering studies also showed Alr3183 to exist as a monomer whereas Alr3183C46S and Alr3183C51S were dimeric. CD spectropolarimetry showed the Alr3183 protein to primarily be an α-helical protein. Reducing the protein with DTT did not significantly alter its secondary structure. Interestingly, Alr3183C46S and Alr3183C51S, in spite of being dimeric, showed only minor changes in the secondary structure when compared with Alr3183, indicating that dimer formation did not cause major alterations in the secondary structure of this protein.

Among the three different reductants (GSH, DTT and TrxA) employed for detoxification of H_2O_2, Alr3183 showed peroxidase activity with TrxA. Along with H_2O_2, Alr3183 could decompose peroxides such as t-butyl hydroperoxide and cumene hydroperoxide using TrxA. Surface Plasmon Resonance (SPR) analysis showed Alr3183 to physically interact with TrxA and interestingly, the DTT-reduced protein showed decreased binding to TrxA as compared to the control Alr3183 protein (i.e. not treated with DTT). Alr3183C46S bound to TrxA in a manner similar to that shown by the wild-type Alr3183, whereas Alr3183C51S and Alr3183CDM showed considerably reduced interaction with TrxA. Thus, the presence of the C_r appears to enhance the binding of the Alr3183 protein to TrxA.

On exposure to elevated temperatures, Alr3183 remained fully functional till 40°C, but a severe drop in its activity was observed beyond 45°C, and the protein was completely

inactive when exposed to 60°C. Interestingly, unlike other Prxs, such as Alr4641 and All1541 from *Anabaena*, Alr3183 protein was active even after treatment with 5 mM H_2O_2, indicating that C_p of Alr3183 was not easily over-oxidized by H_2O_2.The Alr3183C46S protein (that lacks C_p) showed complete absence of peroxidase activity whereas Alr3183C51S (wherein C_r was absent) showed partial activity. However, this activity was several-fold lower than of Alr3183. Moreover, Alr3183C51S required relatively higher concentration of TrxA (2 µM or more) to show any peroxidase activity, whereas the wild-type protein showed peroxidase activity even with 0.5 µM TrxA.

Expression of the Alr3183 protein was monitored in *Anabaena* in response to stresses such as H_2O_2, methyl viologen, salt etc. Only a minor amount of Alr3183 could be detected in the untreated cells and no further induction of the Alr3183 protein was in response to oxidative stress-inducing agents. As the inherent levels of the Alr3183 protein were low in *Anabaena*, it was desired to verify if over-expression of Alr3183 could protect *Anabaena* from oxidative stress. The complete *alr3183* ORF was cloned in between a strong light inducible P_{psbA1}promoter and the *gfpmut2*gene in pAM1956 (construct denoted pAM3183), which was subsequently conjugated into *Anabaena* PCC7120 (to give rise to $An3183^+$). When probed with the Alr3183 antiserum on Western blots, the recombinant $An3183^+$showed considerable production of the Alr3183 protein. The $An3183^+$ strain showed 5-6 times less levels of ROS than the wild-type strain when exposed to 1 mM H_2O_2.Under nitrogen-deficient as well as nitrogen-supplemented conditions, H_2O_2 caused destruction of photosynthetic pigments and cell death in the wild-type *Anabaena* cells, but $An3183^+$was protected from these deleterious effects. The 3183C46S protein was also over-produced in *Anabaena* employing the same strategy used to over-express Alr3183. However, unlike Alr3183, Alr3183C46S was ineffective in offering any protection from oxidative stress, demonstrating that the peroxidase

activity of Alr3183 was essential to protect *Anabaena* from the lethal effects of H_2O_2.

Unlike the results obtained with oxidative stress causing chemicals such as H_2O_2 or methyl viologen, the Alr3183 protein was found to be distinctly induced in response to γ-radiation. Antisense approach was employed to reduce expression of the Alr3183 protein on exposure to gamma radiation. The complete *alr3183* ORF was cloned in the reverse orientation (i.e. antisense) between a strong light inducible P*psbA1* promoter and the *gfpmut2*gene in pAM1956 (construct denoted pAMAS3183), which was subsequently conjugated into *Anabaena* PCC7120 (to give rise to AnAS3183$^+$). As compared to the wild-type *Anabaena*, a distinct decrease in the synthesis of the Alr3183 protein was observed in AnAS3183$^+$ on exposure to γ-radiation. On exposure to 3 kGy dose, AnAS3183$^+$ showed a reduction in growth as compared to the wild-type, suggesting a role for Alr3183 in overcoming γ-radiation stress.

Studies pertaining to the characterization of the Alr4642 protein from *Anabaena* PCC 7120 are described in chapter 4. In *Anabaena*, *alr4642* was located immediately downstream of ORF encoding 2-Cys-Prx i.e. *alr4641*. BLAST search showed the ORF *alr4642* (642-bp, encoding 213 amino acids) from *Anabaena* PCC 7120 to belong to the thioredoxin superfamily and share homology with the Prx-like2 proteins from many other cyanobacteria. Interestingly, similarity of Alr4642 with the other Prx-like2 proteins was observed only from its second methionine, which was 35 amino acids downstream from the first annotated methionine. The protein initiating from the second methionine was therefore designated as AlrT4642, (T for truncated). The Prx-like2 domain of Alr4642 extended from 75thto 196th amino acid. Alr4642 showed presence of CXXC motif similar to that present in thioredoxin (Trx).

The promoter search program, BPROM, identified a promoter that was located right at the beginning of the full-length *alr4642* ORF. Although, the -10 region of the identified promoter showed a good match with the consensus -10 promoter sequences, the -35 region showed poor match with its respective consensus, indicating that the promoter was inherently a weak promoter. A LexA box that overlapped directly with the -10 sequence was identified bioinformatically. Electrophoretic moblity shift assays (EMSAs) showed that LexA protein from *Anabeana* PCC 7120 could bind to the *alr4642* promoter DNA. The *alr4642* transcript could not be detected in control cells or in response to oxidizing agents such as H_2O_2, methyl-viologen and tertiary-butyl hydroperoxide. Thus, possibly due to the presence of a weak promoter and/or possible repression by the LexA protein, the *alr4642* ORF was not expressed in *Anabaena*.

Prx-like proteins have not been characterized from any bacterium. Hence, it was desired to purify the Alr4642 protein for biochemical analysis. As homology with the other Prx-like proteins was observed from the second methionine (Met-36), along with the full-length *alr4642* ORF, a truncated *alr4642* i.e. *alrt4642* (537-bp, encoding a protein extending from 36^{th}residue to 213^{th} residue i.e. 178 amino acids) was also cloned in *E. coli* expression vector pET16b for overproduction of N-terminally His-tagged, Alr4642 or AlrT4642. In spite of abundant production, 10HisAlr4642 or 10HisAlrT4642 were both insoluble in *E. coli* and located exclusively in the inclusion bodies. Attempts to purify Alr4642/AlrT4642 under denaturing conditions and to renature it were also unsuccessful. The over-expressed Alr4642 was eluted from the SDS-polyacrylamide gels and employed to generate polyclonal antiserum in mouse.

As Alr4642could not be expressed in soluble form in *E. coli*, attempts were made to purify Alr4642 after expressing it in *Anabaena*. The complete *alr4642* ORF was cloned in between

a strong light inducible P_{psbA1} promoter and a *gfpmut2* ORF in pAM1956 (construct denoted pAMAlr4642), which was subsequently conjugated into *Anabaena* PCC 7120. When exconjugants were probed with the Alr4642 antiserum on Western blots, the recombinant An4642$^+$ (but not the wild-type *Anabaena*) showed production of a shorter Alr4642 protein, whose size (20.3 kDa) matched with that of AlrT4642, and not the full length Alr4642. This indicated that the codon corresponding to the second methionine was the actual start codon *in vivo* in *Anabaena*.

As the above-mentioned results suggested that AlrT4642 (but not Alr4642) was expressed in *Anabaena*, the His-tagged AlrT4642 protein was over-expressed in *Anabaena* for purification. To accomplish this, the *alrt4642* ORF with 6 additional His codons at its 3' end [i.e. *alrt4642(6His)*] was cloned downstream of P_{psbA1} promoter in pAM1956 (pAMT4642) and conjugated into *Anabaena* to obtain AnT4642(6His)$^+$. Expression of AlrT4642(6His) was verified on Western blots with the Alr4642 antiserum wherein production of a ~21.2 kDa protein was observed (the addition of the 6-His tag increased the size of the protein by ~0.9 kDa). This protein was observed in the cytosolic fraction of *Anabaena* extracts. The AlrT4642 protein could be purified to near homogeneity by affinity chromatography employing the Ni-NTA matrix. The identity of purified AlrT4642 was confirmed by probing it with anti-Alr4642 and anti-polyhistidine antibodies. In metal catalyzed oxidation (MCO) assays, the Alr4642(6His) protein offered distinct protection to DNA. Although this protein failed to show TrxA-dependent Prx activity, Alr3183 did demonstrate a DTT-dependent peroxidase activity**.** The recombinant AnT4642(6His)$^+$ and the wild-type *Anabaena* PCC7120 were monitored for oxidative stress resistance in response to hydrogen peroxide. After 2 days of peroxide treatment, a pronounced bleaching, indicating loss of photosynthetic pigments, was observed in the wild-type cells but not in AnT4642(6His)$^+$ cells, indicating that that over-

expression of AlrT4642 protein can protect *Anabaena* from oxidative stress.

In conclusion, Alr3183 is a monomeric, TrxA-dependent peroxidase whose C_p and C_r, form an intramolecular disulfide bond. The presence of both C_p and C_r prohibits intermolecular disulfide bond formation, but, if either of the catalytic cysteine is absent, the protein becomes dimeric due to formation of intermolecular C_p-C_p or C_r-C_r linkages. C_p is essential for reacting with the peroxidatic substrate whereas the presence of C_r appears to improve the protein's capability to interact with TrxA. *In vivo*, Alr3183 was found to be a stress-inducible protein whose synthesis was upregulated by γ-radiation. Over-expression of Alr3183 protected *Anabaena* from oxidative stress in nitrogen-supplemented as well as nitrogen-deficient conditions. The *alrT4642* is not expressed in *Anabaena*, possibly due to the presence of a weak promoter and repression by the LexA protein. In spite of being insoluble in *E. coli*, the AlrT4642 protein remains soluble when over-expressed (from a strong promoter) in *Anabaena*. The second methionine is the actual start codon of Alr4642 in *Anabaena.* The AlrT4642(6His) protein, purified from *Anabaena*, protected DNA from oxidative damage suggesting that it is indeed an anti-oxidant protein. Over-expression of AlrT4642 protected *Anabaena* from oxidative stress mediated by H_2O_2. These results demonstrate the possible use of both *alr3183* and *alr4642* for construction of stress-tolerant *Anabaena* strains for use as biofertilizers.

References

1. Valko, Marian, C. J. Rhodes, Jan Moncol, M. M. Izakovic, and Milan Mazur. "Free radicals, metals and antioxidants in oxidative stress-induced cancer." Chemico-biological interactions 160, no. 1 (2006): 1-40.
2. Hermes-Lima, Marcelo. "Oxygen in biology and biochemistry: role of free radicals." Functional metabolism: Regulation and adaptation 1 (2004): 319-66.
3. Sen, Chanden K. "Oxygen toxicity and antioxidants: state of the art." Indian journal of physiology and pharmacology 39, no. 3 (1995): 177-196.
4. Mach, William J., Amanda R. Thimmesch, J. Thomas Pierce, and Janet D. Pierce. "Consequences of hyperoxia and the toxicity of oxygen in the lung." Nursing research and practice 2011 (2011).
5. Auten, Richar d L., and Jonathan M. Davis. "Oxygen toxicity and reactive oxygen species: the devil is in the details." Pediatric research 66, no. 2 (2009): 121-127.4.
6. Rolfe, Rial D., David J. Hentges, Benedict J. Campbell, and James T. Barrett. "Factors related to the oxygen tolerance of anaerobic bacteria." Applied and environmental microbiology 36, no. 2 (1978): 306-313.
7. Winterbourn, Christine C. "Reconciling the chemistry and biology of reactive oxygen species." Nature chemical biology 4, no. 5 (2008): 278-286.
8. Halliwell, Barry, and JMe Gutteridge. "Oxygen toxicity, oxygen radicals, transition metals and disease." Biochemical journal 219, no. 1 (1984): 1.
9. Halliwell, Barry. "Reactive oxygen species in living systems: source, biochemistry, and role in human disease." The American journal of medicine 91, no. 3 (1991): S14-S22.
10. Lee, J., N. Koo, and D. B. Min. "Reactive oxygen species, aging, and antioxidative nutraceuticals." Comprehensive reviews in food science and food safety 3, no. 1 (2004): 21-33.
11. Wayne, R. P. "Singlet molecular oxygen." Advances in photochemistry 7, no. 3 (1969): 1.
12. Murphy, Michael P. "How mitochondria produce reactive oxygen species." Biochemical Journal 417, no. 1 (2009): 1-13.
13. Warren, J. S., K. J. Johnson, and P. A. Ward. "Oxygen radicals in cell injury and cell death." Pathology and immunopathology research 6, no. 5-6 (1987): 301-315.
14. Halliwell, B., and J. M. C. Gutteridge. "Free Radicals in Biology and Medicine, 4th edn Oxford University Press." (2007).
15. Cabiscol, Elisa, Jordi Tamarit, and Joaquim Ros. "Oxidative stress in bacteria and protein damage by reactive oxygen species." International Microbiology 3, no. 1 (2010): 3-8.
16. Tiwari, Budhi Sagar, Beatrice Belenghi, and Alex Levine. "Oxidative stress increased respiration and generation of reactive oxygen species, resulting in ATP depletion,

opening of mitochondrial permeability transition, and programmed cell death." Plant physiology 128, no. 4 (2002): 1271-1281.
17. Latifi, Amel, Marion Ruiz, Robert Jeanjean, and Cheng-Cai Zhang. "PrxQ-A, a member of the peroxiredoxin Q family, plays a major role in defense against oxidative stress in the cyanobacterium Anabaena sp. strain PCC7120." Free Radical Biology and Medicine 42, no. 3 (2007): 424-431.
18. Betteridge, D. John. "What is oxidative stress?." Metabolism 49, no. 2 (2000): 3-8.
19. Imlay, James A. "Pathways of oxidative damage." Annual Reviews in Microbiology 57, no. 1 (2003): 395-418.
20. Holmstrom, K. M., and Toren Finkel. "Cellular mechanisms and physiological consequences of redox-dependent signalling." Nat Rev Mol Cell Biol 15, no. 6 (2014): 411-421.
21. Imlay, James A. "Cellular defenses against superoxide and hydrogen peroxide." Annu. Rev. Biochem. 77 (2008): 755-776.
22. Chen, Dongrong, Caroline RM Wilkinson, Stephen Watt, Christopher J. Penkett, W. Mark Toone, Nic Jones, and Jürg Bähler. "Multiple pathways differentially regulate global oxidative stress responses in fission yeast." Molecular biology of the cell 19, no. 1 (2008): 308-317.
23. Brand, Martin D. "The sites and topology of mitochondrial superoxide production." Experimental gerontology 45, no. 7 (2010): 466-472.
24. Sazanov, Leonid A., and Philip Hinchliffe. "Structure of the hydrophilic domain of respiratory complex I from Thermus thermophilus." science 311, no. 5766 (2006): 1430-1436.
25. Hirst, Judy, Martin S. King, and Kenneth R. Pryde. "The production of reactive oxygen species by complex I." (2008): 976-980.
26. Dröse, Stefan, and Ulrich Brandt. "The mechanism of mitochondrial superoxide production by the cytochrome bc1 complex." Journal of Biological Chemistry 283, no. 31 (2008): 21649-21654.
27. Flint, Dennis H., J. F. Tuminello, and M. H. Emptage. "The inactivation of Fe-S cluster containing hydro-lyases by superoxide." Journal of Biological Chemistry 268, no. 30 (1993): 22369-22376.
28. Rada, Balázs, and T. Leto. "Oxidative innate immune defenses by Nox/Duox family NADPH oxidases." In Trends in Innate Immunity, vol. 15, pp. 164-187. Karger Publishers, 2008.
29. Azzam, Edouard I., Jean-Paul Jay-Gerin, and Debkumar Pain. "Ionizing radiation-induced metabolic oxidative stress and prolonged cell injury." Cancer letters 327, no. 1 (2012): 48-60.
30. Khan, K. A. "The radiation chemistry of water." J. Chem. Soc. Pak 3, no. 3 (1981).
31. Foyer, Christine H., and Shigeru Shigeoka. "Understanding oxidative stress and antioxidant functions to enhance photosynthesis." Plant physiology 155, no. 1 (2011): 93-100.

32. Foyer, Christine H., and Graham Noctor. "Redox sensing and signalling associated with reactive oxygen in chloroplasts, peroxisomes and mitochondria." Physiologia Plantarum 119, no. 3 (2003): 355-364.
33. Mehler, Alan H. "Studies on reactions of illuminated chloroplasts: I. Mechanism of the reduction of oxygen and other hill reagents." Archives of Biochemistry and Biophysics 33, no. 1 (1951): 65-77.
34. Asada, Kozi, Kuniaki Kiso, and Kyoko Yoshikawa. "Univalent reduction of molecular oxygen by spinach chloroplasts on illumination." Journal of Biological Chemistry 249, no. 7 (1974): 2175-2181.
35. Laloi, Christophe, and Michel Havaux. "Key players of singlet oxygen-induced cell death in plants." Frontiers in plant science 6 (2015).
36. Telfer, Alison, Suman Dhami, Steven M. Bishop, David Phillips, and James Barber. "beta-Carotene quenches singlet oxygen formed by isolated photosystem II reaction centers." Biochemistry 33, no. 48 (1994): 14469-14474.
37. Hideg, Éva, Tamás Kálai, Kálmán Hideg, and Imre Vass. "Photoinhibition of photosynthesis in vivo results in singlet oxygen production detection via nitroxide-induced fluorescence quenching in broad bean leaves." Biochemistry 37, no. 33 (1998): 11405-11411.
38. Winston, Gary W., and Richard T. Di Giulio. "Prooxidant and antioxidant mechanisms in aquatic organisms." Aquatic toxicology 19, no. 2 (1991): 137-161.
39. Schieber, Michael, and Navdeep S. Chandel. "ROS function in redox signaling and oxidative stress." Current Biology 24, no. 10 (2014): R453-R462.
40. Imlay, J. A., and I. Fridovich. "Suppression of oxidative envelope damage by pseudoreversion of a superoxide dismutase-deficient mutant of Escherichia coli." Journal of bacteriology 174, no. 3 (1992): 953-961.
41. Keyer, Kay, and James A. Imlay. "Superoxide accelerates DNA damage by elevating free-iron levels." Proceedings of the National Academy of Sciences 93, no. 24 (1996): 13635-13640.
42. Fridovich, Irwin. "The biology of oxygen radicals." Science 201, no. 4359 (1978): 875-880.
43. Baron, J. Allen, Kaitlin M. Laws, Janice S. Chen, and Valeria C. Culotta. "Superoxide triggers an acid burst in Saccharomyces cerevisiae to condition the environment of glucose-starved cells." Journal of Biological Chemistry 288, no. 7 (2013): 4557-4566.
44. Guo, W., 2013. Identification and Characterization of Regulators of 2-Cys-Peroxiredoxin A in Arabidopsis thaliana (Doctoral dissertation, Freie Universität Berlin).
45. Augusto, Ohara, and Sayuri Miyamoto. "Oxygen radicals and related species." Principles of free radical biomedicine 1 (2011): 19-42.
46. Halliwell, Barry, John MC Gutteridge, and Carroll E. Cross. "Free radicals, antioxidants, and human disease: where are we now?." The Journal of laboratory and clinical medicine 119, no. 6 (1992): 598-620.

47. Kulkarni, Avanti, and David M. Wilson. "The involvement of DNA-damage and-repair defects in neurological dysfunction." The American Journal of Human Genetics 82, no. 3 (2008): 539-566.
48. Sies, Helmut, and Carlos FM Menck. "Singlet oxygen induced DNA damage." Mutation Research/DNAging 275, no. 3-6 (1992): 367-375.
49. Sies, Helmut. "Strategies of antioxidant defense." European Journal of Biochemistry 215, no. 2 (1993): 213-219.
50. Michiels, Carine. "Physiological and pathological responses to hypoxia." The American journal of pathology 164, no. 6 (2004): 1875-1882.
51. Lipinski, Boguslaw. "Hydroxyl radical and its scavengers in health and disease." Oxidative medicine and cellular longevity 2011 (2011).
52. Kruszewski, Marcin. "The role of labile iron pool in cardiovascular diseases." ACTA BIOCHIMICA POLONICA-ENGLISH EDITION- 51 (2004): 471-480.
53. Gutteridge, J. M. "Lipid peroxidation and antioxidants as biomarkers of tissue damage." Clinical chemistry 41, no. 12 (1995): 1819-1828.
54. Bielski, B. H., Ravindra L. Arudi, and Mark W. Sutherland. "A study of the reactivity of HO2/O2-with unsaturated fatty acids." Journal of Biological Chemistry 258, no. 8 (1983): 4759-4761.
55. Humpries, K. M., and L. I. Sweda. "Selective inactivation of α-ketoglutarate dehydrogenase: reaction of lipoic acid with 4-hydroxy-2-nonenal." Biochemistry 37 (1998): 15835-15841.
56. Cabiscol, Elisa, Eva Piulats, Pedro Echave, Enrique Herrero, and Joaquim Ros. "Oxidative stress promotes specific protein damage in Saccharomyces cerevisiae." Journal of Biological Chemistry 275, no. 35 (2000): 27393-27398.
57. Pompella, Alfonso, Athanase Visvikis, Aldo Paolicchi, Vincenzo De Tata, and Alessandro F. Casini. "The changing faces of glutathione, a cellular protagonist." Biochemical pharmacology 66, no. 8 (2003): 1499-1503.
58. Grill, Dieter. Significance of glutathione to plant adaptation to the environment. Vol. 2. Springer Science & Business Media, 2001.
59. Pastore, Anna, Giorgio Federici, Enrico Bertini, and Fiorella Piemonte. "Analysis of glutathione: implication in redox and detoxification." Clinica chimica acta 333, no. 1 (2003): 19-39.
60. Couto, Narciso, Naglis Malys, Simon J. Gaskell, and Jill Barber. "Partition and turnover of glutathione reductase from Saccharomyces cerevisiae: a proteomic approach." Journal of proteome research 12, no. 6 (2013): 2885-2894.
61. Smirnova, G. V., and O. N. Oktyabrsky. "Glutathione in bacteria." Biochemistry (Moscow) 70, no. 11 (2005): 1199-1211.
62. Oztetik, Elif, and Ayse Cakir. "New food for an old mouth: New enzyme for an ancient archaea." Enzyme and microbial technology 55 (2014): 58-64.
63. Lushchak, Volodymyr I. "Glutathione homeostasis and functions: potential targets for medical interventions." Journal of amino acids 2012 (2012).

64. Lu, Shelly C. "Regulation of glutathione synthesis." Current topics in cellular regulation 36 (2001): 95-116.
65. Michelet, F., Gueguen, R., Leroy, P., Wellman, M., Nicolas, A. and Siest, G., 1995. Blood and plasma glutathione measured in healthy subjects by HPLC: relation to sex, aging, biological variables, and life habits. Clinical chemistry, 41(10), pp.1509-1517.
66. Noctor, Graham, Guillaume Queval, Amna Mhamdi, Sejir Chaouch, and Christine H. Foyer. "Glutathione." The Arabidopsis Book 9, no. 1 (2011): 1-32.
67. Noctor, Graham, Amna Mhamdi, Sejir Chaouch, Y. I. Han, Jenny Neukermans, B. E. L. E. N. MARQUEZ-GARCIA, Guillaume Queval, and Christine H. Foyer. "Glutathione in plants: an integrated overview." Plant, Cell & Environment 35, no. 2 (2012): 454-484.
68. Xiang, Chengbin, Bonnie L. Werner, M. Christensen E'Lise, and David J. Oliver. "The biological functions of glutathione revisited in Arabidopsis transgenic plants with altered glutathione levels." Plant Physiology 126, no. 2 (2001): 564-574.
69. Yen, Gow-Chin, Pin-Der Duh, and Hui-Ling Tsai. "Antioxidant and pro-oxidant properties of ascorbic acid and gallic acid." Food chemistry 79, no. 3 (2002): 307-313.
70. Then, Sue-Mian, Coral Sanfeliu, Gapor M. Top, Wan Zurinah Wan Ngah, and Musalmah Mazlan. "γ-Tocotrienol does not substantially protect DS neurons from hydrogen peroxide-induced oxidative injury." Nutrition & metabolism 9, no. 1 (2012): 1.
71. Yoshida, Yasukazu, Etsuo Niki, and Noriko Noguchi. "Comparative study on the action of tocopherols and tocotrienols as antioxidant: chemical and physical effects." Chemistry and Physics of Lipids 123, no. 1 (2003): 63-75.
72. WEFERS, H. and SIES, H., 1988. The protection by ascorbate and glutathione against microsomal lipid peroxidation is dependent on vitamin E. European journal of Biochemistry, 174(2), pp.353-357.
73. Packer, Lester, Stefan U. Weber, and Gerald Rimbach. "Molecular aspects of α-tocotrienol antioxidant action and cell signalling." The Journal of nutrition 131, no. 2 (2001): 369S-373S.
74. Jackson, George R., Lori Apffel, Karin Werrbach-Perez, and J. Regino Perez-Polo. "Role of nerve growth factor in oxidant-antioxidant balance and neuronal injury. I. Stimulation of hydrogen peroxide resistance." Journal of neuroscience research 25, no. 3 (1990): 360-368.
75. Sen, Chandan K., Savita Khanna, and Sashwati Roy. "Tocotrienols: vitamin E beyond tocopherols." Life sciences 78, no. 18 (2006): 2088-2098.
76. Lu, Dan, Yi Yang, Yongxin Li, and Chengjun Sun. "Analysis of tocopherols and tocotrienols in pharmaceuticals and foods: a critical review." Current Pharmaceutical Analysis 11, no. 1 (2015): 66-78.
77. Pietta, Pier-Giorgio. "Flavonoids as antioxidants." Journal of natural products 63, no. 7 (2000): 1035-1042.

78. Kim, Hyun Pyo, Kun Ho Son, Hyeun Wook Chang, and Sam Sik Kang. "Anti-inflammatory plant flavonoids and cellular action mechanisms." Journal of pharmacological sciences 96, no. 3 (2004): 229-245.
79. Nijveldt, Robert J., E. L. S. Van Nood, Danny Ec Van Hoorn, Petra G. Boelens, Klaske Van Norren, and Paul AM Van Leeuwen. "Flavonoids: a review of probable mechanisms of action and potential applications." The American journal of clinical nutrition 74, no. 4 (2001): 418-425
80. Hertog, Michael GL, Daan Kromhout, Christ Aravanis, Henry Blackburn, Ratko Buzina, Flaminio Fidanza, Simona Giampaoli et al. "Flavonoid intake and long-term risk of coronary heart disease and cancer in the seven countries study." Archives of internal medicine 155, no. 4 (1995): 381-386.
81. Knekt, Paul, Ritva Jarvinen, Antti Reunanen, and Jouni Maatela. "Flavonoid intake and coronary mortality in Finland: a cohort study." Bmj 312, no. 7029 (1996): 478-481.
82. Kirti, Kushwaha, Saini Amita, Saraswat Priti, and Saxena Jyoti. "Colorful world of microbes: carotenoids and their applications." Advances in Biology 2014 (2014).
83. Stahl, Wilhelm, and Helmut Sies. "Antioxidant activity of carotenoids." Molecular aspects of medicine 24, no. 6 (2003): 345-351.
84. Gough, D. R., and T. G. Cotter. "Hydrogen peroxide: a Jekyll and Hyde signalling molecule." Cell death & disease 2, no. 10 (2011): e213.
85. Keyer, Kay, A. Strohmeier Gort, and James A. Imlay. "Superoxide and the production of oxidative DNA damage." Journal of bacteriology 177, no. 23 (1995): 6782-6790.
86. Miller, Anne-Frances. "Superoxide dismutases: ancient enzymes and new insights." FEBS letters 586, no. 5 (2012): 585-595.
87. Halliwell, Barry. "Biochemical mechanisms accounting for the toxic action of oxygen on living organisms: the key role of superoxide dismutase." Cell biology international reports 2, no. 2 (1978): 113-128.
88. Bruno-Bárcena, Jose M., Jason M. Andrus, Stephen L. Libby, Todd R. Klaenhammer, and Hosni M. Hassan. "Expression of a heterologous manganese superoxide dismutase gene in intestinal lactobacilli provides protection against hydrogen peroxide toxicity." Applied and Environmental Microbiology 70, no. 8 (2004): 4702-4710.
89. Fridovich, Irwin. "Superoxide radical: an endogenous toxicant." Annual Review of Pharmacology and Toxicology 23, no. 1 (1983): 239-257.
90. Tyler, DAVID D. "Polarographic assay and intracellular distribution of superoxide dismutase in rat liver." Biochemical Journal 147, no. 3 (1975): 493-504.
91. Peeters-Joris, C. H. A. N. T. A. L., ANNE-MARIE Vandevoorde, and P. Baudhuin. "Subcellular localization of superoxide dismutase in rat liver." Biochemical Journal 150, no. 1 (1975): 31-39.
92. Villafranca, Joseph J., Fred J. Yost, and Irwin Fridovich. "Magnetic Resonance Studies of Manganese (III) and Iron (III) Superoxide Dismutases TEMPERATURE

AND FREQUENCY DEPENDENCE OF PROTON RELAXATION RATES OF WATER." Journal of Biological Chemistry 249, no. 11 (1974): 3531281636
93. Gregory, Eugene M., and Irwin Fridovich. "Induction of superoxide dismutase by molecular oxygen." Journal of Bacteriology 114, no. 2 (1973): 543-548.
94. Hewitt, Joan, and J. G. Morris. "Superoxide dismutase in some obligately anaerobic bacteria." FEBS Lett 50, no. 3 (1975): 315-318.
95. Goscin, Stephen A., and Irwin Fridovich. "The purification and properties of superoxide dismutase from Saccharomyces cerevisiae." Biochimica et Biophysica Acta (BBA)-Enzymology 289, no. 2 (1972): 276-283.
96. Vance, Pat G., Bernard B. Keele, and K. V. Rajagopalan. "Superoxide dismutase from Streptococcus mutans isolation and characterization of two forms of the enzyme." Journal of Biological Chemistry 247, no. 15 (1972): 4782-4786.
97. Beauchamp, C. O., and Irwin Fridovich. "Isozymes of superoxide dismutase from wheat germ." Biochimica et Biophysica Acta (BBA)-Protein Structure 317, no. 1 (1973): 50-64.
98. Misra, Hara P., and Irwin Fridovich. "The role of superoxide anion in the autoxidation of epinephrine and a simple assay for superoxide dismutase." Journal of Biological chemistry 247, no. 10 (1972): 3170-3175.
99. Bihani, Subhash C., Dhiman Chakravarty, and Anand Ballal. "KatB, a cyanobacterial Mn-catalase with unique active site configuration: Implications for enzyme function." Free Radical Biology and Medicine 93 (2016): 118-129.
100. EPP, Otto, Rudolf LADENSTEIN, and Albrecht WENDEL. "The refined structure of the selenoenzyme glutathione peroxidase at 0.2-nm resolution." European Journal of Biochemistry 133, no. 1 (1983): 51-69.
101. Kim, K. A. N. G. H. W. A., I. H. Kim, Ki-Y. Lee, S. G. Rhee, and E. R. Stadtman. "The isolation and purification of a specific" protector" protein which inhibits enzyme inactivation by a thiol/Fe (III)/O2 mixed-function oxidation system." Journal of Biological Chemistry 263, no. 10 (1988): 4704-4711.
102. Wei, K. O. N. G., Susumu SHIOTA, S. H. I. Yixin, Hiroaki NAKAYAMA, and Koji NAKAYAMA. "A novel peroxiredoxin of the plant Sedum lineare is a homologue of Escherichia coli bacterioferritin co-migratory protein (Bcp)." Biochemical Journal 351, no. 1 (2000): 107-114.
103. Rouhier, Nicolas, Eric Gelhaye, Jose M. Gualberto, Marie-Noelle Jordy, Elisabeth De Fay, Masakazu Hirasawa, Sebastien Duplessis et al. "Poplar peroxiredoxin Q. A thioredoxin-linked chloroplast antioxidant functional in pathogen defense." Plant Physiology 134, no. 3 (2004): 1027-1038.
104. Chae, Ho Zoon, Keith Robison, Leslie B. Poole, George Church, Gisela Storz, and Sue Goo Rhee. "Cloning and sequencing of thiol-specific antioxidant from mammalian brain: alkyl hydroperoxide reductase and thiol-specific antioxidant define a large family of antioxidant enzymes."Proceedings of the National Academy of Sciences 91, no. 15 (1994): 7017-7021.

105. Chae, Ho Zoon, Sang Won Kang, and Sue Goo Rhee. "Isoforms of mammalian peroxiredoxin that reduce peroxides in presence of thioredoxin." Methods in enzymology 300 (1999): 219-226.
106. Hofmann, Birgit, H-J. Hecht, and Leopold Flohé. "Peroxiredoxins." Biological chemistry 383, no. 3-4 (2002): 347-364.
107. Seaver, Lauren Costa, and James A. Imlay. "Alkyl hydroperoxide reductase is the primary scavenger of endogenous hydrogen peroxide in Escherichia coli." Journal of bacteriology 183, no. 24 (2001): 7173-7181.
108. Martin, Jennifer L. "Thioredoxin—a fold for all reasons." Structure 3, no. 3 (1995): 245-250.
109. Schröder, Ewald, and Chris P. Ponting. "Evidence that peroxiredoxins are novel members of the thioredoxin fold superfamily." Protein Science 7, no. 11 (1998): 2465-2468.
110. Kim, H. J., H-Z. Chae, Y-J. Kim, Yeul Hong Kim, T-S. Hwang, E-M. Park, and Y-M. Park. "Preferential elevation of Prx I and Trx expression in lung cancer cells following hypoxia and in human lung cancer tissues." Cell biology and toxicology 19, no. 5 (2003): 285-298.
111. Wood, Zachary A., Leslie B. Poole, and P. Andrew Karplus. "Peroxiredoxin evolution and the regulation of hydrogen peroxide signaling." Science 300, no. 5619 (2003): 650-653.
112. Ellis, Holly R., and Leslie B. Poole. "Roles for the two cysteine residues of AhpC in catalysis of peroxide reduction by alkyl hydroperoxide reductase from Salmonella typhimurium." Biochemistry 36, no. 43 (1997): 13349-13356.
113. Woo, Hyun Ae, Ho Zoon Chae, Sung Chul Hwang, Kap-Seok Yang, Sang Won Kang, Kanghwa Kim, and Sue Goo Rhee. "Reversing the inactivation of peroxiredoxins caused by cysteine sulfinic acid formation." Science 300, no. 5619 (2003): 653-656.
114. Woo, Hyun Ae, Sang Won Kang, Hyung Ki Kim, Kap-Seok Yang, Ho Zoon Chae, and Sue Goo Rhee. "Reversible oxidation of the active site cysteine of peroxiredoxins to cysteine sulfinic acid Immunoblot detection with antibodies specific for the hyperoxidized cysteine-containing sequence." Journal of Biological Chemistry 278, no. 48 (2003): 47361-47364.
115. Baier, Margarete, and Karl-Josef Dietz. "The plant 2-Cys peroxiredoxin BAS1 is a nuclear-encoded chloroplast protein: its expressional regulation, phylogenetic origin, and implications for its specific physiological function in plants." The plant journal12, no. 1 (1997):179-190
116. Jeong, Woojin, Mee-Kyung Cha, and Il-Han Kim. "Thioredoxin-dependent hydroperoxide peroxidase activity of bacterioferritin comigratory protein (BCP) as a new member of the thiol-specific antioxidant protein (TSA)/alkyl hydroperoxide peroxidase C (AhpC) family." Journal of Biological Chemistry 275, no. 4 (2000): 2924-2930.

117. Comtois, Spencer L., Mark D. Gidley, and David J. Kelly. "Role of the thioredoxin system and the thiol-peroxidases Tpx and Bcp in mediating resistance to oxidative and nitrosative stress in Helicobacter pylori." Microbiology 149, no. 1 (2003): 121-129.
118. Reeves, Stacy A., Derek Parsonage, Kimberly J. Nelson, and Leslie B. Poole. "Kinetic and thermodynamic features reveal that Escherichia coli BCP is an unusually versatile peroxiredoxin." Biochemistry 50, no. 41 (2011): 8970-8981.
119. Dietz, Karl-Josef. "Peroxiredoxins in plants and cyanobacteria." Antioxidants & redox signaling 15, no. 4 (2011): 1129-1159.
120. Wood, Zachary A., Ewald Schröder, J. Robin Harris, and Leslie B. Poole. "Structure, mechanism and regulation of peroxiredoxins." Trends in biochemical sciences 28, no. 1 (2003): 32-40.
121. Fisher, Aron B., Chandra Dodia, Yefim Manevich, Jin-Wen Chen, and Sheldon I. Feinstein. "Phospholipid hydroperoxides are substrates for non-selenium glutathione peroxidase." Journal of Biological Chemistry 274, no. 30 (1999): 21326-21334.
122. Lee, Sang Pil, Young Sun Hwang, Yong Jun Kim, Ki-Sun Kwon, Hyung Jung Kim, Kanghwa Kim, and Ho Zoon Chae. "Cyclophilin a binds to peroxiredoxins and activates its peroxidase activity." Journal of Biological Chemistry 276, no. 32 (2001): 29826-29832.
123. Peshenko, Igor V., and Hitoshi Shichi. "Oxidation of active center cysteine of bovine 1-Cys peroxiredoxin to the cysteine sulfenic acid form by peroxide and peroxynitrite." Free Radical Biology and Medicine 31, no. 3 (2001): 292-303.
124. Hampton, Mark B., and Karina M. O'Connor. "Peroxiredoxins and the regulation of cell death." Molecules and cells 39, no. 1 (2016): 72.
125. Rhee, Sue Goo, and In Sup Kil. "Mitochondrial H_2O_2 signaling is controlled by the concerted action of peroxiredoxin III and sulfiredoxin: Linking mitochondrial function to circadian rhythm." Free Radical Biology and Medicine 100 (2016): 73-80.
126. Edgar, Rachel S., Edward W. Green, Yuwei Zhao, Gerben van Ooijen, Maria Olmedo, Ximing Qin, Yao Xu et al. "Peroxiredoxins are conserved markers of circadian rhythms." Nature 485, no. 7399 (2012): 459-464.
127. Hoyle, Nathaniel P., and John S. O'Neill. "Oxidation–Reduction Cycles of Peroxiredoxin Proteins and Nontranscriptional Aspects of Timekeeping." Biochemistry 54, no. 2 (2014): 184-193.
128. Clarke, David J., C. Logan Mackay, Dominic J. Campopiano, Pat Langridge-Smith, and Alan R. Brown. "Interrogating the molecular details of the peroxiredoxin activity of the Escherichia coli bacterioferritin comigratory protein using high-resolution mass spectrometry." Biochemistry 48, no. 18 (2009): 3904-3914.
129. Neidhardt, F. C., Vaughn, V., Phillips, T. A. and Bloch, P. L. "Gene-protein index of Escherichia coli K-12." Microbiol. Rev.47, (1983): 231±284
130. Verdoucq, L., Vignols, F., Jaxquot, J.-P., Chartier, Y. and Meyer, Y. "In vivo characterization of a thioredoxin h target protein defines a new peroxiredoxin family" J. Biol. Chem.274, (1999): 19714±19722.

131. Kang, Ga-Young, Eun-Hee Park, Kyunghoon Kim, and Chang-Jin Lim. "Overexpression of bacterioferritin comigratory protein (Bcp) enhance viability and reduced glutathione level in the fission yeast under stress." The Journal of Microbiology 47, no. 1 (2009): 60-67.
132. Brock, Thomas D. "Lower pH limit for the existence of blue-green algae: evolutionary and ecological implications." Science 179, no. 4072 (1973): 480-483.
133. Stanier, R. Y., and G. C. Bazine. "Phototrophic prokaryotes: the cyanobacteria." Annual Reviews in Microbiology 31, no. 1 (1977): 225-274.
134. Fay, Peter. "Oxygen relations of nitrogen fixation in cyanobacteria." Microbiological reviews 56, no. 2 (1992): 340-373.
135. Schopf JW. “Precambrian paleobiology: problems and perspectives”. Ann Rev Earth Planet Sci 3(1975):213-249.
136. Los, Dmitry A., and Norio Murata. "Responses to cold shock in cyanobacteria." J. Mol. Microbiol. Biotechnol 1, no. 2 (1999): 221-230.
137. Dyall, Sabrina D., Mark T. Brown, and Patricia J. Johnson. "Ancient invasions: from endosymbionts to organelles." Science 304, no. 5668 (2004): 253-257.
138. Yamaoka, Takashi, Kazuhiko Satoh, and Sakae Katoh. "Photosynthetic activities of a thermophilic blue-green alga." Plant and Cell Physiology 19, no. 6 (1978): 943-954.
139. Stewart, W. D. P. "Biological and ecological aspects of nitrogen fixation by free-living micro-organisms." Proceedings of the Royal Society of London. Series B, Biological Sciences 172, no. 1029 (1969): 367-388.
140. G. S. Venketraman, Algal inoculation in rice paddy field: In IRRI, nitrogen and rice (1979), The philippines. 311-321.
141. Singh, Rama Nagina. "Reclamation of ‘usar’ lands in India through blue-green algae." (1950): 325-326.
142. Apte, Shree Kumar, and Joseph Thomas. "Possible amelioration of coastal soil salinity using halotolerant nitrogen-fixing cyanobacteria." Plant and soil 189, no. 2 (1997): 205-211.
143. Hoffmann, Lucien. "Algae of terrestrial habitats." The Botanical Review 55, no. 2 (1989): 77-105.
144. Latifi, Amel, Marion Ruiz, and Cheng-Cai Zhang. "Oxidative stress in cyanobacteria." FEMS microbiology reviews 33, no. 2 (2009): 258-278.
145. Stewart, W. D. P. "Some aspects of structure and function in fixing cyanobacteria." Annual Reviews in Microbiology 34, no. 1 (1980): 497-536.
146. Apte, Shree Kumar. "Coping with salinity/water stress: cyanobacteria show the way." PROCEEDINGS-INDIAN NATIONAL SCIENCE ACADEMY PART B 67, no. 5 (2001): 285-309.
147. Singh, Harinder, Tonina Fernandes, and Shree Kumar Apte. "Unusual radioresistance of nitrogen-fixing cultures of Anabaena strains." Journal of biosciences 35, no. 3 (2010): 427-434.

148. Elhai, Jeff, Alexey Vepritskiy, Alicia M. Muro-Pastor, Enrique Flores, and C. Peter Wolk. "Reduction of conjugal transfer efficiency by three restriction activities of Anabaena sp. strain PCC 7120." Journal of Bacteriology 179, no. 6 (1997): 1998-2005.
149. Chaurasia, Akhilesh Kumar, and Shree Kumar Apte. "Improved eco-friendly recombinant Anabaena sp. strain PCC7120 with enhanced nitrogen biofertilizer potential." Applied and environmental microbiology 77, no. 2 (2011): 395-399.
150. Kaneko, Takakazu, Yasukazu Nakamura, C. Peter Wolk, Tanya Kuritz, Shigemi Sasamoto, Akiko Watanabe, Mayumi Iriguchi et al. "Complete genomic sequence of the filamentous nitrogen-fixing cyanobacterium *Anabaena* sp. strain PCC 7120." DNA research 8, no. 5(2001): 205-213.
151. Banerjee, Manisha, Prashanth S. Raghavan, Anand Ballal, Hema Rajaram, and S. K. Apte. "Oxidative stress management in the filamentous, heterocystous, diazotrophic cyanobacterium, *Anabaena* PCC7120." Photosynthesis research 118, no. 1-2 (2013): 59-70.
152. Banerjee, Manisha, Anand Ballal, and Shree K. Apte. "A novel glutaredoxin domain-containing peroxiredoxin 'All1541'protects the N2-fixing cyanobacterium *Anabaena* PCC 7120 from oxidative stress." Biochemical Journal 442, no. 3 (2012): 671-680.
153. Banerjee, Manisha, Anand Ballal, and Shree Kumar Apte. "Mn-catalase (Alr0998) protects the photosynthetic, nitrogen-fixing cyanobacterium *Anabaena* PCC 7120 from oxidative stress." Environmental microbiology 14, no. 11 (2012): 2891-2900.
154. Li, Baojie, Tetsuro Ishii, Choon Ping Tan, Jae-Won Soh, and Stephen P. Goff. "Pathways of Induction of Peroxiredoxin I Expression in Osteoblasts ROLES OF p38 MITOGEN-ACTIVATED PROTEIN KINASE AND PROTEIN KINASE C." Journal of Biological Chemistry 277, no. 14 (2002): 12418-12422.
155. Regelsberger, Günther, Christa Jakopitsch, Lisa Plasser, Hansjörg Schwaiger, Paul Georg Furtmüller, Günter A. Peschek, Marcel Zámocký, and Christian Obinger. "Occurrence and biochemistry of hydroperoxidases in oxygenic phototrophic prokaryotes (cyanobacteria)." Plant Physiology and Biochemistry 40, no. 6 (2002): 479-490.
156. Regelsberger, Günther, Ulrike Laaha, Dagmar Dietmann, Florian Rüker, Antonella Canini, Maria Grilli-Caiola, Paul Georg Furtmüller, Christa Jakopitsch, Günter A. Peschek, and Christian Obinger. "The Iron Superoxide Dismutase from the Filamentous Cyanobacterium Nostoc PCC 7120 LOCALIZATION, OVEREXPRESSION, AND BIOCHEMICAL CHARACTERIZATION." Journal of Biological Chemistry 279, no. 43 (2004): 44384-44393.
157. Raghavan, Prashanth S., Hema Rajaram, and Shree K. Apte. "Nitrogen status dependent oxidative stress tolerance conferred by overexpression of MnSOD and FeSOD proteins in *Anabaena* sp. strain PCC7120." Plant molecular biology 77, no. 4-5 (2011): 407-417.

158. Zhao, Weixing, Qinxi Guo, and Jindong Zhao. "A membrane-associated Mn-superoxide dismutase protects the photosynthetic apparatus and nitrogenase from oxidative damage in the cyanobacterium *Anabaena* sp. PCC 7120." Plant and cell physiology 48, no. 4 (2007): 563-572.
159. Chakravarty, Dhiman, et al. "A Salt-Inducible Mn-Catalase (KatB) Protects Cyanobacterium from Oxidative Stress." Plant physiology (2015): pp-01632.
160. Cui, Hongli, Yipeng Wang, Yinchu Wang, and Song Qin. "Genome-wide analysis of putative peroxiredoxin in unicellular and filamentous cyanobacteria." BMC evolutionary biology 12, no. 1 (2012): 220.
161. Pascual, María B., Alejandro Mata-Cabana, Francisco J. Florencio, Marika Lindahl, and Francisco J. Cejudo. "Overoxidation of 2-Cys Peroxiredoxin in Prokaryotes Cyanobacterial 2-Cys Peroxiredoxins Sensitive to Oxidative Stress." Journal of Biological Chemistry 285, no. 45(2010): 34485-34492
162. Banerjee, Manisha, Dhiman Chakravarty, and Anand Ballal. "Redox-dependent chaperone/peroxidase function of 2-Cys-Prx from the cyanobacterium Anabaena PCC7120: role in oxidative stress tolerance." BMC plant biology 15, no. 1 (2015): 1.
163. Hong, Seung-Keun, Mee-Kyung Cha, and Il-Han Kim. "A glutaredoxin-fused thiol peroxidase acts as an important player in hydrogen peroxide detoxification in late-phased growth of *Anabaena* sp. PCC7120." Archives of biochemistry and biophysics 475, no. 1 (2008): 42-49.
164. Mishra, Yogesh, Neha Chaurasia, and Lal Chand Rai. "AhpC (alkyl hydroperoxide reductase) from *Anabaena* sp. PCC 7120 protects Escherichia coli from multiple abiotic stresses." Biochemical and biophysical research communications 381, no. 4 (2009): 606-611
165. Shrivastava, Alok Kumar, Sarita Pandey, Karl Josef Dietz, Prashant Kumar Singh, Shilpi Singh, Ruchi Rai, and Lal Chand Rai. "Overexpression of AhpC enhances stress tolerance and N 2–fixation in *Anabaena* by upregulating stress responsive genes." Biochimica et Biophysica Acta (BBA)-General Subjects 1860, no. 11 (2016): 2576-2588.
166. Cha, Mee-Kyung, Seung-Keun Hong, and Il-Han Kim. "Four thiol peroxidases contain a conserved GCT catalytic motif and act as a versatile array of lipid peroxidases in *Anabaena* sp. PCC 7120." Free Radical Biology and Medicine 42, no. 11 (2007): 1736-1748.
167. Agrawal, Chhavi, Sonia Sen, Shilpi Singh, Snigdha Rai, Prashant Kumar Singh, Vinay Kumar Singh, and L. C. Rai. "Comparative proteomics reveals association of early accumulated proteins in conferring butachlor tolerance in three N 2-fixing Anabaena spp." Journal of proteomics 96 (2014): 271-290.
168. Panda, Bandita, Bhakti Basu, Hema Rajaram, and Shree Kumar Apte. "Methyl viologen responsive proteome dynamics of *Anabaena* sp. strain PCC7120." Proteomics 14, no. 16 (2014): 1895-1904.

169. Walk, C. P. "Vonshak, 4., Kehoc, P., and Elhai. J: Construction of shuttle vectors capable of conjugative transfer from Escherichia co/i to nitrogen-fixing fitamentous cqanobacteria." Proc. Natl. Acad. Sci. USA 81 (1984): 1561-1565.
170. Haselkorn, Robert. "Heterocysts." Annual Review of Plant Physiology 29, no. 1 (1978): 319-344.
171. Chaurasia, Akhilesh Kumar, Anjali Parasnis, and Shree Kumar Apte. "An integrative expression vector for strain improvement and environmental applications of the nitrogen fixing cyanobacterium, *Anabaena* sp. strain PCC7120." Journal of microbiological methods 73, no. 2 (2008): 133-141.
172. Yoon, Ho-Sung, and James W. Golden. "Heterocyst pattern formation controlled by a diffusible peptide." Science 282, no. 5390 (1998): 935-938.
173. Altschul, Stephen F., Warren Gish, Webb Miller, Eugene W. Myers, and David J. Lipman. "Basic local alignment search tool." Journal of molecular biology 215, no. 3 (1990): 403-410.
174. Schultz, Jörg, Frank Milpetz, Peer Bork, and Chris P. Ponting. "SMART, a simple modular architecture research tool: identification of signaling domains." Proceedings of the National Academy of Sciences 95, no. 11 (1998): 5857-5864.
175. Mazon, G., J. M. Lucena, S. Campoy, AR Fernández De Henestrosa, P. Candau, and J. Barbe. "LexA-binding sequences in Gram-positive and cyanobacteria are closely related." Molecular Genetics and Genomics 271, no. 1 (2004): 40-49.
176. Castenholz, Richard W. "[3] Culturing methods for cyanobacteria." Methods in enzymology 167 (1988): 68-93.
177. Sambrook, Joseph, Edward F. Fritsch, and Tom Maniatis. Molecular cloning. Vol. 2. New York: Cold spring harbor laboratory press, 1989.
178. Apte, Shree Kumar, and Robert Haselkorn. "Cloning of salinity stress-induced genes from the salt-tolerant nitrogen-fixing cyanobacterium *Anabaena* torulosa." Plant molecular biology 15, no. 5 (1990): 723-733.
179. Dagert, M., and S. D. Ehrlich. "Prolonged incubation in calcium chloride improves the competence of Escherichia coli cells." Gene 6, no. 1 (1979): 23-28.
180. Maniatis, T., E. F. Fritsch, and J. Sambrook. "Cold Spring Harbor Laboratory." (1982): 387-389.
181. Lowry, Oliver H., Nira J. Rosebrough, A. Lewis Farr, and Rose J. Randall. "Protein measurement with the Folin phenol reagent." J biol Chem 193, no. 1 (1951): 265-275.
182. Mackinney, Gr. "Absorption of light by chlorophyll solutions." J. biol. Chem 140, no. 2 (1941): 315-322.
183. Wakita, Masahiro, Shinji Masuda, Ken Motohashi, Toru Hisabori, Hiroyuki Ohta, and Ken-ichiro Takamiya. "The significance of type II and PrxQ peroxiredoxins for antioxidative stress response in the purple bacterium Rhodobacter sphaeroides." Journal of Biological Chemistry282, no. 38 (2007): 27792-27801.
184. Stork, Tina, Klaus-Peter Michel, Elfriede K. Pistorius, and Karl-Josef Dietz. "Bioinformatic analysis of the genomes of the cyanobacteria *Synechocystis* sp. PCC

6803 and *Synechococcus elongatus* PCC 7942 for the presence of peroxiredoxins and their transcript regulation under stress." Journal of experimental botany 56, no. 422 (2005): 3193-3206.

185. Pérez-Pérez, María Esther, Alejandro Mata-Cabana, Ana María Sánchez-Riego, Marika Lindahl, and Francisco J. Florencio. "A comprehensive analysis of the peroxiredoxin reduction system in the cyanobacterium *Synechocystis* sp. strain PCC 6803 reveals thatall five peroxiredoxinsare thioredoxin dependent." Journal of bacteriology 191, no. 24 (2009): 7477-7489.
186. Clarke, David J., Ximena P. Ortega, C. Logan Mackay, Miguel A. Valvano, John RW Govan, Dominic J. Campopiano, Pat Langridge-Smith, and Alan R. Brown. "Subdivision of the bacterioferritin comigratory protein family of bacterial peroxiredoxins based on catalytic activity."Biochemistry 49, no. 6 (2010): 1319-1330.
187. Horta, Bruno Brasil, Marcos Antonio de Oliveira, Karen Fulan Discola, José Renato Rosa Cussiol, and Luis Eduardo Soares Netto. "Structural and Biochemical Characterization of Peroxiredoxin Qβ from Xylella fastidiosa Catalytic Mechanism and High Reactivity." Journal of Biological Chemistry 285, no. 21 (2010): 16051-16065.
188. Stork, Tina, Miriam Laxa, Marina S. Dietz, and Karl-Josef Dietz. "Functional characterisation of the peroxiredoxin gene family members of *Synechococcus elongatus* PCC 7942." Archives of microbiology 191, no. 2 (2009): 141-151.
189. Ådén, Jörgen, Marcus Wallgren, Patrik Storm, Christoph F. Weise, Alexander Christiansen, Wolfgang P. Schröder, Christiane Funk, and Magnus Wolf-Watz. "Extraordinary μs–ms backbone dynamics in Arabidopsis thaliana peroxiredoxin Q." Biochimica et Biophysica Acta (BBA)-Proteins and Proteomics 1814, no. 12 (2011): 1880-1890.
190. Nelson, Kimberly J., Stacy T. Knutson, Laura Soito, Chananat Klomsiri, Leslie B. Poole, and Jacquelyn S. Fetrow. "Analysis of the peroxiredoxin family: Using active-site structure and sequence information for global classification and residue analysis."Proteins: Structure, Function, and Bioinformatics 79, no. 3 (2011): 947-964.
191. Lamkemeyer, Petra, Miriam Laxa, Valérie Collin, Wenxue Li, Iris Finkemeier, Mark A. Schöttler, Volker Holtkamp et al. "Peroxiredoxin Q of Arabidopsis thaliana is attached to the thylakoids and functions in context of photosynthesis." The Plant Journal45, no. 6 (2006): 96360081
192. Petersson, Ulrika A., Thomas Kieselbach, José G. García-Cerdán, and Wolfgang P. Schröder. "The Prx Q protein of Arabidopsis thaliana is a member of the luminal chloroplast proteome." FEBS letters 580, no. 26 (2006): 6055-6061.
193. Kiba, Akinori, Masahiro Nishihara, Nobue Tsukatani, Takashi Nakatsuka, Yoshiaki Kato, and Saburo Yamamura. "A peroxiredoxin Q homolog from gentians is involved in both resistance against fungal disease and oxidative stress." Plant and cell physiology 46, no. 6 (2005): 1007-1015.
194. Jing, Li-Wen, Shi-Hua Chen, Xiao-Li Guo, Hui Zhang, and Yan-Xiu Zhao. "Overexpression of a Chloroplast-located Peroxiredoxin Q Gene, SsPrxQ, Increases

the Salt and Low-temperature Tolerance of Arabidopsis." Journal of Integrative Plant Biology 48, no.10(2006): 1244-1249.
195. Pascual, María Belén, Alejandro Mata-Cabana, Francisco Javier Florencio, Marika Lindahl, and Francisco Javier Cejudo. "A comparative analysis of the NADPH thioredoxin reductase C-2-Cys peroxiredoxin system from plants and cyanobacteria." Plant physiology155, no. 4 (2011): 1806-1816.
196. Guo, Xiao-Li, Yang-Rong Cao, Zi-Yi Cao, Yan-Xiu Zhao, and Hui Zhang. "Molecular cloning and characterization of a stress-induced peroxiredoxin Q gene in halophyte Suaeda salsa." Plant science 167, no. 5 (2004): 969-975.
197. Adler, Alan D. "THE CHEMICAL AND PHYSICAL BEHAVIOR OE PORPHYRIN COMPOUNDS AND RELATED STRUCTURES." (1973).
198. Ling, Yan, Jeremy H. Lakey, Claire E. Roberts, and Andrew D. Sharrocks. "Molecular characterization of the B-box protein–protein interaction motif of the ETS-domain transcription factor Elk-1." The EMBO journal 16, no. 9 (1997): 2431-2440.
199. Greenfield, Norma J. "Using circular dichroism spectra to estimate protein secondary structure." Nature protocols 1, no. 6 (2006): 2876-2890.
200. Micsonai, András, Frank Wien, Linda Kernya, Young-Ho Lee, Yuji Goto, Matthieu Réfrégiers, and József Kardos. "Accurate secondary structure prediction and fold recognition for circular dichroism spectroscopy." Proceedings of the National Academy of Sciences 112, no. 24 (2015):E3095-E3103.
201. Rich, Rebecca L., and David G. Myszka. "Higher-throughput, label-free, real-time molecular interaction analysis." Analytical biochemistry 361, no. 1 (2007): 1-6.
202. Zeng, Shuwen, Dominique Baillargeat, Ho-Pui Ho, and Ken-Tye Yong. "Nanomaterials enhanced surface plasmon resonance for biological and chemical sensing applications." Chemical Society Reviews 43, no. 10 (2014): 3426-3452.
203. Barranco-Medina, Sergio, Juan-José Lázaro, and Karl-Josef Dietz. "The oligomeric conformation of peroxiredoxins links redox state to function." FEBS letters 583, no. 12 (2009): 1809-1816.
204. Wood, Zachary A., Leslie B. Poole, Roy R. Hantgan, and P. Andrew Karplus. "Dimers to doughnuts: redox-sensitive oligomerization of 2-cysteine peroxiredoxins." Biochemistry 41, no. 17 (2002): 5493-5504.
205. Matsumura, Tomohiro, Ken Okamoto, Shin-ichiro Iwahara, Hiroyuki Hori, Yuriko Takahashi, Takeshi Nishino, and Yasuko Abe. "Dimer-oligomer interconversion of wild-type and mutant rat 2-Cys peroxiredoxin disulfide formation at dimer-dimer interfaces is notessential for decamerization." Journal of Biological Chemistry 283, no. 1 (2008): 284-293.
206. Bernroitner, Margit, Marcel Zamocky, Paul G. Furtmüller, Günter A. Peschek, and Christian Obinger. "Occurrence, phylogeny, structure, and function of catalases and peroxidases in cyanobacteria." Journal of experimental botany 60, no. 2 (2009): 423-440.

207. Laxa, Miriam, Janine König, Karl-Josef Dietz, and Andrea Kandlbinder. "Role of the cysteine residues in Arabidopsis thaliana cyclophilin CYP20-3 in peptidyl-prolyl cis–trans isomerase and redox-related functions." Biochemical Journal 401, no. 1 (2007):287-297.
208. Wakabayashi, Ken-ichi, and Stephen M. King. "Modulation of Chlamydomonas reinhardtii flagellar motility by redox poise." The Journal of cell biology 173, no. 5 (2006): 743-754.
209. Hara, Satoshi, and Toru Hisabori. "Kinetic analysis of the interactions between plant thioredoxin and target proteins." Thiol-based redox homeostasis and signalling (2014): 129.
210. Chae, Ho Zoon, Sang Jin Chung, and Sue Goo Rhee. "Thioredoxin-dependent peroxide reductase from yeast." Journal of Biological Chemistry 269, no. 44 (1994): 27670-27678.
211. Agrawal, Anjali, and R. K. Kale. "Radiation induced peroxidative damage: mechanism and significance." Indian journal of experimental biology 39, no. 4 (2001): 291-309.
212. Kaplan-Levy, Ruth N., Ora Hadas, and Assaf Sukenik. "Deciphering the mechanisms against oxidative stress in developing and mature akinetes of the cyanobacterium Aphanizomenon ovalisporum." Microbiology 161, no. 7 (2015): 1485-1495.
213. Dietz, Karl-Josef. "The dual function of plant peroxiredoxins in antioxidant defence and redox signaling." In Peroxiredoxin Systems, pp. 267-294. Springer Netherlands, 2007.
214. König, Janine, Helena Galliardt, Patrick Jütte, Simon Schäper, Lea Dittmann, and Karl-Josef Dietz. "The conformational bases for the two functionalities of 2-cysteine peroxiredoxins as peroxidase and chaperone." Journal of experimental botany 64, no. 11(2013): 3483-3497.
215. Nevalainen, Timo J. "1-Cysteine peroxiredoxin: a dual-function enzyme with peroxidase and acidic Ca 2+-independent phospholipase A 2 activities." Biochimie 92, no. 6 (2010): 638-644.
216. Qian, Haifeng, Shuqiong Yu, Zhengqi Sun, Xiucai Xie, Weiping Liu, and Zhengwei Fu. "Effects of copper sulfate, hydrogen peroxide and N-phenyl-2-naphthylamine on oxidative stress and the expression of genes involved photosynthesis and microcystin disposition in Microcystisaeruginosa." Aquatic Toxicology 99, no. 3 (2010): 405-412.
217. Grabski, Anthony, Mark Mehler, and D. Drott. "Unattended high-density cell growth and induction of protein expression with the Overnight Express Autoinduction System." Innovations 17 (2003): 3-8.
218. Studier, F. William. "Protein production by auto-induction in high-density shaking cultures." Protein expression and purification 41, no. 1 (2005): 207-234.
219. Dadheech, Nidheesh. "Desiccation tolerance in cyanobacteria." African Journal of Microbiology Research 4, no. 15 (2010): 1584-1593.

220. Drábková, Michaela, H. C. P. Matthijs, W. Admiraal, and Blahoslav Maršálek. "Selective effects of H2O2 on cyanobacterial photosynthesis." Photosynthetica 45, no. 3 (2007): 363-369.
221. Halliwell, Barry, and John MC Gutteridge. "Iron and free radical reactions: two aspects of antioxidant protection." Trends in biochemical Sciences 11, no. 9 (1986): 372-375.
222. Walker, Graham C. "Mutagenesis and inducible responses to deoxyribonucleic acid damage in Escherichia coli." Microbiological Reviews 48, no. 1 (1984): 60.
223. Patterson-Fortin, Laura M., Kimberley R. Colvin, and George W. Owttrim. "A LexA-related protein regulates redox-sensitive expression of the cyanobacterial RNA helicase, crhR." Nucleic acids research 34, no. 12 (2006): 3446-3454.
224. Kumar, Arvind, Anurag Kirti, and Hema Rajaram. "LexA protein of cyanobacterium Anabaena sp. strain PCC7120 exhibits in vitro pH-dependent and RecA-independent autoproteolytic activity." The international journal of biochemistry & cell biology 59 (2015):84-93.
225. Venkataraman, G. S. "Algal inoculation of rice fields." Nitrogen and rice (1979): 311-321.
226. Choudhury, Shuvasish, Piyalee Panda, Lingaraj Sahoo, and Sanjib Kumar Panda. "Reactive oxygen species signaling in plants under abiotic stress." Plant signaling & behavior 8, no. 4 (2013): e23681.
227. Lindahl, Marika, and Francisco Javier Cejudo. "Comparative analysis of cyanobacterial and plant peroxiredoxins and their electron donors: peroxidase activity and susceptibility to overoxidation." Meth. Enzymol 527 (2013): 257-273.
228. Chakravarty, Dhiman, Manisha Banerjee, Namrata Waghmare, and Anand Ballal. "Cyanobacterial Mn-catalase ‘KatB’: Molecular link between salinity and oxidative stress resistance." Communicative & integrative biology 9, no. 5 (2016): e1216738.

Published Paper(s)

Over-expression of Alr4642, a novel Prx-like peroxiredoxin, defends the cyanobacterium Anabaena *PCC7120 from oxidative stress*

Vijay Tailor & Anand Ballal

Journal of Applied Phycology

ISSN 0921-8971

J Appl Phycol
DOI 10.1007/s10811-014-0503-3

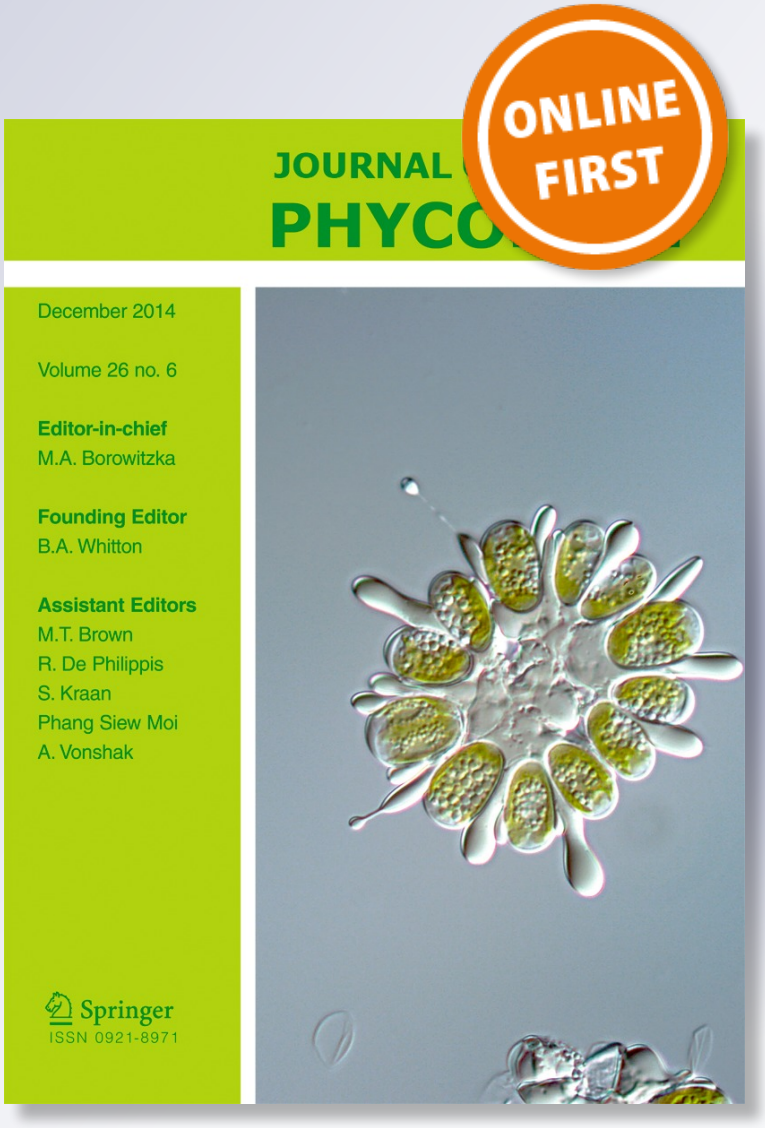

Springer

J Appl Phycol
DOI 10.1007/s10811-014-0503-3

Over-expression of Alr4642, a novel Prx-like peroxiredoxin, defends the cyanobacterium *Anabaena* PCC7120 from oxidative stress

Vijay Tailor · Anand Ballal

Received: 7 October 2014 / Revised: 10 December 2014 / Accepted: 11 December 2014

Abstract Peroxiredoxins (Prxs), proteins that detoxify peroxides, are ubiquitously present in all organisms. In the cyanobacterium *Anabaena* PCC7120, ORF *alr4642* encodes a protein that shows homology to Prx-like family of Prxs. The role of Alr4642 in the oxidative stress management of *Anabaena* was evaluated in this study. Sequence analysis showed the presence of another methionine residue, 35 amino acids away from the first annotated methionine. The similarity of Alr4642 with the other Prx-like proteins was observed only from the second methionine residue. When over-expressed in *Escherichia coli*, both Alr4642 and AlrT4642 (truncated Alr4642, initiating from the second methionine) remained insoluble and could not be purified. Interestingly, expression of the complete *alr4642* ORF in *Anabaena* led to the production of the AlrT4642 protein, suggesting that the second ATG was the actual in vivo start codon of *alr4642* in *Anabaena*. When over-expressed in *Anabaena*, AlrT4642 (with a C-terminal His-tag) remained soluble and could be purified by affinity chromatography. The purified AlrT4642 protected the plasmid DNA from oxidative damage whereas *Anabaena* cells over-expressing AlrT4642 showed improved resistance to H_2O_2 than the wild type. These data indicate that AlrT4642 is indeed an antioxidant protein that is capable of defending *Anabaena* from oxidative stress and suggest that over-expression of Prx-like proteins may be an effective method to improve stress resistance in cyanobacteria. This is the first report wherein a Prx-like family protein has been functionally characterized.

Keywords *Anabaena* · Antioxidant proteins · Peroxiredoxins · Peroxiredoxin-like2 and oxidative stress

V. Tailor · A. Ballal (✉)
Molecular Biology Division, Bhabha Atomic Research Centre, Trombay, Mumbai 400085, India
e-mail: aballal@barc.gov.in

Introduction

Generation of reactive oxygen species (ROS) is an inevitable outcome of metabolic processes that occur during aerobic growth. In photosynthetic organisms like cyanobacteria, ROS are also generated during the light-driven photosynthetic electron transport (Nishiyama et al. 2006). When in excess, ROS can damage all the cellular macromolecules, and hence, ROS have to be effectively eliminated (Imlay 2003). In cells, ROS are detoxified by enzymatic (superoxide dismutase, catalases, peroxidases, etc.) or non-enzymatic (tocopherols, carotenoids, etc.) processes (Storz and Imlay 1999).

Important ROS that occur in the biological systems are the superoxide radical, $O_2^{\cdot-}$ (Zhao et al. 2007), hydrogen peroxide, H_2O_2 (Zamocky et al. 2008), and the hydroxyl radical, $OH^{\cdot}$ (Asada et al. 1974). Electron escape from respiratory electron transport chain (ETC) and reduction of O_2 at the end of the non-cyclic electron transport chain are the two major sources of $O_2^{\cdot-}$ generation (Dietz 2011). Superoxide dismutase (SOD) catalyzed dismutation of $O_2^{\cdot-}$ to H_2O_2 is an important source of intracellular H_2O_2 production (Zamocky et al. 2008). Along with SOD, many oxidases also produce H_2O_2 via oxidation-reduction reactions that utilize molecular O_2 (Collen et al. 1995). The most hazardous ROS, $OH^{\cdot}$, is generated by the Fenton reaction, i.e. $Fe^{2+}+H_2O_2 \rightarrow Fe^{3+}+OH^{\cdot}+OH^{-}$ (Halliwell and Gutteridge 1986).

Peroxiredoxins (Prxs) are ubiquitous thiol peroxidases that function as antioxidant enzymes (Wood et al. 2003). Prxs contain a conserved thiol-specific antioxidant domain, which includes a thioredoxin fold and a catalytic triad (T-C-R). The conserved (peroxidatic) cysteine residue of Prxs reacts with H_2O_2 or other peroxide/peroxynitrite substrates and reduces them to water or corresponding non-toxic alcohols/nitrites (Dietz 2011). Based on the number of cysteine residues directly taking part in catalysis, Prxs are primarily divided into three major classes, i.e. (a) 1-Cys-Prx, (b) typical 2-Cys-Prx

Published online: 07 January 2015

and (c) atypical 2-Cys-Prx, which are further subdivided into PrxQ and type II Prx (Tripathi et al. 2009). Another subfamily of Prxs, Prx-like, has been recently identified in cyanobacteria (Cui et al. 2012). Members of this family show the TSA domain and the CXXC motif, which is characteristic of thioredoxin (TrxA). Although these proteins show the conserved peroxidatic cysteine, the other two conserved residues (i.e. T and R) of the catalytic triad are absent. The Prx-like proteins are further subdivided into Prx-like1 and Prx-like2 (Cui et al. 2012). Prx-like proteins have not been functionally characterized from any bacteria so far. In Prx-like1, the conserved peroxidatic cysteine aligns with the first cysteine of the CXXC motif whereas in the Prx-like2 proteins, the peroxidatic cysteine corresponds to the second cysteine of the abovementioned motif.

Cyanobacteria, the first organisms to generate O_2 during photosynthesis, originated more than three billion years ago and were responsible for the early oxygenation of the earth's atmosphere (Allen and Martin 2007). Therefore, it is likely that these organisms have developed systems to overcome ROS. Diazotrophic strains of cyanobacteria such as *Anabaena* are economically important, eco-friendly source of biofertilizers in the rice paddy fields of Southeast Asia (Venkatraman 1979). Various abiotic stresses (heavy metals, drought, salt, extreme temperatures, high light, herbicides, etc.) that lead to over-production of ROS (Choudhury et al. 2013), adversely affect the biofertilizer potential of *Anabaena*. Thus, understanding the molecular basis of oxidative stress resistance in *Anabaena* is important for the development of newer biofertilizers for use under unfavourable field conditions.

The role played by various proteins in overcoming oxidative stress in the filamentous, heterocystous diazotrophic, cyanobacterium *Anabaena* PCC7120 has generated lots of interest in the recent past (Agrawal et al. 2014; Panda et al. 2014; Cha et al. 2007). Our laboratory is investigating the role played by peroxiredoxins and catalases in overcoming oxidative stress in the filamentous, heterocystous diazotrophic, cyanobacterium *Anabaena* PCC7120 (Banerjee et al. 2012a, b, 2013; Bihani et al. 2013). Bioinformatic analysis showed *Anabaena* PCC7120 to encode several proteins with homology to Prxs (Cui et al. 2012; Banerjee et al. 2013). Among these, the Alr4642 protein displayed similarity to the Prx-like2 family of proteins. As the Prx-like proteins have not been characterized in *Anabaena* or any other bacteria, it was desired to elucidate the role of Alr4642. To verify if Alr4642 could protect *Anabaena* from oxidative stress, the Alr4642 protein was over-expressed in *Anabaena* PCC7120 and the resulting strain was characterized. Results described in this manuscript show that Alr4642 is indeed an antioxidant protein, which can protect *Anabaena* from oxidative damage.

Materials and methods

Axenic *Anabaena* PCC7120 cultures were grown in BG-11 liquid medium (BG-11/N^+, pH 7.2–7.4) containing combined nitrogen (17 mM $NaNO_3$) under continuous illumination (30 μmol photons m^{-2} s^{-1}) with shaking (100 rpm) or as a still culture at 27 °C±2 °C. *Escherichia coli* cells were grown in Luria-Bertani (LB) medium in the presence of appropriate antibiotics at 37 °C with shaking at 150 rpm. The antibiotics used were 10 μg neomycin mL^{-1} (Nm_{10}) in BG-11 liquid media, 25 μg neomycin mL^{-1} (Nm_{25}) in BG-11 agar plates for recombinant *Anabaena* PCC 7120 and 34 μg chloramphenicol mL^{-1} (Cm_{34}), 50 μg kanamycin mL^{-1} (Kan_{50}) or 100 μg carbenicillin mL^{-1} (Cb_{100}) for *E. coli*. The *E. coli* and *Anabaena* strains and plasmids used in the study are indicated in Table 1.

Cloning of *alr4642* and *alrT4642* into pET16b

The *alr4642* or *alrT4642* ORF was PCR amplified using gene-specific primers, *alr*4642fwd and *alr*4642rev or *alr*T4642fwd and *alr*4642rev respectively (Table 2), employing *Anabaena* PCC7120 chromosomal DNA as template. The PCR products were digested with the restriction enzymes *Nde*I and *Bam*HI and cloned separately into similarly digested pET16b to obtain pET4642 and pETT4642 respectively (Table 1). The pET4642 and pETT4642 insert was sequenced to confirm the nucleotide sequence integrity of the cloned gene.

Over-production of the recombinant proteins and generation of the polyclonal antiserum

The plasmid pET4642 or pETT4642 was transformed into *E. coli* BL21 pLysS/codon plus cells. The recombinant *E. coli* cells were grown in Luria-Bertani (LB) medium with appropriate antibiotics to an optical density at 600 nm (OD_{600}) of ~1.0 and induced with 1 mM isopropylthiogalactopyranoside (IPTG) for over-production of proteins. Four hours after induction, cells were harvested, resuspended in lysis buffer (50 mM Tris, 200 mM NaCl, pH 8.0) and lysed by sonication (2 s burst at 250 W with 2 s cooling period between each burst). The lysate was centrifuged at 3000×*g* to remove unbroken cells and other debris. The supernatant obtained was centrifuged at 10,000×*g* for 20 min to separate the inclusion bodies from the soluble cytosolic proteins. The inclusion body pellet containing 10HisAlr4642 was dissolved in 8 M urea and resolved on SDS-PAGE. The 10HisAlr4642 protein was eluted from the gel and employed to raise specific antiserum. The primary immunization (with 100 μg purified protein) and three booster immunizations (50 μg purified protein per booster) in mouse and collection of antiserum were performed at a commercial facility (Merck, India).

Table 1 Strains and plasmids used in this study

Strains/plasmids	Description	Source/reference
E. coli strains		
DH5α	F⁻ *recA*41 *endA*1 *gyrA*96 *thi*-1 *hsd*R17 (rk^- mk^-) *supE*44 *relA*λ Δ*lacU*169	Lab collection
BL21(pLysS)	Cm^r F– *ompT* h_S dS_B (r_B^- m_B^-) *gal dcm* (DE3) pLysS	Novagen
HB 101	F⁻ *mcrB mrr hsd*S20(rB^- mB^-) *recA*13 *leu*B6 *ara*⁻14 *pro*A2 *lac*Y1 *gal*K2 *xyl*⁻5 *mtl*⁻1 *rpsL*20(SmR) *glnV*44 λ⁻	Lab collection
HB101-4642	HB101 strain harbouring pAM4642	This study
HB101T4642(6His)	HB101 strain harbouring pAM4642	This study
HB101R2	Donor strain carrying pRL623(encoding methylase) and pRL443 (conjugal plasmid)	Wolk, C. P.
Anabaena strains		
Anabaena PCC7120	Wild-type strain	Haselkorn, R.
$An4642^+$	*Anabaena* 7120 harbouring pAM4642	This study
$AnT4642(6His)^+$	*Anabaena* 7120 harbouring pAMT4642(6His)	This study
Plasmids		
pBluescriptSKII (pBS)	Amp^r, cloning vector	Stratagene
pET16b	Amp^r, expression vector	Novagen
pAM1956	Kan^r, promoterless vector with *gfpmut2* reporter gene	Golden, J.W.
pFPN	Cb^r, Kan^r, Integrative expression vector	Chaurasia et al. 2008
pET4642	0.642 kb *alr4642* PCR product cloned into *Nde*I and BamHI sites of pET16b	This study
pETT4642	0.537 kb *alrT4642* PCR product cloned into *Nde*I and BamHI sites of pET16b	This study
pFPN4642	0.642 kb *alr4642* fragment cloned in pFPN at NdeI-BamHI restriction sites	This study
pFPNT4642(6His)	0.537 kb *alrT4642* fragment cloned in pFPN at NdeI-BamHI restriction sites	This study
pAM4642	1.2 kb *XmaI-Sal*I fragment from pFPN4642 cloned in pAM1956 vector	This study
pAMT4642(6His)	1.2 kb *XmaI-Sal*I fragment from pFPNT4642(6His) cloned in pAM1956 vector	This study

Protein electrophoresis, Western blotting and immunodetection

After induction with IPTG, *E. coli* BL21 (DE3)/pLysS cells carrying the plasmids pET4642 or pETT4642 were lysed with Laemmli's buffer (Laemmli 1970) and protein extracts were resolved on SDS-polyacrylamide (12 %) gels and stained with Coomassie brilliant blue (CBB). Total cellular proteins from *Anabaena* were extracted using Laemmli's buffer and electrophoretically separated as described above. When required, proteins were electroblotted onto nitrocellulose membrane by electroblotting at 300 mA for 3 h. Subsequently, the blot was allowed to cross-react with the Alr4642 antiserum (1:2000) or the anti-polyhistidine antiserum (1:5000) for 16 h. After washing the primary antibody, the blot was incubated with appropriate secondary antibody linked to alkaline phosphatase. After 1 h, the blot was thoroughly washed and the colour reaction carried out with the chromogenic substrate, nitro blue tetrazolium chloride/5-bromo-4-chloro-3-indolyl phosphate toludine salt (NBT/BCIP), stock solution (Roche).

Table 2 List of primers used in this study

Primer	
*alr*4642fwd	5′-CGGGATCCCATA TGAACGCAGATAGACA CAG-3′
*alr*4642rev	5′-CGGGATCCTTAATCAAATTTTCC TAACAA CTTTTCG-3′
*alr*T4642_Fwd	5′-GCGCGGCA TATGTTAACTTCAACAGATT TCAGTGG-3′
*alr*4642His_Rev	5′-GGATCCTA**ATGATGGTGATGGTGATG** ATCAAATTTTCC TAACAACTTTTCG-3′.
LexA1	GCAGATAGACACAGATATAAAATCAGTGTT AACTCCGG
LexA2	CCGGAGTTAACACTGATTTTATATCTGTGTC TATCTGC

MCO assay and DTT-dependent peroxidase activity

In the metal-catalyzed oxidation (MCO) assay, free radicals were generated by incubating 3 μM $FeCl_3$ and 5 mM DTT for 30 min at room temperature in the presence or the absence of the purified AlrT4642(6His). Plasmid (pBluescript, 1 μg) was added to all tubes, and reaction was allowed to proceed for further 4 h. Subsequently, DNA integrity was assessed by electrophoresis of samples on agarose gels (1 %) (Latifi et al. 2007). DTT-dependent peroxidase activity employing

H_2O_2 as substrate was performed as described by Banerjee et al. (2012b).

Construction of pAM4642/pAMT4642(6His) and transfer to *Anabaena* PCC7120

The *alr4642* DNA fragment (642 bp) from pET4642 was subcloned, downstream of the strong P_{psbA1} promoter, into the pFPN vector (Chaurasia et al. 2008) employing the restriction enzymes *Nde*I and *Bam*HI (plasmid called pFPN4642). Subsequently, the *alr4642* gene along with the P_{psbA1} promoter was transferred as a *Sal*I–*Xma*I fragment from pFPN4642 to appropriately digested *E. coli/Anabaena* shuttle vector pAM1956 (Yoon and Golden 1998) to obtain pAM4642. Using a conjugal *E. coli* donor [HB101(pRL623+pRL443)], pAM4642 was conjugated into *Anabaena* PCC7120 as described earlier (Elhai et al. 1997). Exconjugants were selected on BG-11/N^+ agar plates containing neomycin (25 μg mL^{-1}), transferred to BG-11/N^+ liquid medium containing neomycin (10 μg mL^{-1}) and repeatedly subcultured. The transformed *Anabaena* strain thus obtained (designated *An*4642$^+$) was maintained on BG-11/N^+ plates containing neomycin. The *alrT4642* DNA fragment was amplified from *Anabaena* PCC7120 chromosomal DNA with primers *alr*T4642_Fwd and *alr*4642His_Rev. The forward primer contained a site for the restriction enzyme *Nde* I (underlined) while the reverse primer contained 6 His codons (shown in bold) followed by a stop codon in frame with the last sense codon of the *alrt4642* ORF and a *Bam* HI restriction site (underlined) (Table 2). The *alr*T4642 fragment was cloned into pAM1956 as described for *alr*4642 and pAMT4642(6His) thus obtained was conjugated into *Anabaena* PCC7120 to give rise to AnT4642 (6His)$^+$.

Purification of AlrT4642(6His) protein from *Anabaena* PCC7120

For purification of AlrT4642(6His), AnT4642 (6His)$^+$ cells were grown with aeration (2 L min^{-1}) in the presence of light for 8–10 days until chlorophyll *a* density of 8–10 μg mL^{-1} was reached. Cells were harvested by centrifugation, washed thoroughly with lysis buffer (50 mM Tris, pH 8.0 and 200 mM NaCl), resuspended in the same buffer and subjected to sonication. The cell lysate was centrifuged at 12,000×*g* for 20 min to remove the debris, and the supernatant was allowed to interact with the NiNTA matrix (300 μl slurry, QIAGEN) for 18 h at 4 °C. Subsequently, the matrix was washed five times with 5 mL buffer B (50 mM Tris, 200 mM NaCl, 5 mM imidazole; pH 8.0) and three times with 5 mL buffer C (50 mM Tris, 200 mM NaCl, 20 mM imidazole; pH 8.0). Final elution was performed in buffer D (50 mM Tris, 200 mM NaCl, 250 mM imidazole; pH 8.0).

Oxidative stress tolerance of AnT4642(6His)$^+$

Three-day-old *Anabaena* cultures of the wild-type *Anabaena* PCC7120 (WT) as well as AnT4642(6His)$^+$ were inoculated in a fresh growth medium at a chlorophyll *a* density of 3 μg mL^{-1} and subjected to H_2O_2 (1 mM) stress in tubes (without shaking) under illumination for 2 days. Growth of cultures was monitored by measuring the chlorophyll *a* content. This experiment was repeated three times, and average values are reported.

Analytical procedures and bioinformatic analysis

Protein concentrations were determined by a modified Lowry method (Total Protein Kit, Sigma Cat. No. TP0300) using bovine serum albumin as standard. Growth was assessed as content of chlorophyll *a* mL^{-1} of culture volume (Mackinney 1941). Amino acid sequence was analyzed using BLAST (http://blast.ncbi.nlm.nih.gov/blast) or SMART (http://smart.embl-heidelberg.de/) algorithms (Altschul et al. 1990; Schultz et al. 1998). Multiple sequence alignment was performed with the Clustal W software available at www.ch.embnet.org/software/ClustalW.html. The *alr4642* promoter was identified by a promoter search program available at www.softberry.com. *Anabaena* LexA-binding sequence (TAGTAC TAATGTTCTA, Mazón et al. 2004) was used to identify similar sites in the *alr4642* promoter region using the lalign software (www.ebi.ac.uk/Tools/psa/lalign).

Results

Bioinformatic and expression analysis of Alr4642

The *alr4642* ORF was located immediately downstream (and in the same orientation) of *alr4641*, the ORF encoding the typical 2-Cys-Prx. The ORF *all4643*, encoding the chaperone protein, DnaJ, was located downstream of *alr4642* but in the opposite orientation (Fig. 1a). BLAST search showed the ORF *alr4642* (642-bp, encoding 213 amino acids) from *Anabaena* PCC7120 to belong to the thioredoxin superfamily and share homology with Prx-like2 proteins from many other cyanobacteria (Fig. 1b). Interestingly, similarity of Alr4642 with the other Prx-like2 proteins was observed only from its second methionine, which was 35 amino acids away from the first annotated methionine (Figs. 1b and 2a). The AhpC/TSA domain of Alr4642 extended from the 75th amino acid to the 196th amino acid. Alr4642 showed the presence of CXXC motif (CPFC, in Alr4642) similar to that present in thioredoxin (Trx). The second C of CXXC motif aligned with the peroxidatic cysteine, but the other two residues (T and R) of the catalytic triad were absent. The promoter identified by a

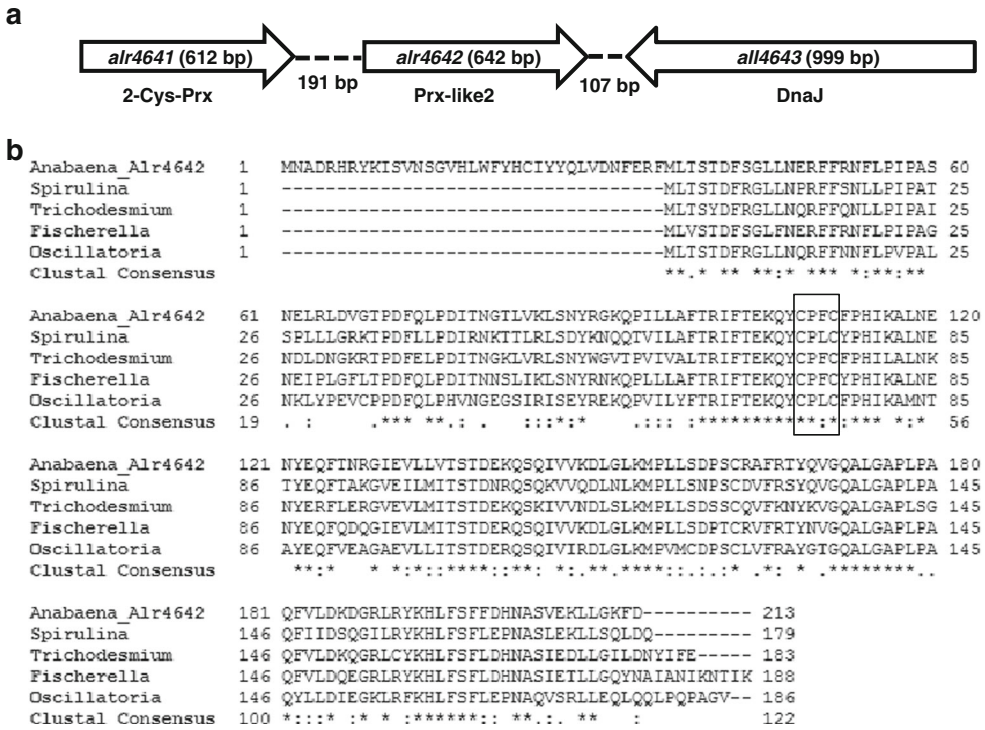

Fig. 1 **a** Location of *alr4642* on *Anabaena* PCC7120 chromosome. The ORF present upstream and downstream of *alr4642* is shown along with its size. The protein encoded by the respective ORF is depicted below the ORF. *Arrowheads* indicate the direction of transcription. The length (in bp) of the intergenic region (*dashed line*) is also represented. **b** Multiple sequence alignment. ClustalW software was employed to obtain alignment of Alr4642-like proteins from different bacteria. Identical amino acids are depicted by *asterisk*, conserve red amino acids are depicted by *colon*, whereas semi-conserved amino acids are depicted by *full stop*. The CXXC motif is *boxed*. The proteins compared include Anabaena_Alr4642 (*Anabaena* PCC7120; NP_4886821), Spirulina (*Spirulina subsalsa*; WP_017304383.1), Trichodesmium (*Trichodesmium erythraeum* IMS101; YP_720195.1), Fischerella (*Fischerella* sp. PCC 9339; WP_017310806.1) and Oscillatoria (*Oscillatoria acuminata* PCC 6304; YP_007086999.1). The name of the bacterium and accession no. of the protein as mentioned in the UniprotKB/Swissprot databases is shown in *parentheses*

promoter search program is shown in Fig. 2a. Interestingly, this promoter sequence was located right at the beginning of the *alr4642* ORF with the −35 region overlapping with the start codon of *alr4642*. Although the −10 region of the identified promoter showed a good match with the consensus −10 promoter sequences, the −35 region showed poor match with its respective consensus, indicating that the promoter was inherently a weak promoter. Homology search with *Anabaena* PCC7120 LexA protein-binding sequence (Mazón et al. 2004) showed the presence of a LexA-binding site that overlapped directly with the −10 sequence (Fig. 2a).

The full-length *alr4642* or a truncated *alr4642*, i.e. *alrT4642* (537 bp, encoding a protein extending from 36th residue to 213th residue, i.e. 178 amino acids), was cloned in *E. coli* expression vector pET16b for over-production of N-terminally His-tagged Alr4642 (10HisAlr4642) or AlrT4642 (10HisTAlr4642) (Fig. 2c). On induction with IPTG, production of the full-length 10HisAlr4642 protein or the 10HisAlrT4642 protein was clearly observed on denatured polyacrylamide gels (Fig. 2d). However, in spite of abundant production, both the over-expressed proteins were located exclusively in the inclusion bodies and could not be purified (data not shown). The 10HisAlr4642 protein was eluted from the gel and employed to raise specific antiserum in mouse.

The Alr4642 antiserum failed to detect the Alr4642 protein in the cell-free protein extracts of unstressed *Anabaena* PCC7120 on Western blots. Even after exposure to oxidizing agents such as H_2O_2 or methyl viologen, expression of Alr4642 could not be observed in *Anabaena* PCC7120 (Fig. 2d). No signal corresponding to *alr4642* could be detected in total RNA isolated from control or H_2O_2/MV-treated cells on Northern blots with the *alr4642* probe (data not shown).

Expression of *alr4642* in *Anabaena* PCC7120 leads to production of AlrT4642

The complete *alr4642* ORF was cloned in between a strong light inducible P_{psbA1} promoter and the *gfp* gene in an *Anabaena* PCC7120-*E. coli* shuttle vector pAM1956 (construct denoted pAM4642), which was subsequently conjugated into *Anabaena* PCC7120 (to give rise to An4642$^+$). In An4642$^+$, both *alr4642* and *gfp* are co-transcribed but

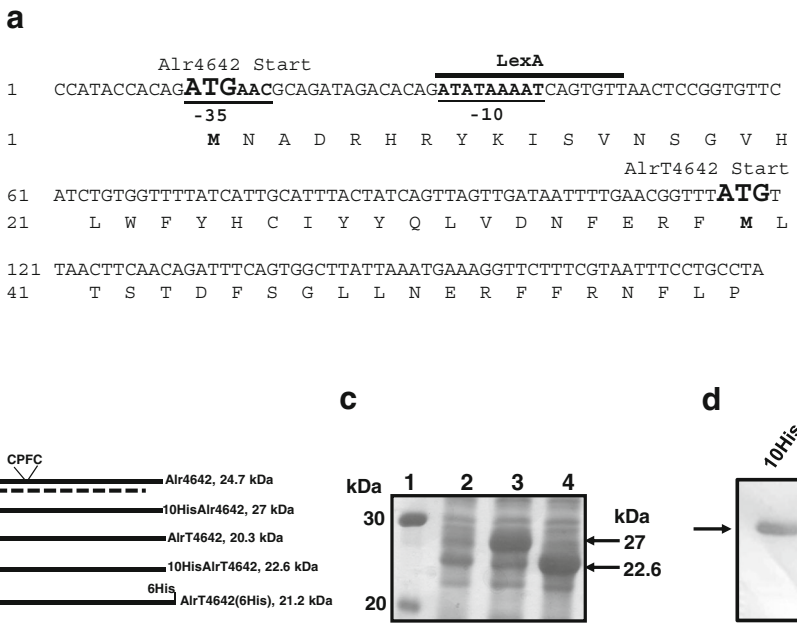

Fig. 2 **a** Schematic representation of the various Alr4642 proteins employed in the study along with their expected molecular weights. The AhpC/TSA domain (*dashed line*) and the position of the CXXC motif (i.e. CPFC in Alr4642) are indicated. The position of the methionine residues (*M*) and the location of the His-tag (if present) are also depicted. **b** Promoter analysis. The nucleotide sequence corresponding to the −10 and −35 region of the promoter are *underlined*. The ATG codons Alr4642 and AlrT4642 are indicated while the LexA-binding sequence that overlaps with the −35 region is depicted by a *thick line*. **c** Production of Alr4642 in *E. coli* BL21 pLysS. The 10HisAlr4642 or 10HisAlrT4642 were over-produced in *E. coli* employing the pET16b expression vector. Four hours after induction with IPTG, proteins (20 μg) were resolved by SDS-PAGE and visualized by staining with Coomassie brilliant blue (CBB). *Lane 1*, BL21pLysS/pET16b; *lane 2*, BL21pLysS/pET4642; and *lane 3*, BL21pLysS/pETT4642. **d** Western blotting-immunodetection analysis with the Alr4642 antiserum. Total protein was isolated from *Anabaena* PCC7120 cells grown in BG-11 medium without or with 2 μM MV (MV) or 1 mM H_2O_2 (H_2O_2). These proteins (50 μg per lane) were resolved by 12 % SDS-PAGE and electroblotted onto the nitrocellulose membrane. Subsequently, the blot was allowed to cross-react with the Alr4642 antiserum (1:2000), followed by secondary anti-mouse IgG (1:5000) coupled to alkaline phosphatase. The 27-kDa band shown by the purified 10HisAlr4642 (100 ng) is depicted by an *arrow*

independently translated resulting in co-expression of both proteins. The An4642$^+$ cells that appeared on the selection medium were verified by monitoring expression of GFP (Fig. 3a). When probed with the Alr4642 antiserum on Western blots, the recombinant An4642$^+$ showed production of a shorter Alr4642 protein, whose size (20.3 kDa) matched with that of AlrT4642 and not the full-length Alr4642 (Fig. 3b). This suggested that codon corresponding to the second methionine was the actual in vivo start codon in *Anabaena*.

Over-production of His-tagged-AlrT4642 in *Anabaena* PCC7120 and its purification

As the second methionine appeared to be the in vivo start codon of *alr4642* in *Anabaena*, attempts were made to over-

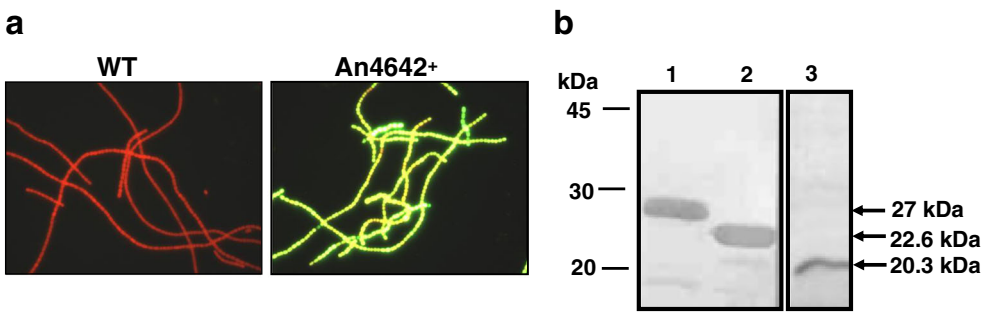

Fig. 3 **a** Fluroescence micrographs of cells grown in BG-11 medium for 3 days (excitation BP, 450–490 nm and emission LP, 515 nm). *WT* wild-type *Anabaena* PCC7120, *An4642*$^+$ recombinant *Anabaena* PCC7120 transformed with pAM4642. **b** 10HisAlr4642 or 10HisAlrT4642 was expressed in *E. coli* whereas Alr4642 (without any tag) was over-expressed in *Anabaena* PCC7120. Total proteins (20 μg per lane) were resolved on SDS-PAGE together and electroblotted onto a nitrocellulose membrane. *Lanes 1* and *2* were probed with the polyhistidine antiserum while *lane 3* was probed with the Alr4642-specific antiserum. *Lane 1*, BL21pLysS/pET16b; *lane 2*, BL21pLysS/pET4642; and *lane 3*, An4642$^+$. The molecular weight of proteins is shown in the figure

express a His-tagged AlrT4642 in *Anabaena* and purify it. To accomplish this, the *alrT4642* ORF with six additional His codons at its 3′ end [i.e. *alrT4642(6His)*] was cloned downstream of P_{psbA1} promoter in pAM1956 (pAMT4642). After conjugating pAMT4642 into *Anabaena* PCC7120, exconjugants [AnT4642(6His)$^+$] were identified by visualizing GFP expression (data not shown). Production of the AlrT4642(6His) protein was verified on Western blots with the Alr4642 antiserum wherein production of a 21.2 kDa protein was observed (Fig. 4a). The His-tagged protein was observed in the cytosolic fraction of *Anabaena* extracts indicating that AlrT4642 remained soluble when over-expressed in *Anabaena*. The AlrT4642 protein could be purified to near homogeneity by affinity chromatography employing the Ni-NTA matrix (Fig. 4b). The identity of purified AlrT4642(6His) was confirmed by probing it with anti-Alr4642 and anti-polyhistidine antiserum (Fig. 4c).

AlrT4642 defends plasmid DNA from oxidative damage

In the absence of the AlrT4642(6His) protein or in the presence of BSA (control protein), complete degradation of the plasmid DNA was observed in the metal-catalyzed oxidation (MCO) assay. However, when the Alr4642(6His) protein was present (Fig. 5a, lanes 3 and 4), a major amount of plasmid DNA was converted only to the linear (L) form and not degraded completely. Also, the proportion of the covalently closed circular (CCC) form of plasmid DNA increased with increasing concentration of the Alr4642(6His) protein. Thus, the addition of purified AlrT4642(6His) conferred considerable protection to DNA from oxidative damage. In DTT-dependent peroxidase activity assays, a distinct reduction in concentration of H_2O_2 was observed in the presence of the Alr4642(6His) protein (Fig. 5b).

Over-expression of AlrT4642 protects *Anabaena* from oxidative stress

As the purified AlrT4642(6His) showed antioxidant activity in vitro, it was desired to verify if over-expression of AlrT4642 would protect *Anabaena* from oxidative stress. To accomplish this, AnT4642(6His)$^+$ and the wild-type *Anabaena* PCC7120 were assessed for oxidative stress resistance in response to hydrogen peroxide. As seen in Fig. 5b, after 2 days of treatment, a pronounced bleaching, indicating loss of photosynthetic pigments, was observed in the wild-type cells but not in AnT4642 (6His)$^+$. AnT4642 (6His)$^+$ showed chlorophyll *a* content comparable to the unstressed AnT4642(6His)$^+$ cells, whereas a clear reduction in chlorophyll *a* was observed in the wild-type cells after 2 days of H_2O_2 stress (Fig. 5c).

Discussion

Many environmental stresses, e.g. salinity, sudden osmotic alterations, desiccation, ionizing and non-ionizing radiations, metal toxicity, high light intensity, etc., result in generation of ROS indicating an obvious cross-talk between these stresses and oxidative stress (Dadheech 2010). Hydrogen peroxide (H_2O_2) is a very common ROS in biological systems, and cyanobacteria, in particular, have been shown to be generally more susceptible to H_2O_2 than other phototrophs (Drabakova et al. 2007). H_2O_2, though relatively stable, can undergo Fenton reaction to generate the most damaging ROS, i.e. $OH^{\cdot}$ (Halliwell and Gutteridge 1986); hence, it is particularly important to remove intracellular H_2O_2. Detoxification of H_2O_2 is largely mediated by peroxidases and catalases that

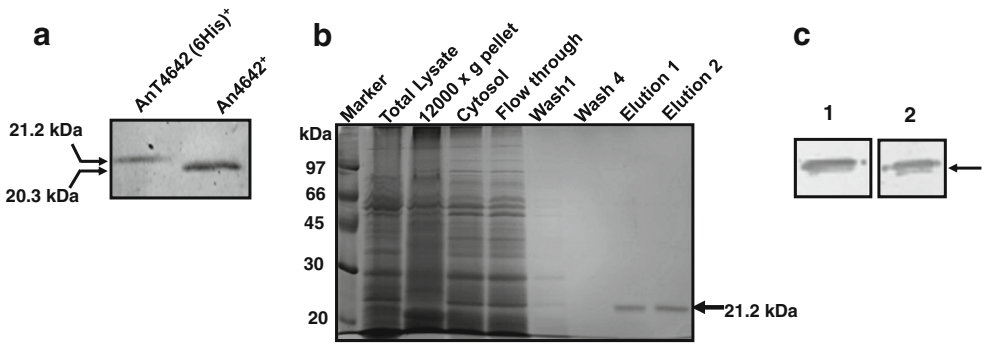

Fig. 4 **a** Total proteins from An4642$^+$ or AnT4642(6His)$^+$ were separated on SDS-PAGE and probed with the Alr4642-specific antiserum. Size of the two proteins is depicted. **b** Purification of AlrT4642(6His). AnT4642(6His)$^+$ culture was grown (with aeration) for 7 days, and purification of the AlrT4642(6His) protein was performed as described in the methods section. Equal volume of different (20 μL each) fractions as indicated in the figure was resolved on SDS-PAGE and visualized by staining with CBB. **c** The purified AlrT4642(6His) was probed with the polyhistidine antiserum (*1*) or with the Alr4642-specific antiserum (*2*). The 21.2-kDa AlrT4642(6His) protein band that appeared after developing the blots is shown by an *arrow*

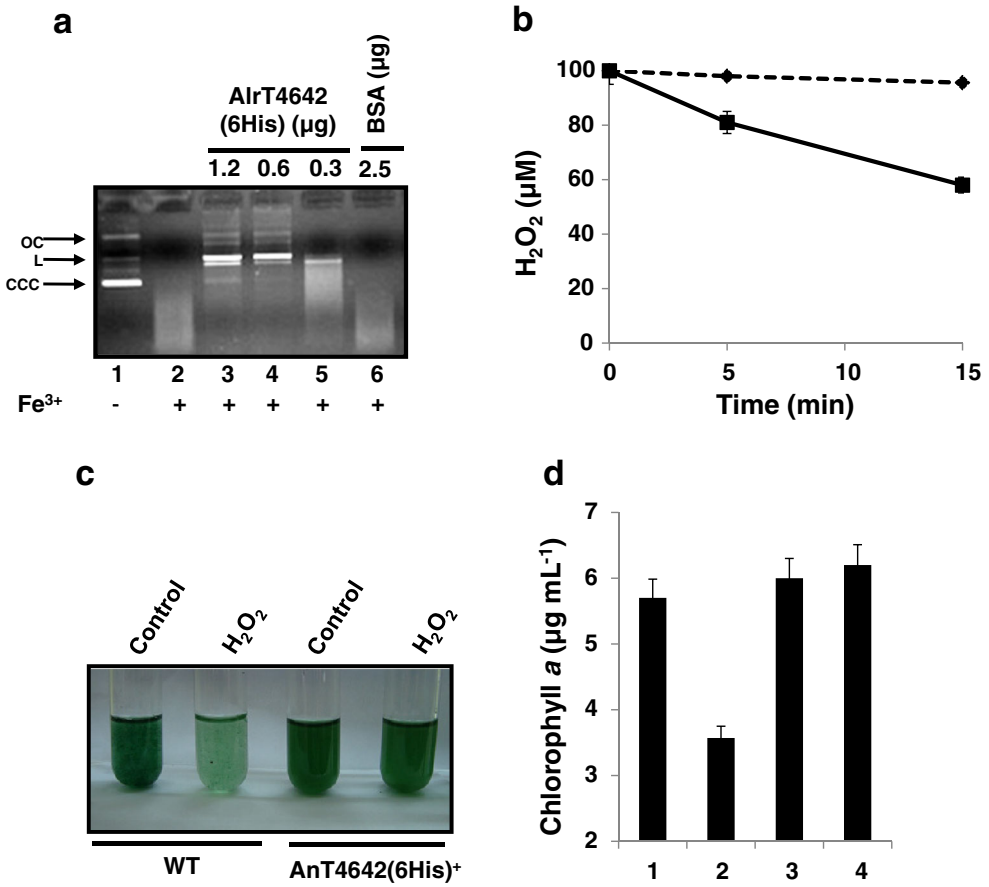

Fig. 5 **a** Metal-catalyzed oxidation (MCO) assay. One microgram of pBluescript DNA (*lane 1*) was subjected to oxidative damage using the MCO reaction [(5 mM DTT+3 μM Fe^{3+}) depicted by Fe^{3+}] to generate ROS in the absence (*lane 2*) or in the presence of purified AlrT4642(6His) (*lanes 3–5*) or BSA (*lane 6*) as indicated. The integrity of DNA was assessed by electrophoresis on a 1 % agarose gel followed by staining with ethidium bromide. The covalently closed circular (*CCC*), linear (*L*) and open circle (*OC*) forms of the plasmid DNA are indicated. **b** DTT-dependent peroxidase activity. Decomposition of H_2O_2 by the purified Alr4642(6His) protein (5 μg) using DTT as reductant. *Dashed line*, no protein; *solid line*, Alr4642(6His). **c** Three-day-old cultures were inoculated in a fresh growth medium and subjected to 1 mM H_2O_2 stress for 2 days. Subsequently, the cultures were photographed. *WT*, wild-type *Anabaena* PCC7120 and $AnT4642^+$, recombinant *Anabaena* PCC7120 over-expressing AlrT4642 (6His) $^+$. **d** The chlorophyll *a* content of cultures shown in **c** was determined after 2 days of exposure to H_2O_2. *1*, WT/control; *2*, WT/H_2O_2; *3*, $AnT4642(6His)^+$/control; and *4*, $AnT4642(6His)^+/H_2O_2$

convert H_2O_2 into harmless water (Bernroitner et al. 2009). As *Anabaena* shows extremely low levels of catalase activity, it is proposed that thiol peroxidases such as Prxs may be the principal components that eliminate H_2O_2 (Banerjee et al. 2012b; Pascual et al. 2010). This view is supported by the relatively large number of *prx* genes present in the genome of *Anabaena* PCC7120 (Kaneko et al. 2001).

The role of hitherto uncharacterized *alr4642* ORF, encoding the Alr4642 protein, was explored in this study. In spite of being located downstream of a gene that is highly expressed (*alr4641* that encodes 2-Cys-Prx) (Pascual et al. 2010), expression of the *alr4642* mRNA or the Alr4642 protein could not be detected under any of the conditions tested. Bioinformatic analysis showed the presence of (1) a relatively weak promoter and (2) the repressor protein LexA-binding site within this promoter. However, when expressed from a strong promoter (P_{psbA}), AlrT4642 protein was readily expressed in *Anabaena*.

The Alr4642 protein, which showed similarity to Prx-like2 group of Prxs, was found to be highly conserved in cyanobacteria and was present in diverse species ranging from the filamentous forms such as *Fischerella muscicola* to unicellular forms such as *Synechococcus* PCC7335 and *Gloeobacter violaceus*. Many of the nitrogen-fixing cyanobacteria, e.g. *Nostoc* sp., *Anabaena* sp. and *Cyanotheceae*, also showed the presence of Alr4642-like ORFs. Interestingly, homology of Alr4642 with other Prx-like2 proteins commenced from its second methionine that was 36 amino acids away from the first methionine annotated in the database (Figs. 1 and 2a). Moreover, in *Anabaena*, expression of the complete *alr4642* ORF (from pAM4642) resulted in production of a smaller protein whose size corresponded to that of AlrT4642 (Fig. 3). These results suggest that the second ATG codon may be the actual in vivo start codon of *alr4642* in *Anabaena*.

Solubility of proteins over-expressed employing the pET-system in *E. coli* is a major problem, and in many cases, the over-produced protein is exclusively present (presumably in inactive form) in the inclusion bodies. Similarly, Alr4642 or AlrT4642 could not be produced in the soluble form in *E. coli*. However, over-expression of *alr4642* or *alrT4642(6His)* in *Anabaena* PCC7120 led to production of soluble AlrT4642 and AlrT4642(6His), respectively (Figs. 3 and 4). In fact, AlrT4642(6His) expressed in *Anabaena* could be purified to near homogeneity by affinity chromatography with the Ni-NTA matrix (Fig. 4). To our knowledge, this is the first instance wherein a protein has been purified from *Anabaena* after over-expression. In an earlier study, over-expression of Mn-catalase (Alr0998 from *Anabaena* PCC7120) in *E. coli* had resulted in production of insoluble protein (i.e. inclusion bodies) that could not be purified. When over-expressed in *Anabaena*, the Alr0998 protein not only remained soluble, but was also active (Banerjee et al. 2012a). These data show the potential use of *Anabaena* PCC7120 for production of soluble *Anabaena* proteins in cases where it is not possible to do so in *E. coli*.

The ability of the purified AlrT4642(6His) to protect the DNA was assessed using the MCO assay. H_2O_2 generated during this reaction undergoes Fenton reaction to produce $OH^{\cdot}$, which degrades DNA. The protection of DNA in the presence of the AlrT4642(6His) protein (Fig. 5a) indicates that it can detoxify H_2O_2, i.e. function as a peroxidase and eventually prevent formation of $OH^{\cdot}$. In addition, the purified protein showed DTT-dependent peroxidase activity (Fig. 5b) indicating that it can indeed function as a peroxidase. Thus, when over-expressed in *Anabaena*, the AlrT4642(6His) protein was not only soluble but was also biologically active.

In cyanobacteria, chlorophyll *a* content is a reliable indicator of growth and is routinely used to assess resistance to various stresses (Alahari and Apte 1998). Excess H_2O_2 resulted in destruction of photosynthetic pigment synthesis and eventually cell death in cyanobacterium *Microcystis aeruginosa* (Qian et al. 2010). In the present study too, treatment of H_2O_2 led to distinct reduction in the chlorophyll *a* content of the wild-type *Anabaena* PCC7120 cells. In contrast, under similar conditions, AnT4642(6His)$^{+}$ cells showed distinct protection of chlorophyll *a* from bleaching (Fig. 5b, c). These results clearly demonstrate that AlrT4642, a Prx-like2 protein, can protect *Anabaena* PCC7120 from oxidative stress.

In conclusion, *alrT4642* is not expressed in *Anabaena*, possibly due to the presence of a weak promoter and probable repression by the LexA protein. In spite of being insoluble in *E. coli*, the AlrT4642 protein remained soluble when over-expressed (from a strong promoter) in *Anabaena*. The second methionine was identified as the actual start codon of Alr4642 in *Anabaena*. The AlrT4642(6His) protein, purified from *Anabaena*, protected DNA from oxidative damage suggesting that it is indeed an antioxidant protein. Over-expression of AlrT4642 protected *Anabaena* from oxidative stress mediated by H_2O_2. These results demonstrate the possible use of *prx-like* genes for construction of stress-tolerant *Anabaena* strains for use as biofertilizers.

Acknowledgments Fellowship provided by Homi Bhabha National Institute to Vijay Tailor is gratefully acknowledged. We wish to thank Dr. S. K. Apte for constant encouragement and Dr. Manisha Banerjee for the helpful suggestions during the course of this study. This work was funded by the XI plan project of DAE, India.

References

Agrawal C, Sen S, Singh S, Rai S, Singh PK, Singh VK, Rai LC (2014) Comparative proteomics reveals association of early accumulated proteins in conferring butachlor tolerance in three N_2-fixing *Anabaena* spp. J Proteomics 96:271–290

Alahari A, Apte SK (1998) Pleiotropic effects of potassium deficiency in a heterocystous, nitrogen-fixing cyanobacterium, *Anabaena torulosa*. Microbiology 144:1557–1563

Allen JF, Martin W (2007) Evolutionary biology: out of thin air. Nature 445:610–612

Altschul SF, Gish W, Miller W, Meyera MW, Lipman DJ (1990) Basic local alignment search tool. J Mol Biol 215:403–410

Asada K, Kiso K, Yoshikawa K (1974) Reduction of molecular oxygen by spinach chloroplast on illumination. J Biol Chem 249:2175–2181

Banerjee M, Ballal A, Apte SK (2012a) Mn-catalase (Alr0998) protects the photosynthetic, nitrogen-fixing cyanobacterium *Anabaena* PCC7120 from oxidative stress. Environ Microbiol 14:2891–2900

Banerjee M, Ballal A, Apte SK (2012b) A novel glutaredoxin domain-containing peroxiredoxin 'All1541' protects the N_2-fixing cyanobacterium *Anabaena* PCC 7120 from oxidative stress. Biochem J 442:671–680

Banerjee M, Raghvan PS, Ballal A, Rajaram H, Apte SK (2013) Oxidative stress management in the filamentous heterocystous, diazotrophic cyanobacterium, *Anabaena* PCC7120. Photosynth Res 118:59–70

Bernroitner M, Zamocky M, Furtmüller PG, Peschek GA, Obinger C (2009) Occurrence, phylogeny, structure, and function of catalases and peroxidases in cyanobacteria. J Exp Bot 60:423–440

Bihani SC, Chakravarty D, Ballal A (2013) Purification, crystallization and preliminary crystallographic analysis of KatB, a manganese catalase from *Anabaena* PCC 7120. Acta Crystallogr Sect F: Struct Biol Cryst Commun 69:1299–1302

Cha MK, Hong SK, Kim IH (2007) Four thiol peroxideses contain a conserved GCT catalytic motif and act as a versatile array of lipid peroxidases in *Anabaena* sp. PCC7120. Free Radic Biol Med 42: 1736–1748

Chaurasia AK, Parasnis A, Apte SK (2008) An integrative expression vector for strain improvement and environmental applications of the nitrogen fixing cyanobacterium, *Anabaena* sp. strain PCC7120. J Microbiol Methods 73:133–141

Choudhury S, Panda P, Sahoo L (2013) Reactive oxygen species signaling in plants under abiotic stress. Plant Signal Behav 8:e23681

Collen J, Del Rio MJ, García-Reina G, Pedersén M (1995) Photosynthetic production of hydrogen peroxide by *Ulva rigida* C. Ag (Chlorophyta). Planta 196:225–230

Cui H, Wang Y, Wang Y, Qin S (2012) Genome-wide analysis of putative peroxiredoxin in unicellular and filamentous cyanobacteria. BMC Evol Biol 12:220

Dadheech N (2010) Desiccation tolerance in cyanobacteria. Afr J Microbiol Res 4:1584–1593

Dietz KJ (2011) Peroxiredoxins in plants and cyanobacteria. Antioxid Redox Signal 15:1129–1159

Drabakova M, Matthijs HCP, Admiraal W, Marsalek B (2007) Selective effects of H_2O_2 on cyanobacterial photosynthesis. Photosynthetica 45:363–369

Elhai J, Vepritskiy A, Muro-Pastor AM, Flores E, Wolk CP (1997) Reduction of conjugal transfer efficiency by three restriction activities of *Anabaena* sp. strain PCC 7120. J Bacteriol 179:1998–2005

Halliwell B, Gutteridge JMC (1986) Oxygen free radicals and iron in relation to biology and medicine: some problems and concepts. Arch Biochem Biophys 246:501–514

Imlay JA (2003) Pathways of oxidative damage. Annu Rev Microbiol 57: 395–418

Kaneko T, Nakamura Y, Wolk CP (2001) Complete genomic sequence of the filamentous nitrogen-fixing cyanobacterium *Anabaena* sp. strain PCC 7120. DNA Res 8:205–213

Laemmli UK (1970) Cleavage of structural proteins during the assembly of the head of bacteriophage T4. Nature 227:680–685

Latifi A, Ruiz M, Jeanjean R, Zhang CC (2007) PrxQ-A, a member of the peroxiredoxin Q family, plays a major role in defense against oxidative stress in the cyanobacterium *Anabaena* sp. strain PCC7120. Free Radic Biol Med 42:424–431

Mackinney G (1941) Absorption of light by chlorophyll solutions. J Biol Chem 140:315–322

Mazón G, Lucena JM, Campoy S, Fernández de Henestrosa AR, Candau P, Barbé J (2004) LexA-binding sequences in Gram-positive and cyanobacteria are closely related. Mol Genet Genomics 271:40–49

Nishiyama Y, Allakhverdiev SI, Murata N (2006) A new paradigm for the action of reactive oxygen species in the photoinhibition of photosystem II. Biochim Biophys Acta 1757:742–749

Panda B, Basu B, Rajaram H, Apte SK (2014) Methyl viologen responsive proteome dynamics of *Anabaena* sp. strain PCC7120. Proteomics 14:1895–1904

Pascual MB, Cabana AM, Florencio FJ, Lindahl M, Cejudo FJ (2010) Overoxidation of 2-Cys peroxiredoxin in prokaryotes: cyanobacterial 2-Cys peroxiredoxins sensitive to oxidative stress. J Biol Chem 285:34485–34492

Qian H, Yu S, Sun Z, Xie X, Liu W et al (2010) Effects of copper sulfate, hydrogen peroxide and N-phenyl-2-naphthylamine on oxidative stress and the expression of genes involved photosynthesis and microcystin disposition in *Microcystis aeruginosa*. Aquat Toxicol 95:405–412

Schultz J, Milpetz F, Bork P, Ponting CP (1998) SMART, a simple modular architecture research tool: identification of signaling domains. Proc Natl Acad Sci U S A 95:5857–5864

Storz G, Imlay JA (1999) Oxidative stress. Curr Opin Microbiol 2:188–194

Tripathi B, Bhatt I, Dietz KJ (2009) Peroxiredoxins: a less studied component of hydrogen peroxide detoxification in photosynthetic organisms. The function of peroxiredoxins in plant organelle redox metabolism. Protoplasma 235:3–15

Venkatraman GS (1979) Algal inoculations in rice fields. In: Brady NC (ed) Nitrogen and rice. International Rice Research Institute, Los Banos, pp 311–321

Wood ZA, Schröder E, Robin-Harris J, Poole LB (2003) Structure, mechanism and regulation of peroxiredoxins. Trends Biochem Sci 28:32–40

Yoon HS, Golden JW (1998) Heterocyst pattern formation is controlled by a diffusible peptide. Science 282:935–938

Zamocky M, Furtmüller PG, Obinger C (2008) Evolution of catalases from bacteria to humans. Antioxid Redox Signal 10:1527–1548

Zhao W, Guo Q, Zhao J (2007) A membrane-associated Mn-superoxide dismutase protects the photosynthetic apparatus and nitrogenase from oxidative damage in the cyanobacterium *Anabaena* sp. PCC 7120. Plant Cell Physiol 48:563–572

Contents lists available at ScienceDirect

Free Radical Biology and Medicine

journal homepage: www.elsevier.com

Original article

Novel molecular insights into the function and the antioxidative stress response of a Peroxiredoxin Q protein from cyanobacteria

Vijay Tailor [a, b], Anand Ballal [a, b, *]

[a] Molecular Biology Division, Bhabha Atomic Research Centre, Trombay, Mumbai 400085, India
[b] Homi Bhabha National Institute, Anushakti Nagar, Mumbai 400094, India

ARTICLE INFO

Keywords:
Stress tolerance
Oxidative stress
Peroxiredoxins
Catalytic cysteines
Cyanobacteria

ABSTRACT

The Peroxiredoxin Q (PrxQ) proteins are thiol-based peroxidases that are important for maintaining redox homeostasis in several organisms. Activity of PrxQs is mediated by two cysteines, peroxidatic (C_p) and resolving (C_r), in association with a reducing partner. A PrxQ, Alr3183, from the cyanobacterium, *Anabaena* PCC 7120, was characterized in this study. Alr3183, which required thioredoxin A (TrxA) for peroxidase activity, was an intramolecular disulfide bond-containing monomeric protein. However, Alr3183 lacking C_p (Alr3183C46S) or C_r (Alr3183C51S) formed intermolecular disulfide linkages and was dimeric. Alr3183C46S was completely inactive, while Alr3183C51S required higher concentration of TrxA for peroxidase activity. Surface plasmon resonance analysis showed that unlike Alr3183 or Alr3183C46S, Alr3183C51S bound rather poorly to TrxA. Also, compared to the oxidized protein, the DTT-treated (reduced) Alr3183 displayed decreased interaction with TrxA. *In vivo*, Alr3183 was found to be induced in response to γ-radiation. On exposure to H_2O_2, *Anabaena* strain over-expressing Alr3183 showed reduced formation of ROS, intact photosynthetic pigments and consequently better survival than the wild-type, whereas overproduction of Alr3183C46S did not provide any protection. Significantly, this study (1) reveals the importance of C_r for interaction with thioredoxins and (2) demonstrates that over-expression of PrxQs can protect cyanobacteria from oxidative stresses.

1. Introduction

Peroxiredoxins (Prxs) are a group of proteins that efficiently detoxify a wide range of peroxide substrates including H_2O_2, the most important peroxide generated in biological systems [19]. Prxs have catalytic cysteine residues which participate in the detoxification reaction, hence these proteins are known as thiol peroxidases ([36]; Woods et al., 2003). Prx, widely distributed across all the phylogenetic kingdoms, are primarily proposed to be high-affinity peroxide-capturing proteins required to maintain the overall desired thiol status within a cell [16]. Depending on the number of catalytic cysteines taking part in the reaction, and their relative locations, Prxs are classified into 3 broad categories namely; 1-Cys Prx; the typical 2-Cys Prx; and the atypical 2-Cys Prx, which are further classified into type II Prx and PrxQ ([36]; Woods et al., 2003). More recently, Cui et al. [15] have identified a new subfamily of Prxs, i.e. Prx-like, in cyanobacteria.

Like all 2-Cys-containing Prxs, the PrxQ proteins contain two conserved cysteine residues, the peroxidatic cysteine (C_p) and the resolving cysteine (C_r) that are essential for peroxidase activity. In spite of showing high degree of similarity amongst them, the relative position of C_r within the PrxQ proteins differs. The C_p is usually located close to the N-terminal end of the protein, whereas C_r is usually 4 residues away from C_p, but in some cases, C_r may be more than 30 amino acids apart from C_p [14]. On reaction with the peroxide substrate, the free thiol group (-SH) of C_p is converted to its sulfenic acid (–SOH) derivative, whereas the peroxide is converted to its corresponding alcohol (or water in the case of H_2O_2) [34]. Subsequently, the free thiol group of C_r reacts with the C_p-SOH, forming an intramolecular disulfide linkage. This disulfide bond is resolved by reductants such as thioredoxin, which regenerates the active (i.e. –SH) form of enzyme, enabling another round of peroxidase activity [4]. Unlike the typical 2-Cys Prx proteins which are obligate dimers, PrxQ may exist as monomers or dimers or as a mixture of both [16].

Although not found in mammals, the PrxQ homologs have been observed in plants and bacteria, including cyanobacteria. The poplar PrxQ protein is targeted to chloroplasts, suggesting its possible role in maintaining the redox status of that organelle [27,35,41]. Over-expression of *Gentiana triflora* (Gt) PrxQ resulted in resistance to fungal infection and methyl viologen in *Nicotiana tabacum* [24], whereas over production of *Suaeda salsa* PrxQ led to tolerance to cold stress in Arabidopsis [21]. Heterologous over-

* Corresponding author at: Molecular Biology Division, Bhabha Atomic Research Centre, Trombay, Mumbai 400085, India.
Email addresses: vijayt@barc.gov.in (V. Tailor); aballal@barc.gov.in (A. Ballal)

http://dx.doi.org/10.1016/j.freeradbiomed.2017.01.031
Received 2 November 2016; Received in revised form 18 January 2017; Accepted 20 January 2017
Available online xxx
0891-5849/

expression of *Synechococcus* PrxQ-A proteins increased ability of *E. coli* to tolerate cumene hydroperoxide [39].

Reactive oxygen species such as superoxide, H_2O_2 and $OH^{\cdot}$ are generated due to the partial reduction of oxygen in all aerobic organisms. Cyanobacteria, the first organisms to evolve oxygen as a by-product of photosynthesis, are expected to harbour complex systems to detoxify the various ROS generated during normal metabolic activity or in response to different environmental stresses [6]. Cyanobacteria remain the only phyla to date whose members can use solar energy to fix atmospheric nitrogen. In fact, strains of the nitrogen-fixing cyanobacterium, *Anabaena*, are widely used as biofertilizers in the paddy fields of Southeast Asia [43]. The filamentous, heterocystous, diazotrophic cyanobacterium *Anabaena* PCC 7120 shows tolerance to stresses such as ionizing radiation and desiccation, which are known to enhance ROS production *in vivo* [38]. For this reason, *Anabaena* PCC 7120 has been used as a model system to decipher adaptive responses to various environmental stresses, especially oxidative stresses, in many laboratories, including ours [12,29,42,8].

Although *Anabaena* possesses two genes encoding catalases, the inherent catalase activity in *Anabaena* appears to be low under normal conditions of growth [5,32]. In view of this, it is proposed that Prxs could be the principal proteins that detoxify H_2O_2 in *Anabaena* [33]. This reasoning is supported by the occurrence of many genes encoding Prxs in *Anabaena* [10]. All the major categories of Prxs are found in *Anabaena*, including four that belong to the PrxQ subtype (i.e. Alr2503, All2375, All2556 and Alr3183) [10,22,28,40]. Chloroplasts, the organelle with highest content of Prxs in a plant cell, are supposed to have evolved from cyanobacteria. Akin to *Anabaena*, chloroplasts also show the presence of the PrxQ proteins and low catalase activity [32,5].

Among the 4 PrxQ proteins present in *Anabaena* PCC 7120, Alr3183 showed highest identity to PrxQ from Arabidopsis [28]. Due to its high degree of similarity with plant PrxQs, Alr3183 was chosen for this study. Several lines of evidence showed the Alr3183 protein to be monomeric, capable of forming intramolecular disulfide bonds. However, when either of the catalytic cysteine was lost, the protein formed intermolecular disulfide bonds and became dimeric. Alr3183 lacking the C_p (Alr3183C46S) was completely inactive, whereas when C_r was absent (Alr3183C51S), the protein required higher concentrations of TrxA to show peroxidase activity. Surface Plasmon resonance (SPR) analysis showed C_r to be necessary for binding of Alr3183 with TrxA. Interestingly, *in vivo* in *Anabaena*, the Alr3183 protein was induced several-fold in response to gamma radiation. Over-expression of Alr3183 increased ability of *Anabaena* to tolerate oxidative stress mediated by H_2O_2. In contrast, *Anabaena* strain overproducing Alr3183C46S remained sensitive to H_2O_2, underscoring the importance of peroxidase activity of Alr3183 for overcoming oxidative stress.

2. Results

2.1. Bioinformatic analysis

The 462-bp long *alr3183* ORF encoded a ~17 kD protein (153 amino acids) that showed homology to the PrxQ family of Prxs. BLAST search indicated the Alr3183 protein to belong to the thioredoxin superfamily, which contain the AhpC/TSA domain. The AhpC/TSA domain of Alr3183 extended from the 5th amino acid to the 128th amino acid and the protein also contained the conserved GCT motif. The cysteine residues at position 46 (Cys-46, which is also a part of the GCT motif) and 51 (Cys-51) were the peroxidatic (C_p) and the resolving cysteine (C_r) residues respectively (Fig. 1A). The amino acid residues of the catalytic triad, T (43), C (46) and R (115), which form the active site, are also shown in the Fig. 1A.

2.2. Absence of catalytic cysteine results in intermolecular disulfide bond formation

The Alr3183 protein from *Anabaena* PCC7120 was over-expressed in *E. coli* with N-terminal His-tag and purified near to homogeneity by affinity chromatography (Fig. 1B). Addition of the N-terminal tag increased the size of Alr3183 by ~2.5 kD, resulting in the production of ~20 kD protein. Under non-reducing conditions (i.e. absence of DTT), the Alr3183 protein was visualized as a single band of 20 kD. Under reducing conditions (i.e. with 1 mM DTT), the Alr3183 protein appeared as two closely spaced bands of

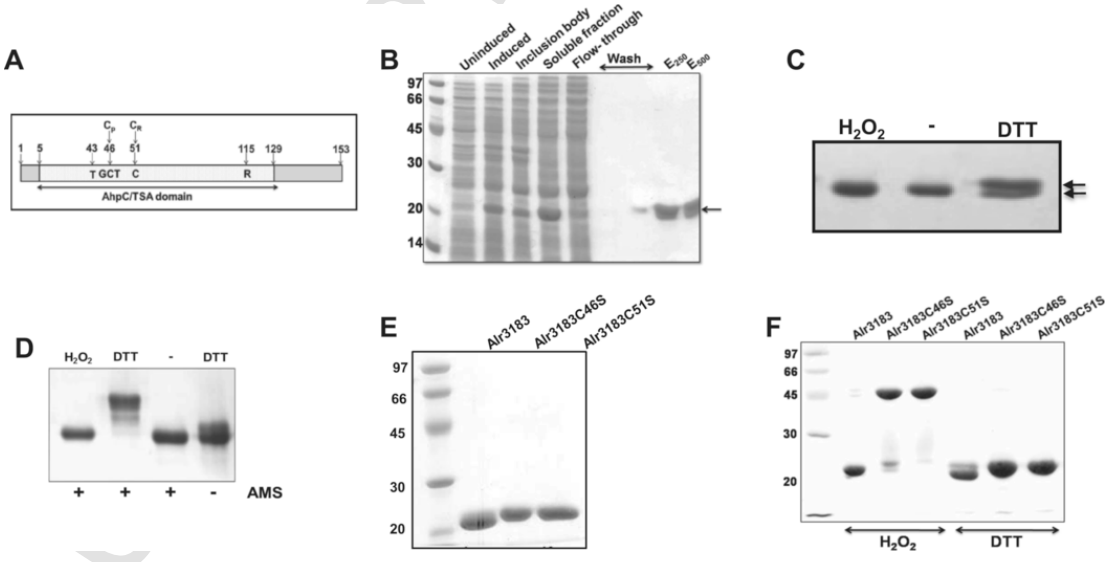

Fig. 1. (A) Schematic representation of the Alr3183 protein. The 153-amino-acid long Alr3183 protein consists of an N-terminal AhpC/TSA domain, which is indicated in the figure. The position and the amino acid residue number of the putative peroxidatic (C_p) and resolving cysteine (C_r) residues are indicated. (B) Purification of the his-tagged Alr3183 from *E. coli.* The various fractions and elutions are indicated in the figure. $Elution_{250}$, elution in buffer containing 250 mM imidazole; $Elution_{500}$, elution in buffer containing 500 mM imidazole. The purified ~20 kD Alr3183 protein is indicated by an arrow. (C) SDS-PAGE analysis of the purified Alr3183 protein. The Alr3183 protein (2 μg) was treated with DTT or H_2O_2 or left untreated (as indicated in panel), solubilized in non-reducing Laemmli's sample buffer, electrophoretically separated by SDS-PAGE (14%) gel and visualized after staining with CBB-G250. The two bands are indicated by arrows. (D) AMS modification of Alr3183. The purified protein was incubated with H_2O_2 (2 mM) or DTT (10 mM), reacted with AMS and precipitated with TCA. The precipitated proteins were solubilized in Laemmli's non-reducing sample buffer, resolved by SDS-PAGE (14% gel) and visualized by staining with CBB. (E) SDS-PAGE analysis of Alr3183C46S and Alr3183C51S. Alr3183, Alr3183C46S and Alr3183C51S were purified by Ni-NTA affinity chromatography under native conditions. Proteins were resolved by SDS-PAGE and visualized by staining with CBB G-250. (F) Mobility of Alr3183 proteins under reducing or non-reducing conditions. Purified proteins (2 μg) were treated with H_2O_2 (2 mM) or DTT (10 mM) solubilized in Laemmli's sample buffer without DTT, electrophoretically separated by SDS-PAGE (14%) gel and visualized by staining with CBB.

~20 kD. (Fig. 1C). However, on increasing the concentration of DTT to 10 mM, only one band, corresponding to the reduced protein was observed (Supp. Fig. 1A). Oxidized Prx proteins are known to form more compact structure than their corresponding reduced forms (Wood et al., 2002), and hence oxidized Prxs generally move more rapidly than their reduced forms on SDS-PAGE. Similarly, the two Alr3183 bands observed in the presence of DTT appear to be the oxidized form (lower band) or the reduced form (upper band) of the Alr3183 protein.

The alkylating agent AMS (4- acetamido-4′-maleimidyl-stilbene-2,2′-disulfonate) was used to verify if Alr3183 could form an intra-molecular disulfide bond. The oxidized form (treated with H_2O_2) or the reduced form (treated with DTT) of the Alr3183 protein was reacted with excess of AMS and resolved on SDS-PAGE. The DTT-treated form of the protein showed retarded mobility as compared to the H_2O_2-treated form of the protein (Fig. 1D). This showed that AMS bound to reduced, but not oxidized, form of the Alr3183 protein. The unavailability of the free thiol group to bind to AMS in oxidized state indicated the presence of an intra-molecular disulfide bond in the Alr3183 protein.

The C_p (Cys-46) and C_r (Cys-51) cysteines of Alr3183 were individually mutated to serine by site specific mutagenesis and the corresponding proteins (Alr3183C46S and Alr3183C51S) were also purified to near homogeneity (Fig. 1E). Interestingly, both cysteine mutants (Alr3183C46S and Alr3183C51S) mostly appeared as dimers on SDS-PAGE when left untreated (Suppl. Fig. 1B) or oxidized with H_2O_2 (Fig. 1F). Under reduced conditions, all the proteins were present in their monomeric forms (Fig. 1F). On SDS–PAGE, both mutant proteins co-migrated with the upper band (reduced form) of the Alr3183 protein. Possibly, due to the absence of intramolecular disulfide bond, the mutant proteins are unable to form a more compact structure like the oxidized form of the wild-type Alr3183 protein.

2.3. Alr3183 exists as a monomer whereas Alr3183C46S and Alr3183C51S are dimers in their native forms

To verify if Alr3183 or its mutant variants formed higher oligomeric structures, the purified proteins were subjected to size-exclusion chromatography. The Alr3183 protein eluted in fraction that corresponded to ~18 kD i.e. its monomeric size, whereas the elution profile of Alr3183C46S (38 kD) and Alr3183C51S (39 kD) indicated that these proteins were dimers (Fig. 2A). DLS analysis showed all the three proteins to be fairly monodispersive. The Alr3183 protein peak obtained from dynamic light scattering (DLS) analysis corresponded to a size of 3.7 nm while Alr3183C46S and Alr3183C51S showed size of 7.4 nm and 7.6 nm respectively (Fig. 2B). The CD spectrum of the Alr3183 protein was consistent with that of a folded protein and further indicated that Alr3183 was mostly α-helical. The Alr3183C51S protein showed a CD spectrum that was very similar to that of the Alr3183 protein, whereas minor changes were observed between the spectra Alr3183 and Alr3183C46S (Fig. 2C). Moreover, the CD spectrum of Alr3183 reduced with DTT was also similar to the CD spectra of DTT-reduced Alr3183 protein (Supp. Fig. 1C). These results suggest that the presence of the intermolecular or intramolecular bonds do not have a major influence on the overall secondary structure of the protein.

2.4. Peroxidase activity of Alr3183

Among the three reducing agents tested (DTT, GSH and TrxA), the purified Alr3183 protein could detoxify H_2O_2 only with TrxA (Fig. 3A). As shown in Fig. 3B, the TrxA-dependent peroxidase activity showed an obvious protein concentration-dependent activity. Alr3183 could also detoxify other peroxides like tert-butyl hydroperoxide and cumene hydroperoxide using TrxA as the reducing agent (Suppl. Fig. 2). The Alr3183 protein also showed high affinity towards H_2O_2 (K_M = 10 μM).

The Alr3183C46S protein (lacking the peroxidatic cysteine) was completely inactive whereas the Alr3183C51S mutant (lacking the resolving cysteine) showed activity that was several fold lower than that shown by the wild-type Alr3183 protein (Fig. 3C). The Alr3183 protein lacking both the catalytic cysteines, Alr3183CDM (cysteine double mutant) was also generated by site-specific mutagenesis, over-expressed in *E. coli* and purified. Like Alr3183C46S, this protein showed the complete absence of peroxidase activity (Fig. 3C). In the absence of TrxA, no activity was detected, whereas, on increasing the concentration of TrxA, a concomitant increase in the peroxidase activity of Alr3183 was observed (Fig. 3D). Unlike the Alr3183 protein, Alr3183C51S required relatively higher concentration of TrxA to show any peroxidase activity i.e. peroxidase activity was observed only when TrxA concentration was 2.5 μM or more (Fig. 3D).

2.5. Physical interaction between TrxA and Alr3183

The physical interaction of Alr3183 with TrxA was studied by Surface Plasmon Resonance (SPR). The TrxA protein was immobilized on a bare gold sensor chip while the purified Alr3183 proteins were present in the mobile phase for interaction. A concentration-dependent increase in the SPR signal confirmed the physical interaction between Alr3183 and TrxA (Fig. 4A). To check the specificity of interaction, another his-tagged protein, KatB (a Mn-catalase), was allowed to interact with TrxA. The SPR profile obtained with KatB was very similar to that obtained with the interaction buffer alone (i.e. no protein present, Suppl. Fig. 3.), indicating that the interaction between TrxA and Alr3183 was indeed specific. The Alr3183 protein was reduced with DTT and allowed to interact with TrxA. Interestingly, the DTT-reduced protein showed decreased binding to TrxA as compared to the control Alr3183 protein (i.e. not treated with DTT) (Fig. 4B).

Interaction of Alr3183C46S and Alr3183C51S with TrxA is shown in the Fig. 4.C. At a comparable concentration, both Alr3183C46S and the wild-type Alr3183 protein showed similar response units at the end of the assay period. However, a distinctly reduced interaction was observed when Al-

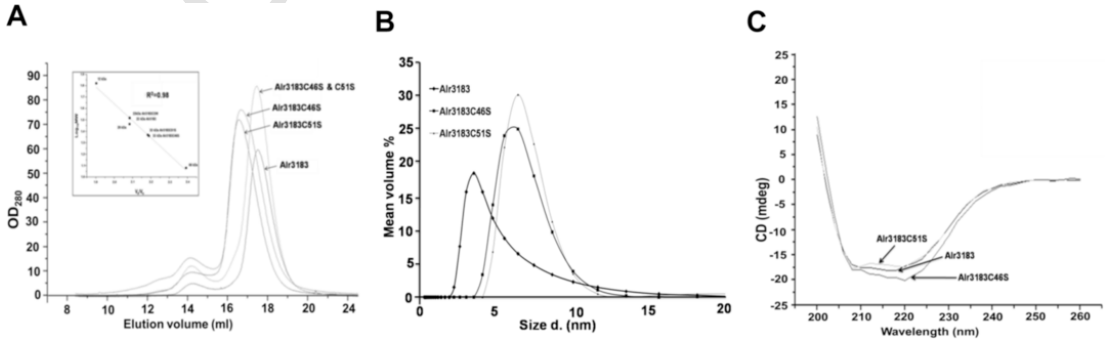

Fig. 2. (A) Size-exclusion chromatography. The column (Superdex 200 10/300) was pre-equilibrated with buffer (20 mM Tris, 50 mM NaCl, pH 7.2) and a 100 μl aliquot of protein (200 μg) was injected. The retention volumes obtained with standard proteins were employed to draw a standard curve (depicted in the insert) that was used to determine the mass of Alr3183 (B) The dynamic light scattering (DLS) profile of the purified Alr3183, Alr3183C46S and Alr3183C51S (in 20 mM Tris, pH 7.2). (C) Secondary structure analysis. The purified Alr3183, Alr3183C46S, Alr3183C51S were analyzed in a CD spectropolarimeter.

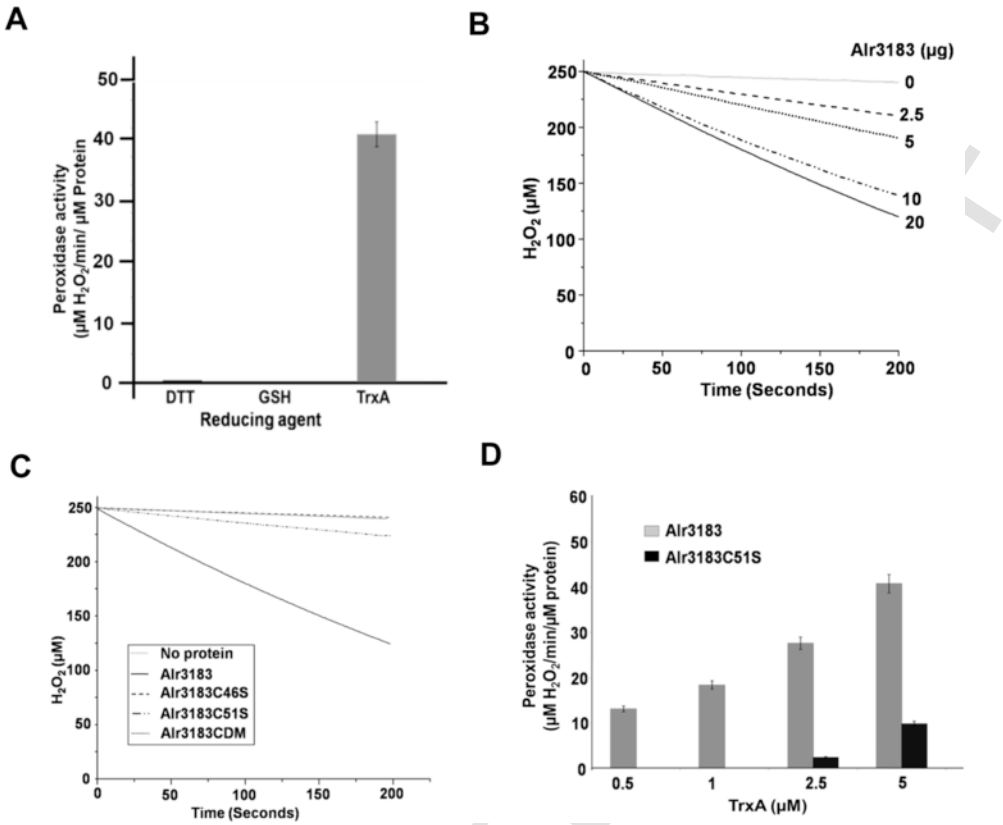

Fig. 3. (A) Peroxidase activity. Relative rates of decomposition of H_2O_2 by the purified Alr3183 protein using various electron donors: GSH, DTT and TrxA. (B) Peroxidase activity of Alr3183, in the presence of TrxA (5 μM), was monitored at various concentrations of protein (as indicated). (C) TrxA-dependent peroxidase activity of the various Alr3183 variants. H_2O_2 (250 μM) as used as the substrate whereas 20 μg of each protein was used in the assay. (D) TrxA-dependent peroxidase activity of Alr3183 and Alr3183C51S at different concentrations of TrxA.

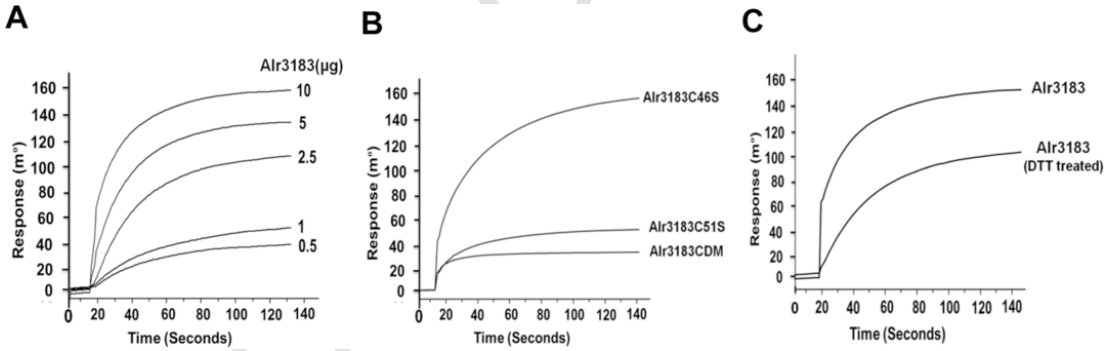

Fig. 4. Surface Plasmon Resonance analysis. The TrxA protein (250 μM) was immobilized on bare gold chip utilizing the EDC-NHS chemistry whereas the Alr3183 proteins were present in the mobile phase. The response was monitored for 120 s (A) Response curve obtained with different concentrations of the Alr3183 (as indicated in the figure). (B) Alr3183 (10 μg) was reduced with DTT and allowed to interact with TrxA. (C) Alr3183C46S, Alr3183C51S or Alr3183CDM (10 μg each) were injected over TrxA and the interaction was monitored over the time period indicated.

r3183C51S was present in the mobile phase. Another Alr3183 variant, i.e. Alr3183 lacking both the cysteines (cystine double mutant, CDM) was employed in the mobile phase for interaction with TrxA. The Alr3183CDM protein, like Alr3183C51S, interacted poorly with TrxA (Fig. 4C). In conclusion, the presence of the resolving cysteine residue appears to enhance the binding of the Alr3183 protein to TrxA.

2.6. *Alr3183 is induced in response to γ-radiation in Anabaena*

The purified Alr3183 protein was employed to raise specific antiserum (in rabbit), which was used to detect the *in vivo* production of the Alr3183 protein in *Anabaena*. On Western blots, in the unstressed control, the Alr3183 protein could not be detected when 20 μg total cellular proteins were loaded per lane. But, on loading higher amount of protein (60 μg) the Alr3183 protein could be detected as a faint band (Fig. 5A). Different oxidizing agents (H_2O_2, methyl viologen and tert-butyl hydroperoxide) did not enhance production of the Alr3183 protein, in fact a decrease in level of the protein was observed (Fig. 5A). Other stresses like salt or desiccation also did not induce synthesis of the Alr3183 protein in *Anabaena*.

Interestingly, Alr3183 protein was found to be distinctly induced in response to γ-radiation (Fig. 5B). At lower doses (0.5 and 1 kGy), the Alr3183 protein was observed 3 h post irradiation and could be clearly observed till day 3, after which it subsequently disappeared by day 5. With increasing dose of γ-radiation (3 and 6 kGy), the levels of Alr3183 protein remained high for a longer duration and gradually decreased with time. For example, noteworthy amount of the Alr3183 protein was observed even after 8 days of exposure to 6 kGy dose of γ-radiation (Fig. 5B). Nitrogen status of the medium did not affect the induction of the Alr3183 protein and even in the absence of combined nitrogen (i.e. under nitrogen-fixing conditions); pro-

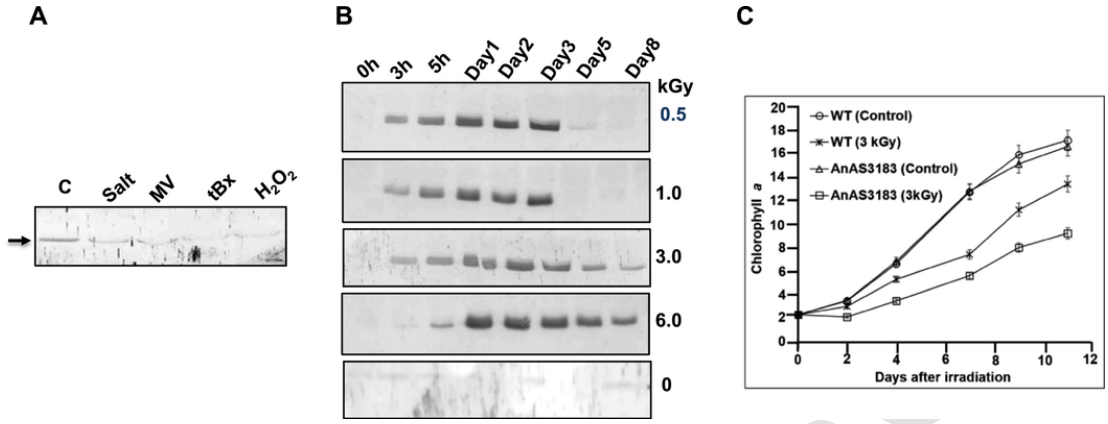

Fig. 5. Expression of Alr3183 in *Anabaena PCC* 7120. (A) *Anabaena* PCC 7120 was grown in BG11 N^+ medium containing methyl viologen (2 μM, MV) or H_2O_2 (1 mM) or tert-butyl hydroperoxide (0.25 mM, tBx) or NaCl (Salt, 200 mM) for 16 h. Total proteins were isolated from each treatment, electrophoretically resolved on SDS-PAGE (60 μg per lane), transferred onto nitrocellulose membranes and probed with the anti-Alr3183 antiserum (1:10000 dilution). The 16.7 kDa Alr3183 band is shown by an arrow. (B) Induction of Alr3183 in *Anabaena* PCC 7120 in response to gamma radiation. Four-day old *Anabaena* PCC 7120 cells grown in BG11N^+ medium was subjected to different doses of gamma radiation (indicated on the right side of each panel), total proteins were extracted at the time points indicated in the figure and probed with the Anti-Alr3183 antibody. 25 μg total protein was loaded in each lane. (C) Growth of *Anabaena* on exposure to radiation. The wild-type (WT) or the AnAS3183 strain was exposed to 3 kGy dose of gamma radiation and allowed to recover in fresh BG-11/N^+ medium under usual growth conditions. Growth was measured as increase in the content of chlorophyll *a*.

duction of Alr3183 was observed on exposure to γ-radiation (Suppl. Fig. 4A). Experiments were performed to verify whether low-dose gamma radiation induced an adaptive response against subsequent challenge by H_2O_2. *Anabaena* culture was exposed to 0.5 kGy of gamma radiation and subsequently treated (after 24 h) with 1 mM H_2O_2. However, no adaptive response was observed, and the gamma radiation-exposed cells were as sensitive to H_2O_2 as the control wild-type culture (Suppl. Fig. 4B).

The inherent expression of Alr3183 was down-regulated in *Anabaena* using an antisense approach. To accomplish this, the *alr3183* ORF was cloned in the reverse orientation downstream of the strong P_{psbA1} promoter and the corresponding construct was inserted into *Anabaena* (to give rise to AnAS3183). The AnAS3183 strain showed decreased production of Alr3183 (with respect to the wild-type *Anabaena*) under normal conditions or in response to gamma radiation (Suppl. Fig. 4C). Interestingly, the AnAS3183 strain showed a reduction in growth as compared to the wild-type cells during recovery from exposure to gamma radiation. These results suggest that the Alr3183 protein helps *Anabaena* recoup from gamma radiation stress (Fig. 5C).

2.7. Overexpression of Alr3183 and Alr3183C46S in Anabaena

It was desired to verify if the ectopic over-expression of Alr3183 could protect *Anabaena* from oxidative stress. The *alr3183* ORF was inserted between a strong light inducible P_{psbA1} promoter and a *gfp* ORF in an *Anabaena* PCC 7120-*E. coli* shuttle vector, pAM1956 (pAM3183) as described in the methods section. In this vector, the *alr3183* and *gfp* are co-transcribed, but independently translated, resulting in production of both the proteins. The pAM3183 construct was transferred into *Anabaena* PCC 7120 by conjugation and exconjugants (An3183$^+$) were selected on solid medium containing the appropriate antibiotic. The recombinant An3183$^+$ showed GFP fluorescence (Fig. 6A) as well as substantial production of the Alr3183 protein as compared to the wild-type cells (Fig. 6B), thus confirming overproduction of Alr3183.

The An3183$^+$ strain showed 4–5 fold less levels of ROS than the wild-type when exposed to H_2O_2 (Fig. 6C). Addition of H_2O_2 caused destruction of photosynthetic pigments and cell lysis in the wild-type *Anabaena* cells (Fig. 6D and E), but An3183$^+$ was protected from these deleterious effects. In addition, after exposure to H_2O_2, the An3183$^+$ retained their viability and could grow on plates whereas the wild-type did not (Fig. 6F). Not only under nitrogen supplemented conditions, under nitrogen-deficient conditions too, An3183$^+$ was protected from the toxic effects of H_2O_2, whereas the wild-type remained susceptible (Suppl. Fig. 5). The AnAS3183 strain and the wild-type *Anabaena* were equally sensitive to H_2O_2, indicating that the endogenous levels of Alr3183 were not adequate to offer protection from H_2O_2.

To overexpress the Alr3183C46S protein in *Anabaena* the *alr3183C46S* ORF was cloned into pAM1956 (pAM3183C46S) and conjugated into *Anabaena*. The recombinant strain, An3183C46S$^+$, showed expression of the GFP, and the Alr3183C46S protein too was readily produced in An3183C46S$^+$(Fig. 7A and B). However, unlike the An3183$^+$ strain, the An3183C46S$^+$ was very sensitive to the oxidative effects of H_2O_2 (Fig. 7C and D), indicating that expression of Alr3183C46S was ineffectual in offering any protection from oxidative stress to *Anabaena*.

3. Discussion

The PrxQ proteins are widely distributed in bacteria, plants and lower eukaryotes. Interestingly, PrxQ proteins have been found in all the sequenced cyanobacterial genomes [15], suggesting that these may play an important role in cyanobacterial physiology. The role of Alr3183, a PrxQ-like protein from *Anabaena* was evaluated in this study.

The nature of the disulfide bond formed (i.e. intermolecular/intramolecular) by a Prx not only depends on the Prx subfamily that particular Prx belongs to, but also depends on the availability of the catalytic cysteines. For example, the wild-type All1541 (Type II Prx from *Anabaena*) is distributed among its monomeric and dimeric forms. However, a mutant version of this protein that lacks the C_p is monomeric, whereas All1541 without the C_r is dimeric [4]. In Alr4641, the 2-Cys-Prx from *Anabaena* PCC 7120, dimerization occurs due to disulfide bond formation between the C_p of one subunit and the C_r of another subunit [7]. But, if any of the two cysteine residue is lost, the 2-Cys-Prx protein is unable to dimerize [7]. The wild-type Alr3183 exists as a monomer, and interestingly, in contrast to All1541 or Alr4641, when either of the cysteine residue is lost (Alr3183C46S or Alr3183C51S) the protein forms intermolecular disulfide bond and becomes dimeric (Figs. 1 and 2). So, the presence of both the cysteines appears to preclude the formation of intermolecular disulfide bond and intermolecular disulfide bond formation predominates in Alr3183. The wild-type Alr3183 shows the best peroxidase activity, Alr3183C51S shows considerably reduced activity whereas Alr3183C46S is completely inactive. Thus, the formation of disulfide bonds alone is not adequate for peroxidase activity; these bonds have to form in the right context, with the right partner.

The SPR technique can be gainfully utilized to explore the influence of the cysteine residues/disulfide bonds on the ability of Prxs to interact with Trxs. Recently, Hara and Hisbori [20] used this technique to observe the interaction of chloroplast Peroxiredoxin Q (PrxQ) from *Arabidopsis thaliana*

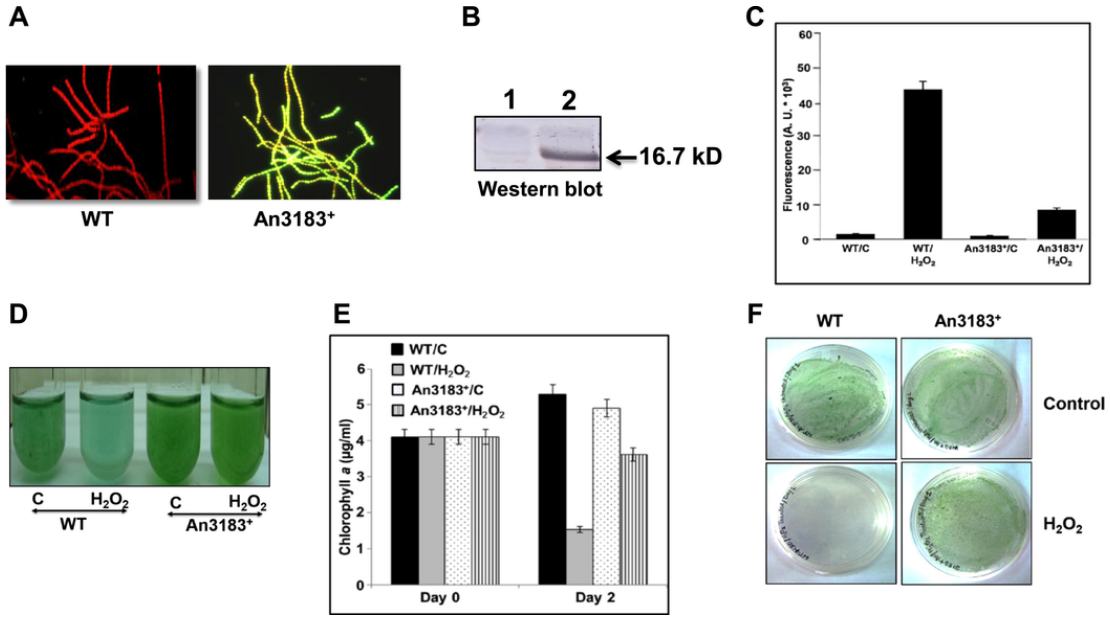

Fig. 6. Over-expression of Alr3183 in *Anabaena*. (A) The wild-type *Anabaena* PCC 7120 (WT) or the recombinant An3183$^+$ cells were visualized under fluorescence microscope (1500X magnification) using Hg-Arc lamp (excitation BP, 450–490 nm and emission LP, 515 nm). (B) Cell-free extracts from wild-type *Anabaena* (lane 1) and An3183$^+$(lane 2) were resolved by SDS-PAGE (30 µg per lane), electro-blotted on to nitrocellulose membrane, and probed with the Alr3183 antiserum (1:10000 dilution). The Alr3183 band is shown by an arrow. (C) Control or 1 mM H_2O_2- exposed wild-type *Anabaena* PCC 7120 (An7120) or An3183$^+$ were allowed to react with the fluorescent probe DCHFDA (final concentration, 10 µM) and emission was measured at 510 nm. (D) Three-day old wild-type *Anabaena* PCC 7120 (WT) or An3183$^+$ were grown in fresh growth medium and subjected to H_2O_2 (1 mM) stress for 2 days and subsequently photographed. C, control; H_2O_2, 1 mM H_2O_2. (E) The chlorophyll *a* content of the wild-type *Anabaena* PCC7120 (WT) and An3183$^+$ shown in (D) was determined immediately (Day 0) or after 2 days of exposure to H_2O_2 (Day 2). (F) 100 µl culture of control or H_2O_2-treated *Anabaena* cells were plated on BG11N$^+$ agar plates. The plates were incubated under continuous illumination for 14 days and photographed.

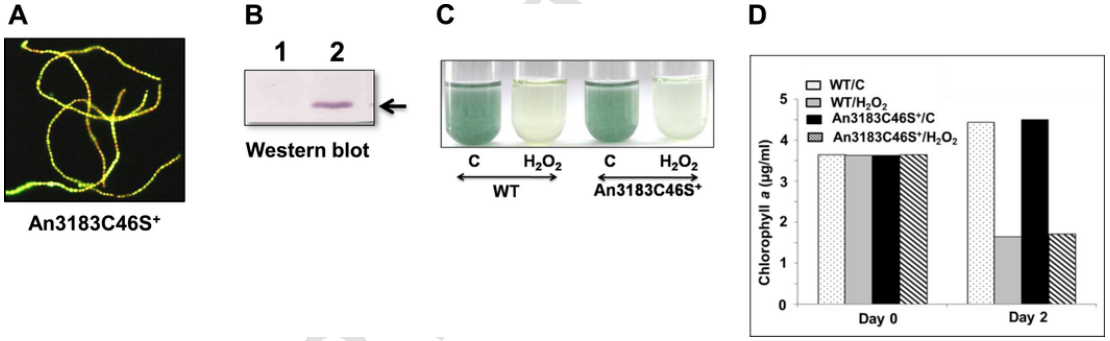

Fig. 7. Over-expression of Alr3183C46S in *Anabaena* (A) The An3183C46S$^+$ culture was visualized under fluorescence microscope using Hg-Arc lamp (excitation BP, 450–490 nm and emission LP, 515 nm). (B) Cell-free extracts from wild-type *Anabaena* (lane 1) or An3183C46S$^+$(lane 2) were resolved by SDS-PAGE (30 µg per lane), electro blotted on to nitrocellulose membrane, and probed with the Alr3183 antiserum (1:10000 dilution). The ~17 kD Alr3183C46S band is shown by an arrow. (C) Three-day old wild-type *Anabaena* PCC 7120 (WT) or An3183$^+$ were subjected to 1 mM H_2O_2 stress in tubes and photographed after 2 days. (D) The chlorophyll a content of the wild-type *Anabaena* PCC 7120 (WT) and An3183$^+$ shown in (D) was determined immediately (Day 0) or after 2 days of exposure to H_2O_2 (Day 2).

with its cognate Trx, Trxh1. However, in their study, the PrxQ protein failed to interact with the wild-type Trxh1 protein, but interaction could be observed only with a mutant $Trxh1_{CS}$ that lacked the second cysteine in its catalytic domain. In contrast, in the present study, the wild-type Alr3183 protein readily interacted with the immobilized TrxA. During the reaction cycle, for regenerating the free thiol form of C_p, the oxidized Prx has to interact with TrxA (for reduction), and once reduced, Prx has to dissociate from TrxA, so that Prx can undergo the next round of reaction [11]. The purified Alr3183 protein (which exists in oxidized state), showed enhanced association with TrxA as compared to the Alr3183 protein that was reduced with DTT (Fig. 4B) Thus, reduction of Alr3183 appears to decrease its ability to interact with TrxA, which in turn may facilitate the dissociation between the two once the disulfide bond exchange has occurred.

The Alr3183 lacking the C_r (Alr3183C51S) also functions as a peroxidase, albeit poorly. Similar to Alr3183C51S, the C_r mutants of PrxQ from Poplar or *Rhodobacter sphaeroides* also dimerize and show peroxidase activity. All the PrxQ homodimers that lack the resolving cysteine are suggested to form an atypical active site that contains the two peroxidatic cysteine residues [44]. It should be noted that Alr3183C51S requires higher concentration of TrxA to show detectable peroxidase activity *in vitro* (Fig. 3). Interestingly, the Alr3183C51S (or Alr3183CDM) that lack C_r show decreased ability to interact with TrxA than the wild-type Alr3183 protein or the Alr3183C46S, which have C_r (Fig. 4). Taken together, these two aspects underscore the importance of C_r for promoting interaction between Alr3183 and TrxA for efficient peroxidase function. The presence of C_r appears to facilitate the recruitment of TrxA, which would rapidly reduce the oxidized cysteines, consequently speeding up the reaction.

Why does *Anabaena* encode so many PrxQ proteins? The presence of multiple PrxQs in *Anabaena*, apparently catalyzing similar reactions, may not be a case of redundancy. A particular PrxQ may be induced in response to a specific stress in *Anabaena*. For example, All2375 alone is induced by NaCl and diamide whereas Alr2503, All2375 and All2556 are all induced by tert-butyl hydroperoxide, but Alr3183 is not [10]. Among the various stresses/oxidizing agents tested, the Alr3183 protein was induced in response to gamma radiation. Ionizing radiation such as gamma radiation not only causes double stranded breaks (dsbs) in DNA, but also causes oxidative

stress. Along with other ROS, exposure to gamma radiation also leads to the formation of H_2O_2 and lipid peroxides [2], both of which are substrates of Alr3183 [10]. Moreover, reduced growth of the AnAS3183 strain in response to 3 kGy gamma radiation (Fig. 5) does argue for a role of Alr3183 in overcoming oxidative stress. Interestingly, Alr3183 expression was also observed when *Anabaena* PCC 7120 was exposed to mitomycin C, an agent that causes DNA double strand breaks (dsbs) (Suppl. Fig. 6), suggesting an apparent link between expression of Alr3183 and formation of DNA dsbs. However, desiccation, another stress causes DNA dsbs [38] failed to induce Alr3183 in *Anabaena*. These results indicate that regulation of Alr3183 is more complex and may not depend solely on DNA damage or ROS levels.

In particular, the filamentous strains of cyanobacteria, including *Anabaena*, are very sensitive to the oxidative effects of H_2O_2 [23,5]. Under normal (i.e. unstressed) conditions, *Anabaena* shows very poor catalase expression and no catalase activity can be detected on zymograms [5]. In fact, H_2O_2 and methyl viologen also fail to induce catalase expression in *Anabaena*. As *Anabaena* shows a preponderance of genes that encode Peroxiredoxins, it is believed that these may be the proteins that defend *Anabaena* from peroxides such as H_2O_2. H_2O_2 and methyl-viologen both induce Alr4641 & All1541, but do not elicit production of Alr3183 in *Anabaena* PCC 7120. Likely, Alr4641 and All1541 (but not Alr3183) could be the principal players that protect cell from H_2O_2 under normal physiological conditions. However, it should be noted that induction of Alr4641 or All541 that normally occurs in response to externally added H_2O_2 is not adequate to protect *Anabaena* from its toxicity. Addition of as little as 1 mM of H_2O_2 causes rapid degradation of chlorophyll *a*, resulting in complete collapse of *Anabaena* cultures and cell death (Fig. 6). However, if Alr3183 is over-expressed in *Anabaena*, cells are protected from the damaging consequences of H_2O_2, both under nitrogen-supplemented as well as nitrogen-deficient conditions. Unlike the wild-type, on exposure to H_2O_2, the An3183$^+$ strain showed substantially reduced ROS formation, lower damage to pigments and consequently, the cells remained viable (Fig. 6).

Although known to function primarily as peroxidases, Prxs are now known to be involved in redox signalling [17] or function as chaperones [25,7] or phospholipases [31]. In fact, the phospholipase or the chaperone activity of Prxs has been shown to be independent of the catalytic cysteine residues. To exclude the possibility that Alr3183 would mediate its protective effect (against H_2O_2) independent of the peroxidase activity, the Alr3183C46S protein (that lacks the peroxidase activity) was over-expressed in *Anabaena*. Like the wild-type strain, the Alr3183C46S$^+$ strain was also very susceptible to H_2O_2. This conclusively demonstrates that the *in vivo* peroxidase activity of Alr3183 is absolutely essential to protect *Anabaena* from the lethal effects of H_2O_2.

In conclusion, Alr3183 is a monomeric, TrxA-dependent peroxidase whose C_p and C_r, form an intramolecular disulfide bond. The presence of both C_p and C_r prohibits intermolecular disulfide bond formation, but, if either of the catalytic cysteine is absent, the protein becomes dimeric due to formation of intermolecular C_p-C_p or C_r-C_r linkages. C_p is essential for reacting with the peroxidatic substrate whereas the presence of C_r appears to improve the protein's capability to interact with TrxA. *In vivo*, Alr3183 was found to be a stress-inducible protein whose synthesis was upregulated by γ-radiation. Over-expression of Alr3183 protected *Anabaena* from oxidative stress in nitrogen-supplemented as well as nitrogen-deficient conditions, indicating the potential of An3183$^+$ to function as stress-resilient biofertilizer.

4. Materials and methods

4.1. Organism and growth conditions

Axenic *Anabaena* PCC 7120 cultures were grown in BG-11 liquid medium (BG-11/N$^+$, pH 7.2–7.4) containing combined nitrogen (17 mM $NaNO_3$) ([9] under continuous illumination (30 μmol photons m^{-2} s^{-1})) with shaking (100 rpm) or as a still culture at 27 °C±2 °C. Growth was assessed as increase in the content of chlorophyll *a* per ml of culture volume [30], whereas viability was verified by determining the ability of cells to grow on BG-11 agar plates. *Escherichia coli* cells were grown in Luria-Bertani (LB) medium in the presence of appropriate antibiotics at 37 °C with shaking at 150 rpm. The antibiotics used were 10 μg neomycin ml^{-1} (Nm_{10}) in BG-11 liquid media, 25 μg neomycin ml^{-1} (Nm_{25}) in BG-11 agar plates for the recombinant *Anabaena* PCC 7120 and 34 μg chloramphenicol ml^{-1} (Cm_{34}), 50 μg kanamycin ml^{-1} (Kan_{50}) or 100 μg carbenicillin ml^{-1} (Cb_{100}) for *E. coli*. The *E. coli* and *Anabaena* strains and plasmids used in the study are indicated in Supp. Table 1.

4.2. Cloning of alr3183, alr3183C46S, alr3183C51S and alr3183CDM (cysteine double mutant i.e. alr3183C46S&C51S) into pET16b

The *alr3183* ORF was PCR amplified using gene-specific primers, *alr3183*fwd and *alr3183*rev (Supp. Table 2), employing *Anabaena* PCC7120 chromosomal DNA as template. The 462-bp PCR product was digested with the restriction enzymes *Nde*I and *Bam*HI and cloned into similarly digested pET16b to obtain pET3183 (Supp. Table 1). The pET3183 insert was sequenced to confirm the sequence integrity of the cloned *alr3183* gene.

A point mutation leading to the substitution of Cys codon (AGA), of Cys-46 or Cys-51, or both (i.e. Cys-46 and Cys-51) to Ser codon (GGA) was introduced into the *ar3183* ORF by PCR- based site-specific mutagenesis using overlapping PCR. A two-step PCR using oligonucleotide primers (Supp. Table 2) that contained mismatched bases at the desired location and the pET3183 DNA (template) was performed. The two PCR products that overlapped in the DNA sequence containing the required mutation were obtained. Subsequently, these fragments were mixed together, denatured by heating and allowed to anneal. Subsequently, the annealed fragments were re-amplified with alr3183 fwd/rev primers, resulting in the formation of the full-length *alr3183C46S* or *alr3183C51S*. These were sub-cloned into pET16b to give rise to pET383C46S and pET3183C51S respectively. For constructing *alr3183CDM*, primers employed to generate the *alr3183C51S* fragment were used to amplify pET3183C46S DNA in the two step PCR. All the above fragments were cloned into pET16b at the *Nde*I and *Bam*HI restriction sites, sequenced to confirm the presence of the desired mutation.

4.3. Overproduction and purification of the various Alr3183 proteins

Overproduction and purification of the His-tagged Alr3183, Alr3183C46S, Alr3183C51S Alr3183CDM proteins from *E. coli* BL21pLysS was performed by affinity chromatography using a Ni-NTA (Ni^{2+}-Nitrilotriacetate) matrix as described previously [3]. The purified Alr3183 protein was also used to immunize rabbits for generating specific antiserum. The primary and booster immunizations and collection of the antiserum were performed at a commercial facility (Merck, India).

4.4. Protein electrophoresis, Western blotting and immunodetection

After induction with IPTG, *E. coli* BL21 (DE3)/pLysS cells over-expressing any of the above-mentioned proteins were lysed in Laemmli's sample buffer [26], protein extracts were resolved on SDS-polyacrylamide (14%) gels and stained with Coomassie brilliant blue (CBB). Total cellular proteins from *Anabaena* were extracted using Laemmli's buffer and electrophoretically separated as described above. When required, proteins were electroblotted onto nitrocellulose membrane by electroblotting at 300 mA for 3 h. Subsequently, the blot was allowed to cross-react with the Alr3183 antiserum (1:5000) or the anti-polyhistidine antiserum (1:5000) for 16 h. After washing the primary antibody, the blot was incubated with appropriate secondary antibody linked to alkaline phosphatase and the colour reaction carried out with the chromogenic substrate, nitro blue tetrazolium chloride/5-bromo-4-chloro-3-indolyl phosphate toluidine salt (NBT/BCIP), stock solution (Roche).

4.5. Peroxidase activity assay

For the DTT-dependent peroxidase assay, a reaction mixture (1 ml) containing 50 mM Hepes/NaOH buffer (pH 7.0) and the desired concentrations of Prx proteins were pre-incubated with DTT (3 mM) for 10 min at 37 °C, followed by the addition of H_2O_2 (200 μM). The residual H_2O_2 remaining in tubes was measured with the peroxoquant kit (Thermo Scientific). The amount of residual H_2O_2 remaining in the reaction was calculated from a standard calibration curve prepared using known concentrations of H_2O_2. For GSH-dependent peroxidase activity, the typical reaction mixture contained 50 mM HEPES/NaOH (pH 7.0), NADPH (0.25 mM), glutathione reductase (GR, 0.2 μM), 1 μg of purified Alr3183 protein and GSH (5 mM). The reaction was started by the addition of 200 μM H_2O_2 and the decrease in the absorbance of NADPH (at 340 nm) was monitored. The TrxA-dependent peroxidase activity of various Alr3183 constructs was measured by monitoring the decrease in absorbance of NADPH at 340 nm using *E. coli* TrxA (1–5 μM, Sigma T0910) and H_2O_2 (200 μM) as the substrate. For calculation of kinetic parameters, the reaction was started by the direct addition of H_2O_2 (ranging from 5 to 250 μM) and the activity was monitored for 5 min. A molar absorption coefficient of 6220 cm^{-1} M^{-1} for NADPH was used to calculate the enzyme activity [10].

4.6. Modification of the proteins with AMS (4-acetamido-4-maleimidylstilbene- 2,2-disulfonate)

The purified Alr3183 protein was incubated in a reaction mixture containing, 10 mM DTT or 2 mM H_2O_2 at 20°C for 20 min. The protein was precipitated with 10% TCA and dissolved in 20 μl of a freshly prepared solution containing 1% SDS, 50 mM Tris/HCl (pH 7.5) and 15 mM of AMS. Proteins were initially incubated with agitation at 20 °C for 30 min after which they were transferred to 37°C for 10 min. Finally, proteins were resolved on SDS/PAGE (14% gel) under non-reducing conditions and visualized by staining with CBB (Coomassie Brilliant Blue).

4.7. Gel-exclusion chromatography

Oligomeric status of Alr3183 and its cysteine mutants was determined by gel permeation chromatography employing the Superdex-200 gel-exclusion column with a bed volume of 24 ml (GE health care, UK). Bovine serum albumin (66 kD), Carbonic anhydrase (29 kD), and Cytochrome C (12.4 kD) were used as protein standards. Approximately 250 μl (concentration of 1 μg/μl) of each of the protein was individually passed through the column at a flow rate of 0.6 ml per min.

4.8. Dynamic light scattering

Hydrodynamic size of Alr3183/Alr3183C46S/Alr3183C51S was determined by dynamic light scattering (DLS) using the instrument, Malvern Zetasizer, nanoseries. Individual proteins (0.4 μg/μl in 20 mM Tris, pH 8), were analyzed in 1 ml cuvettes supplied with the machine.

4.9. CD-spectropolarimetry

For CD spectral analysis, the purified proteins were dialyzed against a buffer containing 20 mM Tris-Cl (pH 8), and CD spectra in the far-UV (190–250 nm) and near-UV (230–350 nm) region were recorded on a Jasco J-720 spectropolarimeter using cylindrical quartz cuvettes of path length 1 and 10 mm respectively. Each spectrum represents the average of five successive scans performed at a scan speed of 20 nm/minute. Appropriate baseline subtraction and noise reduction analysis were performed.

4.10. Surface plasmon resonance (SPR) analysis

Surface plasmon resonance analysis with a bare gold sensor chip was performed using the Autolab Esprit SPR system. At 20 °C, about 200 response units of TrxA was loaded onto the bare gold chip employing the EDC-NHS chemistry (Autolab ESPIRIT User manual SPR) followed by extensive washing with buffer H (20 mM Tris, 100 mM NaCl, pH 7.5). The Alr3183/Alr3183C46S/Alr3183C51S/Alr3183CDM proteins were injected separately onto the TrxA-bound sensor chip at 33.3 μl min^{-1} flow rate in independent experiments. The Alr3183 proteins were allowed to interact with the immobilized TrxA for 300 s before washing off with buffer H containing 0.1% SDS. The Alr3183 protein was reduced with DTT (20 mM) in the above-mentioned buffer for 1 h and the excess DTT was subsequently removed by dialysis. The DTT-reduced protein was also allowed to interact with the immobilized TrxA. The data were processed using Autolab kinetic evaluation software (V5.4) provided with the instrument.

4.11. Construction of pAM3183, pAM3183C46S and pAMAS3183 and their transfer to Anabaena PCC 7120

The ~0.47 kb *alr3183/alr3183C46S* DNA fragment from pET3183/pET3183C46S was subcloned as a NdeI-BamHI fragment, downstream of the strong P_{psbA1} promoter, into pFPN [13] to give rise to pFPN3183 or pFPN3183C46S respectively. For expressing antisense *alr3183* in *Anabaena*, the *alr3183* ORF was cloned in the antisense orientation (using Alr3183ASFwd and Alr3183ASRev primers), downstream of the P_{psbA1} promoter, in pFPN (pFPNAS3183). The *alr3183/alr3183C46S/alrAS3183* DNA fragment along with the P_{psbA1} promoter was transferred as a SalI-XmaI fragment to appropriately digested *E. coli/Anabaena* shuttle vector pAM1956 (Yoon and Golden, 1998) to obtain pAM3183 or pAM3183C46S or pAMAS3183. The various constructs were individually conjugated into *Anabaena* PCC 7120 using a conjugal *E. coli* donor [HB101(pRL623 + pRL443)] [18] which has the AvaI/AvaII methylase encoding plasmid (pRL623) and the conjugal plasmid (pRL443). Exconjugants were selected on BG-11/N^+ plates containing neomycin (25 μg/ml) and repeatedly subcultured. The transformed *Anabaena* strains thus obtained (designated An3183$^+$ or An3183C46S$^+$ or AnAS3183) were maintained on BG-11/N^+ plates containing neomycin.

4.12. Stress tolerance of An3183$^+$ and An3183C46S$^+$

Three-day-old *Anabaena* cultures of the wild-type *Anabaena* PCC 7120 (WT) as well as An3183$^+$ were inoculated in a fresh growth medium at a chlorophyll *a* density of 2–4 μg ml^{-1} and subjected to H_2O_2 (1 mM) stress in tubes (without shaking) under illumination for 2 days. Growth of cultures was monitored by measuring the chlorophyll *a* content of cultures [30]. Radiation experiments were performed as described by [38]. For post-irradiation recovery, the cultures were reincoulated into a fresh medium at chlorophyll *a* density of 2 μg ml^{-1} and their growth was measured as described above.

4.13. Estimation of total ROS content of the whole cells using DCHFDA dye

Total ROS content of the cells were estimated using DCHFDA (SIGMA Aldrich, USA). Briefly 1 ml of cells were taken in 1.5 ml tubes and DCHFDA was added at final concentration of 10 μM and incubated at 37°C for 1 h, in dark and shaking at 150 rpm. After 1 h of incubation, florescence was estimated in triplicates (λ_{ex} = 490 nm, λ_{em} = 520 nm).

4.14. Analytical procedures and bioinformatic analysis

Protein concentrations were determined by a modified Lowry method (Total Protein Kit, Sigma Cat. No. TP0300) using bovine serum albumin as standard. Amino acid sequence was analyzed using BLAST (http://blast.

ncbi.nlm.nih.gov/blast) or SMART (http://smart.embl-heidelberg.de/) algorithms [1,37]. Multiple sequence alignment was performed with the Clustal W software available at www.ch.embnet.org/software/ClustalW.html.

Author contribution

AB conceived and directed the overall study. AB and VT planned the research; VT performed the experiments and both the authors interpreted the results. AB and VT wrote the paper.

Acknowledgements

We would like to thank Dr. S. K. Apte, Dr. Vinay Kumar, Dr. Suprasanna and Dr. Manisha Banerjee for helpful suggestions during the course of this work. Expertise provided by Dr. Subhash Bihani for CD spectropolarimetry and DLS experiments is highly appreciated. Dr. S. Chattopadhyay and Dr. H. S. Misra are thankfully acknowledged for their constant encouragement during the course of this study. Homi Bhabha National Institute (HBNI) is gratefully acknowledged for providing fellowship to Ms. Vijay Tailor.

Appendix A. Supplementary material

Supplementary material associated with this article can be found in the online version at doi:10.1016/j.freeradbiomed.2017.01.031.

References

[1] S.F. Altschul, W. Gish, W. Miller, E.W. Myers, D.J. Lipman, Basic local alignment search tool, J. Mol. Biol. 21 (1990) 5403–5410.
[2] A. Agrawal, R.K. Kale, Radiation induced peroxidative damage: mechanism and significance, Indian J. Exp. Biol. 39 (2001) 291–309.
[3] A. Ballal, S.K. Apte, Characterization of a response regulator protein that binds to Anabaena sp. strain L-31 kdp-promoter region, Arch. Biochem. Biophys. 474 (2008) 65–71.
[4] M. Banerjee, A. Ballal, S.K. Apte, A novel glutaredoxin domain-containing peroxiredoxin 'All1541' protects the N_2-fixing cyanobacterium Anabaena PCC 7120 from oxidative stress, Biochem. J. 442 (2012) 671–680.
[5] M. Banerjee, A. Ballal, S.K. Apte, Mn-catalase (Alr0998) protects the photosynthetic, nitrogen-fixing cyanobacterium Anabaena PCC7120 from oxidative stress, Environ. Microbiol. 14 (2012) 2891–2900.
[6] M. Banerjee, P.S. Raghavan, A. Ballal, H. Rajaram, S.K. Apte, Oxidative stress management in the filamentous, heterocystous, diazotrophic cyanobacterium, Anabaena PCC7120, Photosynth. Res. 118 (2013) 59–70.
[7] M. Banerjee, D. Chakravarty, A. Ballal, Redox-dependent chaperone/peroxidase function of 2-Cys-Prx from the cyanobacterium Anabaena PCC7120: role in oxidative stress tolerance, BMC Plant Biol. 15 (2015) 6015.
[8] L. Botello-Morte, S. Pellicer, V.C. Sein-Echaluce, L.M. Contreras, J.L. Neira, O. Abián, M.T. Bes, Cysteine mutational studies provide insight into a thiol-based redox switch mechanism of metal and DNA binding in FurA from Anabaena sp. PCC 7120, Antioxid. Redox Signal. 24 (2016) 173–185.
[9] R.W. Castenholz, Culturing methods for cyanobacteria, Methods Enzym. 167 (1988) 68–93.
[10] M.K. Cha, S.K. Hong, I.H. Kim, Four thiol peroxidases contain a conserved GCT catalytic motif and act as a versatile array of lipid peroxidases in Anabaena sp. PCC 7120, Free Radic. Biol. Med. 42 (2007) 1736–1748.
[11] H.Z. Chae, T.B. Uhm, S.G. Rhee, Dimerization of thiol-specific antioxidant and the essential role of cysteine 47, Proc. Natl. Acad. Sci. USA 91 (1994) 7022–7026.
[12] D. Chakravarty, M. Banerjee, S. Bihani, A. Ballal, A salt-inducible Mn-Catalase (KatB) protects cyanobacterium from oxidative stress, Plant Physiol. 170 (2016) 761–773.
[13] A. Chaurasia, A. Parasnis, S.K. Apte, An integrative expression vector for strain improvement and environmental applications of the nitrogen fixing cyanobacterium, Anabaena sp. strain PCC 7120, J. Microbiol. Methods 73 (2008) 133–141.
[14] D.J. Clarke, X.P. Ortega, C.L. Mackay, M.A. Valvano, J.R. Govan, D.J. Campopiano, P. Langridge-Smith, A.R. Brown, Subdivision of the bacterioferritin comigratory protein family of bacterial peroxiredoxins based on catalytic activity, Biochemistry 49 (2010) 1319–1330.
[15] H. Cui, Y. Wang, Y. Wang, S. Qin, Genome-wide analysis of putative peroxiredoxin in unicellular and filamentous cyanobacteria, BMC Evol. Biol. 12 (2012) 220.
[16] K.J. Dietz, Peroxiredoxins in plants and cyanobacteria, Antioxid. Redox Signal. 15 (2011) 1129–1159.
[17] K.J. Dietz, The dual function of plant peroxiredoxins in antioxidant defense and redox signaling, Subcell. Biochem. 44 (2007) 267–294.
[18] J. Elhai, A. Vepritskiy, A.M. Muro-Pastor, E. Flores, C.P. Wolk, Reduction of conjugal transfer efficiency by three restriction activities of Anabaena sp. strain PCC 7120, J. Bacteriol. 179 (1997) 1998–2005.
[19] B. Halliwell, M.V. Clement, L.H. Long, Hydrogen peroxide in the human body, FEBS Lett. 486 (2000) 10–13.
[20] S. Hara, T. Hisbori, Kinetic analysis of the interactions between plant thioredoxin and target proteins, Front. Plant Sci. 4 (2014) 508.
[21] L.W. Jing, S.H. Chen, X.L. Guo, H. Zhang, Y.X. Zhao, Overexpression of a chloroplast-located Peroxiredoxin Q gene, SsPrxQ, increases the salt and low-temperature tolerance of arabidopsis, J. Integr. Plant Biol. 48 (2006) 1244–1249.
[22] T. Kaneko, Y. Nakamura, C.P. Wolk, T. Kuritz, S. Sasamoto, A. Watanabe, M. Iriguchi, A. Ishikawa, K. Kawashima, T. Kimura, Y. Kishida, M. Kohara, M. Matsumoto, A. Matsuno, A. Muraki, N. Nakazaki, S. Shimpo, M. Sugimoto, M. Takazawa, M. Yamada, M. Yasuda, S. Tabata, Complete genomic sequence of the filamentous nitrogen-fixing cyanobacterium Anabaena sp. strain PCC 7120, DNA Res. 8 (2001) 205–213.
[23] R.N. Kaplan-Levy, O. Hadas, A. Sukenik, Deciphering the mechanisms against oxidative stress in developing and mature akinetes of the cyanobacterium Aphanizomenon ovalisporum, Microbiology 161 (2015) 1485–1495.
[24] A. Kiba, M. Nishihara, N. Tsukatani, T. Nakatsuka, Y. Kato, S. Yamamura, A Peroxiredoxin Q homolog from gentians is involved in both resistance against fungal disease and oxidative stress, Plant Cell Physiol. 46 (2005) 1007–1015.
[25] J. König, H. Galliardt, P. Jütte, S. Schäper, L. Dittmann, K.J. Dietz, The conformational bases for the two functionalities of 2-cysteine peroxiredoxins as peroxidase and chaperone, J. Exp. Bot. 64 (2013) 3483–3497.
[26] U.K. Laemmli, Cleavage of structural proteins during the assembly of the head of bactetiophage T4, Nature 227 (1970) 680–685.
[27] P. Lamkemeyer, M. Laxa, V. Collin, W. Li, I. Finkemeier, M.A. Schottler, V. Holtkamp, V.B. Tognetti, B.E. Issakidis, A. Kandlbinder, E. Weis, et al., Peroxiredoxin Q of Arabidopsis thaliana is attached to the thylakoids and functions in context of photosynthesis, Plant J. 45 (2006) 968–981.
[28] A. Latifi, M. Ruiz, R. Jeanjean, C.C. Zhang, PrxQ-A, a member of the Peroxiredoxin Q family, plays a major role in defense against oxidative stress in the cyanobacterium Anabaena sp. strain PCC7120, Free Radic. Biol. Med. 42 (2007) 424–431.
[29] R. López-Igual, A. Wilson, R.L. Leverenz, M.R. Melnicki, C.B. de Carbon, M. Sutter, A. Turmo, F. Perreau, C.A. Kerfeld, D. Kirilovsky, Different functions of the paralogs to the N-terminal domain of the Orange Carotenoid Protein in the cyanobacterium Anabaena sp. PCC 7120, Plant Physiol. (2016). (16-00502).
[30] G. Mackinney, Absorption of light by chlorophyll solutions, J. Biol. Chem. 140 (1941) 315–322.
[31] J. Nevalainen, 1-Cysteine peroxiredoxin: a dual-function enzyme with peroxidase and acidic Ca^{2+}-independent phospholipase A2 activities, Biochimie 92 (2010) 638–644.
[32] M.B. Pascual, A. Mata-Cabana, F.J. Florencio, M. Lindahl, F.J. Cejudo, Overoxidation of 2-Cys peroxiredoxin in prokaryotes: cyanobacterial 2-Cys peroxiredoxins sensitive to oxidative stress, J. Biol. Chem. 285 (2010) 34485–34492.
[33] M.B. Pascual, A. Mata-Cabana, F.J. Florencio, M. Lindahl, F.J. Cejudo, A comparative analysis of the NADPH thioredoxin reductase C-2-Cys peroxiredoxin system from plants and cyanobacteria, Plant Physiol. 155 (2011) 1806–1816.
[34] S.A. Reeves, D. Parsonage, K.J. Nelson, L.B. Poole, Kinetic and thermodynamic features reveal that Escherichia coli BCP is an unusually versatile peroxiredoxin, Biochemistry 50 (2011) 8970–8981.
[35] N. Rouhier, E. Gelhaye, J.M. Gualberto, M.N. Jordy, E.D. Fay, M. Hirasawa, S. Duplessis, S.D. Lemaire, P. Frey, F. Martin, W. Manieri, D.B. Knaff, J.P. Jacquot, Poplar Peroxiredoxin Q. A thioredoxin-linked chloroplast antioxidant functional in pathogen defense, Plant Physiol. 134 (2004) 1027–1038.
[36] N. Rouhier, J.P. Jacquot, The plant multigenic family of thiol peroxidases, Free Radic. Biol. Med. 38 (2005) 1413–1421.
[37] J. Schultz, F. Milpetz, P. Bork, C.P. Ponting, SMART, a simple modular architecture research tool: identification of signaling domains, Proc. Natl. Acad. Sci. USA 95 (1998) 5857–5864.
[38] H. Singh, K. Anurag, S.K. Apte, High radiation and desiccation tolerance of nitrogen-fixing cultures of the cyanobacterium Anabaena sp. strain PCC 7120 emanates from genome/proteome repair capabilities, Photosyn. Res. 118 (2013) 71–81.
[39] T. Stork, M. Laxa, M.S. Dietz, K.J. Dietz, Functional characterisation of the peroxiredoxin gene family members of Synechococcus elongatus PCC 7942, Arch. Microbiol. 191 (2009) 141–151.
[40] V. Tailor, A. Ballal, Over-expression of Alr4642, a novel Prx-like peroxiredoxin, defends the cyanobacterium Anabaena PCC7120 from oxidative stress, J. Appl Phycol. 27 (2015) 2261–2270.
[41] U. Petersson, T. Kieselbach, J.G. García-Cerdán, W.P. Schröder, The Prx Q protein of Arabidopsis thaliana is a member of the luminal chloroplast proteome, FEBS Lett. 58 (2006) 6055–6061.
[42] J. Walter, F. Lynch, N. Battchikova, E.M. Aro, P.J. Gollan, Calcium impacts carbon and nitrogen balance in the filamentous cyanobacterium Anabaena sp. PCC 7120, J. Exp. Bot. (2016) http://dx.doi.org/10.1093/jxb/erw112.
[43] G.S. Venkataraman, Algal inoculation in rice field, in: N.C. Brady (Ed.), Nitrogen and Rice, International Rice Research, Los Banos, Philippines, 1979.
[44] M. Wakita, S. Masuda, K. Motohashi, T. Hisabori, Ohta, H, K. Takamiya, The significance of type II and PrxQ peroxiredoxins for antioxidative stress response in the purple bacterium Rhodobacter sphaeroides, J. Biol. Chem. 282 (2007) 27792–27801.